Fault transient analysis of multi-conductor e.h.v. transmission line with particular reference to line protection.

Banerjee, Amiya Ranjan

Award date:
1976

Awarding institution:
University of Bath

75-12146

Fault Transient Analysis Of Multi-Conductor E.H.V. Transmission line with particular Reference To Line Protection.

By

Amiya Ranjan Banerjee

B.Sc. (Engg.), M.Sc. (Engg.), M.I.E.E.E.

Thesis Submitted for the Degree of Doctor of Philosophy

of

The University of Bath

1976

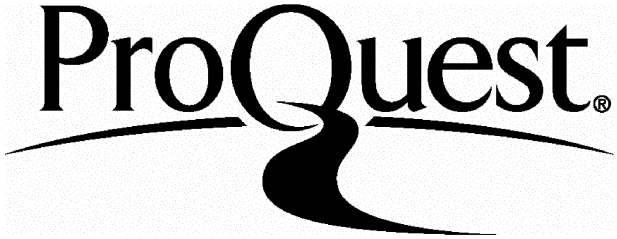

Summary

In this thesis a new analytical technique for the evaluation of fault initiated transients has been developed. The technique is very general and is applicable to both the transposed and untransposed polyphase multi-conductor lines of any configuration, and, can take into account the frequency dependence of the parameters of the system. On the basis of this technique the following types of faults can be easily studied:

(a) shunt faults

(b) series faults

(c) simultaneous shunt or series faults or their combination at one or multiple locations.

The post fault transient behaviour of ehv ac transmission line has been simulated by using digital computer. The fault transient response at the relaying points are presented for a number of interesting cases. This information is of particular interest for the design and development of super-speed protective schemes ehv lines.

The phenomenona of fault induced overvoltage has also been investigated briefly. The results for fault induced overvoltage show excellent agreement with Kimbark's field test results.

Digital simulation of the transient behaviour has been achieved by a very efficient programming technique.

Contents

List of Symbols

Z	=	Series - impedance matrix per Unit length
Y	=	Shunt - admittance matrix per Unit length
Z_o	=	Surge - impedance matrix
Y_o	=	Surge - admittance matrix
Q	=	Eigenvector matrix of voltage
S	=	Eigenvector matrix of current
Υ	=	Diagonal propagation Constant matrix
Z_{os}	=	Self - Surge - impedance
Z_{om}	=	Mutual - Surge - impedance
Z_e	=	Impedance per Unit length of the faulted circuit (Used in Chapter 7 and Appendix 4)
Y_F	=	Fault - admittance matrix
r_e	=	Effective radius of the bundle
r	=	Radius of a Sub-Conductor of a bundle
s	=	Space between the Sub-Conductors

$V_s(t)$, $V_R(t)$, $V_x(t)$ = Instantaneous Value of steady-state Voltage at the Sending end, Receiving end and at Location x

$V_{s_{tr}}(t)$, $V_{R_{tr}}(t)$, $V_{x_{tr}}(t)$ = Instantaneous Value of Voltage at the Sending end, Receiving end and at Location x due to Switching

$V_{s_F}(t)$, $V_{R_F}(t)$, $V_{x_f}(t)$ = Instantaneous Value of Voltage at the Sending end, Receiving end and at Location x after fault inception

$I_s(t)$, $I_R(t)$, $I_x(t)$ = Instantaneous Value of steady-state Current at the Sending end, Receiving end and at Location x

$I_{s_{tr}}(t)$, $I_{R_{tr}}(t)$, $I_{x_{tr}}(t)$ = Instantaneous Value of Current at the Sending end, Receiving end and at Location x due to Switching

$I_{s_F}(t)$, $I_{R_F}(t)$, $I_{x_F}(t)$ = Instantaneous Value of Current at the Sending end, Receiving end and at Location x after fault inception

$E_f(t)$ = Instantaneous Value of e.m.f. of the hypothetical e.m.f. Source

T = Time delay in the arrival of the first incident wave of Fault Surge

T_f = Time delay in the arrival of fast component of the first incident wave of fault surge

T_s = Time delay in the arrival of slow component of the first incident wave of fault surge

T_i = Time interval between any two consecutive reflections

I = Initial jump of Current due to the arrival of the first incident wave of fault surge

$\bar{E}_f$ = Transform of e.m.f. of hypothetical e.m.f. source

$\bar{V}_{RR_1}$, $\bar{V}_{RR_2}$ = Transform of Voltages at the Sending end and the Receiving end

$\bar{I}_{RR_1}$, $\bar{I}_{RR_2}$ = Transform of Currents at the Sending end and the Receiving end

$\bar{I}_f$ = Transform of Current in the fault admittance

$\bar{I}_{s_f}$ = Transform of Current injected at the location of fault

$\bar{I}_{s_{f_1}}$ = Transform of line currents at the location of fault (towards Sending end)

$\bar{I}_{s_{f_2}}$ = Transform of line currents at the location of fault (towards Receiving end)

$\bar{V}_{s_{f_1}}$ = Transform of Voltage at location of fault (location 1)

$\bar{V}_{s_{f_2}}$ = Transform of Voltage at location of fault (location 2)

$\bar{I}_{s_{f_{11}}}$ = Transform of line current at fault location 1 (towards location 2)

$\bar{I}_{s_{f_{12}}}$ = Transform of line current at fault location 1 (towards receiving end)

$\bar{I}_{s_{f_{21}}}$ = Transform of line current at fault location 2 (towards Sending end)

$\bar{I}_{s_{f_{22}}}$ = Transform of line current at fault location 2 (towards location 1)

CHAPTER 1

INTRODUCTION

EHV lines form vital links between remote generating units and are also used for supplying loads from remote generating areas. The other advantages of ehv lines are well known, e.g. large load capacity, better efficiency, and better regulation etc. Because of these advantages of ehv transmission, the transmission voltages are going higher and higher with the growth of load and the increase of the capacity of the generating units. The ehv transmission voltages may be either AC or DC, both have their advantages and disadvantages, however AC is more common.

EHV systems are often subjected to various intended or unintended transient disturbances e.g. switching operations, lightning surges and faults etc. These disturbances produce abnormal voltages and currents and frequencies in the system. It is not possible for a designer to prevent the occurrence of these disturbances, hence the effects of these disturbances are reduced and limited with the protective devices and suitable system design. In order to achieve this aim - proper design of line and protective schemes - it is therefore essential to establish the transient behaviour of the system due to these disturbances. The subject matter of the present work is the investigation of the transient disturbances due to the initiation of fault on ehv AC systems only. The present investigation has been carried out mainly for the purpose of designing and developing a new protective scheme. The phenomenon of fault induced overvoltage has also been investigated briefly, which is useful for the design of line insulation.

The causes of the occurrence of faults on the ehv transmission lines are well-known e.g. insulator breakdown, windblown tree branches, birds etc.

Fault MVA level on these lines is high because of higher transient voltage and low series impedance of the line due to the bundling of conductors. Faults on these systems must be cleared as quickly as possible* in order to prevent disastrous damage to the system due to very high MVA level. The other advantages of fast fault clearance in brief, are as follows:

1. better stability on the system
2. prevention of huge wastage of energy and loss of revenue.
3. prevention of hazards to personnel
4. prevention of escalation of single-line-to-ground fault to double-line-to-ground fault and three-phase faults.

With the advent of very high speed breakers, the need for protecting schemes for detecting the fault and issuing the supply signal for the breakers within the least possible time is very much in demand.

This demand of very fast fault detection - within the least possible time after fault initiation - is not met by the conventional analogue relays or recent protective schemes using digital computers.

The present conventional relays are designed to operate on the basis of the system responses under sustained fault condition with some margin for transient error. Modern static relays operate during the first or second half cycle of supply frequency after the fault initiation.

A particular system has information derived from voltage and current waveforms at the relaying point during the post fault condition to detect a fault condition and initiate appropriate tripping operation. The design and testing of a protective scheme, thus, requires the knowledge of voltage and current signals at the relaying point following the occurrence of any type of fault at a particular location(s). Field

* Envisaged operating time is one cycle (of supply frequency) or less.

tests are not always possible, hence the laboratory generated signals are more frequently used for this purpose.

The generation of realistic test signals is very difficult in the laboratory as it is difficult to simulate the practical polyphase untransposed lines with distributed and frequency dependent parameters. Conventional relays were designed and developed on the basis of test signals from TNA or test models of transmission line represented by one-phase T or Π networks. These system models are found to be suitable for conventional relays with very high operating time and protecting short lines. But these methods of simulating the system are not considered to be suitable for the design and development of superspeed relays protecting long ehv lines:for this purpose-very realistic response from very sophisticated system model are desirable, as the superspeed relays have to perform the assessment within the absolute minimum time and has to derive the current information available at the relaying point. During this period the information is usually very noisy due to high transient content.

Hence for this purpose the recent trend is to use the system response derived from accurate system transient models obtained by programming digital computers. Slemon et al[24] showed using a better system model the errors involved in the traditional relays.

In accurate analysis of transient behaviour, it is thus desirable to study the practical polyphase untransposed line with distributed frequency dependent parameters.

The transient behaviour of these practical lines due to fault initiation has not been studied so far whether for the purpose of developing a new protective scheme or line design.

Most of the recent work for the development of protective schemes using digital computers has been developed on the basis of the system response from very simplified system models. Recent work by Kimbark[26] for the prediction of fault induced overvoltage is based on various simplified assumptions and is applicable for transposed line with frequency invariant parameters.

Fault transient analysis for a wide variety of faults has been carried out by Lewis,[31] but he based his analysis on the simple RL lumped parameter model of the line.

Analysis of practical multiconductor untransposed line for sustained fault condition for common shunt faults at a particular location has been carried out by Wedepohl and others[16] and is well established. The results are very valuable for conventional distance protection schemes protecting long multiconductor lines. They have also pointed out the drawbacks of classical one-phase distributed parameter representation of the line.

In the present work a very general technique for the simulation of the post-fault transient behaviour of the practical multiconductor line has been developed. The method is applicable for both transposed and untransposed line of any configuration, and can take into account the frequency dependence of line parameters. The method is fundamentally based on the application of modal analysis and modified Fourier transform, and the solution is obtained by using digital computer. Fault transient model for such sophisticated transmission line model is not so far available in the literature.

The transmission line parameters suitable for transient studies are described in Chapter 2. The general principle of fault simulation

is described in Chapter 3. The mathematical models for steady state solution are discussed in Chapter 4. The fault transients in single-phase circuit are discussed in Chapter 5. The mathematical fault transient models for practical multiconductor lines are described in Chapter 6 and the digital computer results are presented in Chapter 7 - the system response at the relaying point and the fault induced over-voltages are investigated.

The general conclusions are finally discussed in Chapter 8.

CHAPTER 2

TRANSMISSION LINE PARAMETERS FOR TRANSIENT STUDIES

2.1. Introduction

The parameters of the transmission line are highly frequency dependent and vary widely with frequencies. For the proper simulation of the transient behaviour of the transmission line, the knowledge of these parameters over a wide range of frequencies is essential, in order that the influence of the frequency dependence of the parameters may be taken into account. Hence, in this chapter the parameters of the transmission line are studied.

The basic parameters of a transmission line constitute the series impedance and shunt admittance per unit length of the line. In the case of the multiconductor line these are represented by the series impedance matrix and shunt admittance matrix per unit length of the line. All the other parameters defining a distributed model of the line e.g. surge impedance, surge admittance, propogation constant etc, are derived from these basic parameters and are described in detail in chapter 4.

The basic parameters of the line may be calculated either from the configuration of the line or from the symmetrical component parameters of the line. Both the methods of calculating these parameters of a multiconductor line are briefly described in the following sections.

2.2 Calculation of Basic Parameters from the Configuration of the Conductors

In this method, the physical location of the conductors are defined with respect to a co-ordinate system as shown in Fig. 2.1 and the basic parameters are calculated from the knowledge of the mean heights of the conductors above the ground, the mean spacings between the conductors and other basic data of the line.

Calculation of the basic parameters of the multiconductor line from the physical geometry of its conductors has been described in detail by Galloway et al (2). The equations for the basic parameters developed in this section are mainly based on their

description. The influences of weather conditions, corona loss and the proximity effect on the parameters of the line are neglected in this present analysis.

2.2.1 Calculation of the series impedance matrix

The series impedance matrix Z of a multiconductor line is the sum of the following component matrices:

1. the matrix representing the impedance due to the physical geometry of the conductors.
2. the matrix representing the impedance due to the earth return path.
3. the matrix representing the self-impedance of the conductors.

Thus, the series impedance matrix of a multiconductor line is of the form:

$$Z = R_c + R_e + j(X_g + X_c + X_e) \qquad (2.1)$$

where

$R_c + j X_c$ represents the self impedance of the conductors

$R_e + j X_e$ represents the impedance of the earth-return path

$j X_g$ represents the impedances due to the physical geometry of the conductors.

The impedance matrix Z and each of its component matrices are of the order $3p + q$, where

p = number of circuits

q = number of earth wires

The component matrices are evaluated as follows:

2.2.1.1 Impedance due to physical geometry

The impedance due to the physical geometry of the conductors is of the form

$$j\,X_g = j\,\frac{\omega\mu}{2\pi}\,B \qquad (2.2)$$

where the matrix

B represents the inductances due to the external flux linkages of the conductors and is defined as follows

$$B_{ij} = \log_e \frac{D_{ij}}{d_{ij}} \qquad (2.3)$$

where

D_{ij} = distance between the i^{th} conductor and the image of the j^{th} conductor

d_{ij} = distance between i^{th} conductor and j^{th} conductor for $i \neq j$

= radius of i^{th} conductor (for $i = j$)

If the i^{th} conductor is bundled then the effective radius is used instead of the radius for d_{ij}.

Individual phase conductors of a 400kV line are bundled and each bundle consists of four subconductors at the corners of a square. The effective radius of such a bundle is given by[10]

$$r_e = \sqrt[4]{(\sqrt{2}\ r\ s^3)} \qquad (2.4)$$

2.2.1.2 Impedance of earth-return path

Carson developed equations for the impedance of the earth-return path. Carson's equations have been expressed in suitable computational form by Galloway et al.[2] These modified equations have been used in the present work. Accordingly, the resistance and the reactance components of the impedance of the earth-return path are given by

$$R_e = 2\ P\ \omega\mu/2\pi \tag{2.5}$$

$$X_e = 2\ Q\ \omega\mu/2\pi \tag{2.6}$$

The elements of the matrices P and Q are functions of the elements of the matrices r and θ . The matrices r and θ are defined as follows

$$r_{ij} = \sqrt{\left(\frac{\omega\mu}{\rho_e}\right)\ D_{ij}} \tag{2.7}$$

where

D_{ij} = distance between i^{th} conductor and image of j^{th} conductor

ρ_e = resistivity of earth

μ = permeability

and

θ_{ij} = angle subtended at the i^{th} conductor by the images of i^{th} and j^{th} conductors.

The matrices P and Q are defined in terms of r and θ as follows

For $r_{ij} < 5$

$$P_{ij} = \frac{\pi}{8}(1 - s_4) + \tfrac{1}{2}\log_e\left(\frac{2}{\gamma\,\pi\gamma_{ij}}\right)s_2 + \tfrac{1}{2}\theta_{ij}\,s_2' - \frac{\sigma_1}{\sqrt{2}} + \frac{\sigma_2}{2} + \frac{\sigma_3}{\sqrt{2}} \tag{2.8}$$

$$Q_{ij} = \tfrac{1}{4} + \frac{\log_e\left(\frac{2}{\gamma\,\pi\gamma_{ij}}\right)(1 - s_4)}{2} - \frac{\theta s_4'}{2} + \frac{\sigma_1}{\sqrt{2}} - \frac{\pi s_2}{8} + \frac{\sigma_3}{\sqrt{2}} - \frac{4}{2} \tag{2.9}$$

where $\gamma = 1.7811$ and

s_2, s_2', s_4, s_4', σ_1, σ_2, σ_3, and σ_4 are the infinite series expressed in terms of r_{ij} and θ_{ij}. These series are described in detail in reference 2.

For $r_{ij} > 5$

$$P_{ij} = \frac{\cos\theta_{ij}}{(\sqrt{2})r_{ij}} - \frac{\cos 2\theta_{ij}}{r_{ij}^2} + \frac{\cos 3\theta_{ij}}{(\sqrt{2})r_{ij}^3} + \frac{3\cos 5\theta_{ij}}{\sqrt{2}\,r_{ij}^5} + \cdots\cdots \tag{2.10}$$

$$Q_{ij} = \frac{\cos\theta_{ij}}{(\sqrt{2})\,r_{ij}} - \frac{\cos 3\theta_{ij}}{\sqrt{2}\,r_{ij}^3} + \frac{3\cos 5\theta_{ij}}{\sqrt{2}\,r_{ij}^5} + \cdots\cdots\cdots \tag{2.11}$$

From equations 2.7 to 2.11 it is seen that the matrices P and Q are nonlinear functions of frequency, and hence the impedance due to the earth-return path is highly frequency dependent.

Carson's solution for the impedance of the earth-return path is based on the assumptions that the earth is homogeneous and with constant resistivity, and the permeability and permittivity of the

earth is unity.

Recently a more rigorous and general solution for the impedances of the earth-return path has been developed.[8,9,15] Accordingly, the earth-return path is considered to consist of three layers of differing resistivities, permeabilities and permittivities.

This solution for the impedances of the earth-return path may be interpreted in the study if sufficient information about the different layers of the earth are available, in the absence of such information Carson's equations may be used for design purposes.

2.2.1.3 The self impedance of the conductors

The matrix representing the self impedance of the conductors is a diagonal matrix. The diagonal elements represent the self impedance of the phase conductors and the earth wires. Thus, the self impedance matrix Z_c for a single circuit three-phase line with one earth wire is of the following form

$$[Z_c] = \begin{bmatrix} Z_{cp} & & 0 \\ & Z_{cp} & \\ & & Z_{cp} \\ 0 & & Z_{ce} \end{bmatrix} \qquad (2.12)$$

where

$Z_c = R_c + j X_c$

Z_{cp} = self impedance of the phase conductors

Z_{ce} = self impedance of the earth wire

Usually, the phase conductors of the ehv lines are bundled and the self impedance of the bundled conductors is calculated as follows:

$$Z_{cp} = \frac{\text{self impedance of a sub-conductor of the bundle}}{\text{no. of sub-conductors constituting the bundle}}$$

The conductors used for ehv lines are usually $A_{CS}R$ conductors. The evaluation of the self impedance of such conductors is complicated mainly by the following factors:

1. stranding of the conductors
2. presence of steel core
3. non-uniform current density due to skin effect
4. design features.

The influence of stranding and the steel core are usually insignificant at low frequencies. But at high frequencies both the stranding and the steel core increase the resistance of the $A_{CS}R$ conductors due to the hysteresis loss in the steel core and eddy current losses in both the aluminium and the steel wires.(7)

Skin effect is very prominent at high frequencies. Due to the skin effect the current density is not uniform throughout the overall radius of the conductors. The self impedance of the conductors is very much affected by the non-uniformity of current distribution - the resistance of the conductor increases with the increase of frequency, but its inductance decreases with the increase of frequency and approaches a constant value at very high frequencies.

The self impedance of the $A_{CS}R$ conductors at the power frequency and the frequencies above 2-5 Kc/s (approximately) may be known by the method suggested by Galloway et al.(2) In the intermediate undefined range the self impedance may be evaluated graphically by fitting a curve between the defined values or very approximately analytically.(14) The graphical solution may give better accuracy but may not be com-

putationally very efficient.

In the present work the stranded conductor is substituted by a solid aluminium conductor of the same overall radius, and the self impedance is evaluated on the basis of non-uniform current density due to skin effect. This method is commonly used for design purposes for evaluating the self impedance of $A_{CS}R$ conductors.(7)

The self impedance of a solid conductor with non-uniform current density is defined as follows:(13)

$$Z_c = \frac{\rho \cdot m}{2 \pi r} \left\{ \frac{\text{ber } mr + j \text{ bei } mr}{\text{bei}'mr - j \text{ ber}' mr} \right\} \text{ ohms/meter} \qquad (2.13)$$

where

$$m = \sqrt{\frac{\omega \mu}{\rho}} \qquad (2.14)$$

ρ = resistivity of the conductor in ohms/meter

r = radius of the conductor in meters

$\mu = 4 \times 10^{-7}$ for aluminium conductors

$\omega = 2\pi f$ (where f = frequency in c/s)

The functions ber mr and bei mr are the Bessel functions and ber'mr and bei'mr are respectively the derivatives of these functions with respect to mr. These functions are evaluated for any argument mr by solving their infinite series expansion.

This method is computationally very efficient and the self impedance of the conductor at any frequency may be readily evaluated. However, Kuznetsov(7) pointed out that this method gives somewhat lower value of resistance at high frequencies as the influences of stranding and the steel core are neglected.

According to Kuznetsov's[7] recent investigation better accuracy at any frequency is achieved by direct measurement of the self impedance at that frequency. The measured values of self-impedance over a wide range of frequencies may be stored in the computer and used for theoretical studies. However, for transient studies the self impedance at frequencies other than the measured ones may often be required and their evaluation from the measured data may not be computationally very efficient.

A computationally efficient method for the accurate evaluation of the self impedance at any frequency is desirable, however a very high degree of accuracy in the values of self impedance would be significant for design purposes if all the other data of the line e.g. height, spacings, earth resistivity etc are very accurately known.

2.2.2 Calculation of the shunt admittance matrix

The shunt admittance of the transmission line is mainly due to the mutual capacitances between the conductors and the capacitances between the conductors and earth. The conductances of the air-path surrounding the conductors and the conductances of the insulators supporting the conductors are negligible.

The shunt admittance matrix of a multiconductor line with p circuits and q earth wires is of the order 3p + q and is defined as follows:

$$Y = j\,2\,\pi\,\omega\,\varepsilon\;B^{-1} \qquad (2.15)$$

where B is defined by equation 2.3.

Let $C = B^{-1}$

Then the elements of matrix C define the various capacitances as follows:

$$C_{ij} = -c_{ij} \quad \text{(for } i \neq j\text{)} \tag{2.16}$$

$$C_{ij} = \sum_{j=1}^{n} c_{ij} \quad \text{(for } i=j\text{)} \tag{2.17}$$

where

$n = 3p + q$

c_{ij} = capacitance between conductors i and j for $i \neq j$

c_{ij} = capacitance between conductor i and the earth for $i=j$.

The influence of the earth on the capacitance is very insignificant up to very high frequencies (1Mc/s) and has been considered to be frequency invariant throughout the present work. (3)

2.2.3 Equivalent line and its basic parameters

In the system analysis the actual line is replaced by an equivalent line by eliminating the earth wires. The equivalent line retains the shielding properties of the earth wires and consists of phase circuits only. Thus, the performance of phase conductors, which is of interest, remains unaltered and the system analysis is very much simplified.

The basic Z and Y matrices of the equivalent system may be derived from the corresponding matrices of the actual line by various methods. (11,48) However, in the present work the method suggested by Galloway et al (2) has been used for computational efficiency.

Such equivalent representation is valid only if the earth wires

are at zero potential.

2.3 Calculation of Basic Parameters from the Symmetrical Component Parameters

The equivalent series impedance and shunt admittance matrices of a transposed line may be known from the symmetrical component parameters by symmetrical component transformation of these matrices.

The equivalent Z and Y matrices of three-phase single circuit transposed line are of the following form:

$$Z = \begin{bmatrix} Z_s & Z_m & Z_m \\ Z_m & Z_s & Z_m \\ Z_m & Z_m & Z_s \end{bmatrix} \tag{2.18}$$

$$Y = \begin{bmatrix} Y_s & -Y_m & -Y_m \\ -Y_m & Y_s & -Y_m \\ -Y_m & -Y_m & Y_s \end{bmatrix} \tag{2.19}$$

The elements of these matrices are related to the symmetrical components parameters by the following equations: (11,5)

$$Z_s = \frac{1}{3} \{(r_o + 2r_1) + j\omega(L_o + 2L_1)\} \tag{2.20}$$

$$Z_m = \frac{1}{3} \{(r_o - r_1) + j\omega(L_o - L_1)\} \tag{2.21}$$

$$Y_s = j\,2\,\pi\,\omega\,\varepsilon \times \frac{1}{3}\,(C_o + 2C_1) \tag{2.22}$$

$$Y_m = j\,2\,\pi\,\omega\,\varepsilon \times \frac{1}{3}\,(C_o - C_1) \tag{2.23}$$

The above equations are also sometimes expressed in the following form:

$$Z_s = \frac{1}{3}\left(Z_o + 2Z_1\right) \tag{2.24}$$

$$Z_m = \frac{1}{3}\left(Z_o - Z_1\right) \tag{2.25}$$

$$Y_s = \frac{1}{3}\left(Y_o + 2Y_1\right) \tag{2.26}$$

$$Y_m = \frac{1}{3}\left(Y_1 - Y_o\right) \tag{2.27}$$

where

r_o, L_o, Z_o are the zero sequence resistance, inductance and impedance respectively.

r_1, L_1, Z_1 are the positive-sequence resistance, inductance and impedance respectively.

C_o, Y_o are the zero-sequence capacitance and admittance respectively.

C_1, Y_1 are the positive-sequence capacitance and admittance respectively.

The sequence parameters of a line at power frequency are usually supplied by the manufacturer or may be known by direct measurement on the line.

Z and Y matrices at power frequency may be used for transient studies if the frequency dependence of the parameters is neglected.

If the sequence parameters of a transposed line are measured

over a wide range of frequencies then the frequency dependence of the parameters may be taken into account. Since the measured values are more realistic better accuracy may be achieved from these values. However, this method would be limited to transposed lines only.

2.4 Summary

In this chapter the methods of calculating the basic parameters of a multiconductor line have been described. The series impedance matrix and shunt admittance matrix per unit length are defined as the basic parameters of the line as well as the other important parameters defining a distributed line are known from those parameters.

The basic parameters of both the transposed and untransposed line may be known from the configuration of the line. Symmetrical component parameters are used for calculating the basic parameters of transposed lines only, and may be used for untransposed lines if the asymmetry of the conductors is neglected.

The series impedance matrix is highly frequency dependent due to the skin effect and other losses on the conductors and the frequency dependence of the impedances of the earth return path.

The influences of the earth on the capacitances is very insignificant up to very high frequencies (1Mc/s) and is considered to be frequency invariant in the present work.

For transient studies the values of parameters over a wide and continuous spectrum of frequency is essential in order that the frequency dependence of the parameters may be taken into consideration. Such information about the parameters for both the transposed and untransposed line are readily known from the knowledge of the configuration of the circuit, hence this is very useful for transient

analysis.

However, if the frequency dependence of the parameters is neglected then the parameters at supply frequency evaluated from either methods described in this chapter may be used for transient studies.

The transmission line has been simulated on the basis of these parameters throughout the present work. The importance and usefulness of these parameters is further understood in the subsequent chapters.

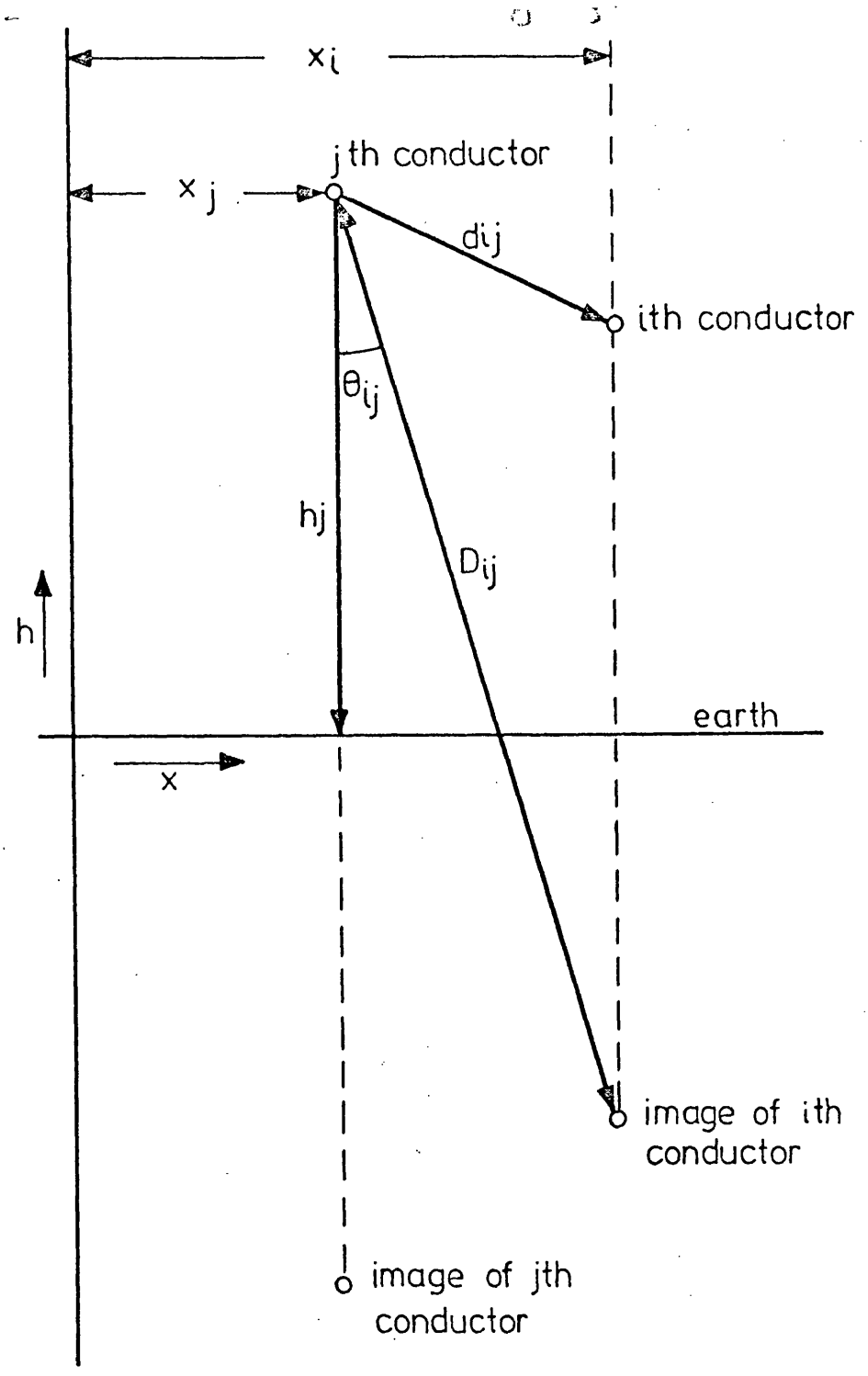

FIG. 2.1 Schematic Diagram of Conductors showing the Physical Location of the Conductors and their Images with Respect to the Co-ordinate System Defined by the Vertical and Horizontal Axes of Reference. The Earth Plane and the Axis of Symmetry of the Tower define respectively the Horizontal and the Vertical Axes of Reference

CHAPTER 3

FAULT SIMULATION

3.1 Introduction

Faults on transmission circuits of a power system are broadly classified into two types, e.g. shunt faults and series faults.

A shunt fault[48] is an unbalance between phases or between phase and neutral. Shunt faults consist of single line-to-ground, line to line, double line to ground, and three-phase faults with or without connection to the ground. These faults may occur either through impedances or direct short circuits.

A series fault[48] is an unbalance in the line impedances and does not involve the neutral or ground nor does it involve any interconnection between phases. One or two open conductors results in this type of fault and occurs either due to the breaking of the conductors or through the action of the circuit breakers and other devices which may not open all the three phases simultaneously.

The majority of faults on power systems are the shunt faults and the typical frequency of occurrence[48] of 3ϕ, 2LG, LL, SLG faults are 5%, 10%, 15% and 70% respectively. The single line-to-ground faults are the most important and common type of fault. There are various other types of fault but the frequency of their occurrence is extremely low.

The faults on power system transmission circuits may produce balanced or unbalanced currents, and accordingly are defined as symmetrical and unsymmetrical faults.

The unsymmetrical faults, e.g. series, SLG, LL, 2LG etc., produce unbalanced current in the circuit. The method of symmetrical components has been widely used for the steady state solution of unsymmetrical faults and also for the transient solution by some authors.[31]

The practical use of this method has, however, been limited to the balanced circuits with lumped parameters. Although this method is theoretically applicable for distributed parameters balanced or unbalanced circuit, the solution in such cases may be extremely complex.

Symmetrical three phase faults on three phase circuits are often solved classically assuming a single phase model of this circuit. However, this method of solution may not be acceptable if the circuit is untransposed and a very high degree of accuracy is desired.

In this chapter, therefore, a very simple and general technique for simulating the ~~series and~~ shunt fault is described. The technique uses phase co-ordinates and is readily applicable for both transient and steady state sustained fault conditions.

3.2 Simulation of Shunt Fault on Single-Phase Circuit

When a fault occurs on a single phase transmission circuit, voltage at the fault point is reduced and the current flows into the fault from the circuit.

The potential difference across the fault is equal to the drop in the fault impedance, and, if the fault impedance is zero, then the voltage is reduced to zero at the location of the fault.

This property of a faulted circuit is simulated by suddenly applying at the point of fault a hypothetical emf source with a series impedance at the instant of fault inception. The emf of the hypothetical source, at every instant of time is equal and opposite to the prefault voltage at the location of fault, and the series impedance of the hypothetical source is equal to the fault impedance. The simulation of the faulted circuit is clearly explained in Figs. 3.1 to 3.6.

Figs. 3.1 and 3.2 show the prefault circuit, which is to be

eventually faulted with the fault impedance Z_f. Let the circuit be under steady state condition before the occurrence of the fault. The current flowing into the fault (Z_f) from the circuit is zero as there is an open circuit at the location of fault.

Let the prefault voltage at the fault point be V_f as shown in Fig. 3.1. The unfaulted circuits of Figs. 3.1 and 3.2 can be simulated as shown in Fig. 3.3. In Fig. 3.3 a hypothetical source (V_f) with a series impedance Z_f is connected at the location of fault. The emf of the hypothetical source is equal to V_f at every instant of time. The connection of this source does not alter the existing circuit condition as no current flows into or out of this hypothetical branch, because the voltages are balanced across it at every instant of time. Fig. 3.4 shows the modified simulation of the prefault circuits of Figs. 3.1, 3.2 and 3.3.

Fig. 3.5 shows the faulted circuit. The fault is applied by switching on Z_f. Then the voltage at the fault point is reduced depending on the value of the fault impedance, and causes the fault current I_f to flow into the fault.

The application of a fault is simulated as shown in Fig. 3.6. In Fig. 3.6 another hypothetical source is switched on, in series with previous ones already connected in the hypothetical branch of Fig. 3.6. The emf of this second source is equal to $-V_f$, i.e. equal and opposite to the voltage existing across the fault impedance in the prefault circuit. The connection of the second source accounts for the voltage reduction at the fault location. The second source balances the voltage of the first at every instant, and the voltage across the fault is equal to the voltage drop in the fault impedance due to the fault current.

Thus the faulted circuit is finally simulated by connecting two more hypothetical emf sources $-(+V_f)$ and $(-V_f)$ at the location of fault - to the prefault circuit. Hence the current or voltage at any point in the faulted circuit is the resultant effect of all the emf sources in the circuit.

The circuit is then solved by the principle of superposition theorem. Accordingly, first shorting out $-V_f$, the current component due to all the emf sources present in the unfaulted circuit and V_f is determined. This current is equal to the prefault steady state current flowing in the circuit as the connection $(+V_f)$ does not alter the prefault steady state condition.

Then the component of current due to $-V_f$ alone is evaluated by shorting out all the emf sources in the prefault circuit and V_f but leaving their respective source impedances in the circuit.

The current at any point in the faulted circuit is defined by the superposition of the two component currents evaluated at that point as described above. The current in the fault is the current due to the switching of $(-V_f)$ alone as the prefault current flowing into the fault is zero. Hence the transient current in the faulted circuit is the sum of the switching transient current due to the hypothetical source $(-V_f)$ alone, when all other emf sources are shorted out, leaving their respective source impedances in the circuit and the prefault steady state current due to all the emf sources present in the prefault circuit. The transient current is measured from the instant of fault inception.

The steady state current in the faulted circuit is the sum of the prefault steady state current and the steady state current due to the switching of $(-V_f)$ alone when all the soures in the prefault circuit

are shorted out leaving their series impedances in the circuit.

Similarly the transient and the steady state voltages at any point in the faulted circuit may be determined by the principle of superposition.

3.3 Simulation of Shunt Faults on a Three-Phase Multiconductor Line

The technique for simulating the shunt faults on a three-phase circuit is based on the principle of superposition and is the extension of the basic idea which is used for the simulation of shunt faults on a single phase circuit.

In a three-phase, n-line circuit every fault impedance constituting the shunt fault is replaced by switching on a hypothetical emf source with a series impedance.

The emf of the hypothetical source at every instant of time is equal and opposite to the prefault potential difference appearing across the particular fault impedance, the source replaces and the series impedance of the source being equal to this fault impedance.

In the case of three-phase to earth faults, there exists a finite fault impedance between each pair of lines, and between each line to earth. For simulating this fault, a hypothetical generator is switched on between each line to line, and each line to earth replacing every line to line, and line to earth fault impedance respectively at the location of the fault.

The emf of a source between a pair of lines is equal and opposite to the line to line voltage between the corresponding lines in the prefault circuit at the location of fault, and its series impedance is equal to the particular fault impedance which appears between these two lines in the faulted circuit.

The emf of the source between a line and the earth is equal and opposite to the voltage of the particular line with respect to earth at the location of fault in the prefault circuit, and its series impedance is equal to the fault impedance connected between this line and the earth.

Thus for three-phase to earth fault all the hypothetical generators between line to line, and line to earth are switched on to the circuit. In the case of balanced three-phase to earth fault in a transposed circuit the lines are symmetrically fed by these generators. For unbalanced faults such as single-line-to-ground, line to line, and double line to earth faults, there is an infinite impedance between each line to line, and between every line to earth in the absence of any similar connection by a finite impedance - the finite fault impedance appearing across the faulted parts only.

Any unbalanced fault, then, may also be simulated by replacing every fault impedance whether finite or infinite by a hypothetical source. The emf and the series impedance of each source is determined as before, accordingly the series source impedance is infinite if the source replaces an infinite impedance, or in other words, the generator representing the infinite fault impedance remains open-circuited, whilst those replacing the finite fault impedance are switched on to the circuit.

In the case of unbalanced faults only, the affected lines are fed by the hypothetical generators, and there is thus unbalanced energisation of the system by these generators at the location of fault.

The current or voltage in a faulted three-phase circuit is then the resultant effect of all the emf sources present in the simulated circuit, i.e. the emf sources present in the unfaulted circuit and the hypothetical sources representing the fault.

As described in the case of the single phase circuit the current or voltage in a faulted three-phase circuit may be obtained by the principle of superposition, and it can similarly be proved, assuming the system to be under steady state condition before the occurrence of the fault that,

The transient current in the faulted circuit

= Prefault steady state current + the switching transient current due to the hypothetical source(s) alone when all the other emf sources are shorted, leaving their respective source impedances in the circuit.

and that,

The steady state current in the faulted circuit

= Prefault steady state current + the steady state current due to the switching of the hypothetical source(s) alone when all the other emf sources are shorted out, leaving their respective source impedances in the circuit.

Similarly, the voltages in the faulted circuit may be evaluated by the principle of superposition both under the steady state and the transient conditions.

The voltage or current at any point in the faulted circuit is determined by the summation of the prefault component and the switching component, each evaluated at the desired point as mentioned above.

The steady state solution of the multiconductor, three-phase circuit is well-defined [1], and is obtained as described in Chapter 4.

Hence the remaining problem in the solution of the faulted three-phase circuit is the solution of the modified circuit (when all the emf sources are shorted out, leaving their respective source impedances in the circuit) due to the switching of the hypothetical sources alone

at the location of the fault. According to the discussion above, the energisation due to the switching of the hypothetical generators may be balanced or unbalanced depending upon the type of fault.

A general solution of the modified circuit for unbalanced or balanced energisation at the location of fault may be achieved by replacing each emf source and its series impedance by an equivalent current generator with a shunt admittance according to Thevenin-Norton's theorem. The source current of the current generator replacing an emf source with infinite series impedance is zero, and the total injected current to a line at the location of fault is the sum of all the individual current generators connected to it. With the knowledge of the injected current to each line, the circuit may easily be solved.

Any type of shunt fault - balanced or unbalanced - on a three-phase, n-line circuit is thus finally simulated by a set of hypothetical current generators and their corresponding shunt admittances, connected between each pair of lines, and between each line to earth. Therefore,

The transient current in the faulted three-phase, multiconductor circuit

= Prefault steady state current + the switching transient current due to the hypothetical current generators alone when all the other emf sources are shorted, leaving their respective source impedances in the circuit.

and the steady state current in the faulted three-phase multiconductor circuit

= Prefault steady state current + the steady state current due to the switching of the hypothetical current generators alone when

all the other emf sources are shorted, leaving their respective source impedances in the circuit.

On the basis of the above principle the simulation of some of the typical faults is illustrated in the following section.

3.4 Simulation of SLG Fault

In the case of SLG fault, the fault impedance between each unfaulted line and the earth, and the line-to-line fault impedance is infinite. Consider a three-phase, three-line circuit, one line of the circuit being connected to earth by the impedance $Z_{f_{10}}$. The simulation of this fault is shown in Fig. 3.7b.

The dummy source is switched on to the faulted line only in place of line to earth fault impedance and all the other dummy emf sources are open-circuited. Finally, Fig.3.7c shows the simulated circuit with the equivalent current generators. The source current of all the generators except the one replacing the fault is zero. However the total injected current to lines at the location of fault is given by

$$I_{S_1} = Y_{10} E_{f_1} \qquad 3.1$$

$$I_{S_2} = 0 \times E_{f_2} \qquad 3.2$$

$$I_{S_3} = 0 \times E_{f_3} \qquad 3.3$$

Expressing the above results in matrix form we obtain

$$\begin{bmatrix} I_{s_1} \\ I_{s_2} \\ I_{s_3} \end{bmatrix} = \begin{bmatrix} Y_{10} & 0 & 0 \\ 0 & 0 & 0 \\ 0 & 0 & 0 \end{bmatrix} \begin{bmatrix} E_{f_1} \\ E_{f_2} \\ E_{f_3} \end{bmatrix} \qquad 3.4$$

where I_{s_1}, I_{s_2}, I_{s_3} are the total injected current due to the dummy generators to the lines 1, 2 and 3 respectively

E_{f_1}, E_{f_2}, E_{f_3} are the emf's of the dummy sources connected between the earth and the lines 1, 2 and 3 respectively.

$Y_{10} = \frac{1}{Z_{f_{10}}}$ where $Z_{f_{10}}$ is the series impedance of the dummy source E_{f_1}.

and

$$E_{f_1} = - V_{f_1}$$

where V_{f_1} is the prefault voltage with respect to the earth on the conductor

3.5 Simulation of Line to Line fault

In the case of line to line fault, the fault impedance between each line to earth and line to line impedance between the lines except the faulted ones is infinite.

The simulation of the line to line fault is shown in Fig. 3.8 for a three-phase, three-line circuit. A dummy emf source is switched on between the lines in place of the line to line fault impedance $Z_{f_{12}}$.

Fig.3.8c shows the simulated circuit with equivalent current generators. Let V_{f_1}, V_{f_2}, V_{f_3} be the prefault voltage with respect to the earth on the lines 1, 2 and 3 and E_{f_1}, E_{f_2}, E_{f_3} be the emf's of the generator connected between the lines 1, 2 and 3 and the

earth respectively. Then, the emf of the dummy source $E_{f_{12}}$ is given by

$$E_{f_{12}} = (E_{f_1} - E_{f_2}) = -(V_{f_1} - V_{f_2}) \qquad 3.5$$

and the source current of the equivalent current generator is given by

$$I_{12} = Y_{12} \times (E_{f_1} - E_{f_2}) \qquad 3.6$$

Hence the total injected current to the lines at the location of the fault is given by

$$\begin{aligned} I_{s_1} &= Y_{12}(E_{f_1} - E_{f_2}) \\ I_{s_2} &= -Y_{12}(E_{f_1} - E_{f_2}) \\ I_{s_3} &= 0 \end{aligned} \qquad 3.7$$

Again, expressing these results in the matrix form, we obtain

$$\begin{bmatrix} I_{s_1} \\ I_{s_2} \\ I_{s_3} \end{bmatrix} = \begin{bmatrix} Y_{12} & -Y_{12} & 0 \\ -Y_{12} & Y_{12} & 0 \\ 0 & 0 & 0 \end{bmatrix} \begin{bmatrix} E_{f_1} \\ E_{f_2} \\ E_{f_3} \end{bmatrix} \qquad 3.8$$

3.6 Three-Phase to Earth Fault

In this case the fault impedance between each line and the earth and that between the line to line is finite. The simulation of three L to earth fault for a three-phase three-line circuit is shown in Fig. 3.10.

Let V_{f_1}, V_{f_2}, V_{f_3} be the prefault line to earth voltage at the location of the fault. Then the emf's of the various dummy sources are as follows:

$$\begin{aligned} &\text{Line 1 to earth} && E_{f_1} = -V_{f_1} \\ &\text{Line 2 to earth} && E_{f_2} = -V_{f_2} \\ &\text{Line 3 to earth} && E_{f_3} = -V_{f_3} \end{aligned} \qquad 3.9$$

The emf of the source connected between line 1 and 2

$$\begin{aligned} &= -(V_{f_1} - V_{f_2}) \\ &= E_{f_1} - E_{f_2} \end{aligned} \qquad 3.10$$

The emf of the source connected between lines 1 and 3

$$\begin{aligned} &= -(V_{f_1} - V_{f_3}) \\ &= E_{f_1} - E_{f_3} \end{aligned} \qquad 3.11$$

The emf of the source connected between lines 2 and 3

$$\begin{aligned} &= -(V_{f_2} - V_{f_3}) \\ &= E_{f_2} - E_{f_3} \end{aligned} \qquad 3.12$$

The total injected current to the line 1 is given by

$$\begin{aligned} I_{s_1} &= Y_{10}E_{f_1} + Y_{12}E_{f_{12}} + Y_{13}E_{f_{13}} \\ &= (Y_{10} + Y_{12} + Y_{13})E_{f_1} - Y_{12}E_{f_{12}} - Y_{13}E_{f_{13}} \end{aligned} \qquad 3.13$$

Similarly, the total injected current to the line 2 is given by

$$I_{s_2} = -Y_{21}E_{f_1} + (Y_{20} + Y_{21} + Y_{23})E_{f_2} - Y_{23}E_{f_3} \qquad 3.14$$

and the total injected current to the line 3 is given by

$$I_{s_3} = -Y_{31}E_{f_1} - Y_{32}E_{f_2} + (Y_{30} + Y_{32} + Y_{33})E_{f_3} \qquad 3.15$$

Expressing the above results in matrix form, we obtain:

$$\begin{bmatrix} I_{s_1} \\ I_{s_2} \\ I_{s_3} \end{bmatrix} = \begin{bmatrix} Y_{10}+Y_{12}+Y_{13} & -Y_{12} & -Y_{13} \\ -Y_{21} & Y_{21}+Y_{20}+Y_{23} & -Y_{23} \\ -Y_{31} & -Y_{32} & Y_{31}+Y_{32}+Y_{30} \end{bmatrix} \begin{bmatrix} E_{f_1} \\ E_{f_2} \\ E_{f_3} \end{bmatrix} \qquad 3.16$$

It is seen from the above results that the emfs of the dummy sources connected between the lines and line to earth are expressed in terms of the prefault line to earth voltage at the location of the fault.

The injected current on each line for any type of shunt fault is given by

$$[I_s] = [Y_f]\,[E_f]$$

I_s represents the injected current to the lines

Y_f represents the fault-admittance matrix

E_f represents the emf's of the generators connected between the lines and earth.

Hence for the evaluation of the injection current matrix for any

type of shunt fault it suffices to evaluate the prefault voltage at the location of the fault and define the Y_f matrix. Y_f matrix depends on the type of fault. For solid faults a suitable numerical value of Y of the order of 10^6 gives correct result.

3.7 Summary and Conclusions

In this chapter a general technique for simulating shunt fault has been developed. The method uses phase co-ordinates and is based on the principle of superposition.

In this approach the shunt fault is simulated by connecting an equivalent injection current matrix and an admittance matrix at the location of fault.

The technique may be extended to simulate also the various types of simultaneous fault occurring at the same instant of time at the same location or different locations.

Once the injection current matrix is evaluated the steady state and the transient solutions of the faulted circuits present no problem.

Using the injection current matrix and the principle of superposition it has been shown in the appendix that the steady state solution of a faulted three phase circuit is the same as that obtained by Wedepohl.[16]

The transient solution of the faulted circuit is evaluated (by the method of Fourier transform) by solving the circuit first in the frequency domain and then the solution in the time domain is obtained by using the inverse Fourier transform. The method of Fourier transform is adopted to take the frequency dependence of the parameters into account.

The Fourier transform of the elements of the injection current matrix

is defined by

$$\left[\bar{I}_s\right] = \left[Y_f\right]\left[\bar{E}_f\right] = \left[Y_f\right]\left[-\bar{V}_f\right]$$

where V_f is the Fourier transform of the sine waves of the prefault line to earth voltages at the location of fault. The waveforms of the prefault line to earth voltages at the location of fault are determined by the sources feeding the system - for sinusoidal sources feeding the system these are sinusoidal, and hence their Fourier transforms are well defined.

The detailed transient solutions for the different types of faulted circuits are described in the next four chapters.

In the case of balanced shunt faults on transposed circuits the simulation technique for the one-phase model is very useful and gives a faster solution. The hypothetical emf source in the solution of one-phase circuit may also be represented by an equivalent current generator. This representation may be of advantage and give a simpler solution when the fault occurs with a fault impedance. But for solid faults each fault impedance constituting the fault may have different values as pointed out earlier and the circuit solution is much easier when the emf sources are replaced by the equivalent current generators and the shunt admittances.

The technique of simulating faults described above are very general and are readily applicable for faulted polyphase circuits with any number of lines, whether they are transposed or untransposed.

Other advantages of this technique are that it can take care of any model of source and transducer provided they can be represented in suitable

linear form in phase co-ordinates.

In short this method is suitable for any complex power system network for any type of fault, as the problem of fault simulation is basically reduced to that of switching.

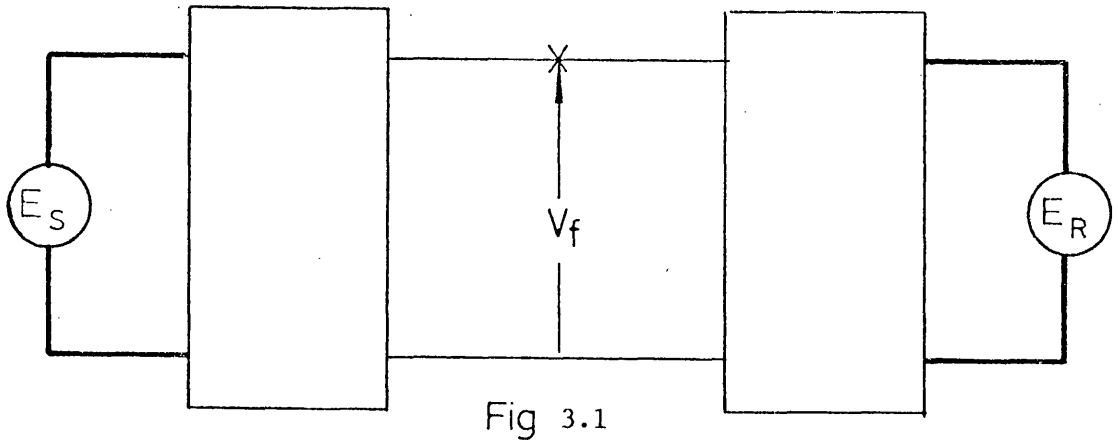

Fig 3.1

Unfaulted Circuit (prefault voltage at the location of fault = V_f)

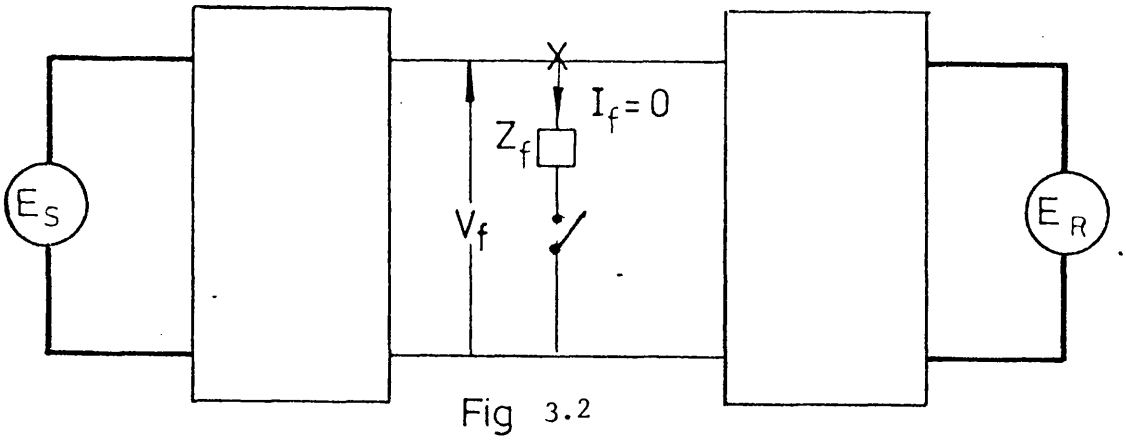

Fig 3.2

Simulation of prefault circuit. The fault impedance Z_f is open-circuited. The current flowing into Z_f = I_f = 0

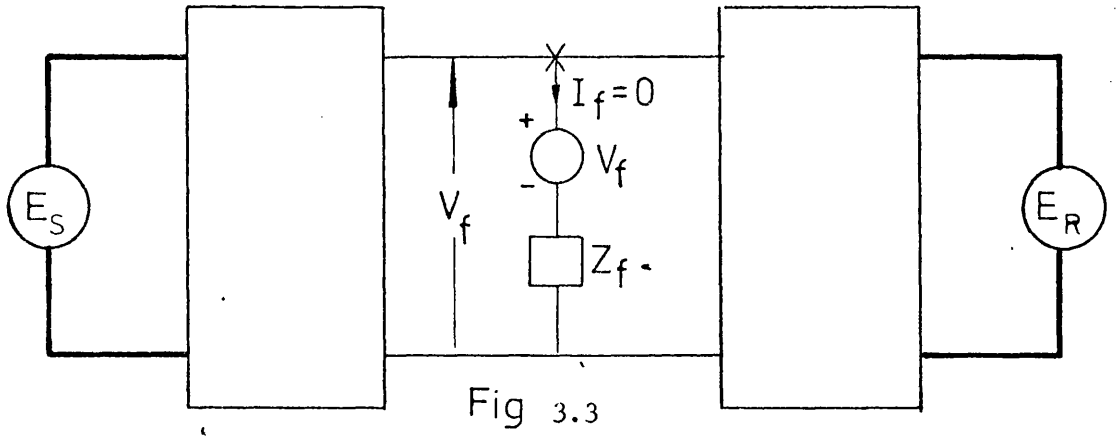

Fig 3.3

Simulation of prefault circuit of Fig. 3.2. Fault impedance of Z_f is replaced by a hypothetical generator with a series impedance. EMF of the generator is equal to the prefault voltage V_f and the series impedance is equal to the fault impedance Z_f. Current flowing into the fault impedance = $I_f = 0$

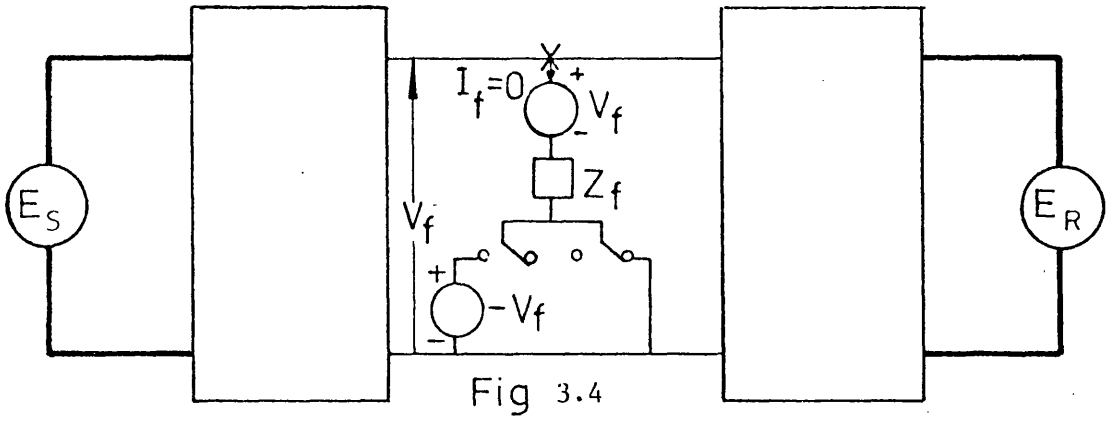

Fig 3.4

Modified simulation of the prefault circuit of Fig.3.3. with another open-circuited hypothetical generator. The emf of this generator is equal and opposite to the prefault voltage i.e. equal to $-V_f$

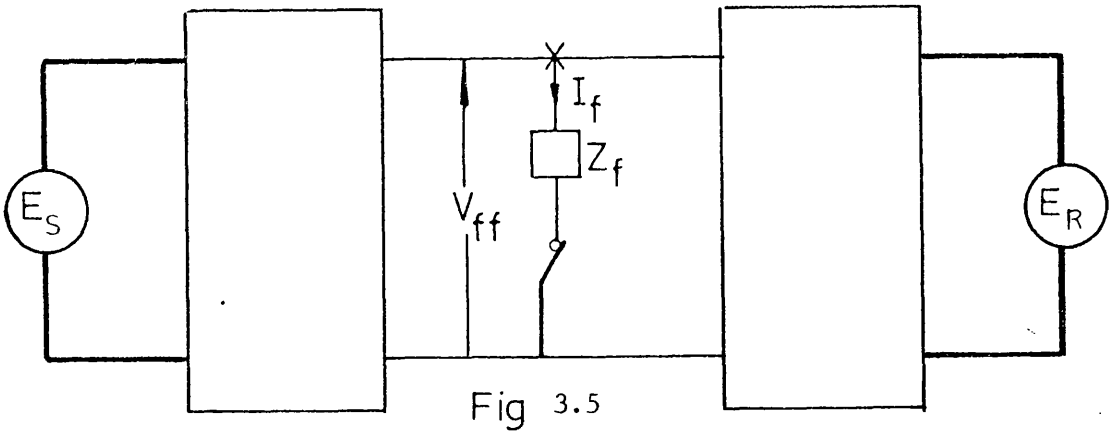

Fig 3.5

Prefault circuit - occurrence of fault is simulated by switching on the fault impedance Z_f. Voltage across the fault is V_{ff} and is equal to the voltage drop in the fault impedance Z_f due to the flow of fault current I_f through it.

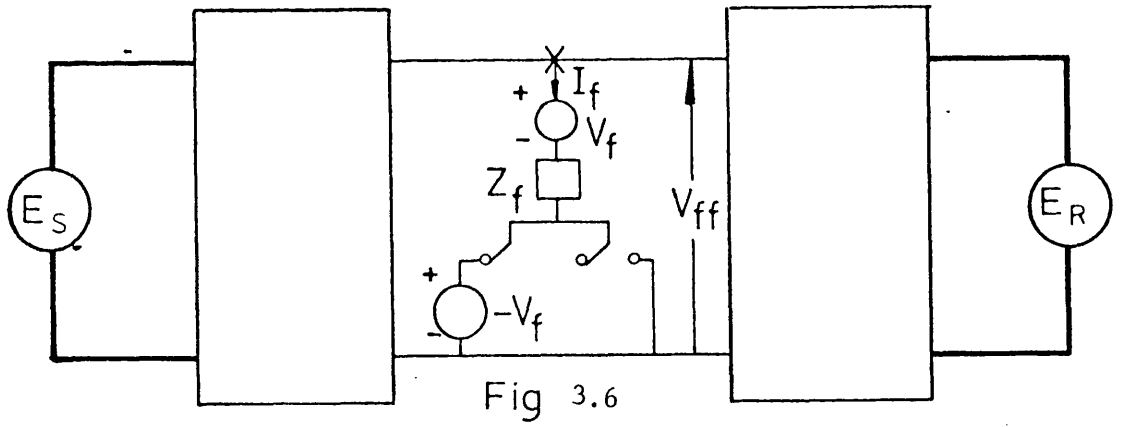

Fig 3.6

Simulation of prefault circuit of Fig. 3.5. Application of fault is simulated by switching the hypothetical generator $-V_f$ in series with the fault impedance Z_f.
Fault current I_f flows through Z_f. The voltage drop across the fault is equal to V_{ff} and is due to the flow of I_f through Z_f as the emf sources $+V_f$ and $-V_f$ balances each other.

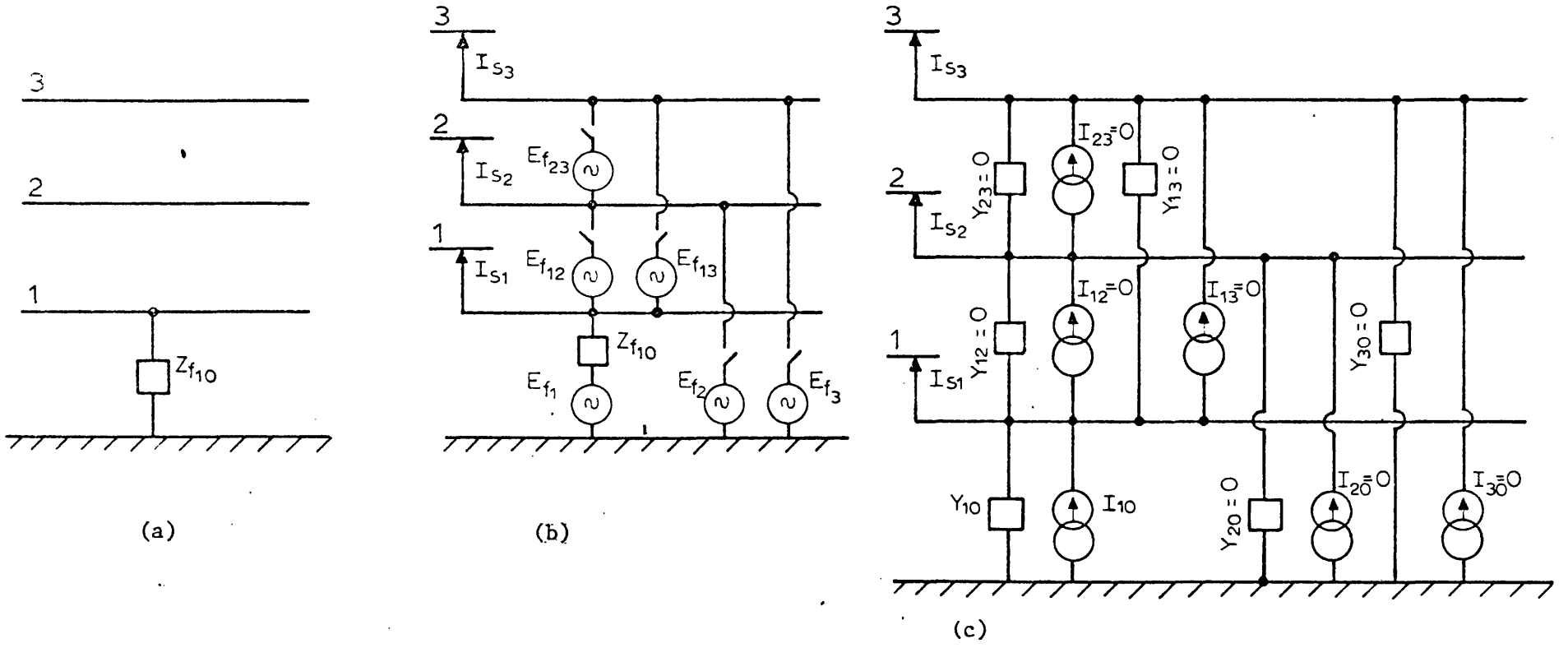

Fig. 3.7 Simulation of Single-Line to Ground Fault

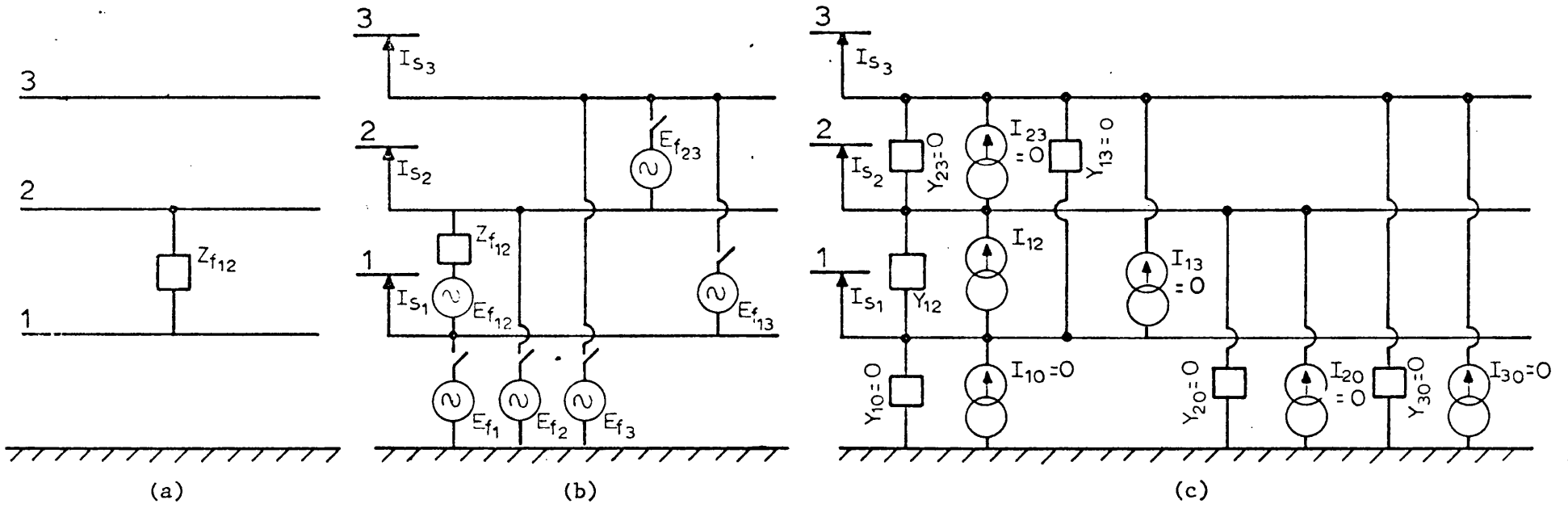

Fig. 3.8 Simulation of Line-to-Line Fault

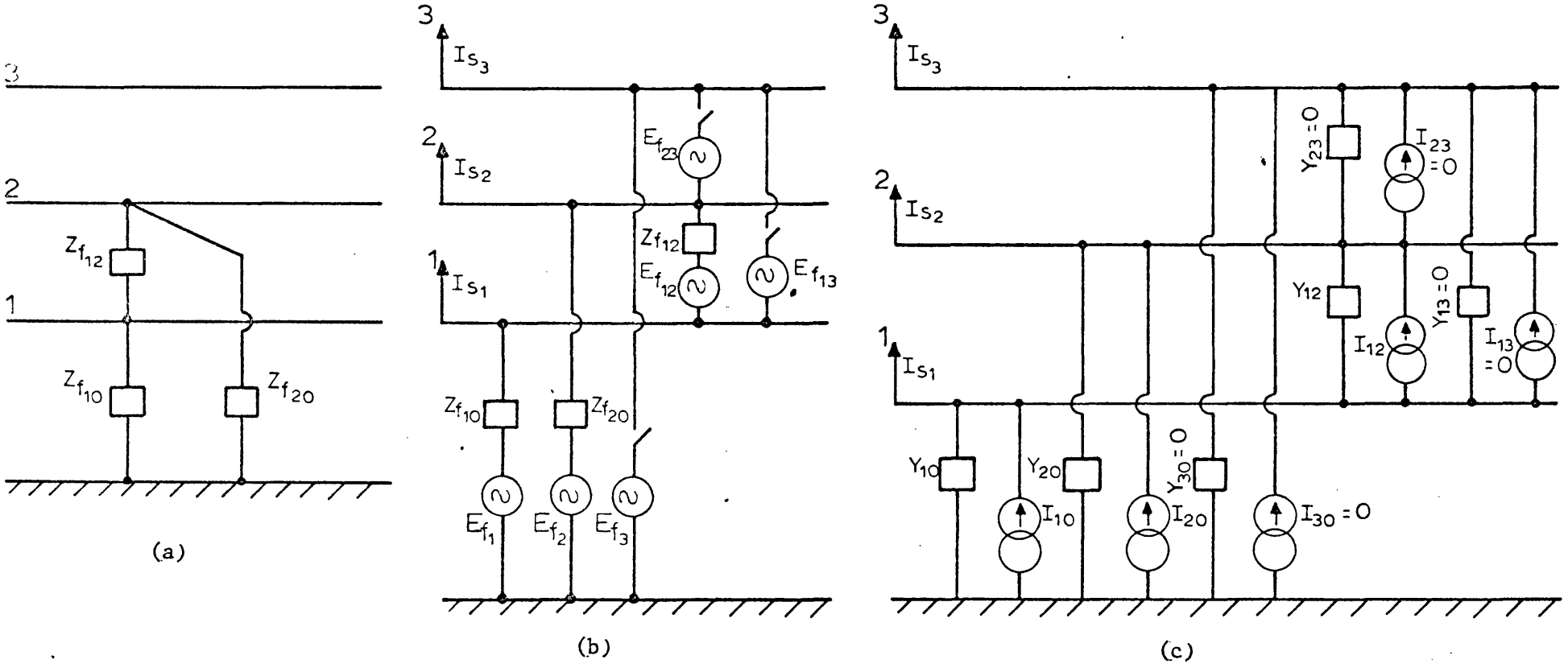

Fig. 3.9 Simulation of Double Line-to-Ground Fault

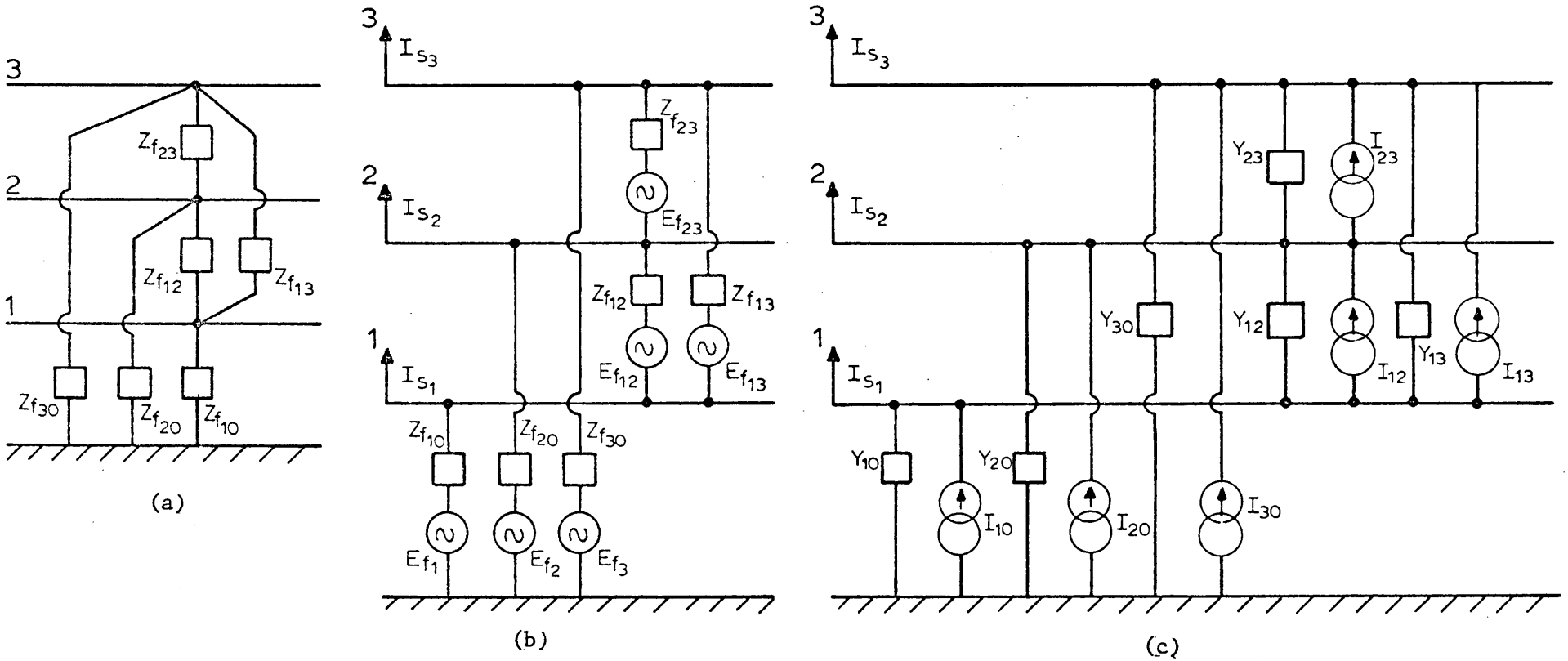

Fig. 3.10 Simulation of Three-Phase to Earth Fault

C H A P T E R 4

MATHEMATICAL ANALYSIS OF TRANSMISSION LINE UNDER STEADY - STATE CONDITION

Introduction

In the previous chapters it was seen that the fault transients depend on the prefault voltage at the location of fault. Usually, the power systems are under steady state condition before the occurrence of the fault. Hence the knowledge of the prefault steady state voltage at the location of fault is essential in order to predict the transients due to faults.

If there is no prefault power transfer in a very short line, then the prefault voltage at the location of fault is usually assumed to be equal to the terminal voltage and an approximate solution of the fault transients may be evaluated. However, if this line is long and there is prefault power transfer then the prefault voltage at the location of fault is not equal to the terminal voltage and needs to be evaluated accurately for the correct evaluation of the fault transients. Hence, in this chapter, the evaluation of the steady state solution of transmission line is described.

The steady state solutions for the multi-conductor polyphase system and its simplified single phase model are presented. The simplified model is sometimes useful for balanced faults, however, it does not show the influences of the multi-velocity propagation on the transmission line, hence both the simplified and general polyphase model are studied.

In this chapter, the distributed model of the transmission line is considered. The solution for the polyphase case is based on Wedepohl's[1] theory of natural modes. This method is very general and takes into account the multivelocity propagation on the transmission line, and the formulations are readily programmable.

4.2 Steady State Solution of the Simplified Model of the Polyphase Line

Classically a polyphase line is often represented on a per phase basis assuming the polyphase line to be ideally balanced. Fig. 4.1 shows a single phase model consisting of one phase and neutral of a three phase uniformly distributed line.

Let the series impedance and shunt admittance per unit length per phase be Z and Y respectively. Consider a very small element in the line, then the difference in voltage between the ends of the elements is given by

$$dV = -I\,Z\,dx$$ where $Z\,dx$ = series impedance of the elemental length of the line.

or,

$$\frac{dV}{dx} = -I\,Z \tag{4.1}$$

Now differentiating equation 4.1 with respect to x and replacing $\frac{dI}{dx}$ with equation 4.2 gives

$$\frac{d^2V}{dx^2} = Z\,Y\,V \tag{4.3}$$

Similarly, from equations 4.2 and 4.1

$$\frac{d^2I}{dx^2} = Z\,Y\,I \tag{4.4}$$

The solution of the differential equations 4.3 and 4.4 is given by[13]

$$V = \frac{V_R + I_R Z_o}{2} e^{\gamma x} + \frac{V_R - I_R Z_o}{2} e^{-\gamma x} \tag{4.5}$$

$$I = \frac{\frac{V_R}{Z_o} + I_R}{2} e^{\gamma x} - \frac{\frac{V_R}{Z_o} - I_R Z_o}{2} e^{-\gamma x} \tag{4.6}$$

where $Z_o = \sqrt{\frac{Z}{Y}}$ and is called the characteristic impedance of the line.

$\gamma = \sqrt{ZY}$ and is called the propagation constant of the line.

Z_o tends to be real with the increase of frequency for a typical line. The real part of γ is called the attenuation constant and the quadrature part is called the phase constant. Thus Z_o and γ define the uniformly distributed line.

V_R and I_R are the rms values of the phase voltage and current respectively at the receiving end of the line.

By re-arranging equations 4.5 and 4.6 and substituting hyperbolic functions for exponential terms, the voltage and current at a distance x from the receiving end is given by

$$V_x = V_R \cosh \gamma x + I_R Z_o \sinh \gamma x \tag{4.7}$$

$$I_x = I_R \cosh \gamma x + \frac{V_R}{Z_o} \sinh \gamma x \tag{4.8}$$

Equations 4.7 and 4.8 give the rms values of voltage and current and their phase angle at any distance x along the line measured from the receiving end.

At the sending end, $x = \ell$ and the voltage and current are given by

$$V_s = V_R \cosh \gamma\ell + I_R Z_o \sinh \gamma\ell \tag{4.9}$$

$$I_s = I_R \cosh \gamma\ell + \frac{V_R}{Z_o} \sinh \gamma\ell \tag{4.10}$$

Equations 4.9 and 4.10 may be solved for I_s and I_R in terms of V_s and V_R to give

$$I_s = \frac{V_s}{Z_o} \coth \gamma\ell - \frac{V_R}{Z_o} \operatorname{cosech} \gamma\ell$$

$$= Y_o \coth \gamma\ell \; V_s - Y_o \operatorname{cosech}\gamma\ell \; V_R \tag{4.11}$$

where $Y_o = \frac{1}{Z_o}$ and is called the surge admittance.

$$I_R = \frac{V_s}{Z_o} \operatorname{cosech} \gamma\ell - \frac{V_R}{Z_o} \coth \gamma\ell$$

$$= Y_o \operatorname{cosech} \gamma\ell \; V_s - Y_o \coth \gamma\ell \; V_R \tag{4.12}$$

or,

$$-I_R = -Y_o \operatorname{cosech} \gamma\ell \; V_s + Y_o \coth \gamma\ell \; V_R \tag{4.13}$$

where $(-I_R)$ defines the current flowing into the receiving end.

The equations 4.11 and 4.13 are sometimes usefully represented in the matrix form as follows

$$\begin{bmatrix} I_s \\ I_R \end{bmatrix} = \begin{bmatrix} Y_o \coth \gamma\ell & -Y_o \operatorname{cosech} \gamma\ell \\ -Y_o \operatorname{cosech} \gamma\ell & Y_o \coth \gamma\ell \end{bmatrix} \begin{bmatrix} V_s \\ V_R \end{bmatrix} \tag{4.14}$$

4.3 Steady State Solution of a Multiconductor Polyphase Line

4.3.1 Basic equations

Fig. 4.2 shows a system of n-phase transmission line conductors parallel to each other and to the ground plane. Let the conductors be uniformly distributed and mutually coupled electromagnetically and electrostatically.

Consider a very small element Δx on each of the conductors as shown in Fig. 4.2.

The difference in voltage ΔV_1 across the element in conductor 1 at a discrete frequency is given by

$$\Delta V_1 = -(Z_{11}.\Delta x.I_1 + Z_{12}.\Delta x.I_2 + \ldots\ldots + Z_{1n}.\Delta x.I_n)$$

or,

$$\frac{\Delta V_1}{\Delta x} = -(Z_{11}.I_1 + Z_{12}.I_2 + \ldots\ldots\ldots + Z_{1n}.I_n)$$

or,

$$\frac{dv_1}{dx} = -(Z_{11}.I_1 + Z_{12}.I_2 + \ldots\ldots\ldots + Z_{1n}.I_n)$$

Similarly, for other conductors

$$\frac{dV_2}{dx} = -(Z_{21}.I_1 + Z_{22}.I_2 + \ldots\ldots\ldots + Z_{2n}.I_n)$$

$$\vdots$$

$$\frac{dV_n}{dx} = -(Z_{n1}.I_1 + Z_{n2}I_2 + \ldots\ldots\ldots + Z_{nn}I_n)$$

The above equations can be represented in general as follows

$$\left[\frac{dV}{dx}\right] = -\left[Z\right]\left[I\right] \qquad (4.15)$$

where $[Z]$ = series impedance matrix for unit length and is of the order nxn

$[I]$ = column vector of current phasors I_1, I_2,..... I_n and is of the order nxl

and I_1, I_2,.....I_n represent the rms value of the current in phase 1, 2, ...n respectively.

The difference in the current between the ends of the element in conductor 1 is given by

$$\Delta I_1 = \Delta I_{11} + \Delta I_{12} + \ldots\ldots\ldots + \Delta I_{1n}$$

where

$$\Delta I_{11} = -Y_{11}.\Delta x.V_1$$

$$\Delta I_{12} = -Y_{12}.\Delta x.(V_1 - V_2)$$

$$\vdots$$

$$\Delta I_{1n} = -Y_{1n}.\Delta x.(V_1 - V_n)$$

or,

$$\Delta I_1 = -(Y_{11}.\Delta x + Y_{12}.\Delta x + \ldots\ldots\ldots + Y_{1n}.\Delta x)\, V_1 + Y_{12}.\Delta x.V_2 + \ldots\ldots\ldots\ldots + Y_{1n}.\Delta x.V_n$$

or,

$$\frac{\Delta I_1}{\Delta x} = -(Y_{11} + Y_{12} + \ldots\ldots\ldots + Y_{1n})V_1 + Y_{12}V_2 + \ldots\ldots + Y_{1n}V_n$$

or,

$$\frac{dI_1}{dx} = -(Y_{11} + Y_{12} + \ldots\ldots\ldots + Y_{1n})V_1 + Y_{12}V_2 + \ldots\ldots + Y_{1n}V_n$$

Similarly for other conductors

$$\frac{dI_2}{dx} = Y_{21}V_1 - (Y_{21} + Y_{22} + \ldots\ldots\ldots + Y_{2n})V_2 + \ldots\ldots + Y_{2n}V_n$$

$$\vdots$$

$$\frac{dI_n}{dx} = Y_{n1}V_1 + Y_{n2}V_2 + \ldots\ldots\ldots\ldots - (Y_{n1} + Y_{n2} + \ldots\ldots + Y_{nn})V_n$$

or,

$$\begin{bmatrix} \frac{dI_1}{dx} \\ \frac{dI_2}{dx} \\ \vdots \\ \frac{dI_n}{dx} \end{bmatrix} = - \begin{bmatrix} (Y_{11}+Y_{12}+\ldots\ldots+Y_{1n}) & -Y_{12} & -Y_{1n} \\ -Y_{21} & (Y_{21}+Y_{22}+\ldots+Y_{2n}) & -Y_{2n} \\ \vdots & & \\ -Y_{n1} & -Y_{n2} & (Y_{n1}+Y_{n2}+\ldots+Y_{nn}) \end{bmatrix} \begin{bmatrix} V_1 \\ V_2 \\ \vdots \\ V_n \end{bmatrix}$$

or in general the above equation may be represented as follows

$$\left[\frac{dI}{dx}\right] = -\left[Y\right] \quad \left[V\right] \tag{4.16}$$

where $\left[Y\right]$ = shunt-admittance matrix per unit length and is of order nxn.

$\left[V\right]$ = column vector of voltage phasors $V_1, V_2, \ldots\ldots V_n$ and is of order nx1.

$V_1, V_2, \ldots\ldots V_n$ represent the rms values of voltage with respect to ground of phases 1,2,..... and n respectively.

Evaluation of the matrices Z and Y has been described in Chapter 2.

Hereafter the matrices Z, Y, and the vectors V, I, $\frac{dV}{dx}$ and $\frac{dI}{dx}$ will be represented without the matrix notation for simplicity.

Now, differentiating equation 4.15 a second time with respect to x and replacing $\frac{dI}{dx}$ with equation 4.16 gives

$$\frac{d^2V}{dx^2} = - Z \frac{dI}{dx} = Z Y V$$
$$= P V \qquad (4.17)$$

where

$$P = Z.Y$$

and similarly, from equations 4.16 and 4.15

$$\frac{d^2I}{dx^2} = Y Z I$$
$$= Y_t Z_t I \quad (\because Z = Z_t \text{ and } Y = Y_t \text{ for the transmission line because it is a passive network})$$
$$= (ZY)_t I$$
$$= P_t I \qquad (4.18)$$

4.3.2 Modal Linear Transformation and Diagonalisation

The solution of the second order differential equations 4.17 and 4.18 are very much simplified by the modal linear transformation of the phase voltages and currents and subsequent diagonalisation of the equations[1].

Let $V = Q V_c$ (4.19)

and $I = S I_c$ (4.20)

where S and Q are non-singular transformation matrices of order nxn and yet to be defined.

V_c = column vector of the n component voltages V_{c1}, V_{c2}....V_{cn} etc

I_c = column vector of the n component currents I_{c1}, I_{c2}....I_{cn} etc

Now substituting equation 4.19 in equation 4.17 gives

$$Q \frac{d^2V_c}{dx^2} = P Q V_c$$

or,

$$\frac{d^2V_c}{dx^2} = Q^{-1}P Q V_c$$

$$= \gamma^2 V_c \qquad (4.21)$$

where

$$\gamma^2 = Q^{-1}P Q \qquad (4.22)$$

Similarly, substituting equation 4.20 in equation 4.18 gives

$$\frac{d^2I_c}{dx^2} = S^{-1} P_t S I_c$$

$$= {}^1\gamma^2 I_c \qquad (4.23)$$

where ${}^1\gamma^2 = S^{-1}P_tS$ (4.24)

Now if the matrices Q and S are such that the matrices γ^2 and ${}^1\gamma^2$ are diagonal matrices of order nxn given by

$$[\gamma^2] = \begin{bmatrix} \gamma_1^2 & & & 0 \\ & \gamma_2^2 & & \\ & & \ddots & \\ 0 & & & \gamma_n^2 \end{bmatrix} \qquad (4.25)$$

and

$$\left[\frac{1}{\gamma^2}\right] = \begin{bmatrix} \frac{1}{\gamma_1^2} & & \\ & \frac{1}{\gamma_2^2} & 0 \\ & & \ddots \\ & 0 & \frac{1}{\gamma_n^2} \end{bmatrix} \qquad (4.26)$$

Then substituting for γ^2 in equation 4.21 gives

$$\frac{d^2V_{c1}}{dx^2} = \gamma_1^2 V_{c1}$$

$$\frac{d^2V_{c2}}{dx^2} = \gamma_2^2 V_{c2}$$

$$\vdots$$

$$\frac{d^2V_{cn}}{dx^2} = \gamma_n^2 V_{cn} \qquad (4.27)$$

Solving this differential equation 4.27 gives

$$V_{c1} = e^{-\gamma_1 x} V_{ci1} + e^{\gamma x} V_{cr1}$$

$$V_{c2} = e^{-\gamma_2 x} V_{ci2} + e^{\gamma x} V_{cr2}$$

$$\vdots$$

$$V_{cn} = e^{-\gamma_n x} V_{cin} + e^{\gamma_n x} V_{crn} \qquad (4.28)$$

or, in general $V_c = e^{-\gamma x} V_{ci} + e^{\gamma x} V_{cr}$ (4.29)

where

$$\left[V_{ci}\right] = \begin{bmatrix} V_{ci1} \\ V_{ci2} \\ \vdots \\ V_{cin} \end{bmatrix} \quad \text{and} \quad \left[V_{cr}\right] = \begin{bmatrix} V_{cr1} \\ V_{cr2} \\ \vdots \\ V_{crn} \end{bmatrix} \tag{4.30}$$

V_{ci} and V_{cr} are the constants of integration of equation 4.21 and may be evaluated from the defined boundary conditions.

Comparing the equation 4.28 with equation 4.5, it is seen that γ_1 γ_2,..... γ_n define the propagation constant of the component voltages V_{c1}, V_{c2},.....V_{cn} respectively.

Similarly substituting equation 4.26 in equation 4.23 gives

$$\begin{aligned} I_{c1} &= e^{-\gamma_1^1 x} I_{ci1} + e^{\gamma_1^1 x} I_{cr1} \\ I_{c2} &= e^{-\gamma_1^1 x} I_{ci2} + e^{\gamma_1^1 x} I_{cr2} \\ &\vdots \\ I_{cn} &= e^{-\gamma_n^1 x} I_{cin} + e^{\gamma_n^1 x} I_{crn} \end{aligned} \tag{4.31}$$

or in general

$$I_c = e^{-\gamma^1 x} I_{ci} + e^{\gamma^1 x} I_{cr} \tag{4.32}$$

where

$$\left[I_{ci}\right] = \begin{bmatrix} I_{ci1} \\ I_{ci2} \\ \vdots \\ I_{cin} \end{bmatrix} \quad \text{and} \quad \left[I_{cr}\right] = \begin{bmatrix} I_{cr1} \\ I_{cr2} \\ \vdots \\ I_{crn} \end{bmatrix} \tag{4.33}$$

I_{ci} and I_{cr} are the constants of integration and may be known from the defined boundary conditions.

$\gamma_1^1, \gamma_2^1 \ldots\ldots \gamma_n^1$ define the propagation constants of the component currents $I_{c1}, I_{c2} \ldots\ldots I_{cn}$ respectively.

The component voltages (V_c) and the component currents (I_c) may be evaluated by solving for the constants of integration from the defined boundary conditions. Once the component voltages and currents are known the corresponding phase quantities may be evaluated from equations 4.19 and 4.20 respectively.

The above simplified solutions of the components of voltages and currents illustrate the advantage of the modal linear transformation and diagonalisation - the mutual effects are eliminated and the equations are solved as a series of simple wave equations[1] as in the case of single phase.

Thus, if the diagonalisation is achieved, then the solution of the differential equation is very easily obtained - just in terms of the components and then transforming the components into the phase quantities.

It is seen from the previous sections that the key to the simplified solution of the second order differential equations 4.17 and 4.18 is based on the following conditions:-

1. The matrices γ^2 and $^1\gamma^2$ are diagonal where γ^2 and $^1\gamma^2$ are defined by equations 4.22 and 4.24.

2. The matrices

$$[Q] \neq [0]$$

and

$$[S] \neq [0]$$

It has been shown in the appendix2that the above conditions are satisfied if the following relations hold true, e.g.

$$\det(P - \gamma^2) = 0 \tag{4.34}$$

and

$$\det(P_t - {}^1\gamma_2) = 0 \tag{4.35}$$

In this case the diagonal elements of the matrix γ^2 are the eigenvalues and the columns of the Q matrix are the corresponding eigenvectors of the P matrix. Similarly, the matrices ${}^1\gamma_2$ and S are defined from the matrix P_t.

It has been shown in the appendix2that the propagation constants of the voltage and current of the same mode are equal to each other i.e. $\gamma = {}^1\gamma$, and that S and Q matrices are related to each other by the relationship

$$S = Y Q D \tag{4.36}$$

and $S = [Q_t]^{-1} D$ where D is any arbitrary diagonal matrix. Hence, once Q is known, the matrix S may be easily evaluated from the above relation (equation 4.36).

4.3.3 Evaluation of Voltages and Currents on the Systems

4.3.3.1 Voltages and currents at the boundaries

In this section the voltage and current at the terminals or at any other point along the system are evaluated. If the state of the system at any of the terminals is known then the voltage and current at any point along the system may be evaluated in terms of these conditions.

The evaluation of the terminal condition involves the evaluation of the 2n constants of integration defined by either V_{ci} or V_{cr} or I_{ci} and I_{cr}. These constants may be evaluated either in terms of the sending end or the receiving end boundary conditions.

In this section the constants of integration I_{ci} and I_{cr} are evaluated in terms of the sending end condition and the receiving end conditions are derived in terms of the constants.

Let the phase voltages and currents at the sending end of the line be V_s and I_s respectively. At the sending end x = 0 and substituting for x in equation 4.29 gives

$$V_s^c = V_{ci} + V_{cr}$$

or,

$$V_s = Q\, V_s^c$$

$$= Q\,[V_{ci} + V_{cr}] \qquad (4.37)$$

Now, substituting for V_{ci} and V_{cr} respectively from equations 38 and 39 (Appendix 2) in equation 4.37 gives

$$V_s = Q\, Z^c\, [I_{ci} - I_{cr}] \qquad (4.38)$$

or,

$$[I_{ci} - I_{cr}] = Z^{c\,-1}\, Q^{-1} V_s\, [I_{ci} - I_{cr}] \qquad (4.39)$$

Similarly, substituting for x in equation 4.32 gives

$$I_s^c = I_{ci} + I_{cr}$$

or,

$$I_s = S\,[I_{ci} + I_{cr}] \tag{4.40}$$

or.

$$[I_{ci} + I_{cr}] = S^{-1} I_s \tag{4.41}$$

Now solving for I_{ci} and I_{cr} from equations 4.39 and 4.41, I_{ci} and I_{cr} are given by

$$I_{ci} = [Z^{c-1} Q^{-1} V_s + S^{-1} I_s]\,/2 \tag{4.42}$$

$$I_{cr} = [S^{-1} I_s - Z^{c-1} Q^{-1} V_s]\,/2 \tag{4.43}$$

Let the voltages and currents at the receiving end be V_R and I_R respectively. At the receiving end of this line $x = \ell$ and substituting for x in equation 4.29 gives

$$V_R^c = e^{-\gamma\ell} V_{ci} + e^{\gamma\ell} V_{cr}$$

or,

$$V_R = Q\, V_R^c$$

$$= Q\,[e^{-\gamma\ell} V_{ci} + e^{\gamma\ell} V_{cr}] \tag{4.44}$$

or,

$$Q^{-1} V_R = e^{-\gamma\ell} V_{ci} + e^{\gamma\ell} V_{cr} \tag{4.45}$$

Now substituting for V_{ci} and V_{cr} from equations 38 and 39 (Appendix 2) in equation 4.45 gives

$$Q^{-1}V_R = e^{-\gamma\ell} Z^c I_{ci} - e^{\gamma\ell} Z^c I_{cr} \qquad (4.46)$$

Again, substituting for I_{ci} and I_{cr} in equation 4.46 gives

$$Q^{-1}V_R = \frac{e^{-\gamma\ell}Z^c}{2} [Z^{c-1}Q^{-1}V_s + S^{-1}I_s] - \frac{e^{\gamma\ell} Z^c}{2} [S^{-1}I_s - Z^{c-1}Q^{-1}V_s] \qquad (4.47)$$

or,

$$Q^{-1}V_R = \frac{e^{\gamma\ell} + e^{-\gamma\ell}}{2} Q^{-1}V_s - \frac{e^{\gamma\ell} - e^{-\gamma\ell}}{2} Z^c S^{-1} I_s$$

$$= \cosh \gamma\ell \, Q^{-1}V_s - \sinh \gamma\ell \, Z^c S^{-1} I_s$$

$$= \cosh \gamma\ell \, Q^{-1}V_s - Z^c \sinh \gamma\ell \, S^{-1} I_s \qquad (4.48)$$

($\because Z^c$ and $\sinh \gamma\ell$ are both diagonal matrices)

or,

$$V_R = Q \cosh \gamma\ell \, Q^{-1} V_s - Q Z^c \sinh \gamma\ell \, S^{-1} I_s$$

$$= Q \cosh \gamma\ell \, Q^{-1}V_s - Q Z^c S^{-1}S \sinh \gamma\ell \, S^{-1} I_s$$

$$= Q \cosh \gamma\ell \, Q^{-1} V_s - Z_o S \sinh \gamma\ell \, S^{-1}I_s \qquad (4.49)$$

(It has been shown in the appendix that $Z_o = QZ^cS^{-1}$).

I_s is sometimes expressed in terms of V_s and V_R. From equation 4.48,

$$[\sinh \gamma\ell \, Z^c S^{-1}] I_s = \cosh \gamma\ell \, Q^{-1}V_s - Q^{-1}V_R$$

$\therefore$ I_s is given by

$$I_s = [\sinh \gamma \ell \; Z^c \; S^{-1}]^{-1} \cdot [\cosh \gamma \ell \; Q^{-1} V_s - Q^{-1} V_R]$$

$$= S \; Z^{c-1} [\sinh \gamma \ell]^{-1} [\cosh \gamma \ell \; Q^{-1} V_s - Q^{-1} V_R]$$

$$= S \; Z^{c-1} \coth \gamma \ell \; Q^{-1} V_s - S Z^{c-1} \operatorname{cosech} \gamma \ell \; Q^{-1} V_R \qquad (4.50)$$

$$= Y_o Q \coth \gamma \ell \; Q^{-1} V_s - Y_o \; Q \operatorname{cosech} \gamma \ell \; Q^{-1} V_R \qquad (4.51)$$

(It has been shown in the appendix that $SZ^{c-1} = Y_o Q$).

or,

$$I_s = Y_o \coth \psi \ell \; V_s - Y_o \operatorname{cosech} \psi \ell \; V_R \qquad (4.52)$$

where $\psi = Q \gamma Q^{-1}$

and

$$Q \coth \gamma \ell \; Q^{-1} = \coth \psi \ell$$

$$Q \operatorname{cosech} \gamma \ell \; Q^{-1} = \operatorname{cosech} \psi \ell$$

[$\because$ from the theory of matrix functions $f(\psi) = Q f(\gamma) Q^{-1}$]

Similarly, I_R may be evaluated by substituting $x = \ell$ in equation 4.35 as follows

$$I_R^c = e^{-\gamma \ell} I_{ci} + e^{\gamma \ell} I_{cr}$$

or,

$$I_R = S \; I_R^c$$

$$= S [e^{-\gamma \ell} I_{ci} + e^{\gamma \ell} I_{cr}]$$

or,

$$S^{-1}I_r = e^{-\gamma\ell} I_{ci} + e^{\gamma\ell} I_{cr} \qquad (4.53)$$

Now substituting for I_{ci} and I_{cr} from equations 4.42 and 4.43 in equation 4.52 gives

$$S^{-1}I_r = \frac{e^{-\gamma\ell}}{2} [Z^{c^{-1}} Q^{-1}V_s + S^{-1}I_s] + \frac{e^{\gamma\ell}}{2} [S^{-1}I_s - Z^{c-1}Q^{-1}V_s]$$

$$= [\frac{e^{\gamma\ell} + e^{-\gamma\ell}}{2}] S^{-1}I_s - [\frac{e^{\gamma\ell} - e^{-\gamma\ell}}{2}] Z^{c-1}Q^{-1}V_s$$

$$= \cosh \gamma\ell \, S^{-1} I_s - \sinh \gamma\ell \, Z^{c-1}Q^{-1}V_s \qquad (4.54)$$

or.

$$I_R = S \cosh \gamma\ell \, S^{-1}I_s - S \sinh \gamma\ell \, Z^{c-1}Q^{-1}V_s \qquad (4.55)$$

I_R may also be expressed in terms of V_s and V_R as follows. Substituting for I_s from equation 4.50 in equation 4.54 gives

$$S^{-1}I_R = [\cosh \gamma\ell \, S^{-1}] [SZ^{c-1} \coth \gamma\ell \, Q^{-1}V_s - SZ^{c-1}\operatorname{cosech} \gamma\ell \, Q^{-1}V_R]$$
$$- \sinh \gamma\ell \, Z^{c-1} Q^{-1}V_s$$

$$= \cosh \gamma\ell \, S^{-1} S Z^{c-1} \coth \gamma\ell \, Q^{-1} V_s - \cosh \gamma\ell \, S^{-1} S Z^{c-1}$$
$$\operatorname{cosech} \gamma\ell \, Q^{-1}V_R - \sinh \gamma\ell \, Z^{c-1} Q^{-1}V_s$$

$$= Z^{c-1} \cdot \cosh^2 \gamma\ell \cdot [\sinh \gamma\ell]^{-1} Q^{-1}V_s - Z^{c-1}\coth \gamma\ell \, Q^{-1}V_R$$
$$- \sinh \gamma\ell \, Z^{c-1} Q^{-1}V_s$$

$$= Z^{c-1}\{\cosh^2 \gamma\ell\left[\sinh\gamma\ell\right]^{-1} - \sinh\gamma\ell\}\, Q^{-1}V_s - Z^{c-1}\coth\gamma\ell\, Q^{-1}V_R$$

$$= Z^{c-1}\,\text{cosech}\,\gamma\ell\, Q^{-1}V_s - Z^{c-1}\coth\gamma\ell\, Q^{-1}V_R \qquad (4.56)$$

or,

$$I_R \simeq SZ^{c-1}\,\text{cosech}\,\gamma\ell\, Q^{-1}V_s - SZ^{c-1}\coth\gamma\ell\, Q^{-1}V_R$$

$$= Y_o Q\,\text{cosech}\,\gamma\ell\, Q^{-1}V_s - Y_o Q\coth\gamma\ell\, Q^{-1}V_R$$

$$= Y_o\,\text{cosech}\,\psi\ell\, V_s - Y_o\coth\psi\ell\, V_R \qquad (4.57)$$

and

$$-I_R = -Y_o\,\text{cosech}\,\psi\ell\, V_s + Y_o\coth\psi\ell\, V_R \qquad (4.58)$$

where $(-I_R)$ represents the current flowing into the receiving end and if the current flowing into the receiving end is considered to be positive then

$$I_R = -Y_o\,\text{cosech}\,\psi\ell\, V_s + Y_o\coth\psi\ell\, V_R \qquad (4.59)$$

Equations 4.52 and 4.59 may be represented in the matrix form as follows

$$\begin{bmatrix} I_s \\ I_R \end{bmatrix} = \begin{bmatrix} Y_o\coth\psi\ell & -Y_o\,\text{cosech}\,\psi\ell \\ -Y_o\,\text{cosech}\,\psi\ell & Y_o\coth\psi\ell \end{bmatrix} \begin{bmatrix} V_s \\ V_R \end{bmatrix} \qquad (4.60)$$

$$\text{or,} \quad \begin{bmatrix} I_s \\ I_R \end{bmatrix} = \begin{bmatrix} A_\ell & B_\ell \\ B_\ell & A_\ell \end{bmatrix} \begin{bmatrix} V_s \\ V_R \end{bmatrix} \tag{4.61}$$

where $A_\ell = Y_o \coth \psi\ell$

$B_\ell = -Y_o \operatorname{cosech} \psi\ell$

If only the currents at either end are defined then the voltages V_s and V_R may be evaluated from equation 4.61 as follows

$$\begin{bmatrix} V_s \\ V_R \end{bmatrix} = \begin{bmatrix} A_\ell & B_\ell \\ B_\ell & A_\ell \end{bmatrix}^{-1} \begin{bmatrix} I_s \\ I_R \end{bmatrix} \tag{4.62}$$

Thus the solution of the boundary condition may be evaluated from equations 4.49 and 4.55 or from the equation 4.60. Equation 4.49 requires the knowledge of both the eigenvector matrices S and Q for the solution, whereas equation 4.60 is in terms of only the eigenvector matrix Q, hence equation 4.60 has been used throughout the present work for the efficient numerical evaluation of the steady state solution.

Voltages and Currents at any Point on the System

The voltages and currents at any point along the line may be evaluated from the known boundary conditions. Fig. 4.2 shows a simplified diagram of a polyphase system. Let V_s and I_s respectively the sending end voltages and currents be known, then the voltages (V_x) and current (I_x) at a distance x from the sending end may be evaluated from the relation given by

$$\begin{bmatrix} I_s \\ I_x \end{bmatrix} = \begin{bmatrix} A_x & B_x \\ B_x & A_x \end{bmatrix} \begin{bmatrix} V_s \\ V_x \end{bmatrix} \tag{4.63}$$

where $A_x = Y_o \coth \psi x$

$B_x = -Y_o \operatorname{cosech} \psi x$

Now solving for V_x and I_x from equation 4.63, V_x and I_x are given by

$$V_x = B_x^{-1} (I_s - A_x V_s)$$

and

$$I_x = B_x V_s + A_x V_x \tag{4.64}$$

Similarly, if V_R and I_R be the receiving end voltages and currents respectively, then the voltages and currents at a distance x from the receiving end are given by the relation

$$\begin{bmatrix} I_x \\ I_R \end{bmatrix} = \begin{bmatrix} A_x & B_x \\ B_x & A_x \end{bmatrix} \begin{bmatrix} V_x \\ V_R \end{bmatrix} \tag{4.65}$$

Solving for V_x and I_x from equation 4.65 gives

$$V_x = B_x^{-1} (I_R - A_x V_R)$$

and

$$I_x = A_x V_x + B_x V_R \tag{4.66}$$

Summary

In this chapter, the mathematical analysis for the steady state solutions for the general polyphase line and the simplified single phase representation of the polyphase line is described. The transmission line is considered to be uniformly distributed. The solution for polyphase line is based on Wedepohl's[1] theory of natural modes.

Single phase uniformly distributed transmission line is defined by the parameters Z_o and γ. In this case the voltage and current at any point along the system are defined by equations 4.5 to 4.14.

The polyphase homogeneous line may be defined by the matrices Y_o, Q and γ. These parameters are evaluated from the basic parameters of the system - the series impedance and shunt admittance matrices per unit length of the transmission line. Once the matrices Y_o, Q and γ are known the steady state solution is easily evaluated from equations 4.60 to 4.63.

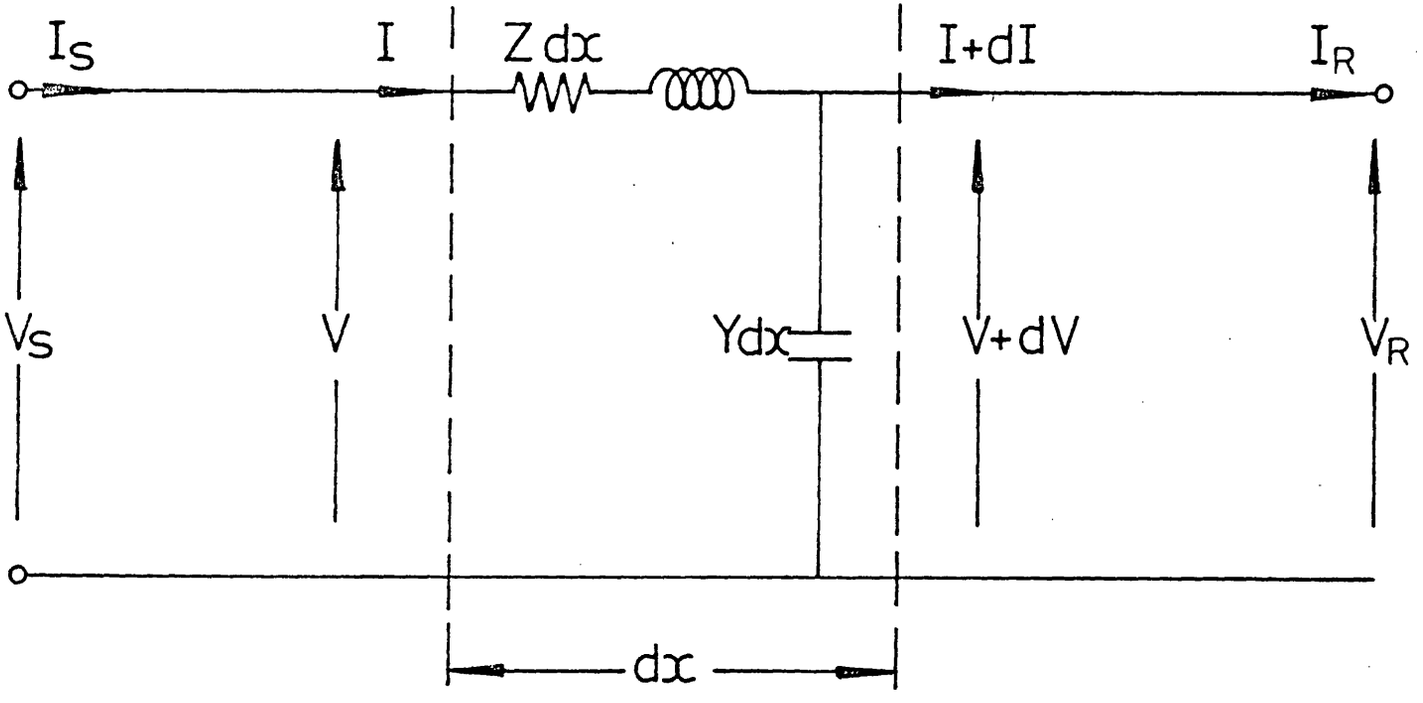

FIG. 4.1 Schematic Diagram of the Single Phase Model of a Three-Phase Line showing One Phase and Neutral Return and an Elementary Line Segment.

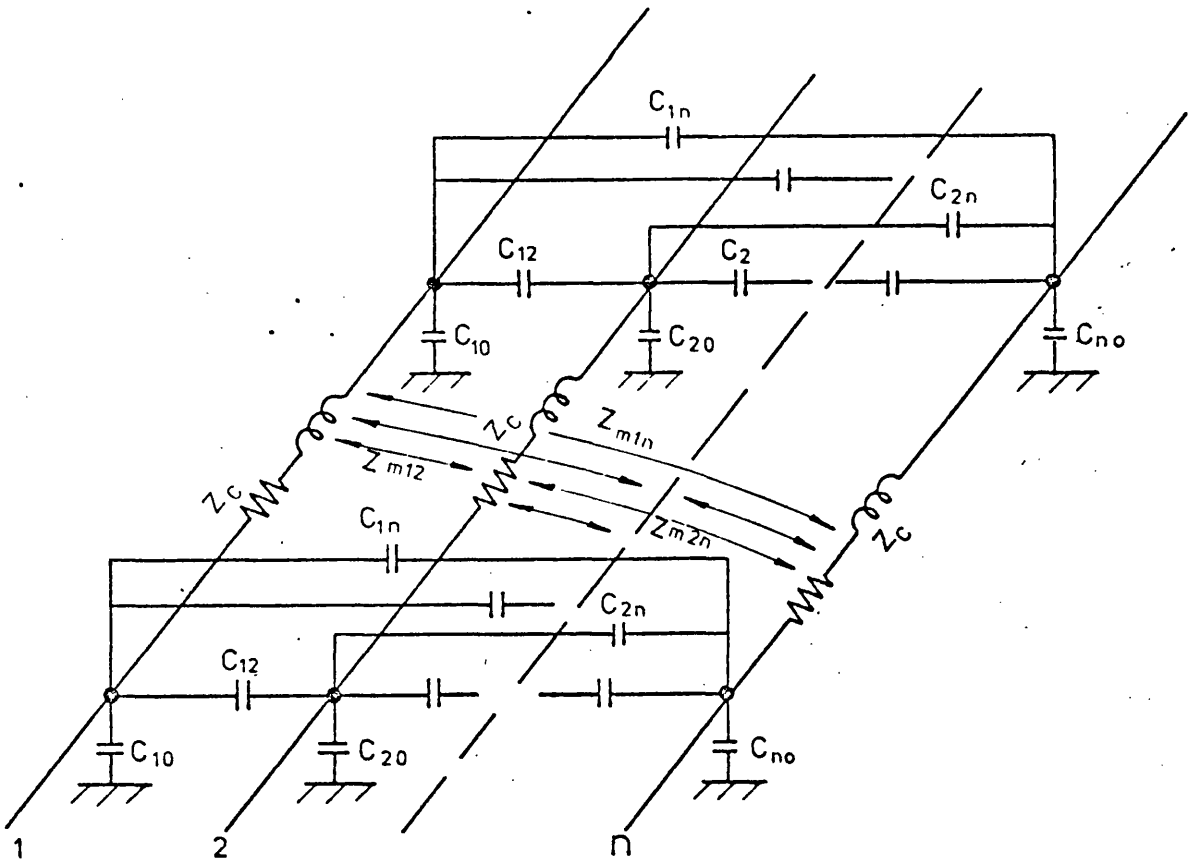

FIG. 4.2 Equivalent Circuit of a General Multiconductor Transmission Line

C H A P T E R 5

SIMPLIFIED FAULT TRANSIENT MODELS

5.1 Introduction

Power systems normally operate with balanced loads and the transmission lines are either transposed or untransposed. However, classically, the effect of slight dissymmetry due to untransposition is neglected and the lines are assumed to be perfectly transposed. Thus, the three-phase power system is assumed to be ideally balanced and is solved as a single-phase circuit composed of one of the three phases and a neutral return. Calculations made for this equivalent single-phase circuit are then extended to the whole three-phase circuit by assigning the appropriate phase-angles to the respective phases. This approach has the obvious advantage of simplifying the circuit and hence any calculations to a great extent.

In this chapter this simplified classical approach of representing the power system by a single-phase circuit is adopted so that the merits or demerits of such representations can be assessed in relation to the new technique of evaluating fault transients outlined in the previous chapters.

In the classical approach the equivalent distributed circuit of the transmission line is represented by various simplified models, e.g.

(a) the equivalent series impedance circuit - in this case the distributed shunt admittance is neglected.

(b) the cascaded sections of T or π network. The equivalent series impedance circuit is usually selected to represent a very short line and the cascaded sections of the T or π circuits represent the medium/long line.

These models are suitable within the reasonable degree of accuracy for the steady state solutions of the line but are a rather poor model

for transient studies, especially for long lines.

The shortcomings of the transient responses of these models are well documented in the literature[12,24,33] e.g. the response of the lumped series impedance circuit does not contain any travelling waves although these are present in practice, irrespective of the length of the line.

The response of the cascaded T or π circuit contains some high frequency components but the steep wavefronts observed on actual lines are sloped off in this case[33]. Such inaccuracies in the response are not acceptable to designers of future superspeed relays.

In this chapter, therefore, the most accurate model of the transmission line consisting of the distributed parameters is selected and the transient response is evaluated using the techniques outlined in the previous chapters.

5.2 Mathematical Analysis of Fault Transients

In this section the mathematical analysis for the fault transients in the single phase models of a typical power systems is presented. The analysis for the sudden occurrence of shunt faults at any location on the transmission circuit is discussed in detail. In this study the fault impedance is considered to be linear but it may have any finite value. The mathematical analysis is based on the modified Fourier transform, and is capable of taking into account the frequency dependence of the line parameters.

5.2.1 Single-end fed single-phase circuit

Consider a single-phase transmission line fed from an infinite busbar source as shown in Fig. 5.1. A single-phase transmission line with distributed parameters is defined by the parameters Z_o, α, β, and γ

where these have their usual meanings.

Let the receiving end condition of the system be known and let V_R be the reference vector. The sending end voltage and current are given by

$$V_s = V_R \cosh \gamma l + I_R Z_o \sinh \gamma l \tag{5.1}$$

$$I_s = I_R \cosh \gamma l + \frac{V_R}{Z_o} \sinh \gamma l$$

$$= I_{SM} \angle \theta_{si} \tag{5.2}$$

where I_{SM} = RMS value of current at the sending end

θ_{si} = Phase angle of I_s with respect to V_R

The steady state voltage at a distance x from the receiving end is given by

$$V_x = V_R \cosh \gamma x + I_R Z_o \sinh \gamma x$$

$$= V_{xM} \angle \theta_x \tag{5.3}$$

where V_{xM} = RMS voltage at x

θ_x = phase angle of voltage vector V_x with respect to V_R.

The positive direction of V_s, V_R, I_s, I_R are as shown in Fig. 5.2.

Let the receiving end voltage vary sinusoidally and a shunt short circuit fault occur at a distance x from the receiving end. Then the emf of the hypothetical source simulating the fault is given by

$$E_f(t) = -\sqrt{2}\ V_{xM} \sin(\omega t + \theta_x + \phi_f) \tag{5.4}$$

where $E_f(t)$ = instantaneous emf of the hypothetical source

ϕ_f = point on the waveform of V_R at which the fault occurs

The instantaneous value of steady state current at the sending end due to the main emf source alone measured from the instant of fault inception is given by

$$I_{ss}(t) = \sqrt{2}\ I_{SM} \sin(\omega_s t + \theta_{si} + \phi_f) \tag{5.5}$$

The switching transient current due to the hypothetical source alone is derived by solving the circuit shown in Fig. 5.3.

The Fourier transforms of the sine waves of energising voltage E_f are given by

$$\overline{E_f} = \sqrt{2}\ V_{xM} \left\{ \frac{\omega_s}{\omega_s^2 - \omega^2} \times \cos(\theta_x + \phi_f) + \frac{j\omega}{\omega_s^2 - \omega^2} \times \sin(\theta_x + \phi_f) \right\} \tag{5.6}$$

The Fourier transform of the current at the sending end is then given by

$$\overline{I}_{s\omega} = \overline{E}_f \times \frac{1}{Z_o \times \sinh \gamma(\ell - x)} \tag{5.7}$$

The inverse Fourier transform of $\overline{I_{s\omega}}$ gives the switching transient current at the sending end $I_{str}(t)$. The inverse Fourier transform of $\overline{I_{s\omega}}$ is evaluated by the method of modified Fourier transform as suggested by Ametani[51], Wedepohl[17] and others[49,50,54,55,57].

The transient fault current at the sending end is then given by

$$I_{fs}(t) = I_{ss}(t) - I_{str}(t) \tag{5.8}$$

Similarly, the transient fault current and voltage at any point on the transmission line may be evaluated as described above by the principle of superposition.

5.3 Digital Computer Studies

Fault transients results for the distributed parameter model of the transmission line fed at the sending end from an infinite bus are presented here. The mathematical model for this case has been described in Section 5.2.1.

The parameters of the line are considered to be frequency invariant for simplicity although their frequency dependence may be taken into account.

For all the cases studied here, the line was energised at the sending end, and was open circuited at the receiving end before the sudden occurrence of fault, although any other prefault condition may be simulated.

The results are evaluated at the sending end relaying point for a solid earth fault at the receiving end of the line. The voltage at the sending end is not affected as the source is an infinite bus, hence the variation of transient current only for different fault conditions are described here.

The study of this simple model has been taken up here as a means of establishing the validity of the technique of evaluating the fault

transients outlined in the previous sections. However, the influencing factors such as the source impedance on the fault transients at the relaying point or any other point of interest may also be studied on the basis of this technique.

5.3.1 Description of the circuit

The studies presented here have been performed for the circuit shown in Fig. 5.1. The data of the circuit studied are as follows:-

(A) Prefault boundary condition:

(a) the sending end source is infinite busbar

(b) supply frequency is 50Hz

(c) the receiving end voltage = $\frac{400}{\sqrt{3}}$ KV (rms phase to earth)

(d) the line is energised at the sending end and the receiving end is open-circuited before the fault inception

(B) The parameters[18] of the transmission line are as follows

(a) R_L = 2.125×10^{-2} ohms/Km

(b) L = 0.8875 mH/Km

(c) C = 1.306×10^{-2} μF/Km

(d) Z = 0.279 ohm/Km (at 50Hz)

(e) Z_o = $260.8 - j\ 9.41 = 261.0\ \underline{/-2.064^{o}}$ ohm

(f) γ = $0.107\ \underline{/87.94^{o}}$

(g) velocity of propagation = 293440 Km/sec

(h) attenuation = 0.3852 nepers/Km

(The parameters of the line are considered to be frequency invariant).

(C) Details of the fault:

(a) the location of the fault is the receiving end

(b) the fault impedance = 0Ω

(D) Number of samples used in Fourier transform = 400

5.3.2 20-mile line

5.3.2.1 20-mile line, 2 ms observation period, $\phi = \pi/2$

Fig. 5.4 shows the transient fault current at the sending end relaying point after the occurrence of fault at the receiving end. The voltage at the location of fault was at its positive peak value at the instant of fault inception.

The variation of the fault transient current in this case is easily understood from the phenomena of the propagation of the fault surge. The occurrence of the fault initiates a surge of voltage and current waves which travel near the velocity of light.

The initial jump of the current is due to the arrival of the first incident wave of the fault surge and prior to its arrival the current at the sending end varies according to the prefault boundary condition. The prefault current in this case is the charging current of the line.

The incident wave of the fault surge is reflected from the sending end and travels towards the fault, where it is again reflected and then travels back to the sending end. This process of travelling forwards and backwards of the fault surge between the sending end and the fault point continues until the energy of the surge is fully dispersed and the sustained steady state fault condition is reached.

Thus the build-up of the current at the sending end is due to the arrival of the incident waves and its successive reflections. This Figure is very similar to the classical staircase build-up of current at the short-circuited receiving end of a distributed L-C circuit due to the sudden application of a step voltage at its sending end. The classical staircase solution has been obtained in the past by Bewley's lattice diagram method.

According to the lattice diagram solution the time 'T' for the first incident wave initiated by the fault to reach the sending end is given by

T = distance to fault from the sending end/velocity of propagation

The time interval 'T_i' between any two consecutive reflections is given by

$$T_i = 2T$$

and the initial jump 'I_j' of the current at the sending end for the infinite bus source and the zero fault impedance is given by

$$I_j = -2I$$

where

$I = V/Z_o$

V = the instantaneous magnitude of the voltage at the fault point at the instant of fault inception

$Z_o = \sqrt{\frac{L}{C}} \simeq$ surge impedance

The magnitudes of the successive jumps are also equal to the initial jump neglecting the slight variation of voltage during the short period of observation in this case.

From the Fig. 5.4 it is seen that the waveforms, the time of arrival of the first incident wave, the time interval between the arrival of the successive reflections, the magnitudes of the initial and the successive jumps agree well with the Bewley's lattice diagram solution.

The close agreement with Bewley's solution confirms the validity of the results and the mathematical technique presented here.

5.3.2.2 20-mile line, 20 ms observation period, $\phi = \pi/2$

Fig. 5.5 shows the transient current at the sending end relaying point over a period of 20 ms for the same prefault condition as described above.

The response of the distributed model is full of ripples due to the reflections of the fault surge between the sending end and the fault. In this case, the location of fault being very near to the relaying point the reflections arrive at very short intervals and the build-up of the current is very similar to that in the simplified series impedance model.

The variation of current in the equivalent lumped series impedance model is given by

$$I(t) = I_m \left\{ \sin(\omega t + \phi - \theta) - e^{-\frac{R}{L} t} \sin(\phi - \theta) \right\} \qquad (5.8)$$

where I_m, θ, and ϕ are as defined in Appendix .

In this case, $\phi = \pi/2$

$\theta \simeq \pi/2$ as $R_L \neq 0$ and is very small compared to ωL

Hence, $I(t) \simeq I_m \sin(\omega t)$ (5.9)

Thus the variation of the transient current in the equivalent lumped circuit is sinusoidal and the overall response of the distributed model is in agreement with this result.

However, there is a difference in these two responses e.g. the current in the distributed model remains at its prefault charging current until the arrival of the first incident wave, whereas the current varies sinusoidally after the fault inception in the case of the lumped model - its prefault current being zero. But the difference in response is very small and it is very clear from Figs. 5.4 and 5.5 that the response of the equivalent series circuit is approximately the mean value of the response of the distributed model.

It may, therefore, be observed that the short lines may be represented by the equivalent lumped series impedance circuit, if very high degree of accuracy is not required. This result is in agreement with the classical approximation of a short line by a lumped series impedance circuit.

The close agreement between these two results also confirms the validity of the mathematical model for the evaluation of fault transients in the distributed circuit outlined in the previous sections.

However, the disadvantage of the lumped circuit representation is that the true mechanism of the build-up of current in the practical circuit is not clearly shown by the response, although the overall response is approximately equal to that of the distributed model.

5.3.2.3 20-mile line, $\phi = 0$

Fig. 5.6 shows the fault transient current at the sending end when a solid fault occurs at the receiving end when the voltage there passes through zero.

In this case the initial value of the voltage step applied at the location of fault by the hypothetical source simulating the fault is zero. Hence the magnitude of the incident wave is zero, however, the current increases gradually because the magnitude of the successive reflections increases with the gradual increase of the voltage of the hypothetical source simulating the fault.

Fig. 5.7 shows the current at the sending end over a period of 20ms and in this case the variation of the transient current is very similar to that in the equivalent lumped series circuit.

The transient current in the equivalent lumped series circuit is given by

$$I(t) = I_m \left\{ \sin(\omega t + \phi - \theta) - e^{-\frac{R}{L}t} \sin(\phi - \theta) \right\} \qquad (5.10)$$

for $\phi = 0$, $\theta \simeq \pi/2$ i.e. for $R_L << \omega L$

$$I(t) \simeq I_m \left\{ 1 - \cos \omega t \right\} \qquad (5.11)$$

For the fault inception angle equal to zero, the difference between the transient currents of the distributed and the lumped series circuit is very small and the close agreement between these two results also confirm the observation made in section 5.3.2.2.

5.3.3

5.3.3.1 100-mile line, 20ms Observation period, $\phi = \pi/2$

Fig. 5.8 shows the variation of the transient current at the sending end relaying point after the inception of fault at the receiving end. The fault occurs when the voltage at the point of fault is at its positive peak value.

The current remains at its prefault value which is the charging current of the line and then suddenly jumps to a very high value. The sudden jump is due to the arrival of the first incident wave of the fault surge and is approximately equal to (2I) where the value of I is as defined in section 5.3.2.1.

Thereafter, the current goes on building up due to the arrival of the successive reflections from the fault point. The interval of time between any two consecutive reflections agree well with the time taken by the wave to travel at its velocity of propagation - twice the distance to fault from the relaying point.

The disturbances in the transient current due to the reflections from the fault do not die out within a cycle (20ms) after the fault inception as in the case of the 20 mile line.

5.3.3.2 100-mile line, 20ms Observation period, $\phi = 0$

Fig. 5.9 shows the variation of the transient current at the sending end for the above line when the magnitude and phase angle of the prefault voltage at the location of fault are zero and zero degrees respectively. In this case the difference between the responses of the distributed and the equivalent lumped series impedance model is very small, and for this particular case of fault inception even a long line may be represented by the equivalent lumped model without involving much inaccuracy.

5.4 Summary and General Conclusions

In this chapter a mathematical model for evaluating the fault transient in the simplified single phase representation of the balanced three-phase power system has been studied. The uniformly distributed parameter model of the transmission line has been considered, and the mathematical model is based on the technique of fault simulation outlined in the previous chapter.

The following conclusions may be drawn from the mathematical analysis and the digital computer results presented in the previous sections:

1. The method of evaluating the fault transients in the distributed model described in this chapter is very general and can take into account the influence of the frequency dependence of the line parameters, the effect of the fault impedance and the source impedance on the fault transients.

2. If a very high degree of accuracy is not desired then the fault transients may be obtained by the classical Bewley lattice diagram - the effect of the line resistance and the frequency dependence of the line parameters may be neglected in this case.

3. The waveform of the transient current and its magnitude at a particular instant of time after the fault inception depends on the following factors:-

   (a) the phase angle of the prefault voltage at the location of fault at the instant of fault inception.

   (b) the location of fault

   (c) the fault impedance

   (d) the impedance of the source

4. There is good agreement in the results of the distributed model and the equivalent lumped series impedance model for the short line, or for the close-up faults. Hence such cases may be analysed from the equivalent lumped circuit, if a very high degree of accuracy is not required.

For longer lines error in the responses of the above two models depends on the phase angle of the voltage at the instant of fault inception and is different for different phase angles, e.g. the error is very small for $\phi = 0$ and very large for $\phi = \pi/2$.

5. The zero crossings of the response of the distributed model do not occur at the same intervals of time as that obtained from the lumped series impedance model of the line for the same prefault condition. The error in the zero crossings may give rise to problems in the operation of conventional analogue relays which depend for their operation on the time interval between zero-crossings. Similar observation has already been made by Robertson and others.[24]

6. The relay does not receive the information about occurrence of the fault immediately at the instant of fault inception. The information from the fault point travels towards the relaying point at approximately the velocity of light and the time delay depends therefore upon the distance of the fault from the relaying point. Hence no superspeed relay can be designed to detect the fault exactly at the instant of fault inception or in other words no relay can be designed to operate faster than the propagation velocity of the fault surge, as the relay has to wait till the information reaches it.

7. The response of the lumped series impedance circuit is approximately the mean value of that of the distributed model. This is one of the

reasons why the many classical relays work well. However the waveform of the response of the distributed model for long distance fault may differ considerably (e.g. for $\phi = \pi/2$) from that of the lumped series impedance model, hence, for very accurate design of superspeed relays the response of the distributed model should be taken into account.

8. The limitation of the study of the simplified single phase circuit of the three phase system is that only the balanced faults on balanced systems can be analysed. Hence, in the next chapter both transposed and untransposed three-phase systems are studied in detail.

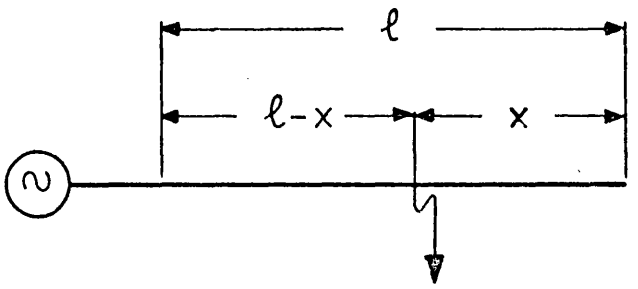

FIG. 5.1 On-Line Diagram of the Single-Phase Transmission Line Fed from an Infinite Busbar

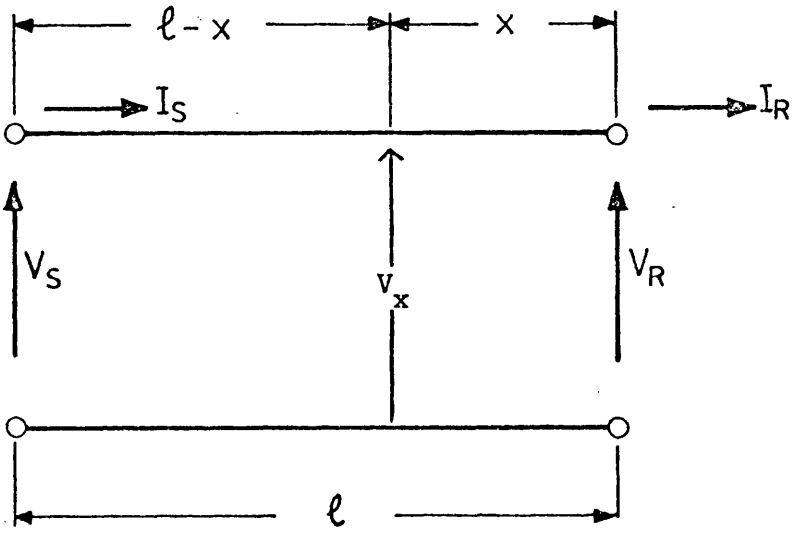

FIG. 5.2 Equivalent Block Diagram of the System

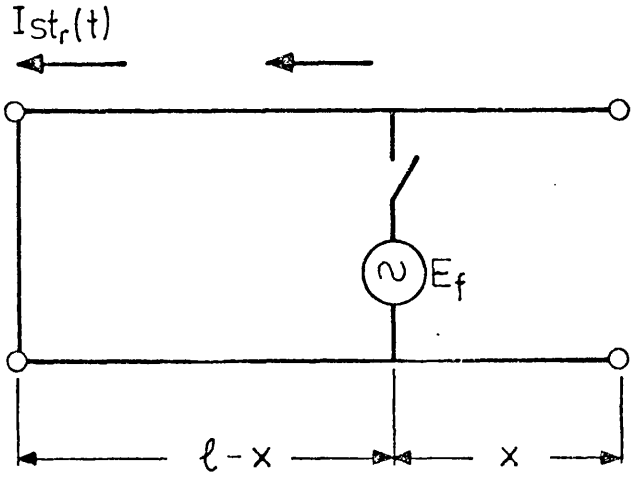

FIG. 5.3 Equivalent Circuit of the System for the Evaluation of Switching Transient Component due to the Hypothetical EMF Source Simulating the Fault.

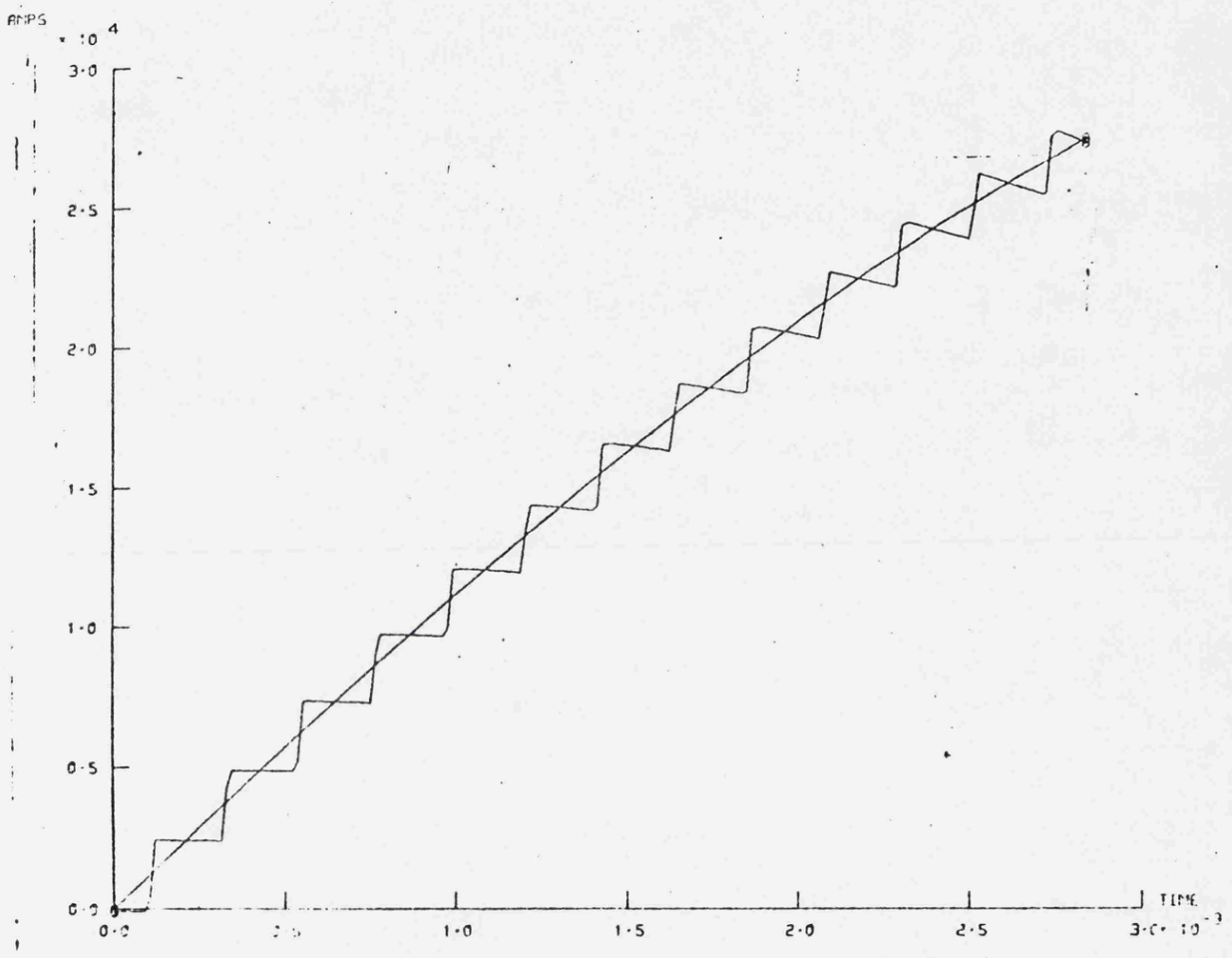

FIG. 5.4 Transient Fault Current at the Sending End
(32Km line, 3ms observation period, $\phi = \pi/2$)

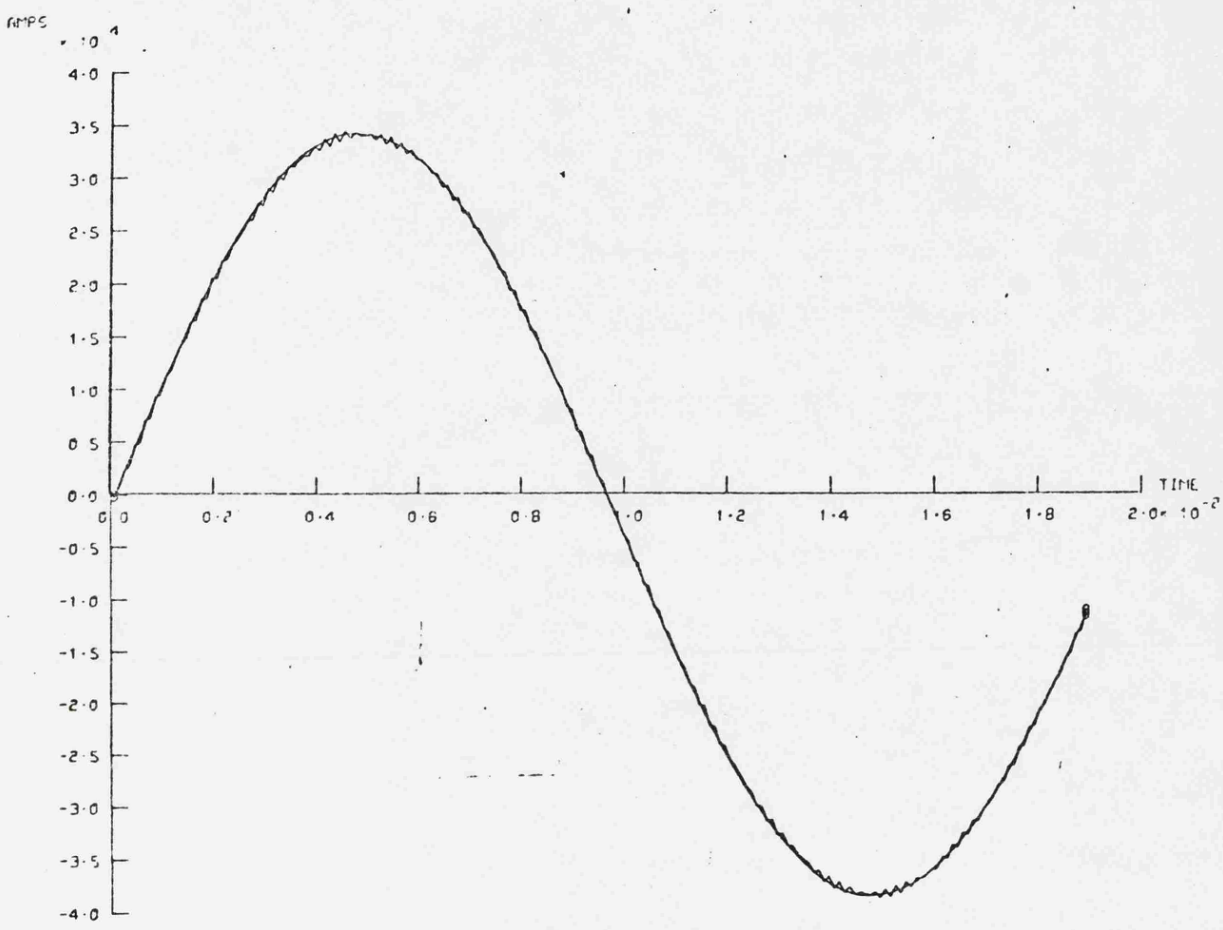

FIG. 5.5 Transient Fault Current at the Sending End
(32Km line, 20ms observation period, $\phi = \pi/2$)

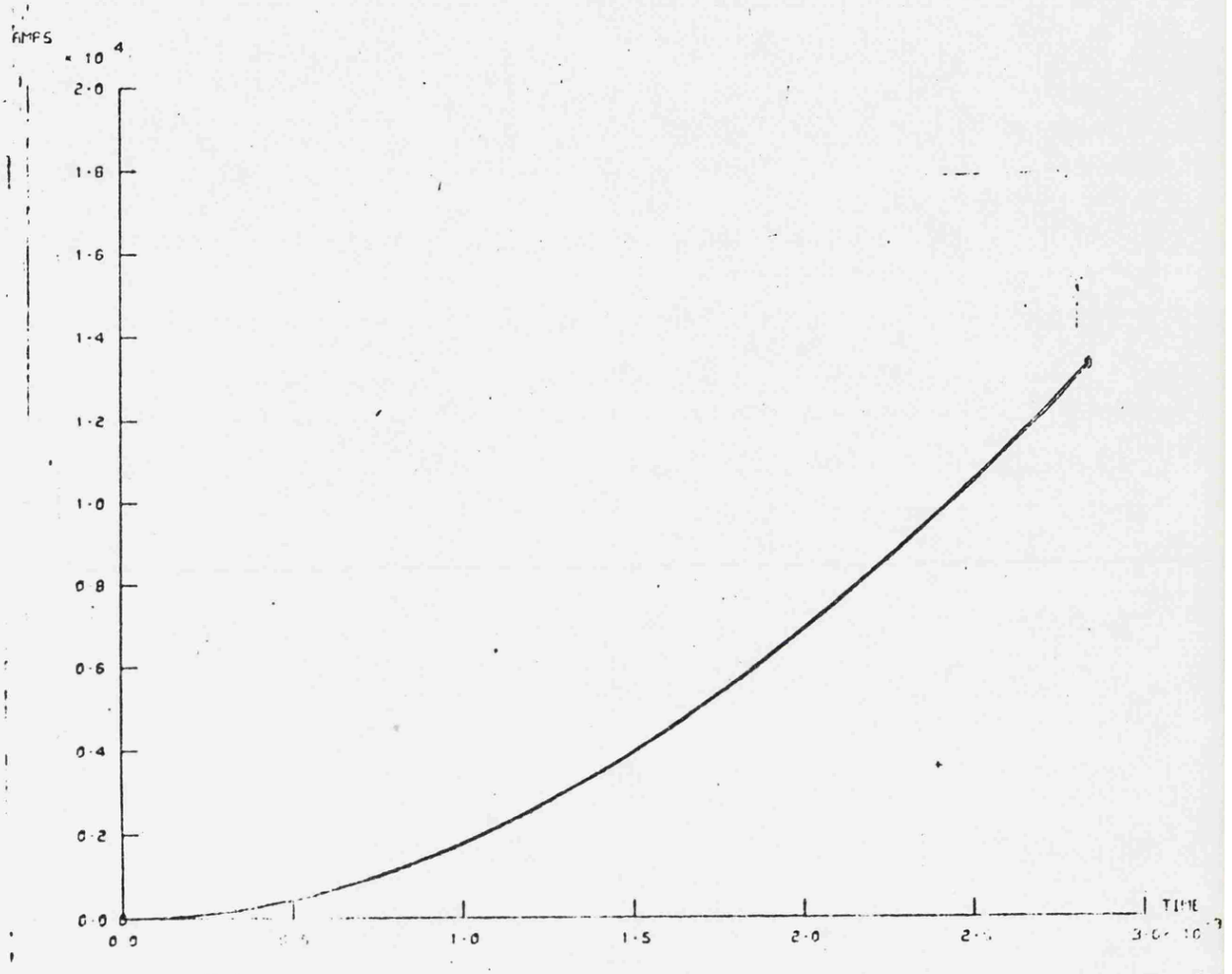

FIG. 5.6 Transient Fault Current at the Sending End
(32Km line, 3ms observation period, ϕ = 0)

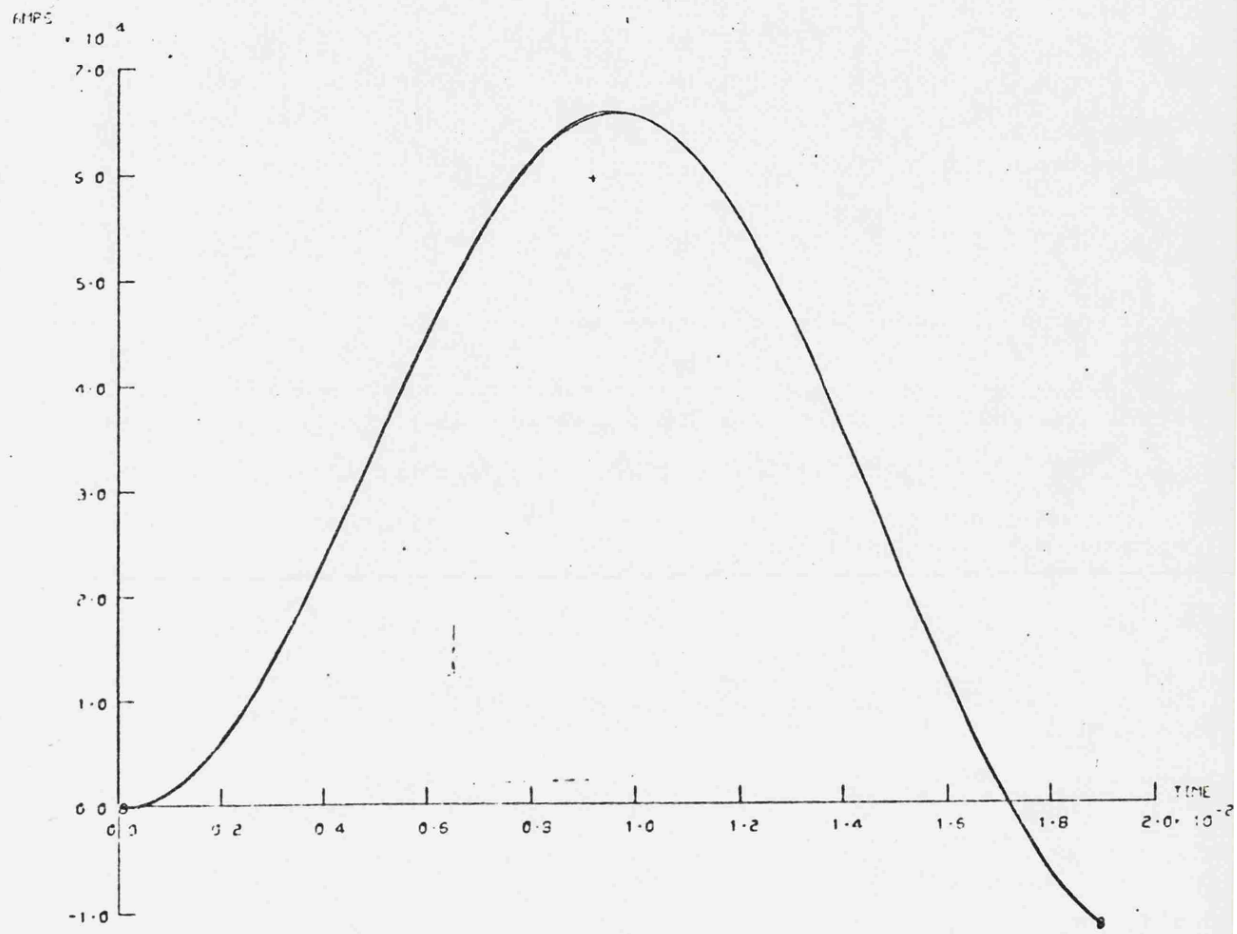

FIG. 5.7 Transient Fault Current at the Sending End
(32Km line, 20ms observation period, ϕ = 0)

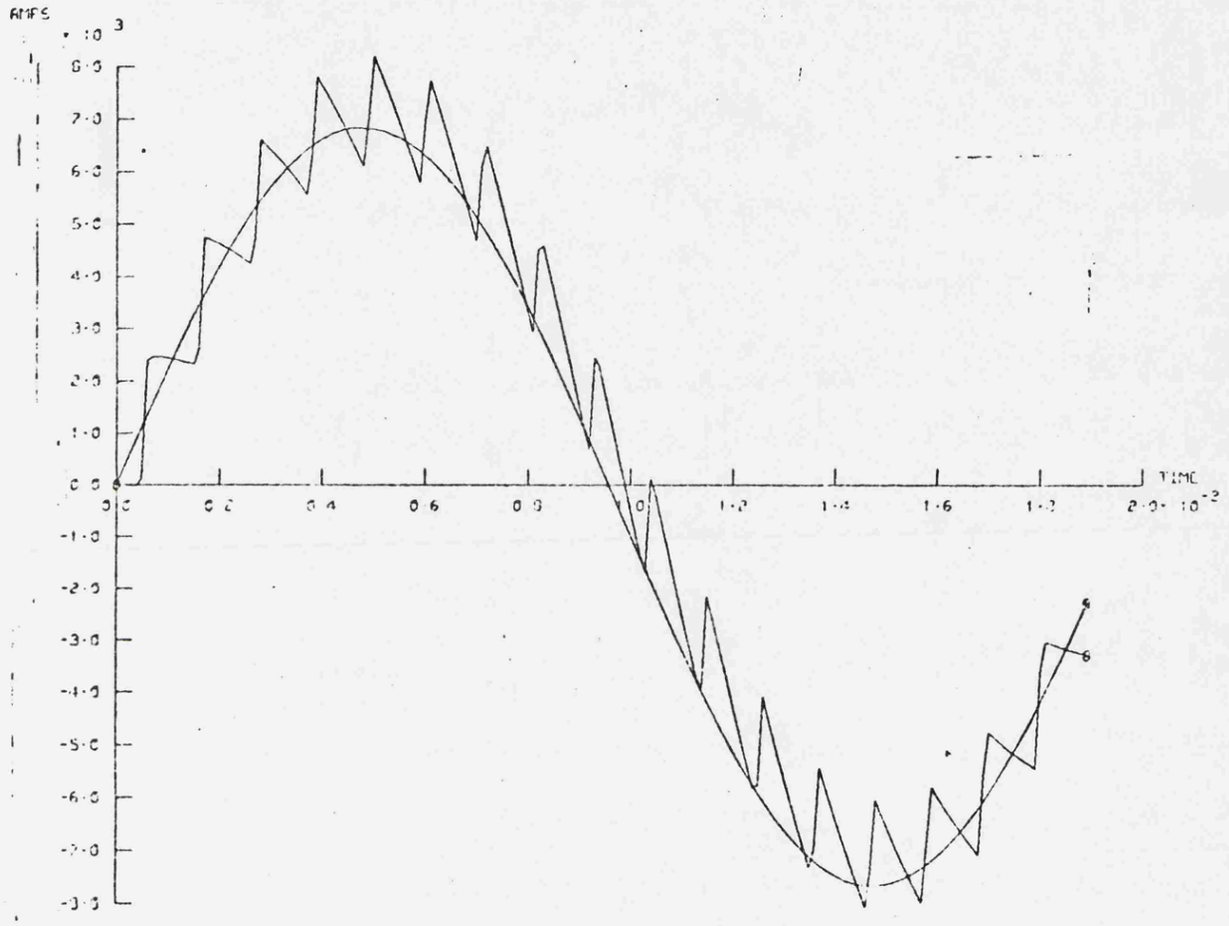

FIG. 5.8 Transient Fault Current at the Sending End
(160Km line, 20ms observation period, $\phi = \pi/2$)

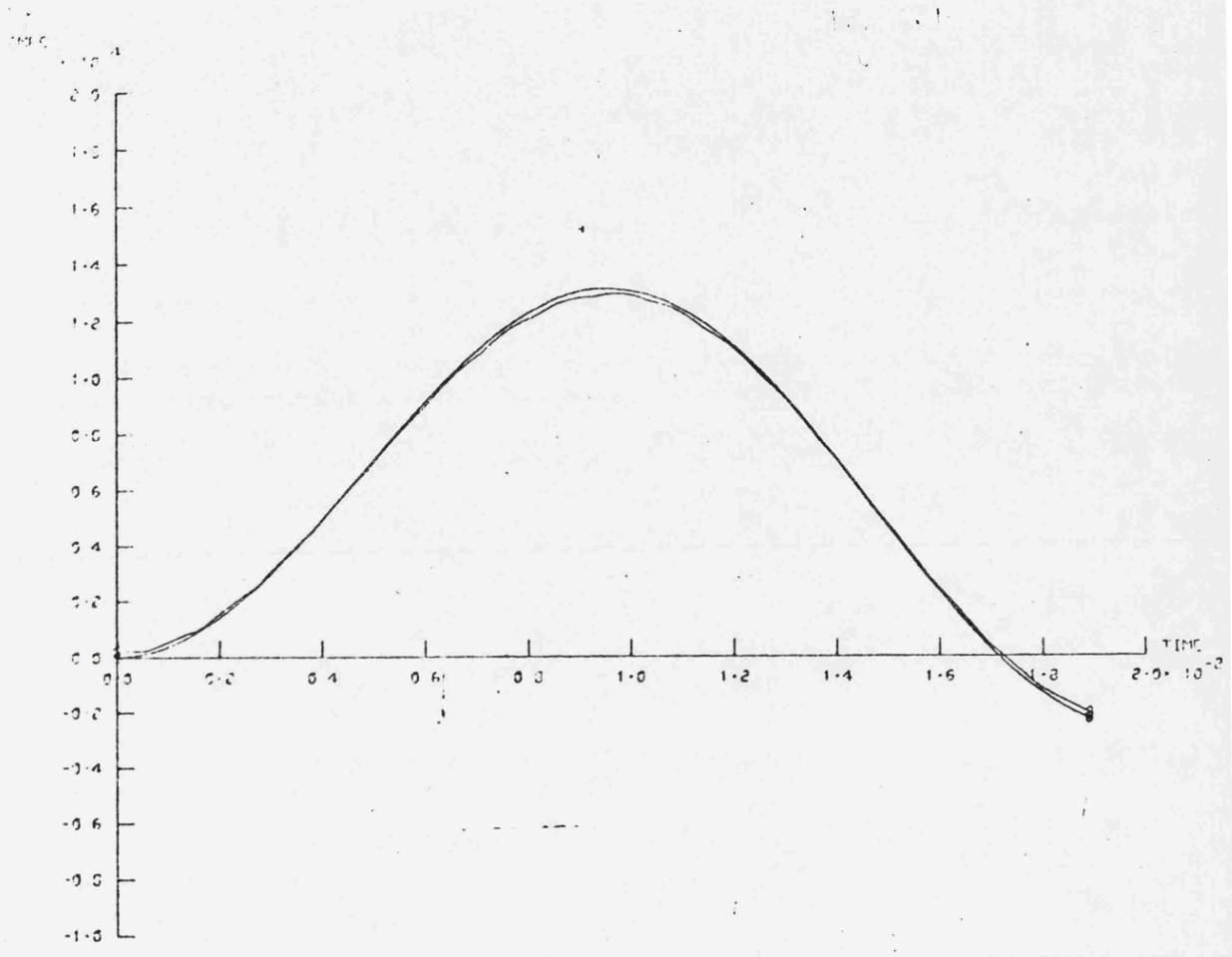

FIG. 5.9 Transient Fault Current at the Sending End
(160Km line, 20ms observation period, ϕ = 0)

CHAPTER 6

MATHEMATICAL ANALYSIS OF FAULT TRANSIENTS IN PRACTICAL TRANSMISSION LINES

6.1 Introduction

In the previous chapter the fault transients in the single phase circuit have been studied. In practice, most of the lines are three-phase untransposed lines and all the conductors of these lines are electromagnetically and electrostatically coupled. The simplified analysis - single phase representation of the three phase system - neglects the presence of other conductors and, hence the mutual effects. Neglecting the influence of mutual effects affects the results and in the words of Bewley, "sometimes their influence is so vital as to change the characteristics of the phenomenon completely and entirely erroneous results are obtained if they are not considered."[44] A good example of this statement is the overvoltage phenomenon in the sound phases due to the SLG fault on one of the phases. This phenomenon cannot be observed from the study of the single-phase circuit. All the conductors are monitored constantly by the protective relays and hence knowledge of the overall picture of the transient behaviour of all the conductors is essential for protective schemes in order to assess the performance of the present protective relays (for long lines) and for the design and development of the improved protective scheme for the future. This information is also of great importance for the design of lines.

Such information can be obtained only from the study of practical three-phase lines as the application of this simplified analysis is restricted to the limited practical cases only - single-phase circuits, balanced faults on balanced systems.

In this chapter, therefore, the study of the three-phase system is taken up and a very general mathematical technique for the evaluation of fault transients is developed.

6.2 Mathematical Analysis

In the following sections the detailed mathematical analysis for fault transients in some typical three-phase systems is presented.

The source is represented by the simplified classical models e.g. infinite busbar source and lumped parameter source. The source usually influences the nature of the transients to a great degree. The simulation of the source is a very complicated problem e.g. the proper representation of the distributed generators and the infeeds. In the present analysis very approximate models are considered as the primary objective of this present study is to establish the fault transients due to the transmission lines only.

The transmission line is considered to be homogeneous multi-conductor line with distributed and frequency dependent parameters.

The mathematical analysis is based on the modal analysis and the application of modified Fourier transform.[17] The method of modified Fourier transform is well documented in the literature.[49,50,51,54,55,57] ~~and is briefly described in the Appendix~~.

The system is considered to be under steady state condition before the occurrence of the fault and the fault is simulated on the basis of the technique described in Chapter Three.

The anslysis of the shunt faults only is presented. The analysis of series faults, and simultaneous shunt faults are described in the Appendix 3.

6.2.1 Double-End Fed System

6.2.1.1 Infinite busbar source

Consider the system fed from the infinite busbar source at either end as shown in Fig. 6.1. Let the sending and receiving-end voltages be known and be represented as follows

$$V_s = \begin{bmatrix} V_{s_1} \\ V_{s_2} \\ V_{s_3} \end{bmatrix} = \begin{bmatrix} V_{sM_1} \angle\theta_{vs_1} \\ V_{sM_2} \angle\theta_{vs_2} \\ V_{sM_3} \angle\theta_{vs_3} \end{bmatrix} \qquad 6.1$$

$$V_R = \begin{bmatrix} V_{R_1} \\ V_{R_2} \\ V_{R_3} \end{bmatrix} = \begin{bmatrix} V_{RM_1} \angle\theta_{vr_1} \\ V_{RM_2} \angle\theta_{vr_2} \\ V_{RM_3} \angle\theta_{vr_3} \end{bmatrix} \qquad 6.2$$

where

$$\theta_{vs_1} = 0, \quad \theta_{vs_2} = 2\pi/3, \quad \theta_{vs_3} = 4\pi/3$$

$$\theta_{vr_1} = \theta_{vs_1} - \beta, \quad \theta_{vr_2} = \theta_{vs_2} - \beta, \quad \theta_{vr_3} = \theta_{vs_3} - \beta$$

β = phase angle between the sending end and the receiving end voltages and defines the prefault power transfer between the two ends

The suffices 1,2,3 refer to the phases1, 2 and 3 respectively.

The system may be defined by the two-port matrix equation 4.60. Accordingly, I_s and I_R are defined in terms of V_s and V_R as follows:

$$I_s = A_L V_s + B_L V_R \qquad 6.3$$

$$= I_{SM} \angle \theta_{is}$$

$$I_R = B_L V_s + A_L V_R \qquad 6.4$$

$$= I_{RM} \angle \theta_{ir}$$

where the line constants A_L and B_L are defined by equation 4.58.

The voltages and currents at a distance x from the receiving end are defined by the system equation 4.65 as follows:

$$V_x = B_x^{-1} (I_R - A_x . V_R) \qquad 6.5$$

$$= V_{xM} \angle \theta_{vx}$$

$$I_x = B_x V_x + A_x V_R \qquad 6.6$$

$$= I_{xM} \angle \theta_{ix}$$

where the line constants A_x and B_x are defined by equation 4.63.

The steady state instantaneous values of the voltages and currents at the sending end, receiving end and at a distance x from the receiving end may be defined as follows:

$$V_{s_k}(t) = \sqrt{2}\ V_{sM_k} \cos(\omega_s t + \theta_{vs_k} + \phi) \qquad 6.7$$

$$I_{s_k}(t) = \sqrt{2}\ I_{sM_k} \cos(\omega_s t + \theta_{is_k} + \phi) \qquad 6.8$$

$$V_R(t) = \sqrt{2}\, V_{RM_k} \cos(\omega_s t + \theta_{vr_k} + \phi) \qquad 6.9$$

$$I_R(t) = \sqrt{2}\, I_{RM_k} \cos(\omega_s t + \theta_{ir_k} + \phi) \qquad 6.10$$

$$V_x(t) = \sqrt{2}\, V_{xM_k} \cos(\omega_s t + \theta_{vx_k} + \phi) \qquad 6.11$$

$$I_x(t) = \sqrt{2}\, I_{xM_k} \cos(\omega_s t + \theta_{ix_k} + \phi) \qquad 6.12$$

where

$$V_{s_k} = V_{sM_k} \angle \theta_{vs_k}$$

$$I_{s_k} = I_{sM_k} \angle \theta_{is_k}$$

$$V_{x_k} = V_{xM_k} \angle \theta_{vx_k}$$

$$I_{x_k} = I_{xM_k} \angle \theta_{ix_k}$$

$$V_{R_k} = V_{RM_k} \angle \theta_{vr_k}$$

$$I_{R_k} = I_{RM_k} \angle \theta_{ir_k}$$

ϕ = point on the reference vector V_{s_1} from which the time t is measured

k = 1, 2 or 3 and refers to the phases 1, 2 or 3 respectively.

The voltages and currents expressed as complex quantities or as a function of time are represented as column vectors in the present analysis and the elements of the column vectors may be determined from equations 6.1 to 6.12.

Let a shunt fault occur at a distance x from the receiving end when the phase angle of the reference vector V_{s_1} is ϕ. The shunt fault is simulated as described in Chapter Three. Accordingly, the emf's of the hypothetical sources simulating the shunt fault are defined by

$$[E_f] = [-V_x] \qquad 6.13$$

and the instantaneous values of the emf's are given by

$$[E_f(t)] = [-V_x(t)] \qquad 6.14$$

where

$$E_{f_k}(t) = -\sqrt{2}\, V_{xM_k} \cos(\omega_s t + \theta_{vx_k} + \phi)$$

The total energising current fed to each line by the equivalent current generators representing the hypothetical emf sources are

$$I_{s_f} = Y_F E_f \qquad 6.15$$

where

Y_F = shunt admittance matrix and is defined according to the type of fault as described in Chapter Three.

The Fourier transform of the energising currents are defined as follows:

$$\overline{I_{s_f}} = Y_F \overline{E_f} \qquad 6.16$$

where the elements of $\overline{E_f}$ represent the Fourier transforms of the

sinusoidal waves of the emf of the hypothetical source. The switching transients due to the hypothetical emf sources alone are evaluated by solving the circuit of Fig. 6.2.

The Fourier transforms of the system equations for the section Y of the system are defined as follows:

$$\begin{bmatrix} \bar{I}_{s_{f_1}} \\ \bar{I}_{RR_1} \end{bmatrix} = \begin{bmatrix} A_Y & B_Y \\ B_Y & A_Y \end{bmatrix} \begin{bmatrix} \bar{V}_{s_f} \\ \bar{V}_{RR_1} \end{bmatrix} \qquad 6.17$$

where

$$A_Y = Y_o \cot h\, \psi\, y$$

$$B_Y = -Y_o \operatorname{cosec} h\, \psi\, y$$

From equation 6.17 $\bar{I}_{s_{f_1}}$ and $\bar{I}_{RR_1}$ may be expressed as follows

$$\bar{I}_{s_{f_1}} = A_Y \bar{V}_{s_f} + B_Y \bar{V}_{RR_1} \qquad 6.18$$

$$\bar{I}_{RR_1} = B_Y \bar{V}_{s_f} + A_Y \bar{V}_{RR_1} \qquad 6.19$$

The Fourier transforms of the system equations for the section x are given by

$$\begin{bmatrix} \overline{I_{s_{f_2}}} \\ \overline{I_{RR_2}} \end{bmatrix} = \begin{bmatrix} A_x & B_x \\ B_x & A_x \end{bmatrix} \begin{bmatrix} \overline{V_{s_f}} \\ \overline{V_{RR_2}} \end{bmatrix} \qquad 6.20$$

where

$$A_x = Y_o \cot h\, \psi x$$

$$B_x = -Y_o \operatorname{cosec} h\, \psi x$$

From equation 6.20 $\overline{I_{s_{f_2}}}$ and $\overline{I_{RR_2}}$ may be expressed as follows:

$$\overline{I_{s_{f_2}}} = A_x \overline{V_{s_f}} + B_x \overline{V_{RR_2}} \qquad 6.21$$

$$\overline{I_{RR_2}} = B_x \overline{V_{s_f}} + A_x \overline{V_{RR_2}} \qquad 6.22$$

In the system shown in Fig. 6.2 the terminal voltages V_{RR_1} and V_{RR_2} are zero. Therefore

$$\begin{bmatrix} \overline{V_{RR_1}} \end{bmatrix} = \begin{bmatrix} 0 \end{bmatrix} \qquad 6.23$$

and

$$\begin{bmatrix} \overline{V_{RR_2}} \end{bmatrix} = \begin{bmatrix} 0 \end{bmatrix} \qquad 6.24$$

Substituting for $\overline{V_{RR_1}}$ from equation 6.23 in equations 6.18 and 6.19, and for $\overline{V_{RR_2}}$ from equation 6.24 in equations 6.21 and 6.22 gives

$$\overline{I_{s_{f_1}}} = A_Y \overline{V_{s_f}} \qquad 6.25$$

$$\bar{I}_{RR_1} = B_Y \bar{V}_{s_f} \tag{6.26}$$

$$\bar{I}_{s_{f_2}} = A_x \bar{V}_{s_f} \tag{6.27}$$

$$\bar{I}_{RR_2} = B_x \bar{V}_{s_f} \tag{6.28}$$

The Fourier transform of the currents in the shunt admittance of the current generator is given by

$$\bar{I}_f = Y_F \bar{V}_{s_f} \tag{6.29}$$

Thus the currents at the various points in the system are known in terms of $\bar{V}_{s_f}$ and the line constants. $\bar{V}_{s_f}$ may be determined by solving for the currents at the location of fault.

At the location of fault the currents are related as follows:

$$\bar{I}_{s_f} = \bar{I}_{s_{f_1}} + \bar{I}_{s_{f_2}} + \bar{I}_f \tag{6.30}$$

Substituting for $\bar{I}_{s_{f_1}}$, $\bar{I}_{s_{f_2}}$ and $\bar{I}_f$ from equations 6.25, 6.27 and 6.29 respectively in equation 6.30 gives

$$\bar{I}_{s_f} = (A_Y + A_x + Y_F) \bar{V}_{s_f} \tag{6.31}$$

or,

$$\bar{V}_{s_f} = (A_Y + A_x + Y_F)^{-1} \bar{I}_{s_f}$$

$$= (A_Y + A_x + Y_F)^{-1} Y_F \bar{E}_f \quad (\because \bar{I}_{s_f} = Y_F \bar{E}_f) \tag{6.32}$$

The inverse Fourier transform of $\overline{I}_{RR_1}$ and $\overline{I}_{RR_2}$ defines the instantaneous values of the switching transient currents $I_{s_{tr}}(t)$ and $I_{R_{tr}}(t)$ at the sending end and the receiving end respectively.

The fault transient currents at the sending end and the receiving end may then be evaluated as follows:

$$I_{s_F}(t) = I_s(t) + I_{s_{tr}}(t) \qquad 6.33$$

$$I_{R_F}(t) = I_R(t) + I_{R_{tr}}(t) \qquad 6.34$$

The voltages at the sending end and the receiving end are unaltered by the occurrence of the fault as both the ends are connected to the infinite busbar source.

Transient voltages and currents at the fault point

The transient voltage at the location of fault is determined as follows:

$$V_{x_F}(t) = V_x(t) + V_{x_{tr}}(t) \qquad 6.35$$

where

$V_{x_{tr}}(t)$ = inverse Fourier transform of $\overline{V}_{s_f}$, $\overline{V}_{s_f}$ being determined by equation 6.32.

Similarly, the fault transient current at the location of fault may be evaluated. The inverse Fourier transform of $\overline{I}_{s_{f_1}}$ and $\overline{I}_{s_{f_2}}$ defines the instantaneous values of line currents on the either side of the fault due to the switching only and the prefault steady state current is defined by equation 6.12.

The voltages and currents at any other point on the system due to the fault at a distance x from the receiving end

Let the distance of the point from the receiving end be x'. The steady state voltages and currents on the system at x' are determined by substituting x' for x, in equation 4.63 as follows:

$$V_{x'} = B_{x'}^{-1} (I_R - A_{x'} V_R) \qquad 6.36$$

$$I_{x'} = B_{x'} V_{x'} + A_{x'} V_R \qquad 6.37$$

where

$$A_{x'} = Y_o \cot h \psi x' \qquad B_{x'} = -Y_o \operatorname{cosec} h \psi x'$$

The system condition at the location of fault is defined as described earlier by equations 6.5 and 6.6.

For the point in section y (i.e. for x' > x) the switching transients at x' due to the fault at x are evaluated as follows:

$$\begin{bmatrix} \bar{I}_{s_{f_1}} \\ \bar{I}_{x'} \end{bmatrix} = \begin{bmatrix} A_d & B_d \\ B_d & A_d \end{bmatrix} \begin{bmatrix} \bar{V}_{s_f} \\ \bar{V}_{x'} \end{bmatrix} \qquad 6.38$$

where $\bar{I}_{s_{f_1}}$ and $\bar{V}_{s_f}$ are defined by equations 6.18 and 6.32.

From equation 6.38

$$\bar{V}_{x'} = B_d^{-1} (\bar{I}_{s_{f_1}} - A_d \bar{V}_{s_f}) \qquad 6.39$$

$$\bar{I}_{x'} = B_d \bar{V}_{s_f} + A_d \bar{V}_{x'} \qquad 6.40$$

Similarly, for the point in section x (i.e. for $x' < x$) $\overline{V}_{x'}$ and $\overline{I}_{x'}$ are defined as follows:

$$\overline{V}_{x'} = B_d^{-1} (\overline{I}_{s_{f_2}} - A_d \overline{V}_{s_f}) \qquad 6.41$$

$$\overline{I}_{x'} = B_d \overline{V}_{s_f} + A_d \overline{V}_{x'} \qquad 6.42$$

where

$$d = |x' - x|$$

$$A_d = Y_o \coth \psi d$$

$$B_d = -Y_o \operatorname{cosech} \psi d$$

Fault transient voltages and currents at x' may be evaluated as follows:

$$V_{x'F}(t) = V_{x'}(t) + V_{x'_{tr}}(t) \qquad 6.43$$

$$I_{x'F}(t) = I_{x'}(t) + I_{x'_{tr}}(t) \qquad 6.44$$

where

$V_{x'_{tr}}(t)$ = inverse Fourier transform of $\overline{V}_{x'}$

$I_{x'_{tr}}(t)$ = inverse Fourier transform of $\overline{I}_{x'}$

6.2.1.2 Lumped parameter source

Consider the system shown in Fig. 6.3. Let the emf's per phase, the series impedance per phase and the neutral impedance of the sources at either end be known.

For this system the sending end terminal voltages may be determined as follows:

$$V_s = \begin{bmatrix} V_{s_1} \\ V_{s_2} \\ V_{s_3} \end{bmatrix} = \begin{bmatrix} E_{s_1} \\ E_{s_2} \\ E_{s_3} \end{bmatrix} - \begin{bmatrix} Z_g & 0 & 0 \\ 0 & Z_g & 0 \\ 0 & 0 & Z_g \end{bmatrix} \begin{bmatrix} I_{s_1} \\ I_{s_2} \\ I_{s_3} \end{bmatrix} - \begin{bmatrix} Z_{ns} & Z_{ns} & Z_{ns} \\ Z_{ns} & Z_{ns} & Z_{ns} \\ Z_{ns} & Z_{ns} & Z_{ns} \end{bmatrix} \begin{bmatrix} I_{s_1} \\ I_{s_2} \\ I_{s_3} \end{bmatrix} \quad 6.45$$

or,

$$V_s = E_s - Z_s I_s \quad 6.46$$

where

$$[Z_s] = \begin{bmatrix} Z_{g_s}+Z_{ns} & Z_{ns} & Z_{ns} \\ Z_{ns} & Z_{g_s}+Z_{ns} & Z_{ns} \\ Z_{ns} & Z_{ns} & Z_{g_s}+Z_{ns} \end{bmatrix}$$

Similarly the terminal voltages at the receiving end may be defined as follows

$$V_R = E_R - Z_R I_R \quad 6.47$$

where

$$Z_R = \begin{bmatrix} Z_{g_r}+Z_{nr} & Z_{nr} & Z_{nr} \\ Z_{nr} & Z_{g_r}+Z_{nr} & Z_{nr} \\ Z_{nr} & Z_{nr} & Z_{g_r}+Z_{nr} \end{bmatrix}$$

The system currents I_s and I_R may be expressed in terms of V_s and V_R according to the relation defined by equations 6.3 and 6.4.

Substituting for V_s and V_R from equations 6.46 and 6.47 in equation 6.3 gives

$$I_s = A_L(E_s - Z_s I_s) + B_L(E_R - Z_R I_R) \qquad 6.48$$

or,

$$(1 + A_L Z_s)I_s + B_L Z_R I_R = A_L E_s + B_L E_R \qquad 6.49$$

Similarly, from equations 6.46, 6.47 and 6.48 I_R is given by

$$B_L Z_s I_s + (1 + A_L Z_R)I_R = B_L E_s + A_L E_R \qquad 6.50$$

Equations 6.49 and 6.50 may also be expressed as follows:

$$\begin{bmatrix} 1 + A_L Z_s & B_L Z_R \\ B_L Z_s & 1 + A_L Z_R \end{bmatrix} \begin{bmatrix} I_s \\ I_R \end{bmatrix} = \begin{bmatrix} A_L & B_L \\ B_L & A_L \end{bmatrix} \begin{bmatrix} E_s \\ E_R \end{bmatrix} \qquad 6.51$$

If $Z_s = Z_R = 0$ then $V_s = E_s$ and $V_R = E_R$, and for the particular case equation 6.51 reduces to equation 4.58.

I_s and I_R may be determined directly from equation 6.51 as follows:

$$\begin{bmatrix} I_s \\ I_R \end{bmatrix} = \begin{bmatrix} 1 + A_L Z_s & B_L Z_R \\ B_L Z_s & 1 + A_L Z_R \end{bmatrix}^{-1} \begin{bmatrix} A_L & B_L \\ B_L & A_L \end{bmatrix} \begin{bmatrix} E_s \\ E_R \end{bmatrix} \qquad 6.52$$

I_s and I_R may also be expressed in the simplified forms. From equation 6.49 I_R may be determined as follows:

$$I_R = - B_L Z_R^{-1} \left\{ (1 + A_L Z_s) I_s - (A_L E_s + B_L E_R) \right\} \qquad 6.53$$

and, substituting for I_R from 6.53 in equation 6.50 I_s may be defined as follows:

$$I_s = D^{-1} C \qquad 6.54$$

where

$$C = \left\{ (B_L E_s + A_L E_R) - (1 + A_L Z_R)(B_L Z_R)^{-1} (A_L E_s + B_L E_R) \right\}$$

$$D = \left\{ -(1 + A_L Z_R)(B_L Z_R)^{-1} (1 + A_L Z_s) + B_L Z_s \right\}$$

Thus I_s is defined and once I_s is known, I_R, V_s and V_R may be determined from the relations defined by equations 6.53, 6.54 and 6.47 respectively.

Then the voltages and currents at a distance x from the receiving end may be evaluated in terms of V_R and I_R from equations 6.5 and 6.6.

The instantaneous values of the steady state voltages and currents at the various points on the system are known from the relations defined by equations 6.7 to 6.12.

The shunt fault at a distance x from the receiving end is simulated as described in the previous section and $E_f(t)$ and I_{s_f} are determined according to the relations defined by equations 6.14 and 6.16 respectively.

The switching transients in the system due to the hypothetical emf sources simulating the fault are obtained by solving the circuit shown in Fig. 6.4.

In the system of Fig. 6.4 $\overline{V_{RR_1}}$ and $\overline{V_{RR_2}}$ may be defined as follows:

$$\overline{V_{RR_1}} = - Z_s \overline{I_{RR_1}} \qquad 6.55$$

and,

$$\overline{V_{RR_2}} = - Z_R \overline{I_{RR_2}} \qquad 6.56$$

$\overline{I_{RR_1}}$ may be defined by equation 6.19 and substituting for V_{RR_1} from equation 6.55 in equation 6.19 gives

$$\overline{I_{RR_1}} = B_y \overline{V_{s_f}} - A_y Z_s . \overline{I_{RR_1}}$$

or,

$$\overline{I_{RR_1}} = (1 + A_y Z_s)^{-1} B_y \overline{V_{s_f}} \qquad 6.57$$

$\overline{I_{s_f}}$ may be defined by equation 6.19 and substituting for $\overline{V_{RR_1}}$ and $\overline{I_{RR_1}}$ from equations 6.55 and 6.57 respectively in 6.19 gives

$$\overline{I_{s_{f_1}}} = A_y \overline{V_{s_f}} - B_y Z_s (1 + A_y Z_s)^{-1} B_y \overline{V_{s_f}}$$

$$= C_y \overline{V_{s_f}} \qquad 6.58$$

where

$$C_y = A_y - B_y Z_s (1 + A_y Z_s)^{-1} B_y$$

Proceeding similarly $\bar{I}_{RR_2}$ and $\bar{I}_{s_{f_2}}$ may be defined as follows:

$$\bar{I}_{RR_2} = (1 + A_x Z_R)^{-1} B_x \bar{V}_{s_f} \qquad 6.59$$

$$\bar{I}_{s_{f_2}} = \left\{ A_x - B_x Z_R . (1 + A_x Z_R)^{-1} B_x \right\} \bar{V}_{s_f}$$

$$= C_x \bar{V}_{s_f} \qquad 6.60$$

where

$$C_x = A_x - B_x Z_R (1 + A_x . Z_R)^{-1} B_x$$

The Fourier transform of the currents in the shunt admittance of the current generator may be defined by equation 6.29.

The currents at the location of fault are related by equation 6.30, and substituting for $\bar{I}_{s_{f_1}}$, $\bar{I}_{s_{f_2}}$ and $\bar{I}_f$ respectively from equations 6.58, 6.60 and 6.29 in equation 6.30 gives

$$\bar{I}_{s_f} = C_Y \bar{V}_{s_f} + C_x \bar{V}_{s_f} + Y_F \bar{V}_{s_f}$$

or,

$$V_{s_f} = -(C_Y + C_x + Y_F)^{-1} \bar{I}_{s_f}$$

$$= -(C_Y + C_x + Y_F)^{-1} Y_F \bar{E}_f \qquad 6.61$$

Thus $\bar{V}_{s_f}$ is known and $\bar{V}_{RR_1}$, $\bar{I}_{RR_1}$, $\bar{V}_{RR_2}$ and $\bar{I}_{RR_2}$ may be evaluated in terms of $\bar{V}_{s_f}$ from the relations defined by equations 6.55, 6.57, 6.56

and 6.59 respectively.

Then the fault-transient voltages and currents at the sending end and the receiving end may be determined as follows:

$$V_{s_F}(t) = V_s(t) + V_{s_{tr}}(t) \qquad 6.62$$

$$I_{s_F}(t) = I_s(t) + I_{s_{tr}}(t) \qquad 6.63$$

$$V_{R_F}(t) = V_R(t) + V_{R_{tr}}(t) \qquad 6.64$$

$$I_{R_F}(t) = I_R(t) + I_{R_{tr}}(t) \qquad 6.65$$

Similarly the fault transient voltages and currents at any other point on the system may be evaluated.

6.2.2 Single-End Fed System

6.2.2.1 Infinite busbar source

Consider the system shown in Fig. 6.5. The system is fed at the sending end from the infinite busbar source and the receiving end is open-circuited.

Let the voltages at the receiving end of the system be known and be represented as follows:

$$V_R = \begin{bmatrix} V_{R_1} \\ V_{R_2} \\ V_{R_3} \end{bmatrix} = \begin{bmatrix} V_{RM} \underline{/\theta_{vr1}} \\ V_{RM} \underline{/\theta_{vr2}} \\ V_{RM} \underline{/\theta_{vr3}} \end{bmatrix} \qquad 6.66$$

where

$$\theta_{vr1} = 0, \quad \theta_{vr2} = 2\pi/3, \quad \theta_{vr3} = 4\pi/3$$

In this system $[I_R] = [0]$ and V_s and I_s may be determined in terms of V_R and I_R as follows:

From equation 6.4, V_s is given by

$$V_s = B_\ell^{-1} (I_R - A_\ell V_R)$$

$$= -B_\ell^{-1} A_\ell V_R \qquad (\because I_R = 0)$$

$$= V_{SM} \underline{/\theta_{vs}} \qquad 6.67$$

and substituting for V_s and V_R from equations 6.67 and 6.66 in equation 6.3 gives

$$I_s = A_\ell V_s + B_\ell V_R$$

$$= I_{SM} \underline{/\theta_{is}} \qquad 6.68$$

The system voltages and currents at a distance x from the receiving end are defined by equation 4.6ϕ and for the receiving end open circuited these are defined as follows:

$$V_x = -B_x^{-1} A_x V_R$$

$$= V_{xM} \angle \theta_{vx} \qquad 6.69$$

$$I_x = A_x V_x + B_x V_R$$

$$= I_{xM} \angle \theta_{ix} \qquad 6.70$$

The instantaneous values of the steady state voltages and currents on the system may be evaluated according to the relation defined by equations 6.7 to 6.12. In this system V_{R_1} is the reference vector and all the phase angles are determined with respect to V_{R_1}.

Any shunt fault at a distance x from the receiving end may be simulated as described in the previous sections. Accordingly E_f, $E_f(t)$, I_{s_f} and $\overline{I_{s_f}}$ are determined from the relation defined by equations 6.13 to 6.16.

The switching transients only due to the emf sources simulating the fault in this system may be determined by solving the circuit shown in Fig. 6.6. In this circuit,

$$\left[V_{RR_1}\right] = \left[0\right] \qquad 6.71$$

and

$$\left[I_{RR_2}\right] = \left[0\right] \qquad 6.72$$

The Fourier transform of the equations for the section y of the system may be defined by the equation 6.17 and substituting for $\overline{V_{RR_1}}$ from equation 6.71 in equation 6.17 gives

$$\overline{I_{s_{f_1}}} = A_y \overline{V_{s_f}} \qquad 6.73$$

$$\overline{I_{RR_1}} = B_y \overline{V_{s_f}} \qquad 6.74$$

The section x of the system may be defined by equation 6.20. Accordingly,

$$\overline{V_{RR_2}} = -A_x^{-1} B_x \overline{V_{s_f}} \quad (\because \left[I_{RR_2}\right] = \left[0\right]) \qquad 6.75$$

Now, substituting for $\overline{V_{RR_2}}$ from equation 6.75 in equation 6.20 gives

$$\overline{I_{s_{f_2}}} = (A_x - B_x A_x^{-1} B_x)\overline{V_{s_f}} \qquad 6.76$$

The Fourier transform of the current in the shunt admittance of the equivalent current generator may be defined in terms of $\overline{V_{s_f}}$ by equation 6.29.

Now, $\overline{V_{s_f}}$ may be evaluated from the relation defined by equation 6.30, and substituting for $\overline{I_{s_{f_1}}}$, $\overline{I_{s_{f_2}}}$ and $\overline{I_f}$ from equations 6.73, 6.76 and 6.29, respectively in equation 6.30 gives

$$\overline{V_{s_f}} = (A_y + A_x - B_x A_x^{-1} B_x + Y_F)\overline{I_{s_f}}$$

or,

$$\overline{V_{s_f}} = (A_y + A_x - B_x A_x^{-1} B_x + Y_F)Y_F \overline{E_f} \qquad 6.77$$

($\because I_{s_f} = Y_F E_f$ according to equation 6.16).

For the fault at the receiving end

$$\left[\overline{I_{s_{f_2}}}\right] = \left[0\right] \qquad 6.78$$

and $\overline{V_{s_f}}$ is given by

$$\overline{V_{s_f}} = (A_y + Y_F)^{-1} \overline{I_{s_{f_1}}} \qquad 6.79$$

$$= (A_y + Y_F)^{-1} Y_F \overline{E_f} \qquad 6.80$$

Now, I_{RR_1} may be evaluated in terms of $\overline{V_{s_f}}$ by substituting equation 6.80 in equation 6.74. Then the fault transient current at the sending end is given by

$$I_{s_F}(t) = I_s(t) + I_{s_{tr}}(t) \qquad 6.81$$

where

$I_{s_{tr}}(t)$ = inverse Fourier transform of $\overline{I_{RR_1}}$

Similarly, the fault transient voltages and currents at any point on the system may be evaluated.

6.3 Summary and Conclusions

In this chapter a very general mathematical analysis of the evaluation of fault transients due to shunt faults in some typical three phase systems has been described. The analysis is based on the modal analysis and the application of modified Fourier transforms. The analysis of some other types of faults - series faults, simultaneous ~~faults~~ Shunt faults - are described in the Appendix 3.

The transmission line has been represented by a very sophisticated model and very approximate simplified conventional source models are con-

sidered, as it is easier to establish the transient behaviour of the transmission line with these source models. However, any complicated model of source may be incorporated provided they are suitably represented.

Typical system models considered here highlight the influences of different terminal conditions on the mathematical complexity of the analysis.

Analysis of the single-end fed system may be used for the study of the mid-point fault on the double-end fed system, and for this particular case the analysis of the double-end fed system is very much simplified.

Some other important features of this analysis may be summarised as follows:

(1) The analysis is very general and is applicable for both the transposed and the untransposed lines of any configuration.

(2) The frequency dependence of the system parameters may be taken into consideration.

(3) The analysis is suitable for any type of linear shunt fault.

(4) The analysis is suitable for any length of line.

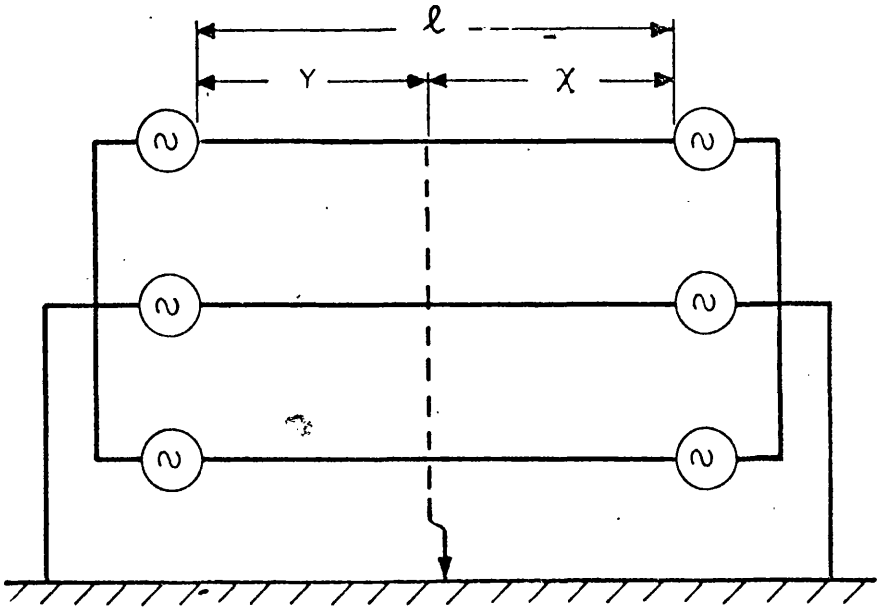

Fig. 6.1a Circuit of the Double-End Fed System (Infinite busbar source)

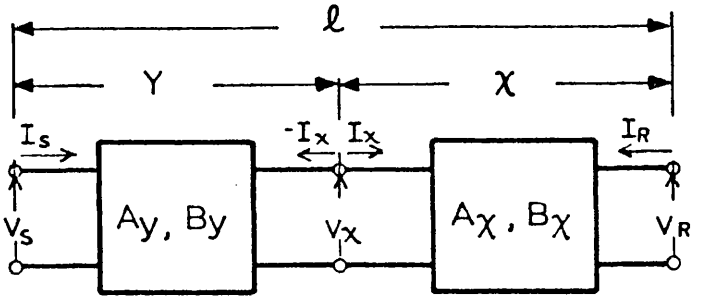

Fig. 6.1b Equivalent Block Diagram of the System

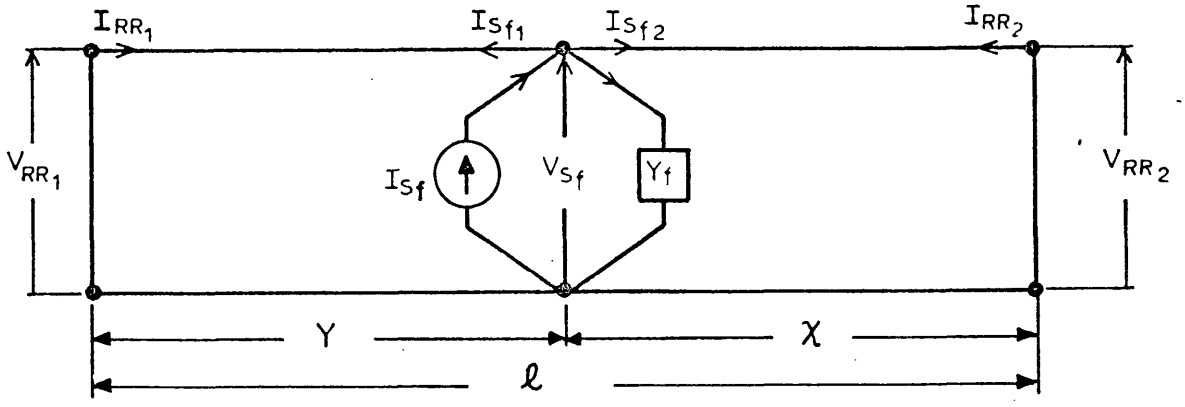

Fig. 6.2 One-line diagram of the faulted power system in which the hypothetical emf source simulating the fault is replaced by the equivalent current generator and the shunt admittance Y_f at the location of fault. The emf sources at either end in the prefault circuit are replaced by their respective source impedances.

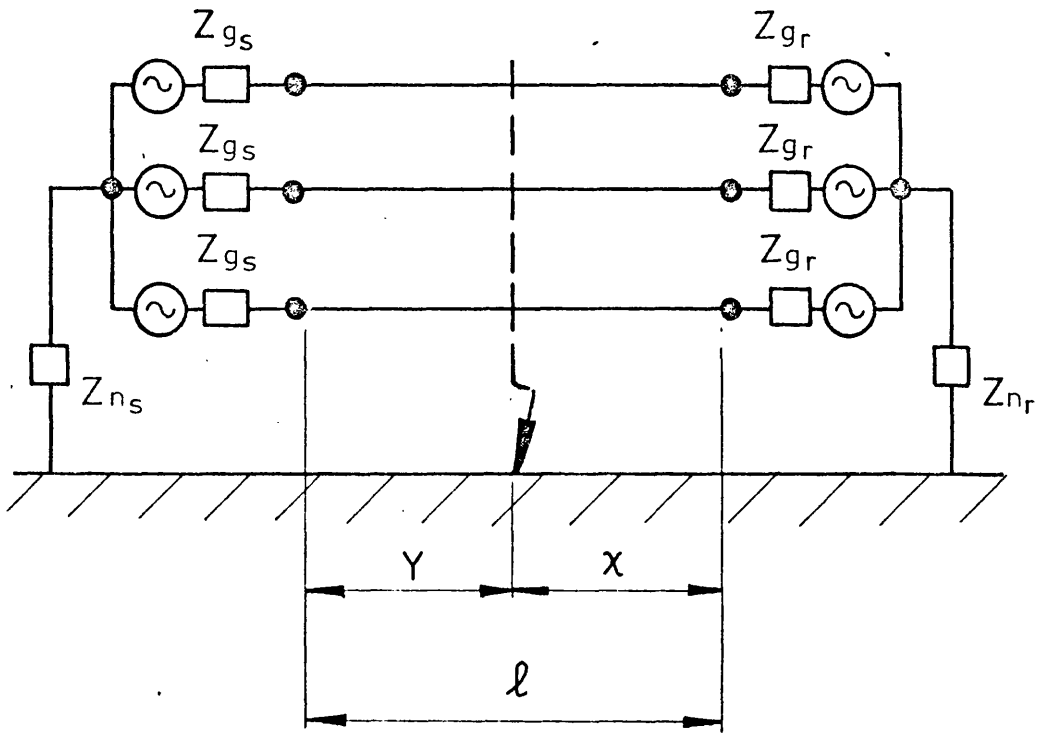

Fig. 6.3 Circuit of double-end fed system (Lumped parameter source)

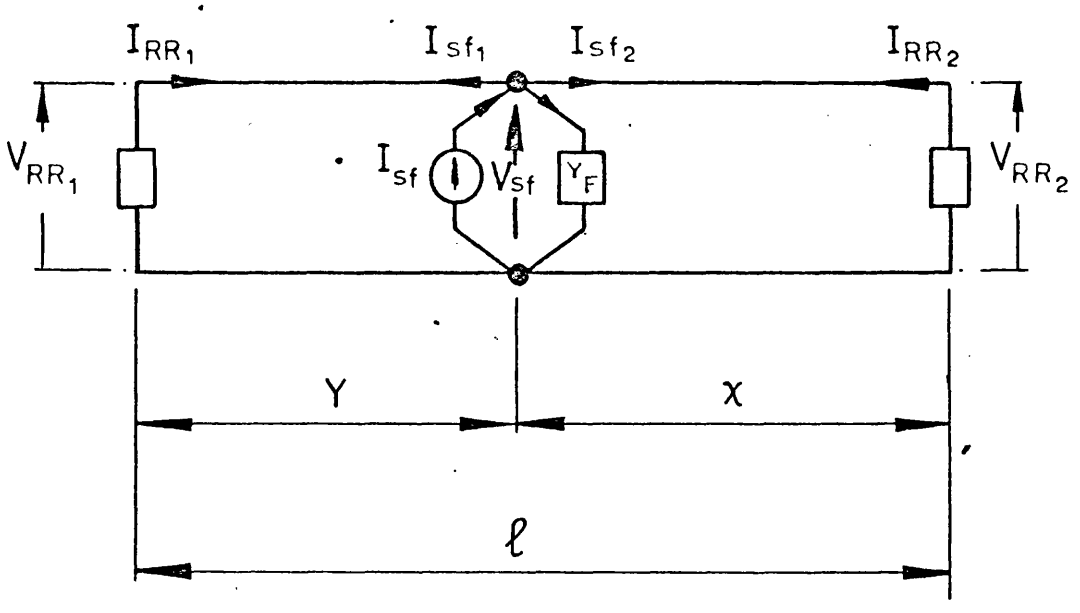

Fig. 6.4 One-line diagram of the faulted power system(shown in Fig. 6.3), in which the hypothetical emf source simulating the fault is replaced by the equivalent current generator and the shunt admittance Y_f at the location of fault. The emf sources at either end in the prefault circuit are replaced by their respective source impedances.

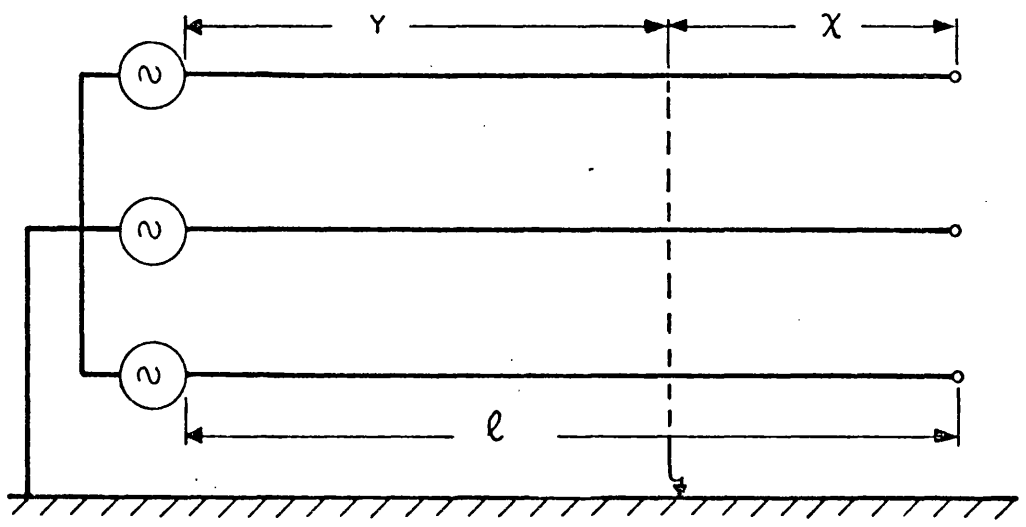

Fig. 6.5a Circuit of the Single-End Fed System

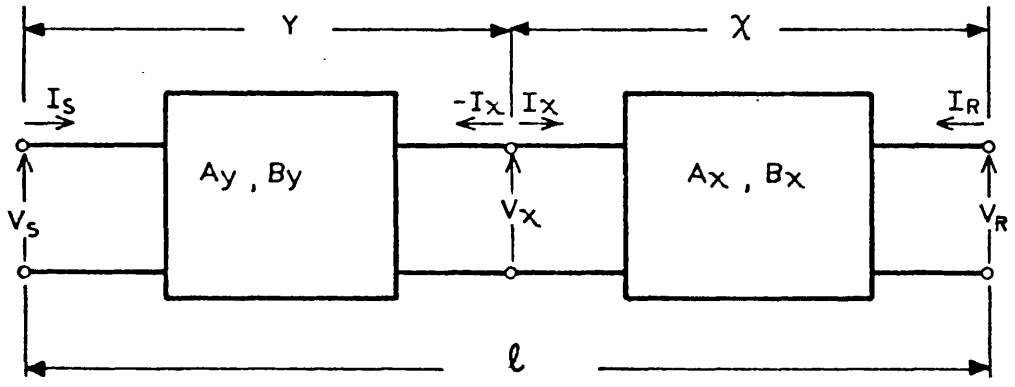

Fig. 6.5b Equivalent Block Diagram of the System

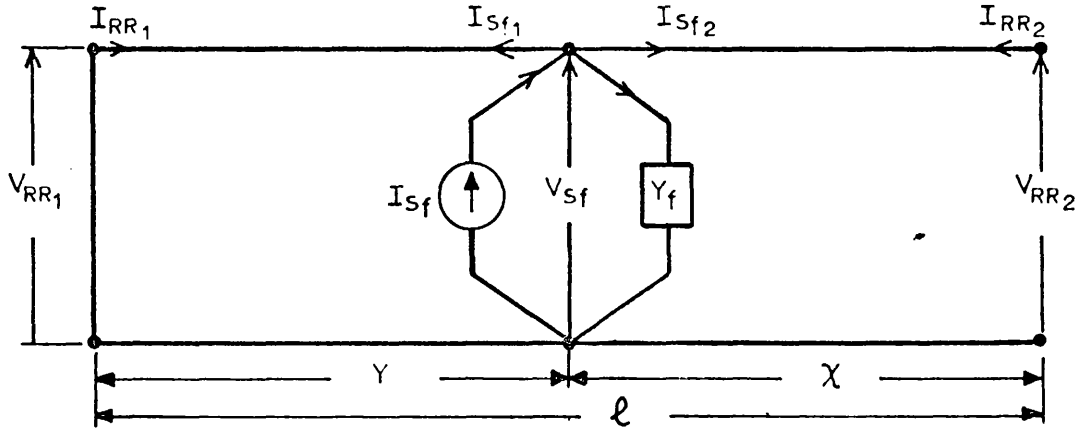

Fig. 6.6 One-line diagram of the faulted power system in which the hypothetical emf source simulating the fault is replaced by the equivalent current generator and the shunt admittance Y_f at the location of fault. The emf source at the sending end in the prefault circuit is replaced by its source impedance

CHAPTER 7

COMPUTATIONAL RESULTS FOR PRACTICAL LINES

7.1 Introduction

In this chapter the digital computer results for the fault transients due to the various types of shunt faults on the practical three-phase lines are presented.

The system models with the transmission system consisting of three phase transposed or untransposed line with uniformly distributed parameters have been studied. The source has been represented by simplified models in order that the transient response of the line may be established easily.

The system is considered to be under steady state condition before the occurrence of the fault and the results of the transient response are obtained by programming the formulations described in Chapter 6. The digital computer programme is described in the Appendix 5.

The transient response is evaluated at the sending and the receiving end relaying points only, as these are of main interest for the protective schemes. The results for the fault induced overvoltages are also presented and show excellent agreement with Kimbark's field test results.

7.2 Transposed Line

The data for the transposed line studied in this section are shown in Table 1. The parameters of the line are considered to be frequency-invariant and the constant 50Hz parameters are used throughout the study of the transposed line. The series impedance and the shunt admittance matrices per unit length are evaluated from the sequence parameters on the basis of the formulations described in Chapter 2.

7.2.1 Single end fed system, infinite busbar source

The system is energised at the sending end and the receiving end is open circuited before the occurrence of the fault.

The prefault voltages at the receiving end are defined as follows

$$\begin{bmatrix} V_{R1} \\ V_{R2} \\ V_{R3} \end{bmatrix} = \begin{bmatrix} \frac{400}{\sqrt{3}} & \underline{/0} \\ \frac{400}{\sqrt{3}} & \underline{/2\pi/3} \\ \frac{400}{\sqrt{3}} & \underline{/4\pi/3} \end{bmatrix} \quad \text{KV} \qquad \ldots \quad 7.1$$

where V_{R1}, V_{R2}, V_{R3} are the rms values of phase to neutral voltages of phases 1, 2 and 3 respectively.

In each case described in sections 7.2.1.1 and 7.2.1.2 the fault occurs at the receiving end, when the voltage of the reference vector V_{R1} is at its peak value.

The impedance of the fault is assumed to be 0.1Ω whether this fault is between line to ground or between line to line for each type of fault described in section 7.2.1.1 and 7.2.1.2.

The number of samples used is 256 for the evaluation of the solution in the time domain by the technique of modified Fourier transform.

The voltage at the sending end relaying point remains unaltered even after the inception of the fault since the source is infinite busbar, hence the results for the transient fault currents are only presented.

7.2.1.1 32 Km transposed line

This line is selected for the study as it is easier to verify the accurate formulation described in section 6.2.2.The results from the accurate formulation and the approximate formulations described in Appendix 4 are recorded on the same graph for the purposes of comparison. The approximate formulations neglect the influence of the distributed shunt capacitances as it is well known that for short lines the influence of the shunt capacitance is negligible. In the approximate model the influence of the prefault charging current is neglected.

In each of the following studies the line resistance is assumed to be zero and the influence of the fault impedance is neglected for the evaluation of the results from the approximate formulations, as the line impedance is much higher than the fault impedance.

The transient fault current at the sending end are evaluated from the accurate formulations described in Section 6.2.2 after forming the suitable Y_F matrix depending on the type of fault. The transient fault current at the sending end for the approximate model is evaluated on the basis of the solution described in Appendix 4.

SLG Fault

The sending end current for SLG fault at the receiving end, according to the approximate formulations are defined as follows:-

$$I_s(t) = I_m \left\{ \cos(\omega_s t + \phi - \theta) - e^{-\frac{R_s t}{L_s}} \cos(\phi - \theta) \right\} \qquad 7.2$$

for

$R_s = 0$ and $R_m = 0$, equation 7.2 reduces to the form

$$I_s(t) = I_m \left\{ \cos(\omega_s t + \phi - \theta) - \cos(\phi - \theta) \right\} \qquad 7.3$$

where

$$I_m = \frac{V_{s\ peak}}{Z_e}$$

$$Z_e = \sqrt{R_s^2 + (\omega_s L_s)^2}$$

$V_{s\ peak} = V_{R\ peak}$ (in this case)

$$\theta = \tan^{-1} \frac{\omega L_s}{R_s} = \pi/2 \quad (\because R_s = 0)$$

ϕ = phase angle of sending end voltage at the instant of fault inception.

= 0 for phase 1

= $(2/3)\pi$ for phase 2

= $\frac{4}{3}\pi$ for phase 3.

Double-line to ground fault

According to the approximate formulation, the sending end current due to line to ground faults on phases 1 and 2 are given by

$$I_{s_1}(t) = \frac{I_a(t) + I_b(t)}{2} \qquad 7.4$$

$$I_{s_2}(t) = \frac{I_a(t) - I_b(t)}{2} \qquad 7.5$$

where

$$I_a(t) = I_{ma}\left\{\cos(\omega_s t + \phi_a - \theta) - \cos(\phi_a - \theta)\right\}$$

$$I_b(t) = I_{mb}\left\{\cos(\omega_s t + \phi_b - \theta) - \cos(\phi_b - \theta)\right\}$$

for $R_s = R_m \simeq 0$

$$I_{ma} = (V_{s_1} + V_{s_2})/(Z_s + Z_m)$$

$$I_{mb} = (V_{s_1} - V_{s_2})/(Z_s - Z_m)$$

ϕ_a = phase angle of the vector $V_{s_1} + V_{s_2}$ at the instant of fault inception

ϕ_b = phase angle of the vector $V_{s_1} - V_{s_2}$ at the instant of fault inception

In this case,

$$\theta = \tan^{-1}\frac{\omega L}{R} = \pi/2 \quad (\because R = 0)$$

and for fault on phases 1 and 2, ϕ_a and ϕ_b are defined as follows

$$\phi_a = \pi/3$$

$$\phi_b = -\pi/3$$

ϕ_a and ϕ_b for faults involving phases 1 and 3, and 2 and 3 are defined by the vectors V_{s_1} and V_{s_3}, and vectors V_{s_2} and V_{s_3} respectively.

Line to line fault

The sending end current for the line to line fault on phases 1 and 2 are given by

$$I_{s_1} = I_m \left\{ \cos(\omega_s t + \phi - \theta) - \cos(\phi - \theta) \right\} \qquad 7.6$$

$$(\because R = 0)$$

and

$$I_{s_2} = -I_{s_1}$$

where

$$I_m = \frac{V_{s\ peak}}{Z_e}$$

$$Z_e = 2(Z_s - Z_m)$$

ϕ = phase angle of vector $V_{s_1} - V_{s_2}$ at the instant of fault inception.

The results for faults involving phases 1 and 3, and phases 2 and 3 are obtained by substituting suitable values of ϕ in the above equations. The value of ϕ in these cases are defined by the phase angles of the line-to-line voltage between phases 1 and 3 and phases 2 and 3 respectively.

Three-phase fault

The sending end current due to three-phase fault at the receiving end is given by

$$I_s(t) = I_m \left\{ \cos(\omega_s t + \phi - \theta) - \cos(\phi - \theta) \right\} \qquad 7.7$$

where

$$I_m = \frac{V_{s\ peak}}{Z_e}$$

$$Z_e = Z_s - Z_m$$

ϕ = phase angle of the sending end voltage at the instant of fault inception.

= 0 for phase 1

= $(2/3)\pi$ for phase 2

= $(4/3)\pi$ for phase 3

Fig. 7.1a, 7.1b, 7.1c show the transient fault current at the sending end due to SLG fault on phases 1, 2 and 3 respectively.

The results for double line to ground fault involving phases

(a) 1 and 2

(b) 1 and 3

(c) 2 and 3

are shown in Figs. 7.2a, 7.2b, 7.2c respectively.

The results for line to line fault involving phases

(a) 1 and 2

(b) 1 and 3

(c) 2 and 3

are shown in Figs. 7.3a, 7.3b, 7.3c respectively.

Fig. 7.4 shows the transient fault current at the sending end due to the three-phase fault at the receiving end.

These results for faults on short line are well-known. In each case, excellent agreement is seen between the results of the accurate

and the approximate model. The close agreement between the results of both the methods confirm the validity of the formulation developed in Section 6.2.2.

The above results also confirm that the distributed shunt capacitance may be neglected for short line studies without any significant error.

7.2.1.2 160 Km transposed line, single end fed system, infinite busbar source

SLG fault

*Figs. 7.5a, 7.5b, 7.5c show the transient fault current at the sending end due to the occurrence of single line to ground fault at the receiving end respectively on phases 1, 2 and 3.

The build up of current in the faulted phases in this case is due to the arrival of the first incident fault surge and its successive reflection between the sending end and the fault, and the mechanism is similar to that for the single phase case.

The fault current due to SLG fault consists of two components - aerial mode and the earth mode. The presence of these two components is clearly seen in Fig. 7.5a. The difference in the time of arrival of these components is responsible for the formation of a very small step on the sending end current due to the arrival of the first incident wave of fault surge. This small step is distinguishable in this case because of very large difference in the velocity of propagation of these two component waves.

The values of time delay in the arrival of the first incident wave of fault surge, the time interval between any consecutive reflections and the peak value of the sending end current due to the arrival of the

* These results show the influence of frequency invariant line parameters and the large difference in the velocities of propagation of the slow and fast components on the fault transient waveform due to SLG fault.

first incident wave of fault surge obtained from Fig 7.5a are in good agreement with the velocities of propagation and surge impedance of the line. These quantities, hereafter, will be referred to as T, Ti and I. The values of T and I are shown in table 2 for each type of fault.

The currents in the unfaulted phases are also disturbed. This is due to the mutual electromagnetic and electrostatic coupling of these phases with the faulted phase.

The induced current in the unfaulted phases are equal because the line is ideally transposed. However, from Figs. 7.5a, 7.5b and 7.5c it is seen that the total current in these two phases are not exactly equal - this is due to the difference in the prefault charging current flowing in these phases.

From Figs. 7.5a, 7.5b and 7.5c it is seen that the waveform of the transient fault current depends on the phase angle of the prefault voltage at the location of fault at the instant of fault inception. It is further observed from these figures that the peak value of the total build-up of current (positive or negative) also depends upon the phase angle at the instant of fault inception of the prefault voltage at the location of fault.

Double line to ground fault

The transient fault current at the sending end due to the double line to ground fault involving phases (a) 1 and 2, (b) 1 and 3, (c) 2 and 3 are shown in Figs. 7.6a, 7.6b and 7.6c respectively.

It is seen from these figures that the waveform and the peak value of the total build-up of current in the faulted phases depend on the phase angles at the instant of fault inception of the prefault voltages at the location of fault.

It is further observed from Figs. 7.6a and 7.6b that the current due to double line to ground fault constitutes mainly of the aerial mode, as the time interval between any two consecutive reflections agrees with velocity of propagation of the aerial mode in these cases

The values of T and I obtained from Fig. 7.6a are in good agreement and are shown in Table 2.

In this case the currents in the faulted phases are not exactly equal to each other as in the case of line to line fault, hence the current in the unfaulted phase is somewhat disturbed.

Line to line fault

The transient fault current at the sending end due to the line to line fault involving phases (a) 1 and 2, (b) 1 and 3, (c) 2 and 3 are shown in Figs. 7.7a, 7.7b and 7.7c respectively.

In the case of line to line fault the current in the faulted phases due to the hypothetical emf sources simulating the fault is exactly equal and opposite to each other, as the line is ideally transposed. However, the fault currents in these lines are slightly different from each other, due to the difference in the prefault charging currents in these phases.

Since the line is ideally transposed and the currents in the faulted phases are equal and opposite to each other neglecting the slight difference due to the prefault current, the induced current in the unfaulted phase should be ideally zero, and the prefault current should flow in this phase unaffected. However, some disturbance is observed in the fault current in the unfaulted phase, and is due to the error in the numerical evaluation of the induced current. The numerical error is comparable with the low value of charging current, hence the

disturbance in these look somewhat prominent.

It is seen from these figures that the waveform and the peak value of the total build up of current depends on the phase angle at the instant of fault inception of the prefault voltage at the location of fault.

It is further observed from Figs. 7.7a and 7.7b that the current due to line to line fault consists of aerial mode components only.

The values of T and I are in good agreement and are shown in Table 2.

Three-phase fault

Fig. 7.8 shows the transient fault current at the sending end due to three phase fault at the receiving end.

It is seen from Fig. 7.8 that at every instant of time

$$I_{s_1} + I_{s_2} + I_{s_3} = 0 \qquad (7.8)$$

which is expected for a balanced fault on an ideally transposed line.

The values of T and I obtained from Fig. 7.8 are in good agreement and are shown in Table 2.

It is further observed from Fig. 7.8 that the current due to three phase fault consists of aerial mode components only, because the delay time T, and the time interval between any two consecutive reflections T_i agree with velocity of propagation of the aerial mode.

7.2.2 Double-end fed system, 288Km line, infinite bus-bar source

The system studied consists of the transmission line described in section 7.2.1. The data of the line is the same as that studied by Kimbark[26]. The system is fed at the sending- and receiving-ends from the infinite busbar source, The terminal voltages are defined as follows

$$\left[V_s\right] = \left[V_R\right] = \begin{bmatrix} \frac{400}{\sqrt{3}} & \angle 0 \\ \frac{400}{\sqrt{3}} & \angle 2\pi/3 \\ \frac{400}{\sqrt{3}} & \angle 4\pi/3 \end{bmatrix} \quad \text{KV (rms. phase to neutral)} \qquad (7.9)$$

The length of the line is 288Km and the parameters of the line are considered to be frequency invariant.

The solid fault is simulated by assuming the fault impedance to be $10^{-6}\Omega$. The total number of samples used for the solution of the inverse Fourier transform is 256.

In this section the results are presented for SLG fault only and the phenomenon of the fault induced overvoltage is studied.

The transient fault currents at the relaying points at the sending end and the receiving end for shunt faults, at the midpoint of the system will be very similar to those for the single-ended system described in section 7.2.1.2. There will be some differences in the results because the distance to fault from the sending end in single-ended system is slightly different from that in the case of double-ended system, however the general nature of the waveform in both cases will be very similar and hence these are not separately evaluated again in this section.

7.2.2.1 SLG fault at midpoint of line

The system and its prefault condition is exactly the same as that considered by Kimbark. The results for SLG fault are obtained on the

basis of the fomulation described in chapter 6 and are compared with those predicted by Kimbark et al.

The fault occurs when the voltage at the location of fault is near its (-)ve peak value. Similar instant of fault initiation has been considered by Kimbark and others.[26]

Fig. 7.9α shows the variation of voltages on the different phases both under the prefault and post-fault conditions at the location of fault.

The voltage on the faulted phase should ideally drop down to zero and the voltages on the unfaulted phases jump up at the instant of fault inception at the location of fault, according to the predicted results of Kimbark and others.

However, in this case some time delay is observed in the occurrence of such change and this is due to the time delay inherent to the technique of modified Fourier transform. The reason for this is the finite truncation of the Fourier integral[21].

The initial jump in the unfaulted phases is due to the mutual electromagnetic and electrostatic coupling of all the phases. It is seen from Fig. 7.9α that the value of the initial jump is approximately 0.3p.u. at the instant of fault inception, neglecting the slight time delay due to the reason mentioned above. This value of initial jump shows excellent agreement with Kimbark's prediction and is in proportion to the mutual surge impedances of the unfaulted phases with respect to the faulted phase.

The value of the initial jump may be determined from the surge impedance of the line as follows:

let the injected current to the faulted phase at the location of the fault be I_f. The injected current to the unfaulted phase is zero. Let the emf of the hypothetical source (simulating the fault) at the instant

of fault inception be V_1.

Then the induced voltages on the unfaulted phases may be evaluated from the following relation

$$[V] = [Z_o][I]$$

or,

$$V_1 = Z_{o_s} I_1$$

or,

$$I_1 = V_1/Z_{o_s}$$

and

$$V_2 = V_3 = Z_{o_m} I_1 = \frac{Z_{o_m}}{Z_{o_s}} V_1 \qquad 7.10$$

where V_2 and V_3 are the induced voltages on phases 2 and 3 respectively.

Substituting for the values of self- and mutual surge impedance from Table 1 in equation 7.9a gives

$$V_2 = V_3 \simeq 0.3 \qquad 7.11$$

The formation of pulse in this case is mainly due to the difference in the velocities of propagation of the aerial and earth modes.[26] The times of arrival of these components (at the location of fault) after their first reflection at the terminals of the line may be determined as follows

Time of arrival of aerial mode $= \frac{\ell}{V_f} = 0.977$ ms

Time of arrival of earth mode $= \frac{\ell}{V_s} = 1.605$ ms

These values are also observed from Fig. 7.9a.

The peak value of the pulse = 1·9 (from Fig.7·9a)

= 2·0 (Predicted)

Thus, the peak value of pulse, the time of arrival of the aerial and earth modes after their first reflection at the sending and receiving end terminals also show excellent agreement with the predicted results.

Fig. 7.9b shows the result for the above case but for longer observation period. In this case, it is seen that pulses are periodic as predicted by Kimbark.

7.2.2.2. SLG fault, 96Km from sending end

Fig 7·10a shows the variation of phase voltages at the location of fault after the occurrence of fault at 96 KM from the sending-end. It is seen from this figure that the peak value of the pulse is less than that in the case of the fault at the mid-point of the line and as predicted by Kimbark.

Fig 7·10b shows the variation of voltage at the location of fault for the above case for a longer observation time. In this case it is seen that the pulses are not periodic and is in agreement with Kimbark's prediction.

7.3 Untransposed Line

Details of the Line

400KV untransposed line shown in Fig. 7.11 is chosen for the study. This is a typical example of an untransposed line and its conductors are not symmetrically arranged about each other as is usually the case with horizontal lines. The circuit configuration of the line, the mean heights of the conductors above the ground, and the mean spacings between the conductors are shown in Fig. 7.11.

The data for the line conductors are as follows. The phase conductors consist of a bundle of quad conductors. Each subconductor of this bundle is of size 54/7/0.125 SCA and is arranged at the corners of a square with 1 foot sides.

The earth wire consists of 1 x 54/7/0.125 SCA. The earth is assumed to be homogeneous throughout and its resistivity is assumed to be 30Ω-m throughout the calculation.

The parameters of the line are considered to be distributed and frequency dependent and are evaluated directly from the knowledge of the heights and spacings of the conductors on the basis of the formulations described in Chapter 2.

7.3.1 Double end fed system, infinite busbar source

The system studied consists of the transmission line described above and is fed at either end from the infinite busbar source. The system is considered to be under steady state condition before the occurrence of the fault. The prefault sending end and the receiving end terminal voltages are defined as follows:

$$\left[V_s\right] = \begin{bmatrix} \frac{400}{\sqrt{3}} & \underline{/0} \\ \frac{400}{\sqrt{3}} & \underline{/2\pi/3} \\ \frac{400}{\sqrt{3}} & \underline{/4\pi/3} \end{bmatrix} \quad \text{KV (RMS phase to neutral)}$$

$$\left[V_R\right] = \begin{bmatrix} \frac{400}{\sqrt{3}} & \underline{/-\beta} \\ \frac{400}{\sqrt{3}} & \underline{/2\pi/3 - \beta} \\ \frac{400}{\sqrt{3}} & \underline{/4\pi/3 - \beta} \end{bmatrix} \quad \text{KV (RMS phase to neutral)}$$

where

β = phase angle between the sending end and the receiving end terminal voltages and represents the prefault power transfer

In sections 7.3.1.1 and 7.3.1.2 the results are presented for $\beta = 0$ and represents a system energised at either end without any prefault power transfer before the fault inception. In section 7.3.1.3 the results are presented for $\beta = \pi/6$.

In each of the following cases the fault occurs when the reference vector V_{s_1} is at its peak value.

The impedance of the fault is considered to be 0.1Ω for the fault between the line to ground or line to line.

The transient solutions are evaluated by programming the equations described in chapter 6 .

256 samples are used for the evaluation of the solution in the time domain from the frequency domain by the method of modified Fourier transform.

7.3.1.1 320Km untransposed line, double end fed system, infinite busbar source, mid-point fault, $\beta = 0$

In this section, the variations of the transient fault current at the sending end only is described as the receiving end current will be exactly the same as the sending end current due to the symmetrical location of the fault with respect to the other end.

SLG fault

Fig. 7.12a shows the transient fault current at the sending end due to the single line to ground fault on phase 1.

The variation of current in the faulted phases is due to the arrival of the first incident wave of fault surge and its successive reflection between the sending end and the location of fault.

It is seen from Fig. 7.12a that the transient disturbance almost disappears within a cycle after the fault inception.

In Fig. 7.5a, however, the transient disturbance in the faulted phase current is quite prominent over a cycle after the fault inception. The results for Fig. 7.5a, are obtained for the frequency invariant parameters, whereas the results for Fig. 7.12 are for frequency dependent parameters. Thus, the quick disappearance of the transient disturbance is due to the influence of the frequency dependence of the line parameters, neglecting the slight difference in 50Hz parameters of these two lines.

The frequency dependence of the line parameters is due to the influence of the earth and the skin effect and other line losses. The transient current due to the SLG fault consists of aerial mode and the earth mode. The earth mode is heavily attenuated due to the influence of the earth and the aerial mode is attenuated due to the line losses.

The results of Fig. 7.5a and 7.12a may be compared as the influence of the fault at the midpoint of a double end fed system is similar to that of the fault at the receiving end of a single ended system for the similar prefault condition and for the same distance of the fault from the sending end.

The currents in the unfaulted phases 2 and 3 are also disturbed and these currents are not equal to each other. The slight differences are due to the difference in the prefault charging current in these conductors and also due to the difference in the induced currents. The induced currents in the unfaulted phases are slightly different due to the untransposition of the lines.

The values of T and I obtained from Fig. 7.12a are in good agreement, and are shown in Table 3.

Figs. 7.12b and 7.12c show the transient fault current at the sending end due to the SLG fault on phases 2 and 3 respectively at the midpoint of the line. The influences of the frequency dependence of the parameters are also seen from these figures. These figures also show the influence of the phase angle (at the instant of fault inception) of the prefault voltage at the location of fault on the transient fault current.

Double line to ground fault

Fig. 7.13a shows the transient fault current at the sending end due to the double line to ground fault on phases 1 and 2 at the midpoint of the line.

From Fig. 7.13a it is seen that the transient disturbance in the sending end current is prominent within a cycle after the fault inception. The current due to the double line to ground fault consists mainly of the aerial mode, which has low attenuation, therefore,

the disturbance persists for a longer time.

The values of T_r and I obtained from Fig. 7.13a are in good agreement. The values are shown in Table 3.

Figs. 7.13b and 7.13c show the transient fault current at the sending end due to the double line to ground fault involving (a) phases 1 and 3, (b) phases 2 and 3 respectively.

Figs. 7.13a, 7.13b, 7.13c show the influence of the phase angles of the prefault voltages at the location of fault on the transient fault current.

Line to line fault

Fig. 7.14a shows the transient fault current at the sending end due to the line to line fault involving phases 1 and 2 at the midpoint of the line.

From Fig. 7.14a it is seen that the transient disturbance in the sending end fault current is present within a cycle (approx.) after the fault inception. This is due to the low attenuation of the aerial mode which consists of the fault current due to the line to line fault.

Fig. 7.14b and 7.14c show the transient fault currents at the sending end due to the line to line fault involving phases 1 and 3, and phases 2 and 3 respectively.

It is seen from these figures that the current in the faulted phases are almost equal and opposite to each other, and the differences in these currents is not very significant, neglecting the small difference in the prefault charging current. Hence it may be concluded that influences of untransposition of the line is not very significant.

Figs. 7.14a, 7.14b and 7.14c shows the influence of the phase angles

(at the instant of fault inception) of the prefault line to line, voltages at the location of fault on the waveform of the fault transient current.

The values of T and I obtained from Fig. 7.14a are in good agreement and are shown in Table 3.

Three-phase fault

Fig. 7.15 shows the transient fault current at the sending end due to the three-phase fault at the midpoint of the line.

The current due to the three-phase fault consists of the aerial mode components, hence the transient disturbance is persistent within a period of a cycle (approx.) after the fault inception.

It is seen from Fig. 7.15 that

$$I_{s_1} + I_{s_2} + I_{s_3} = I_n$$

where

$$I_n \neq 0$$

However the value of I_n is very small and it may again be concluded that that influence of untransposition is very insignificant at least for 160Km untransposed lines as I_n is very small.

The values of T and I obtained from Fig. 7.15 are in good agreement, and are shown in Table 3.

7.3.1.2 320 Km untransposed line, double end fed system, infinite busbar source, off-centre fault (32 Km from sending end), $\beta = 0$

In the present analysis the location of fault is considered to be at 32Km from the sending end.

The transient fault current at the sending end and the receiving end for the following types of fault

(a) SLG fault on phase 1

(b) double line to ground fault on phases 1 and 2

(c) line to line fault on phases 1 and 2

(d) three-phase fault.

are shown in Figs. 7.16, 7.17, 7.18 and 7.19 respectively.

The following expected general features are observed in each of these figures:

(1) the time delay for the fault surge to reach the sending end is negligible, whereas this is quite appreciable for the receiving end.

(2) the variation of current at the sending end is similar to that in a series RL circuit and hf transient disturbances are non-existent.

In the receiving end the hf components due to the fault surge are quite prominent.

(3) The magnitude of peak value of positive current is much higher at the sending end than at the receiving end.

7.3.1.3 320Km untransposed line, double end fed system, infinite busbar source, midpoint fault, $\beta = \pi/6$

In this case the prefault currents at the sending end and the receiving end are different due to the difference in the phase angles of the terminal voltages. Hence the fault transient currents at these ends are different in magnitude and the waveform, although the switching transient components at the either ends are the same due to the symmetrical position of the location of fault with respect to each end.

The influence of considerable prefault power transfer on the fault transient current is seen from Figs. 7.20 to 7.23.

SLG fault

Fig. 7.20 shows the sending end and the receiving end current due to SLG fault on phase 1 at the midpoint of the line. The fault occurs when the voltage on phase 1 at the midpoint is near its positive peak value.

In this case, the magnitude of the absolute peak value of current in each phase is much higher than the case (Fig. 7.12a) when the prefault power transfer is negligible.

The disturbance in the unfaulted phases is not very significant compared to the prefault current.

Three-phase fault

Fig. 7.23 shows the sending end and the receiving end transient fault current due to the three-phase fault at the midpoint of the line. In this case it is again observed that the magnitude of the absolute peak value of current is similar to that in the case (Fig. 7.15) when the prefault power transfer is negligible.

The neutral currents at the sending end and the receiving end are very small. Hence, it is again observed that the influence of untransposition is not very significant.

Line to line fault

Fig. 7.22 shows the transient fault current at the sending end and the receiving end due to the line to line fault on phases 1 and 2 at the midpoint of the line.

The current in the faulted phases are almost equal and opposite to each other at either ends. The slight difference is due to the difference in the prefault currents in these phases and due to the untransposition of the line.

From Fig. 7.22 it is seen that the disturbance in the unfaulted phase is negligible and the variation of current in this phase is according to its prefault value.

320 Km untransposed line, double end fed system, lumped parameter source. Midpoint fault, $\beta = 0$

Figs. 7.24a, 7.24b show the influences of purely inductive terminals on the transient voltages and currents at the sending end due to SLG fault on phase 1 at the midpoint of the line. The variation of the voltages and currents at the receiving end will be exactly similar to that at the sending end due to the symmetrical position of the fault with respect to the either end and are not shown separately.

The sending end voltage of the faulted phases drops down on the arrival of the first incident wave of fault surge at the sending end from the location of fault. This is due to the well-known behaviour of the inductive terminal, which, when energised momentarily behaves as an open circuit first and then acts as a short circuit.

The voltages on all the phases are disturbed due to the mutual coupling (electromagnetic and electrostatic) of the phase conductors. The maximum disturbance, however, occurs on the faulted phase.

The variation of current is similar to that in the case of infinite busbar source. The current is momentarily zero on the arrival of the first incident wave of fault surge at the sending end and then the current is doubled because the inductances act as short circuits.

From Fig.7.24b it is seen that T, T_i are in good agreement with the velocity of propagation and the peak value of the current due to the arrival of the first incident wave is in good agreement with the surge impedance of the line. The values of T and I are shown in Table 3.

7.4 Summary and Conclusions

In this chapter digital computer results for fault initiated transients have been described. The results are presented for each of the following types of shunt fault at one particular location only:

(a) single line to ground fault

(b) double line to ground fault

(c) line to line fault

(d) three-phase fault

The digital computer results are obtained on the basis of the formulations described in Chapter Six and confirm the validity and the generality of the formulations. The influence of the following factors on the transient response due to each of the above mentioned faults has been investigated:

(a) location of fault and the line length

(b) transposition and untransposition of line

(c) terminations - both stiff and weak source

(d) frequency dependence and frequency invariance of line parameters

(e) pre-fault power transfer

(f) fault impedance - low impedance faults only.

The following results and observations vividly confirm the validity of the formulations described in Chapter Six:

(a) excellent agreement with Kimbark's results for fault induced over-voltage due to SLG fault in the double end fed system.

(b) excellent agreement of the results of the sophisticated model and approximate model for short line fault

(c) excellent agreement of the time delay in the arrival of first incident wave of fault surge from the location of fault to the relaying point and

the time interval between any consecutive reflections.

(d) excellent agreement of the magnitude of first incident wave with surge impedance of line (assuming the surge impedance to be purely resistive).

On the basis of the results described in this chapter, the following conclusions and observations may be made.

(1) For each type of shunt fault the waveform of transient current depends upon the phase angle of the prefault voltage at the location of fault at the instant of fault inception. Similar influence of phase angle of the prefault voltage on the transient response was also observed in the single-phase circuit and is well-known.

(2) The peak value of the total build-up of current depends on the following factors:-

(a) the phase angle of the prefault voltage at the location of fault at the instant of fault inception.

(b) the location of fault

(3) The magnitude of the first incident wave of current defines the instant of fault inception.

(4) If the prefault current is neglected then the nature of the variation of current gives a clear indication of the type of fault, e.g.

(a) If the variation of current in one phase is much higher than that in the other phases then the fault is a single line to ground.

(b) If the variation of current is very large only in any two phases, but these currents are not equal and opposite to each other at every instant of time then these lines are involved in line to ground fault, i.e. this is a case for double line to ground fault.

(c) If the variation of current is very large in any two phases and these currents are equal and opposite to each other then these phases are involved in line to line fault.

(d) If the variation of current in each of the phases is very high and the sum of the phase currents is zero or approximately zero at every instant of time then this is the case for three-phase fault.

Conclusions (a) to (c) are true if the prefault current is negligible however, if the prefault current is not negligible then in this case the prefault current may be estimated during the post fault period and subtracted from the total fault current in order to establish the type of fault.

Thus, the type of fault and the instant of fault inception can be easily established from the current waveform.

(5) For a defined phase angle of the prefault voltage at the instant of fault inception the peak value of the total build-up of current is a clear indication of the location of fault. The location of fault may also be known from the time delay in the arrival of the first incident wave of fault surge or the time interval between any two consecutive reflections and the propagation velocities.

(6) Thus, the current waveform is very useful as far as the simplified sources - infinite busbar and the lumped parameter source - are concerned. For both these sources the variation of current is similar at the terminals of the line as the source impedance is usually very much less than the self-surge impedance of the line. For infinite bus bar source the voltage at the terminals are unaffected due to any type of fault. But for lumped parameter source the terminal voltage

are very much disturbed with main disturbance appearing on the faulted phase(s).

(7) The influence of untransposition is very insignificant - this is clearly seen from the results of line to line fault and three-phase to earth fault. Hence, the influence of untransposition may be neglected if very high degree of accuracy is not desired. Moreover, the study of the transposed line may be further justified because of the computational efficiency and economy in computation time.

(8) The results presented are for very low values of fault impedance only in order to get the maximum of current. But the fault transients due to high resistance fault or any other constant value of fault impedance may be evaluated by this method.

(9) The results for the fault induced overvoltages in unfaulted phases due to SLG fault on one phase show excellent agreement with Kimbark's results and the maximum overvoltage is observed for mid-point fault (in the case of the double end fed system).

These results do not show the superimposition of unwanted hf oscillations as observed in the results of TNA or those obtained by the technique of Laplace transform[25]. The cause of the oscillation is the lumpiness of the circuit parameters of TNA and the numerical noise in the case of the analytical technique using Laplace transform. Results free from such oscillations were expected by Kimbark and others but was not successfully achieved before. Thus, these results prove the superiority of the analytical technique described in Chapter Six over other methods.

On the basis of this technique the results for off-centre fault may be very easily obtained, whereas it is very complicated to achieve

the solution for such cases by Kimbark's lattice diagram method.

Furthermore, the technique can be readily applied to transposed or untransposed line with frequency dependent or frequency invariant parameters. Kimbark's method is applicable for transposed lines with frequency invariant parameters only. Moreover, on the basis of this technique the fault induced overvoltage due to other types of faults e.g. double line to ground fault, combination of SLG fault and open conductor fault at a particular location etc. Can be easily determined .

(10) The results for fault induced overvoltage for mid-point fault is an excellent example of the interaction of modal components, especially in this particular example due to the large difference in the propagation velocities of the two components.

From the results of Fig. 7.9 and 7.10 it may be observed that the less the difference in the velocities of propagation of two modes the better, and if the two velocities are exactly equal to each other (this is practically impossible and is very academic) and the magnitudes of modal components are equal then there would be no overvoltage on the unfaulted phases due to SLG fault.

Hence it is desirable that by suitable design of the line, the difference in the velocities of propagation and the magnitude of the two modal components are kept as low as possible in order that both the duration and the peak value of the pulse are reduced.

(11) It may again be observed as in the case of the simplified model (single-phase circuit) that any superspeed relay cannot detect the fault exactly at the instant of fault inception. This is due to the time delay in the arrival of fault initiated surge from the location of fault to the relaying point.

(12) The influence of the frequency dependence of the line parameters is very significant in the case of SLG fault. The hf disturbances are very prominent for comparatively longer duration of time in the case of frequency invariant parameters than in the case of frequency dependent parameters. Thus, the frequency dependence of parameters is a boon for slow relays, as the waveform would be less noisy after about one half cycle or so of the supply frequency. However, the disturbance is very similar in either case - with frequency dependent or invariant parameters - during a period of 5ms or less after the fault inception. Hence, the influence of the frequency dependence of the parameters would not be significant as far as the design of superspeed relays with operating time 5ms or less are concerned.

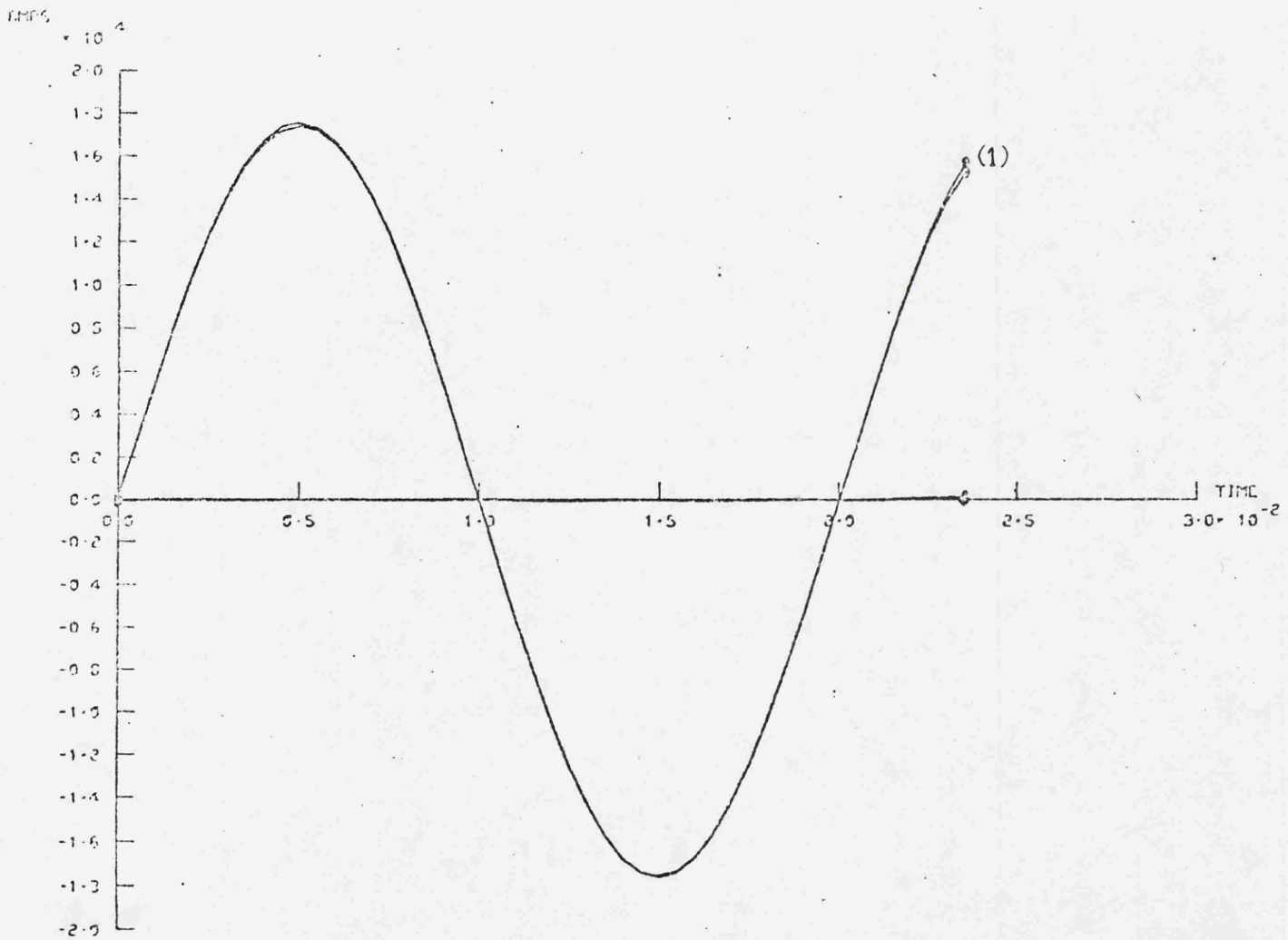

Fig. 7.1 a

Transient Fault Current at the Sending End
(400KV, 3-phase, single-end fed system, 32 Km transposed line)

Type of Fault - Single line to ground

Location of Fault - Receiving End

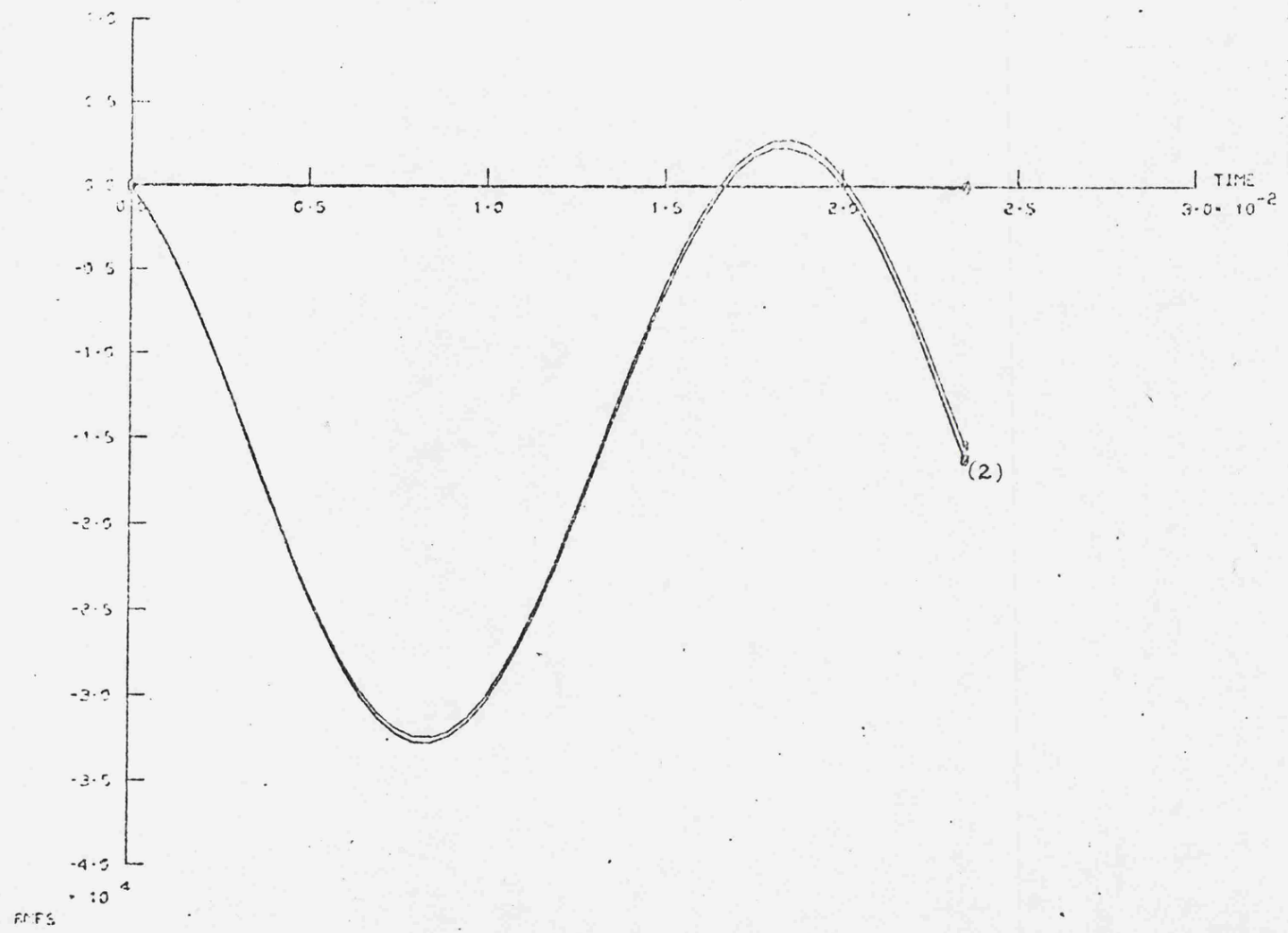

Fig. 7.1b

Transient Fault Current at the Sending End
(400KV, 3-phase, single-end fed system, 32 Km transposed line)

Type of Fault- Single line to ground

Location of Fault - Receiving End

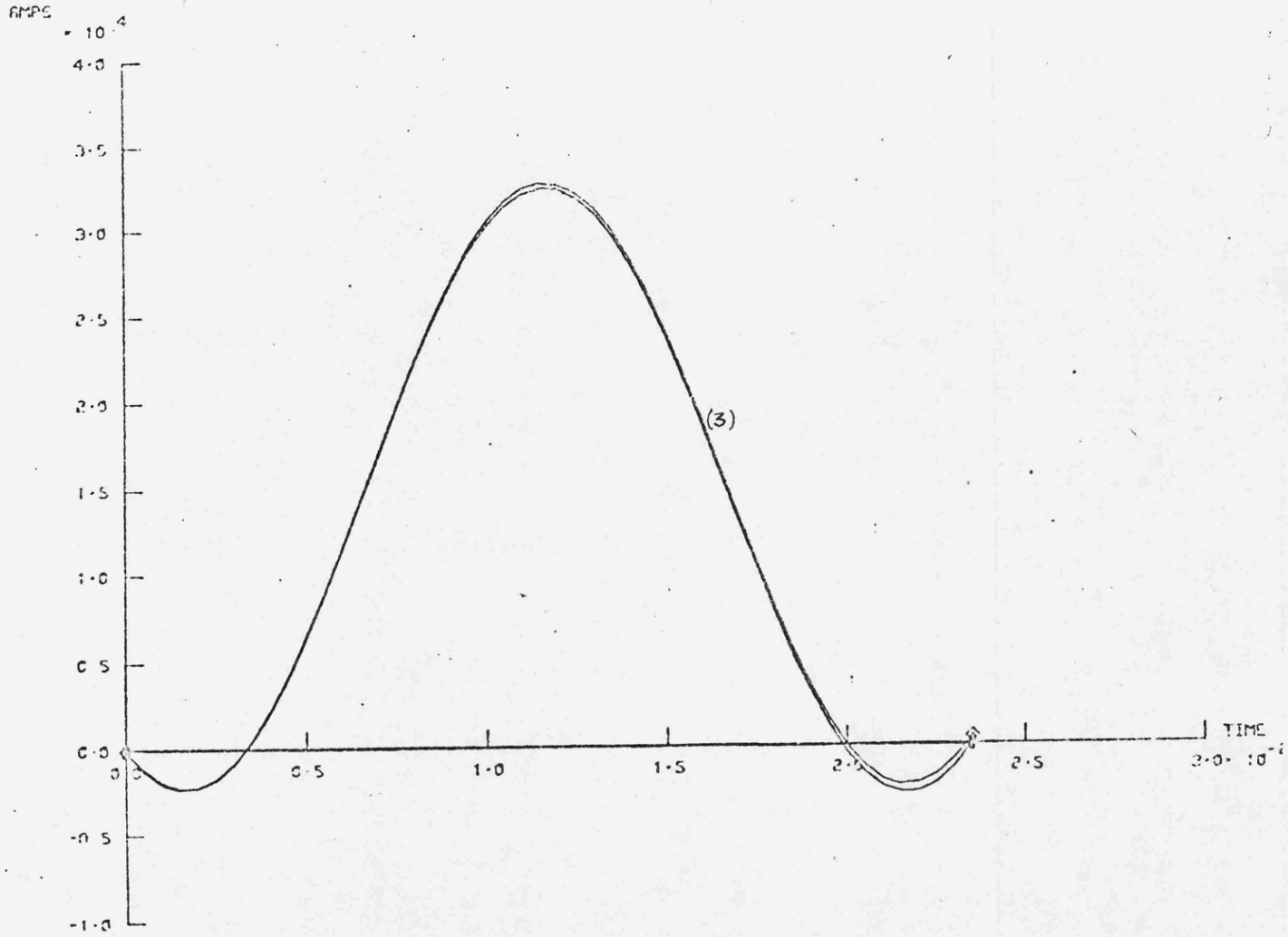

Fig. 7.1c

Transient Fault Current at the Sending End
(400KV, 3-phase, single-end fed system, 32Km transposed line)

Type of Fault - Single line to ground

Location of Fault - Receiving End

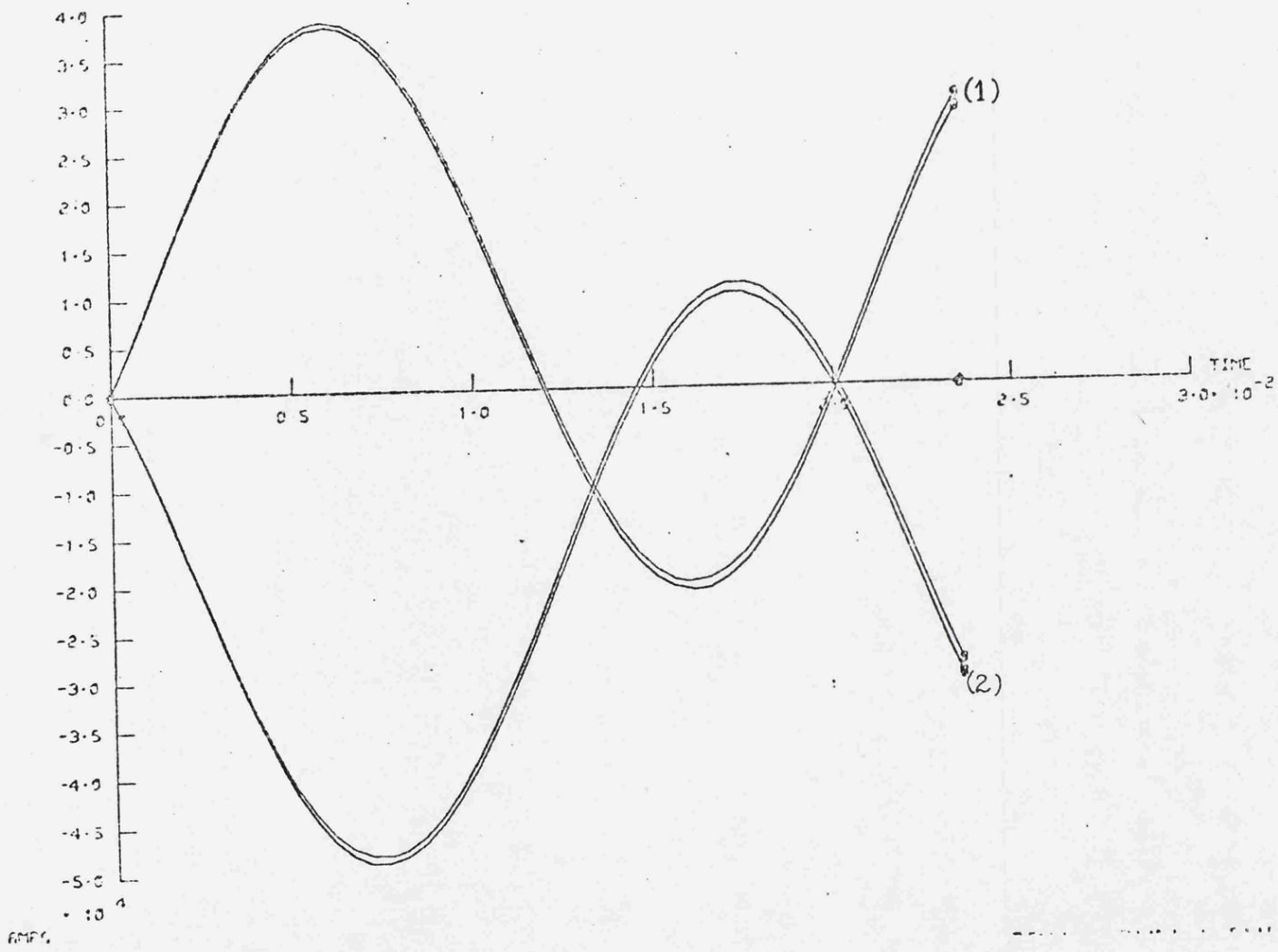

Fig. 7.2a
Transient Fault Current at the Sending End

(400KV, 3-phase, single-end fed system, 32Km transposed line)

Type of Fault - Double line to ground

Location of fault - Receiving End

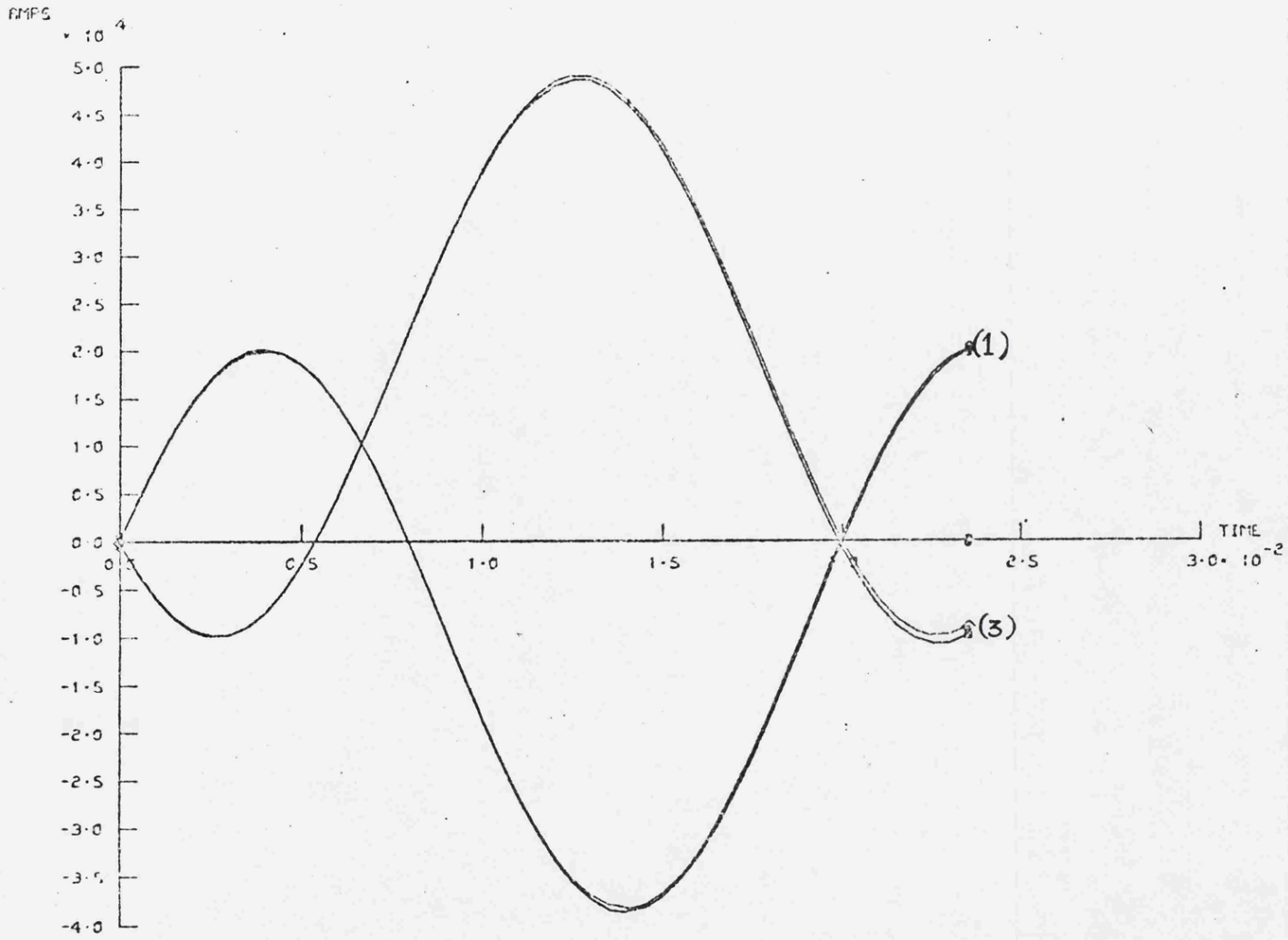

Fig. 7.2b

Transient Fault Current at the Sending End

(400KV, 3-phase, single-end fed system, 32Km transposed line)

Type of Fault - Double line to ground

Location of Fault - Receiving End

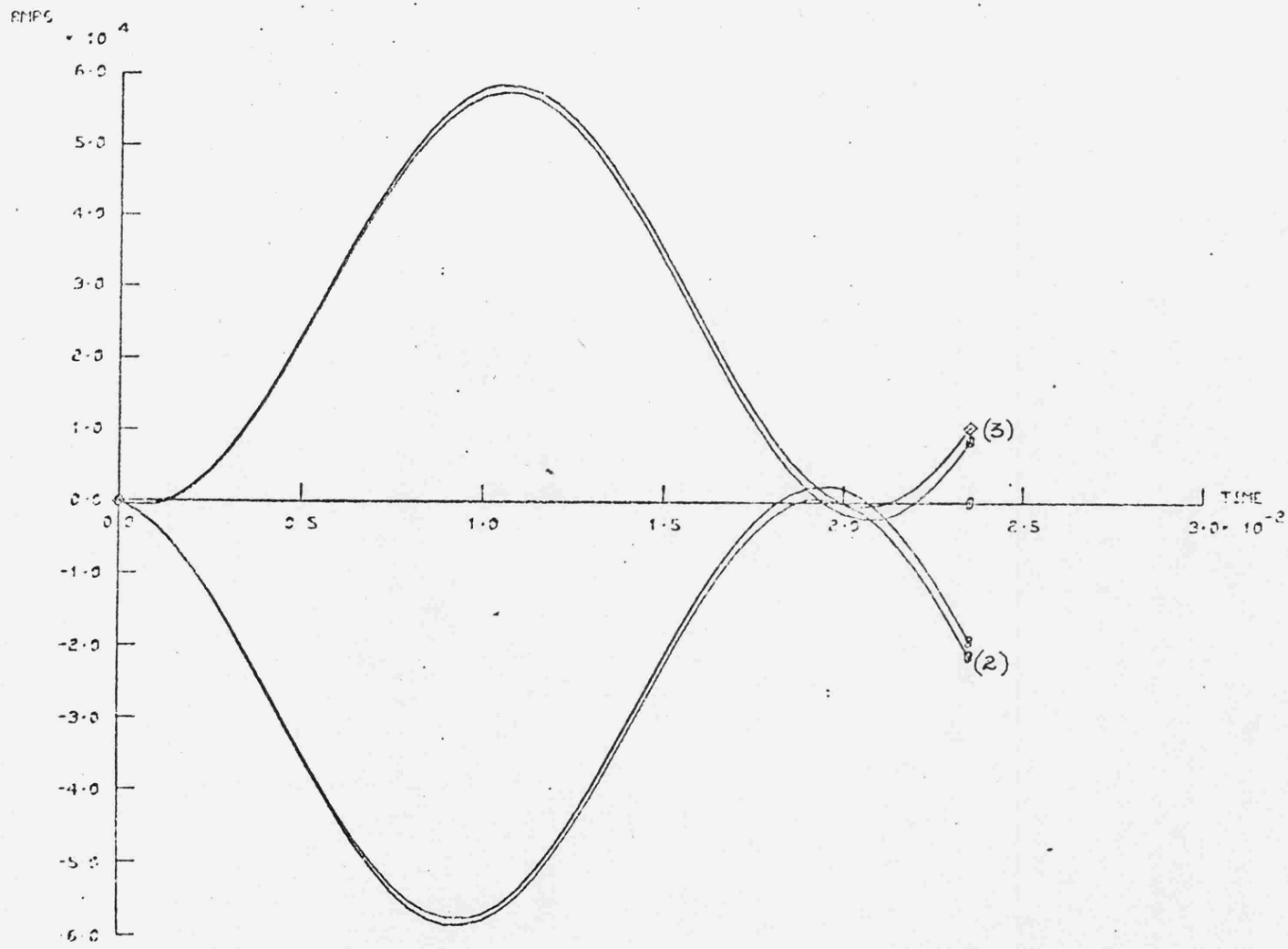

Fig. 7.2c

Transient Fault Current at the Sending End

(400KV, 3-phase, single-end fed system, 32Km transposed line)

Type of Fault - Double line to ground

Location of Fault - Receiving End

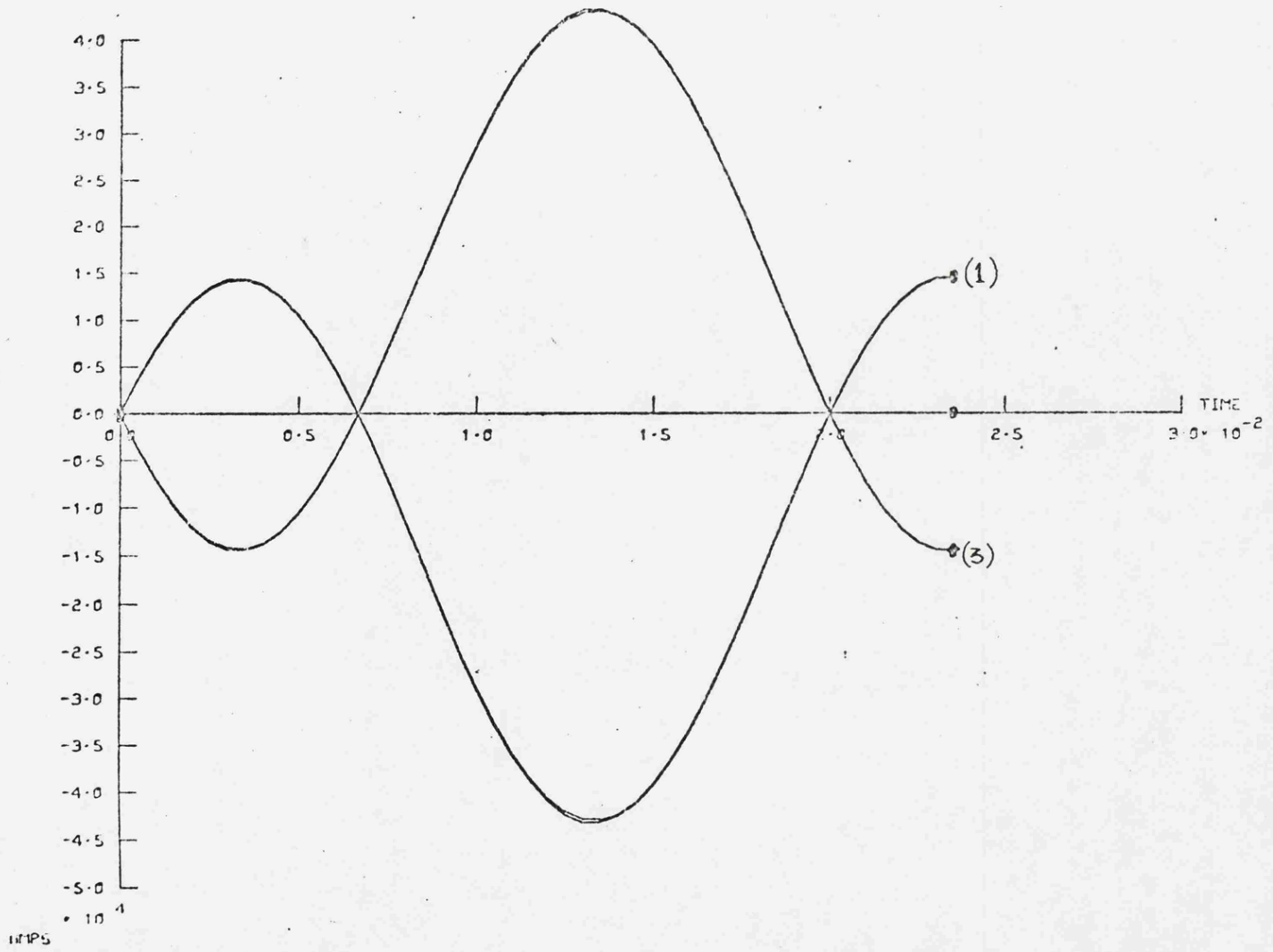

Fig. 7.3a

Transient Fault Current at the Sending End

(400KV, 3-phase, single-end fed system, 32Km transposed line)

Type of Fault - line to line

Location of Fault - Receiving End

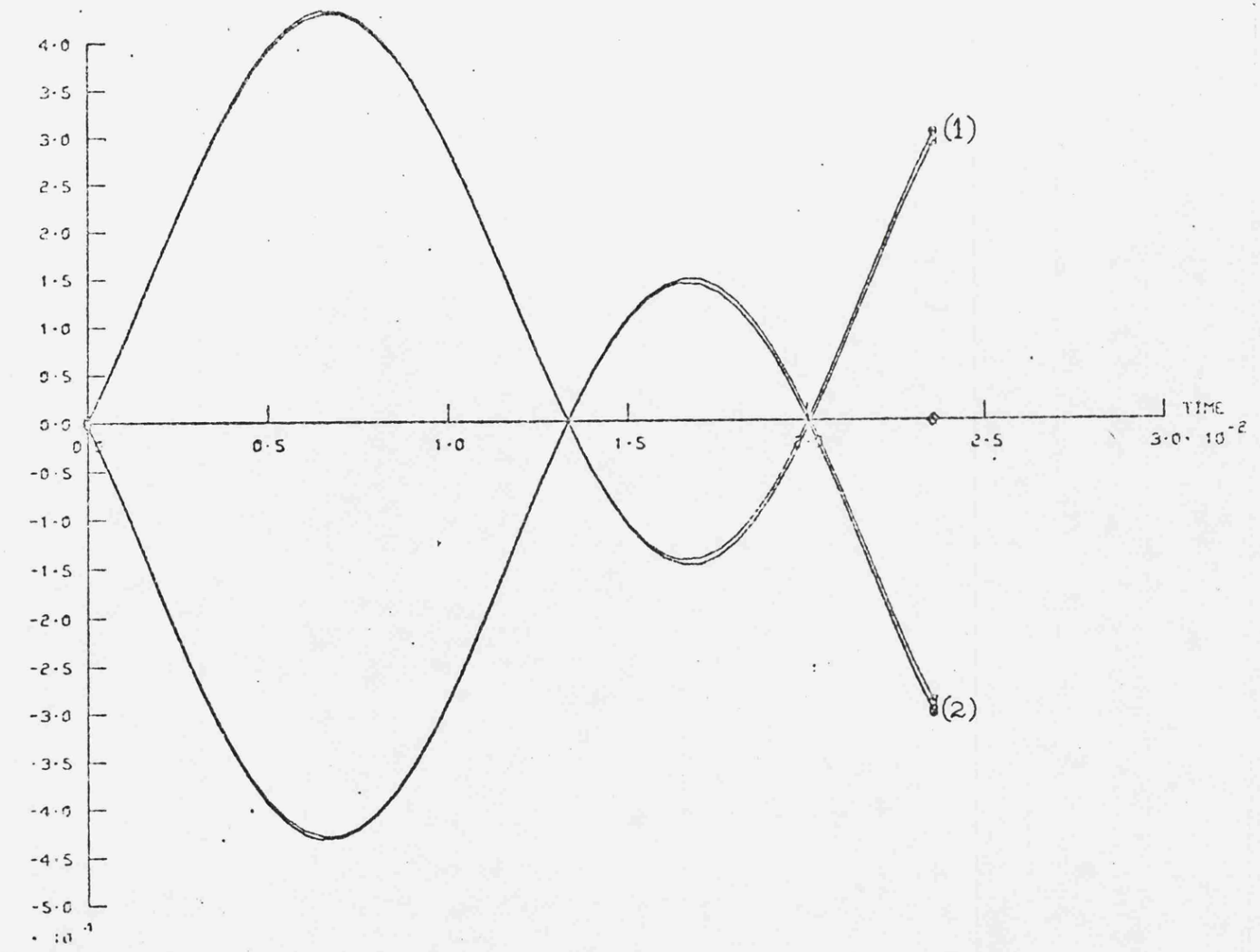

Fig. 7.3b

Transient Fault Current at the Sending End

(400KV, 3-phase, single-end fed system, 32Km transposed line)

Type of Fault - line to line

Location of Fault - Receiving End

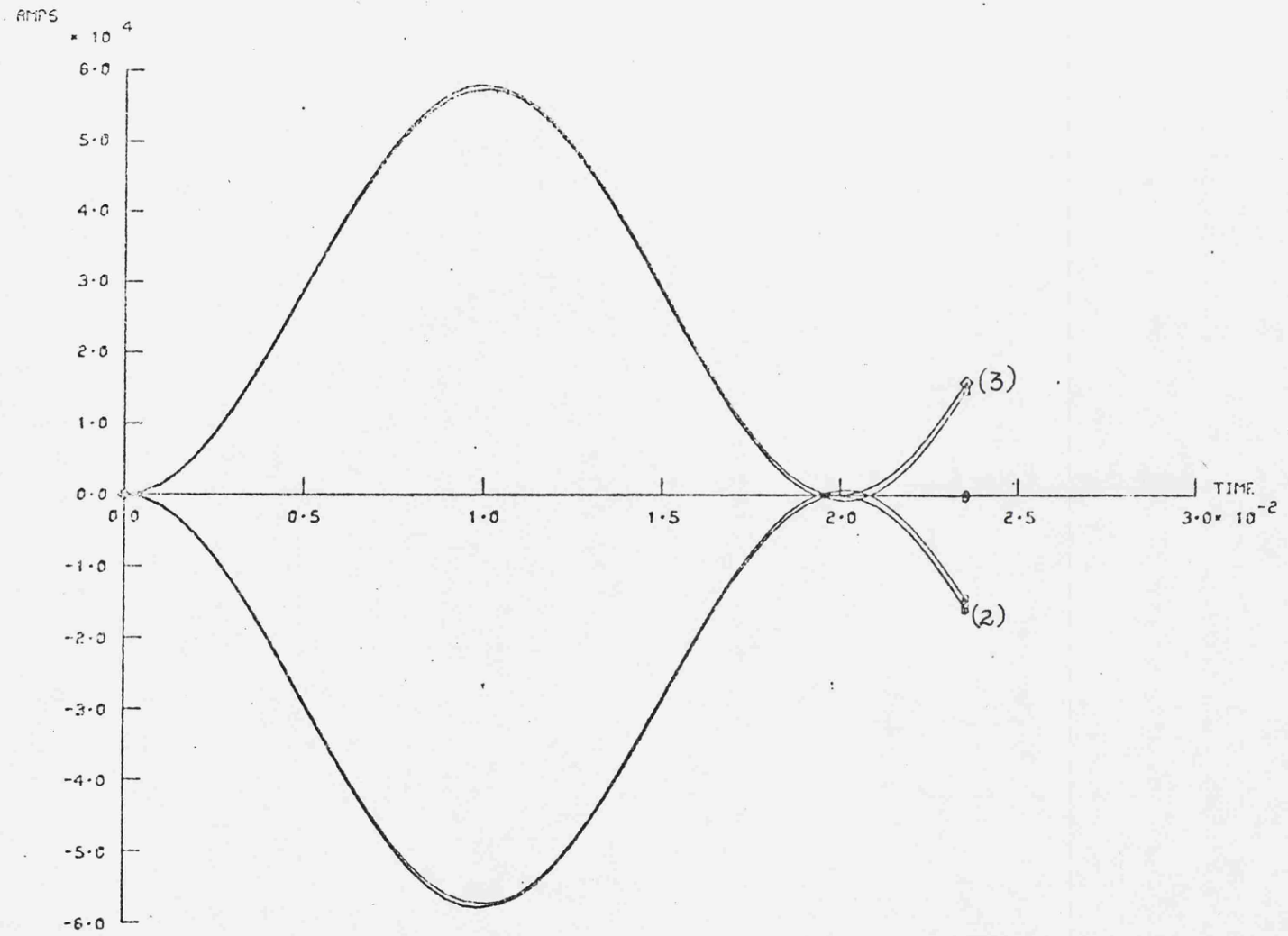

Fig. 7.3c

Transient Fault Current at the Sending End

(400KV, 3-phase, single end fed system, 32Km transposed line)

Type of Fault - line to line

Location of Fault- Receiving End

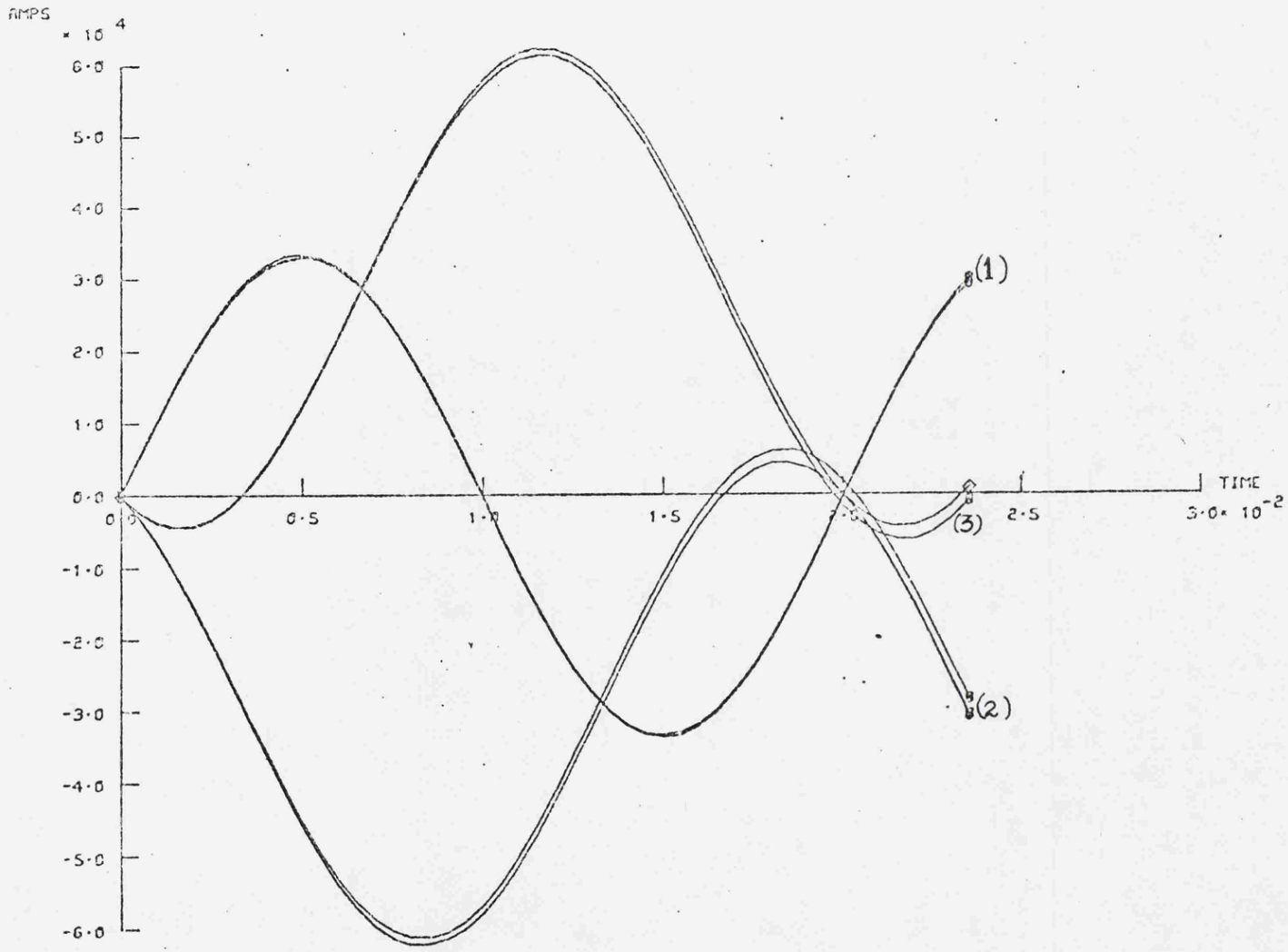

Fig. 7.4

Transient Fault Current at the Sending End

(400KV, 3-phase, single-end fed system, 32Km transposed line)

Type of Fault - Three-phase

Location of Fault - Receiving End

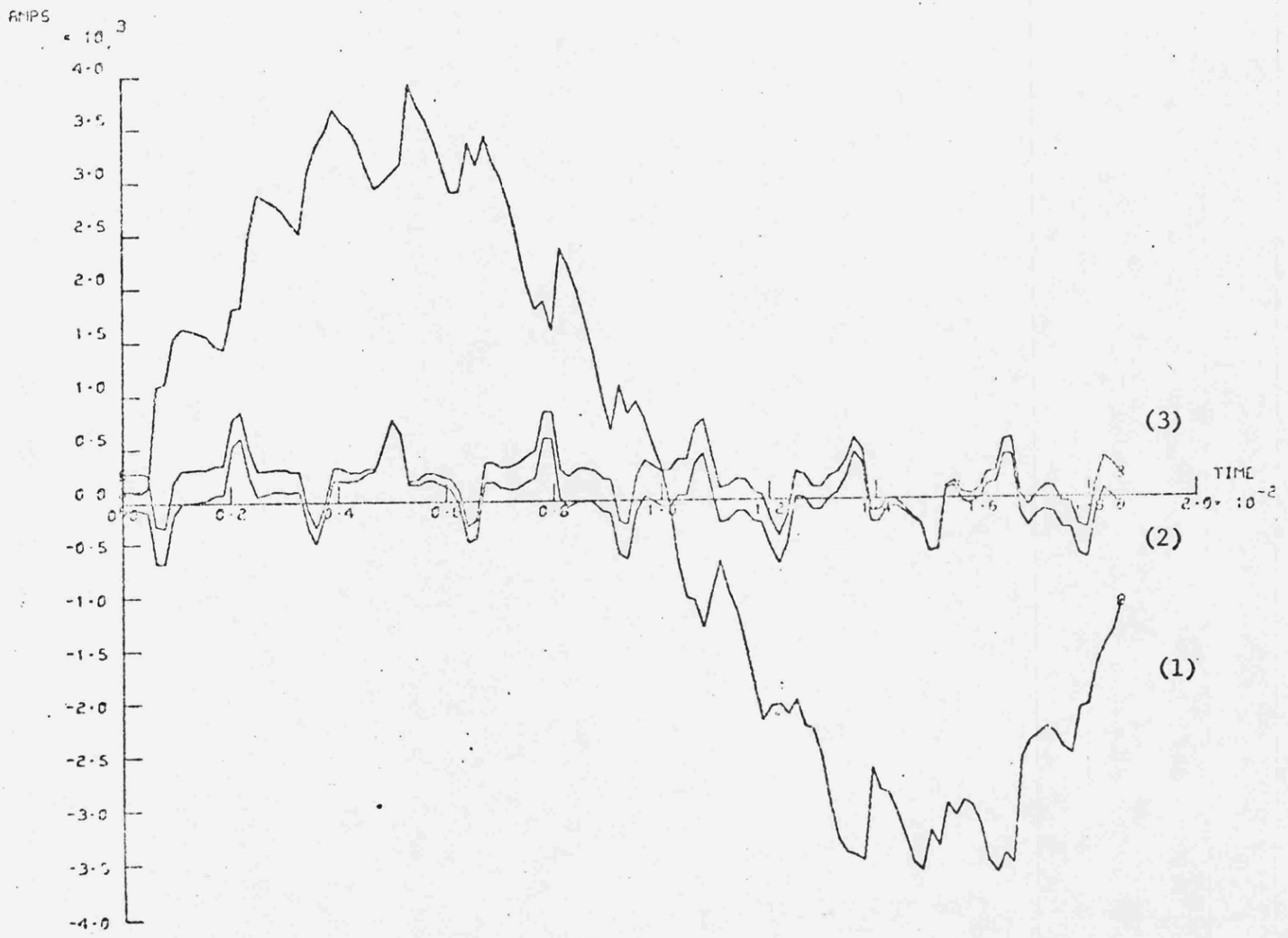

Fig. 7.5a

Transient Fault Current at the Sending End

(400KV, 3-phase, single-end fed system, 160 km transposed line)

Type of Fault - Single line to ground

Location of Fault - Receiving End

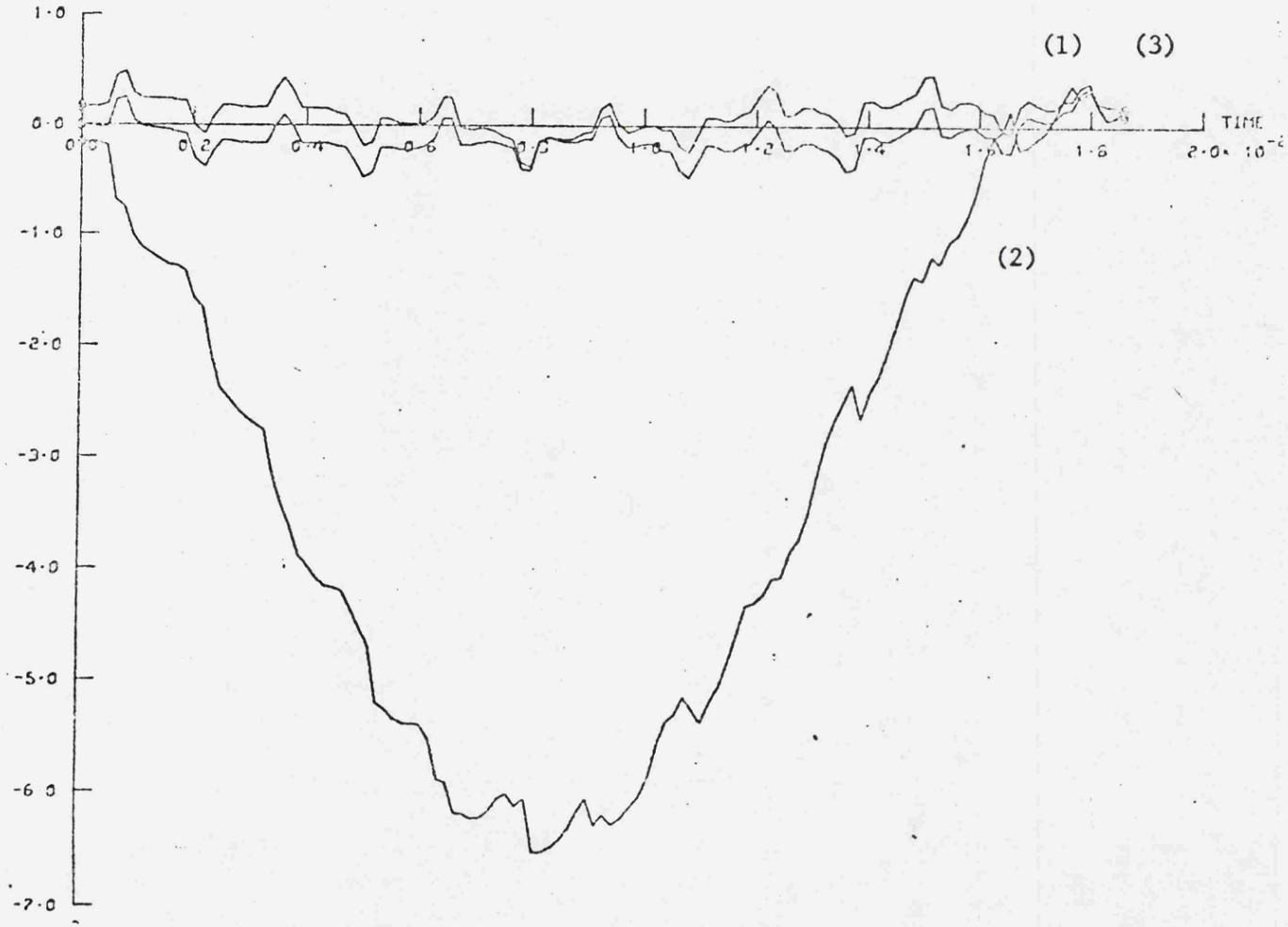

Fig. 7.5b

Transient Fault Current at the Sending End

(400KV, 3-phase, single-end fed system, 160Km transposed line)

Type of Fault - Single line to ground

Location of Fault - Receiving End

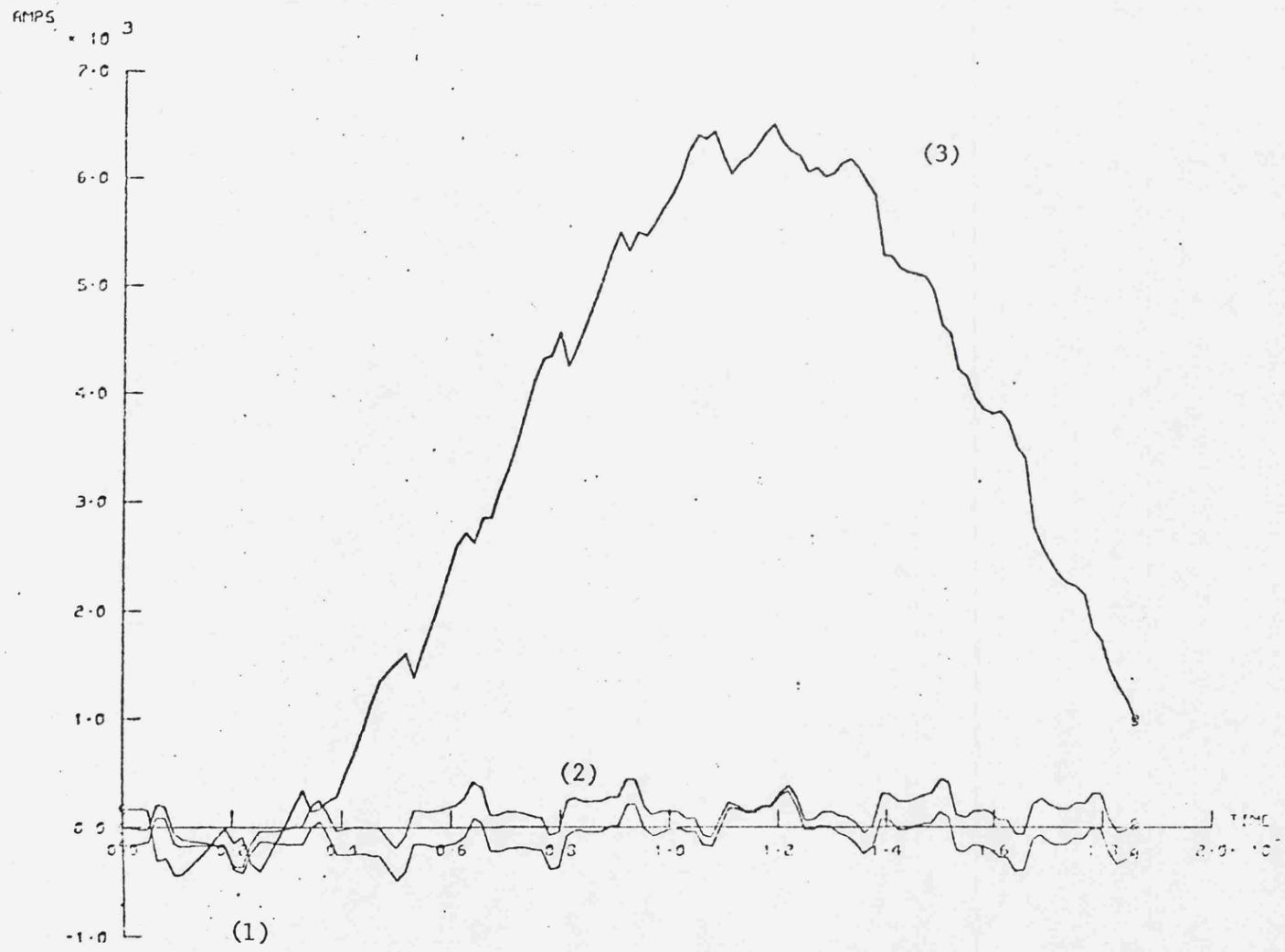

Fig. 7.5c

Transient Fault Current at the Sending End

(400KV, 3-phase, single-end fed system, 160Km transposed line)

Type of Fault - Single line to ground

Location of Fault - Receiving End

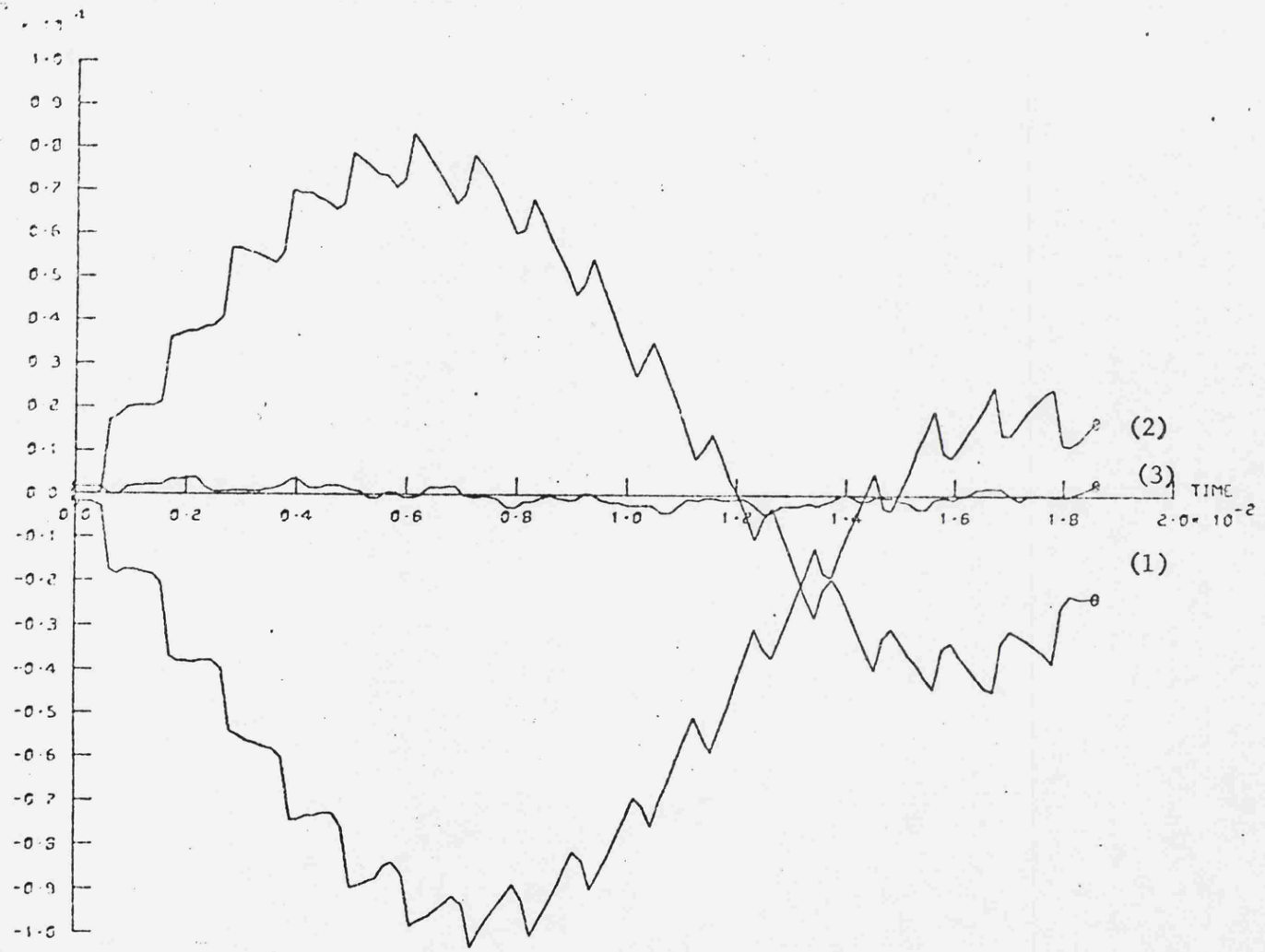

Fig. 7.6a

Transient Fault Current at the Sending End

(400KV, 3-phase, single-end fed system, 160Km transposed line)

Type of Fault - Double line to ground

Location of Fault - Receiving End

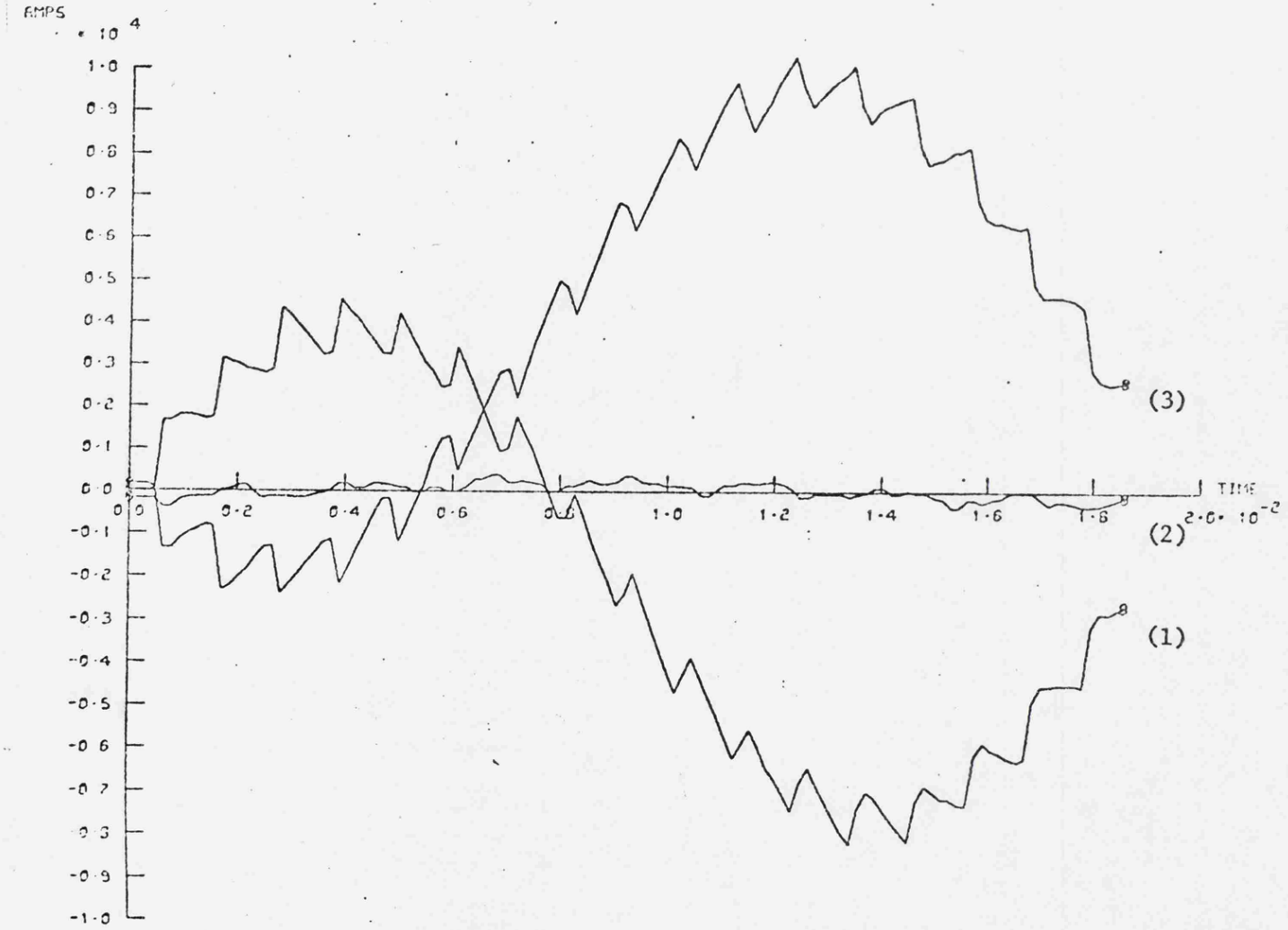

Fig. 7.6b

Transient Fault Current at the Sending End

(400KV, 3-phase, single-end fed system, 160Km transposed line)

Type of Fault - Double line to ground

Location of Fault - Receiving End

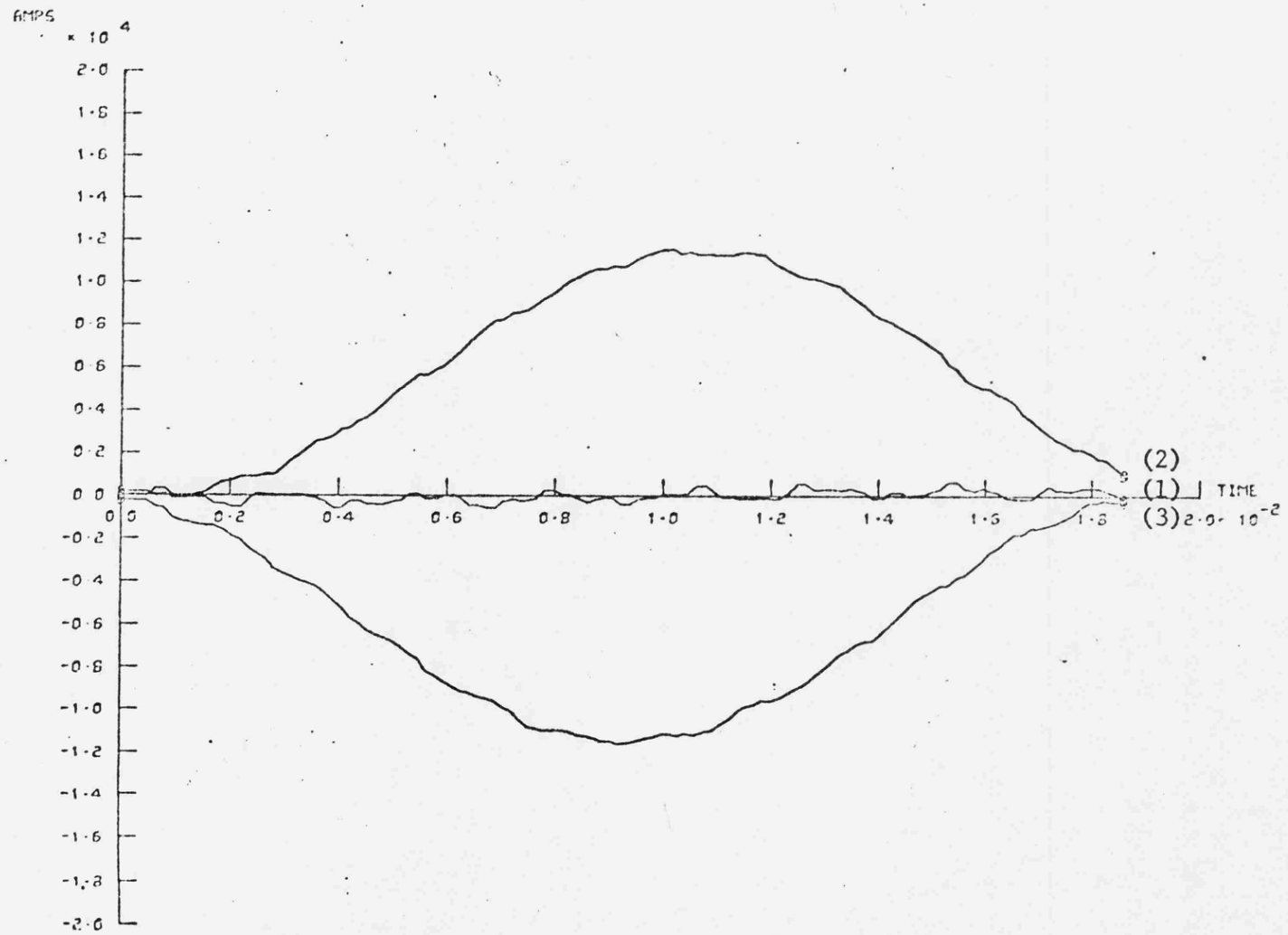

Fig. 7.6c

Transient Fault Current at the Sending End

(400KV, 3-phase, single-end fed system, 160Km transposed line)

Type of Fault - Double line to ground

Location of Fault - Receiving End

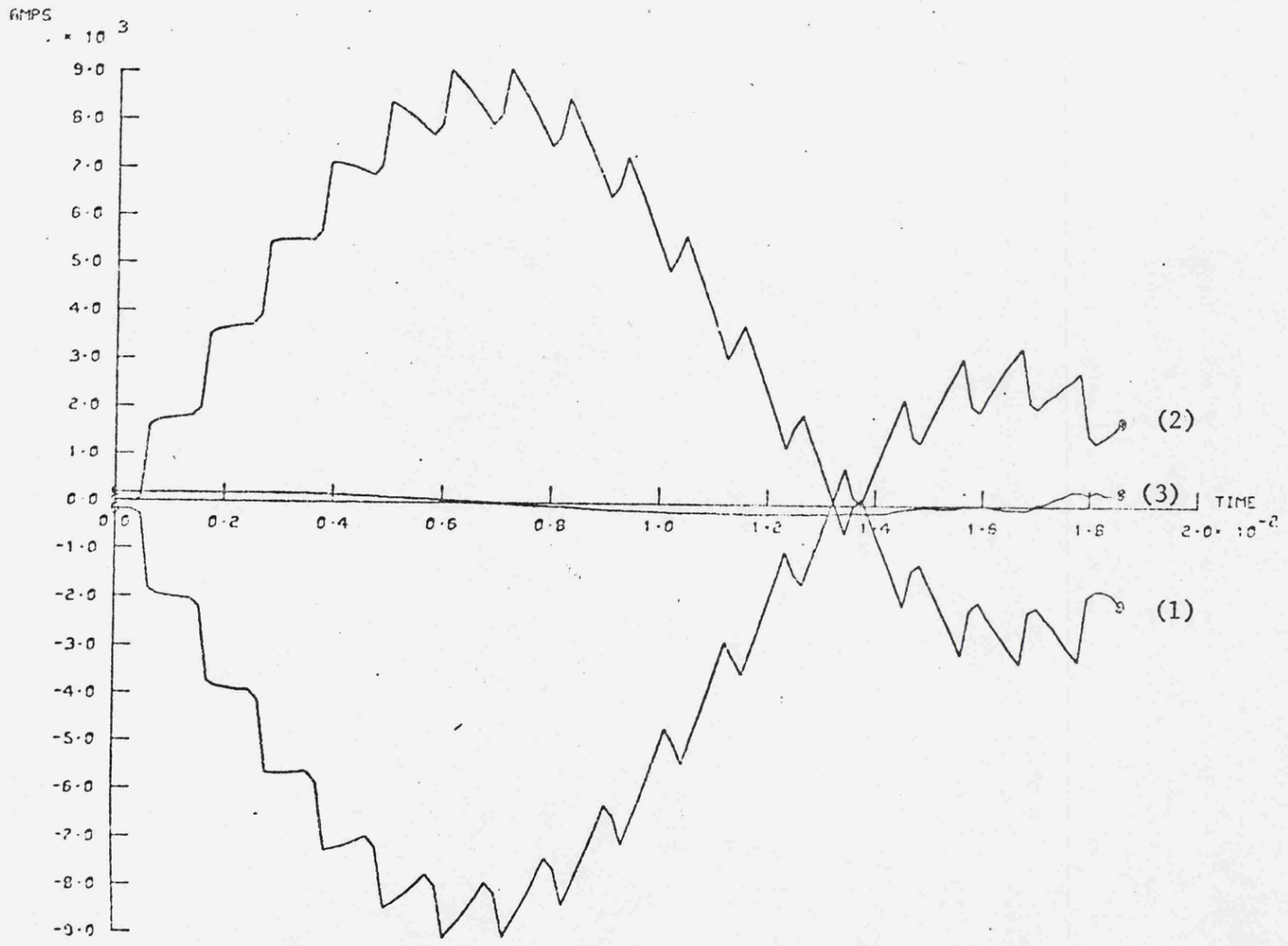

Fig. 7.7a

Transient Fault Current at the Sending End

(400KV, 3-phase, single-end fed system, 160Km transposed line)

Type of Fault - line to line

Location of Fault - Receiving End

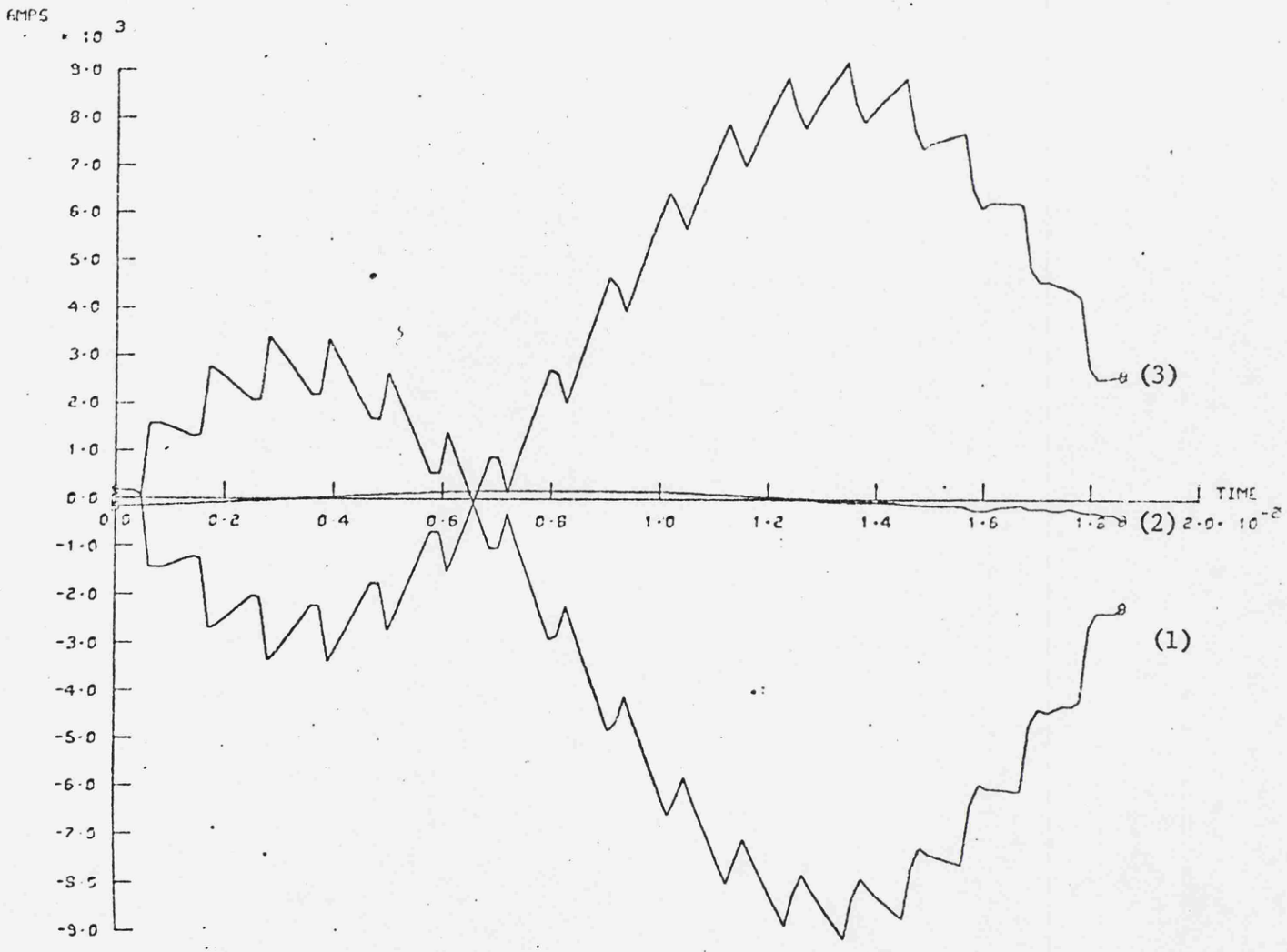

Fig. 7.7b

Transient Fault Current at the Sending End

(400KV, 3-phase, single-end fed system, 160 Km transposed line)

Type of Fault - line to line

Location of Fault - Receiving End

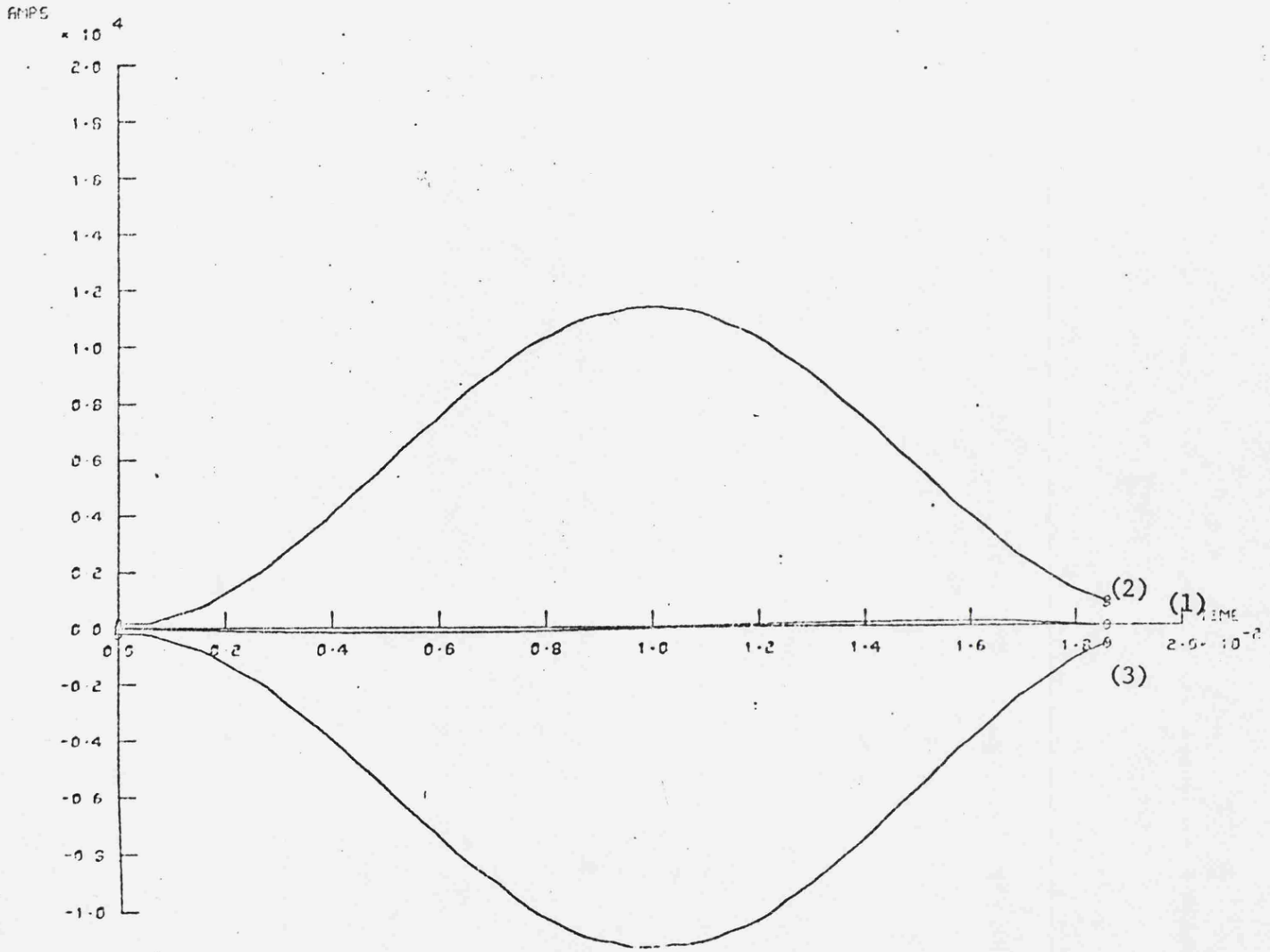

Fig. 7.7c

Transient Fault Current at the Sending End

(400KV, 3-phase, single-end fed system, 160Km transposed line)

Type of Fault - line to line

Location of Fault - Receiving End

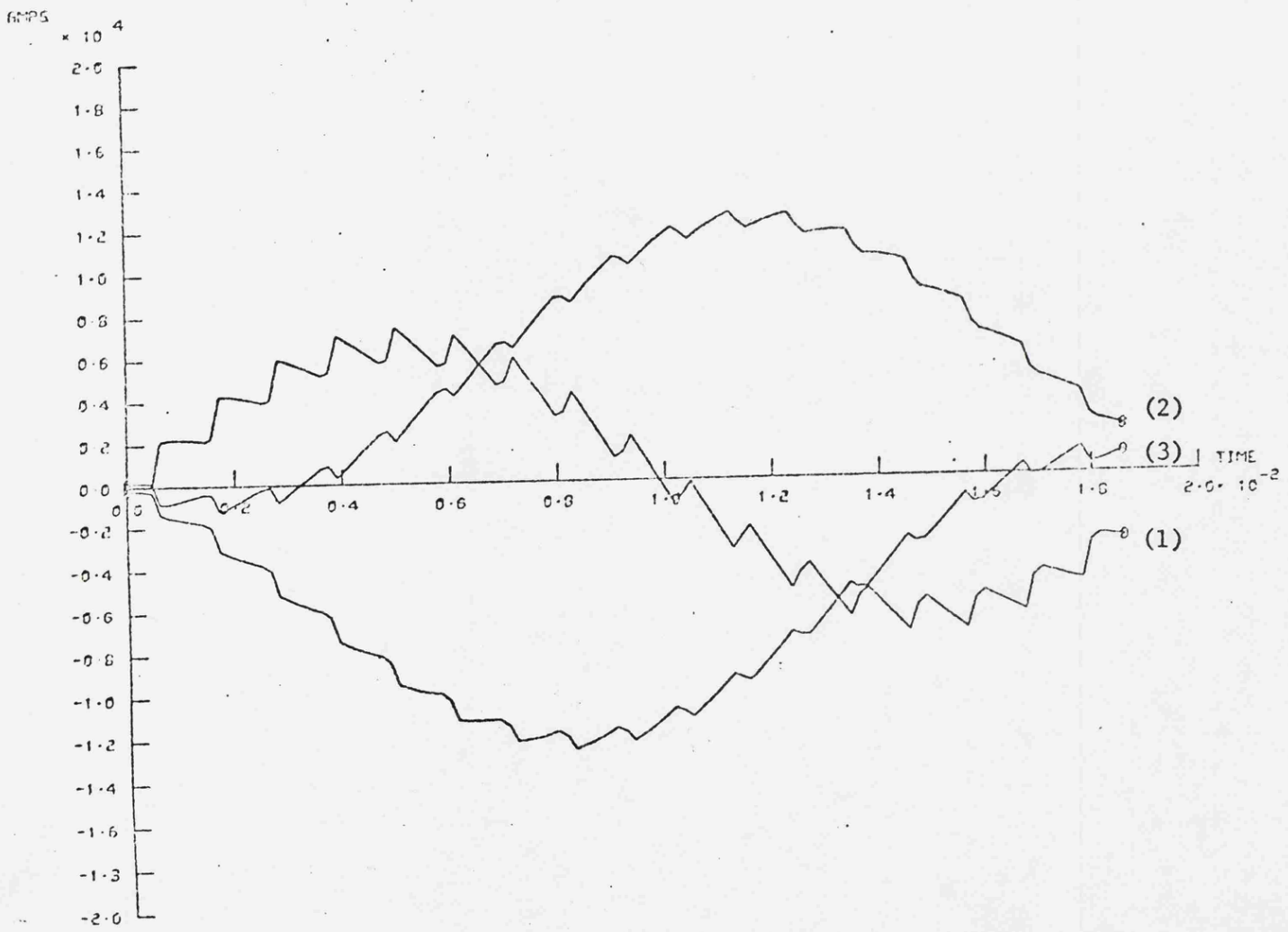

Fig. 7.8

Transient Fault Current at the Sending End

(400KV, 3-phase, single-end fed system, 160Km transposed line)

Type of Fault - Three-phase fault

Location of Fault - Receiving End

Fig. 7.9a Observation period - 2ms

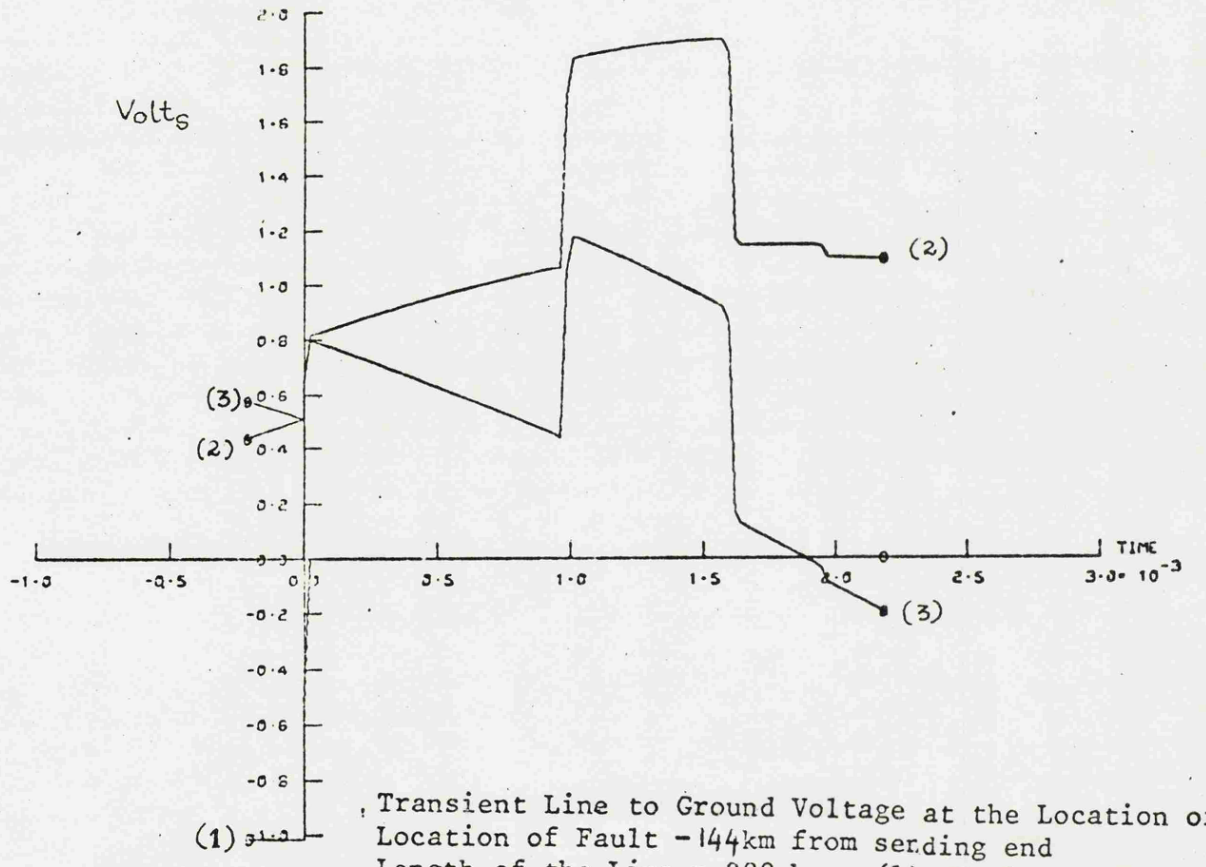

Transient Line to Ground Voltage at the Location of Fault
Location of Fault - 144km from sending end
Length of the Line - 288 km (1) Faulted phase
(2) & (3) Sound phases

Fig. 7.9b Observation period - 15ms

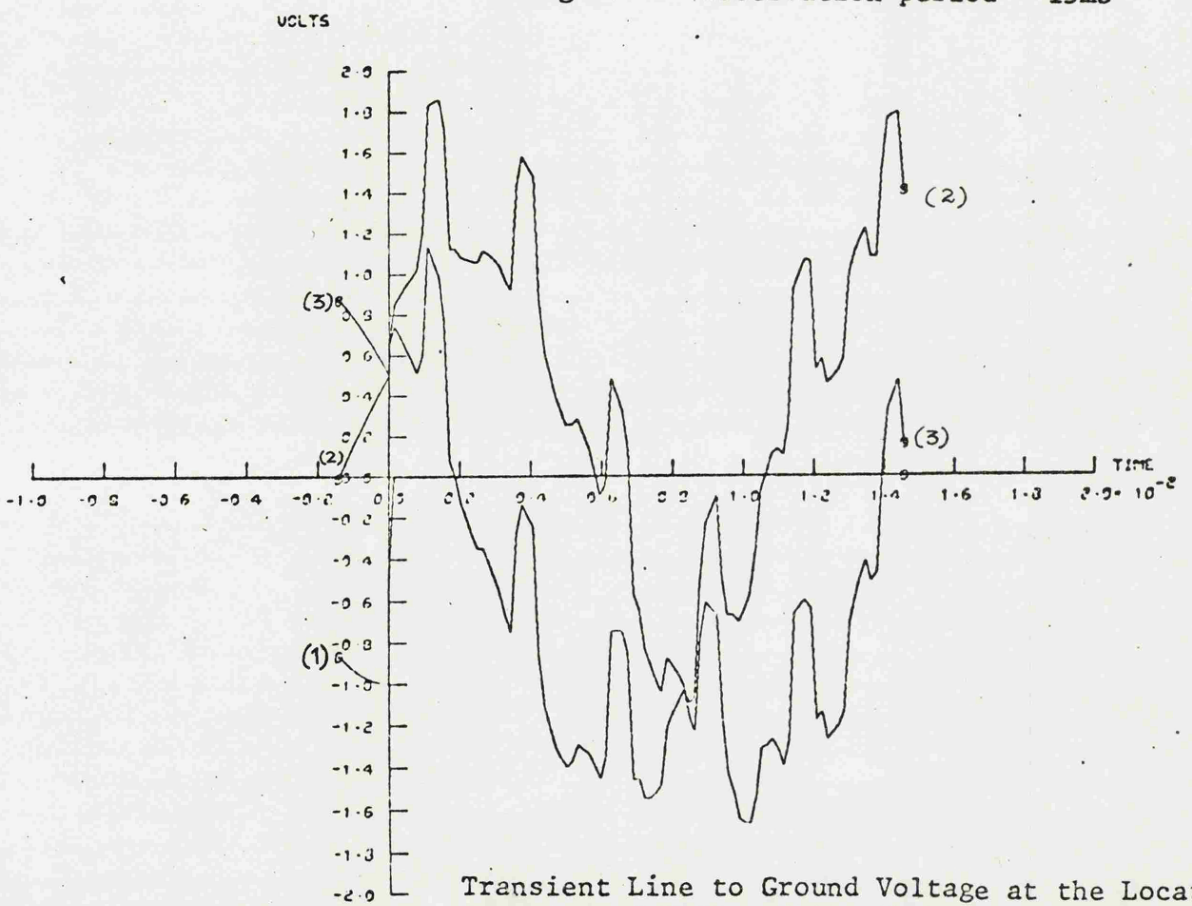

Transient Line to Ground Voltage at the Location of Fault
Location of Fault - 144km from sending end
Length of the Line - 288 km (1) Faulted phase
(2) and (3) Unfaulted phases

Fig. 7.10a Transient Line to Ground Voltage at the Location of Fault
Location of Fault - 96km from sending end
Length of the Line - 288 km (1) Faulted phase
(2) & (3) Sound phases

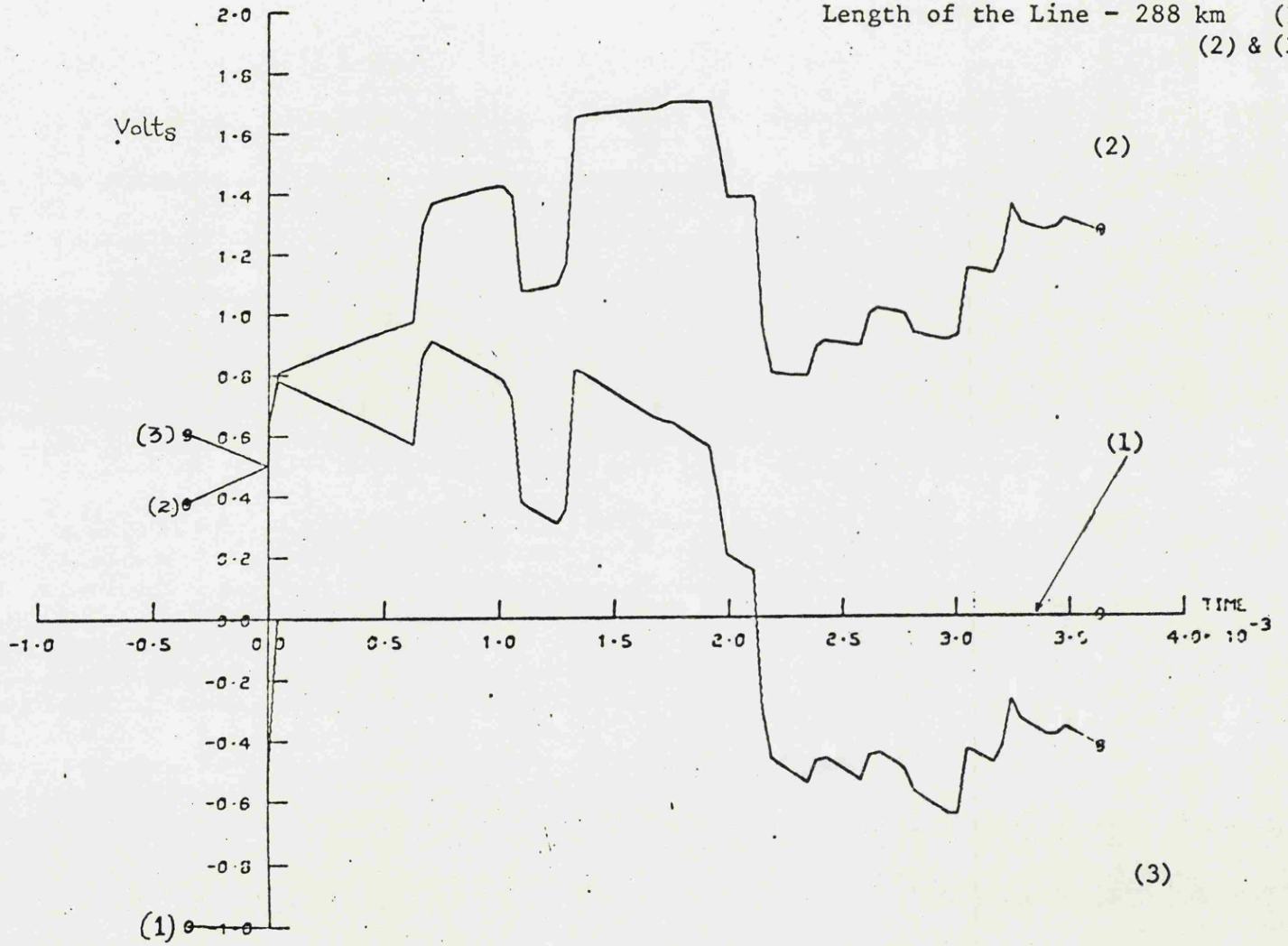

Observation period - 2ms

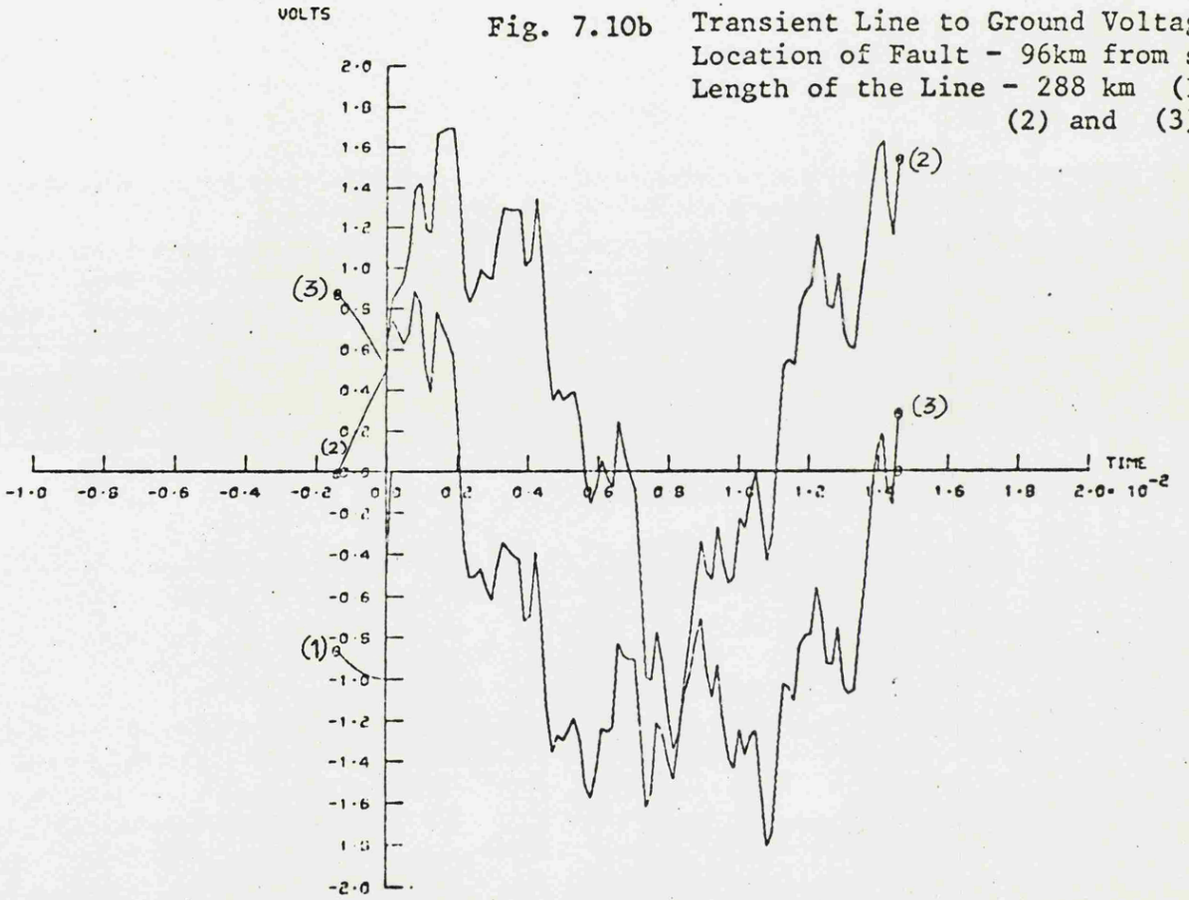

Fig. 7.10b Transient Line to Ground Voltage at the Location of Fault
Location of Fault - 96km from sending end
Length of the Line - 288 km (1) Faulted phase
(2) and (3) Unfaulted phases

Observation period 15ms

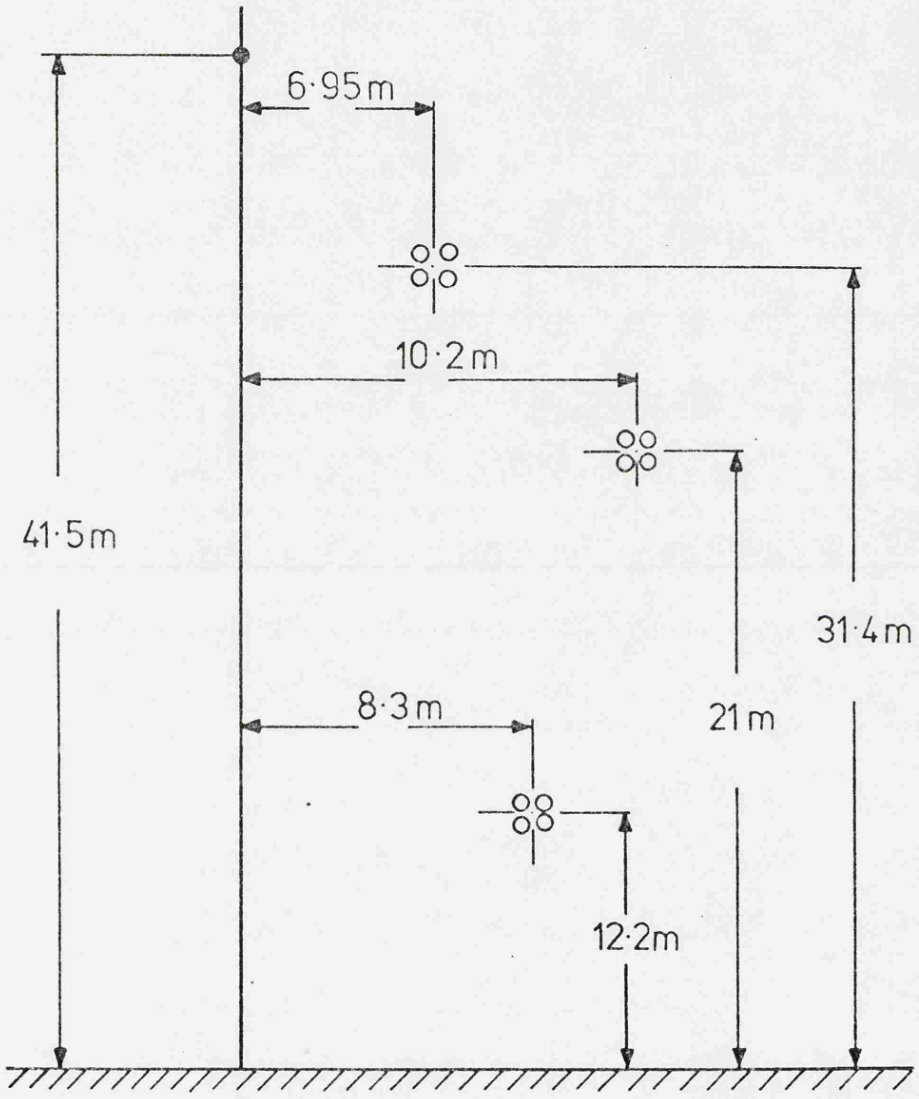

FIG. 7.11 400KV Quad-Conductor Single Circuit Vertical Untransposed Line

Fig. 7.12a Transient Fault Current at the Sending End
(400kv, 3-phase double-end fed system, 320km untransposed line)
Location of Fault - mid-point of line
Type of Fault - single line to ground
Prefault power transfer negligible

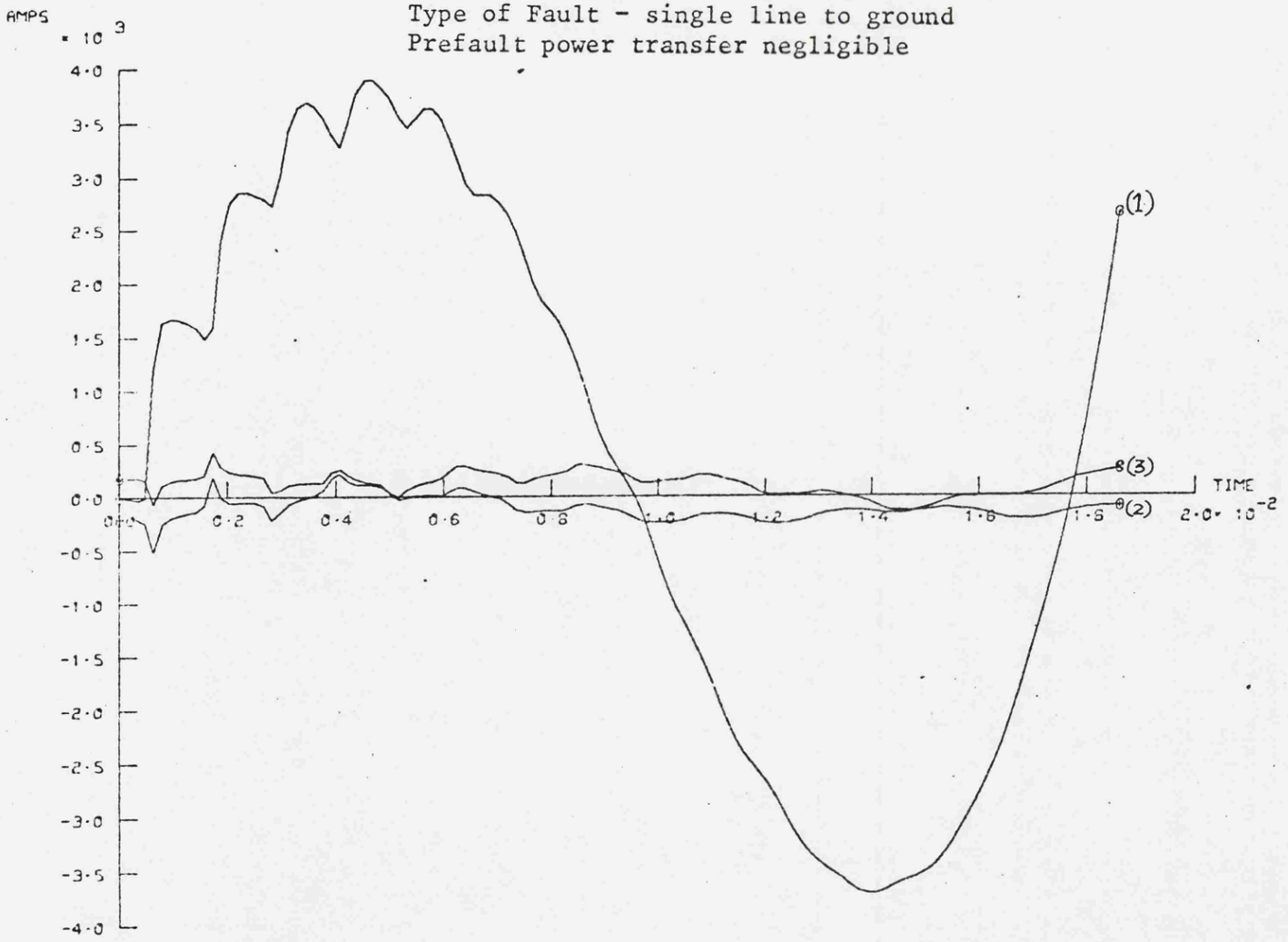

Fig. 7.12b Transient Fault Current at the Sending End
(400kv, 3-phase double end fed system, 320km untransposed line)

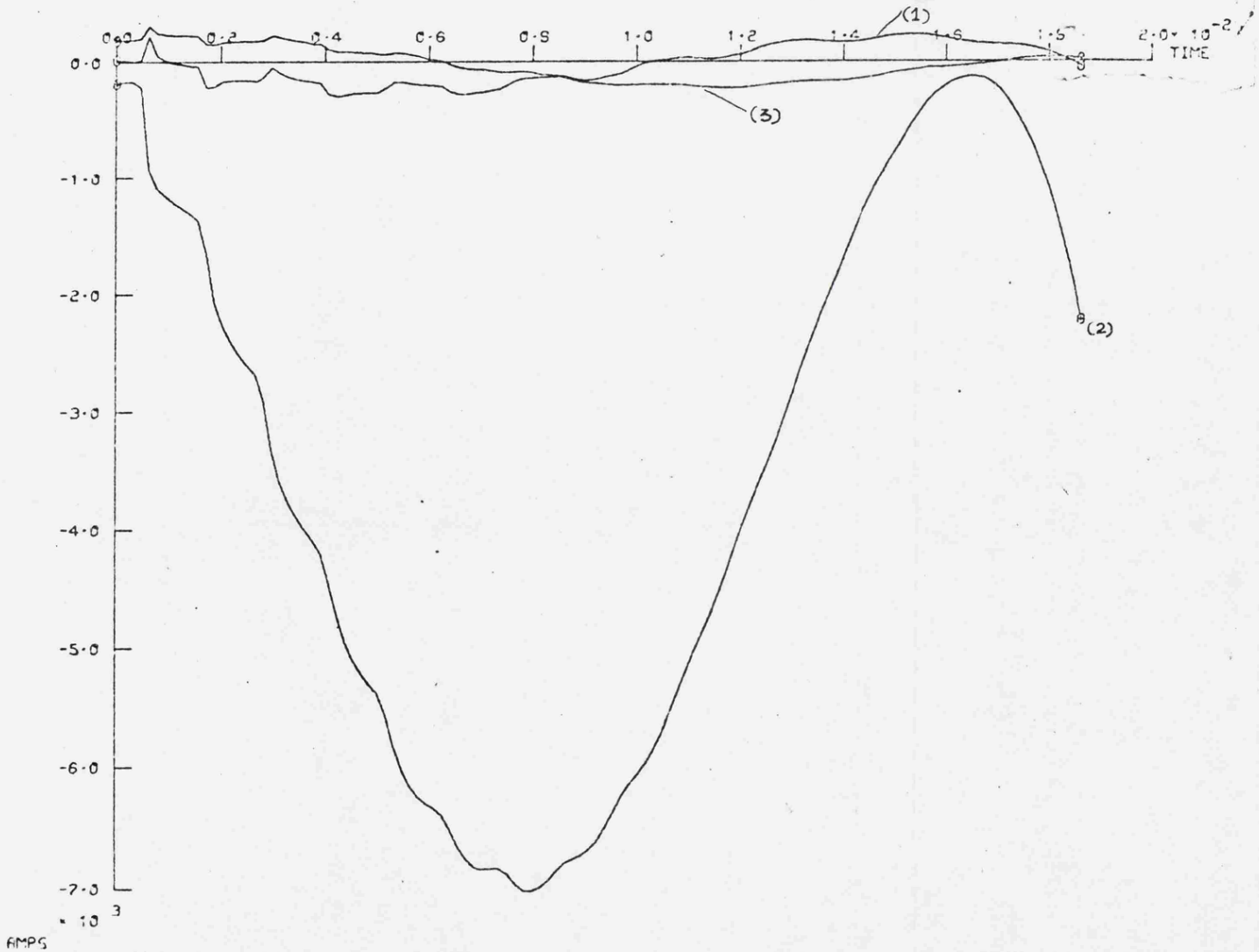

Location of fault - mid-point of line
Type of Fault - single line to ground
Prefault power transfer negligible

Fig 7.12c

Transient Fault Current at the Sending End
(400kv 3-phase double end fed system, 320km untransposed line)
Location of fault - mid-point of line, Type of fault - single line to ground
Prefault power transfer negligible

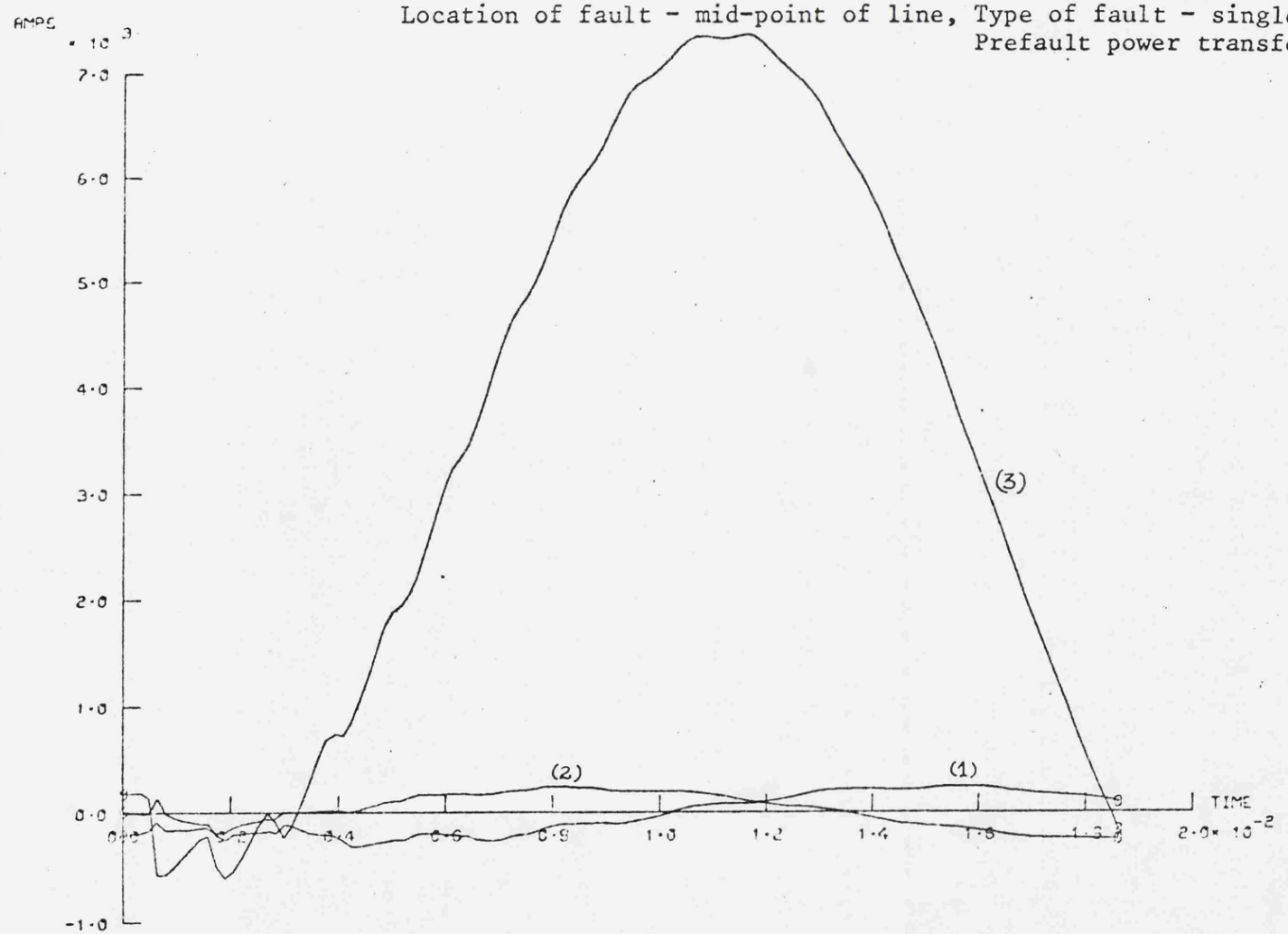

Fig. 7.13a Transient Fault Current at the Sending End
(400kv, 3-phase double end fed system, 320km untransposed line)
Location of fault - mid-point of line; Type of fault - double line to ground
Prefault power transfer negligible

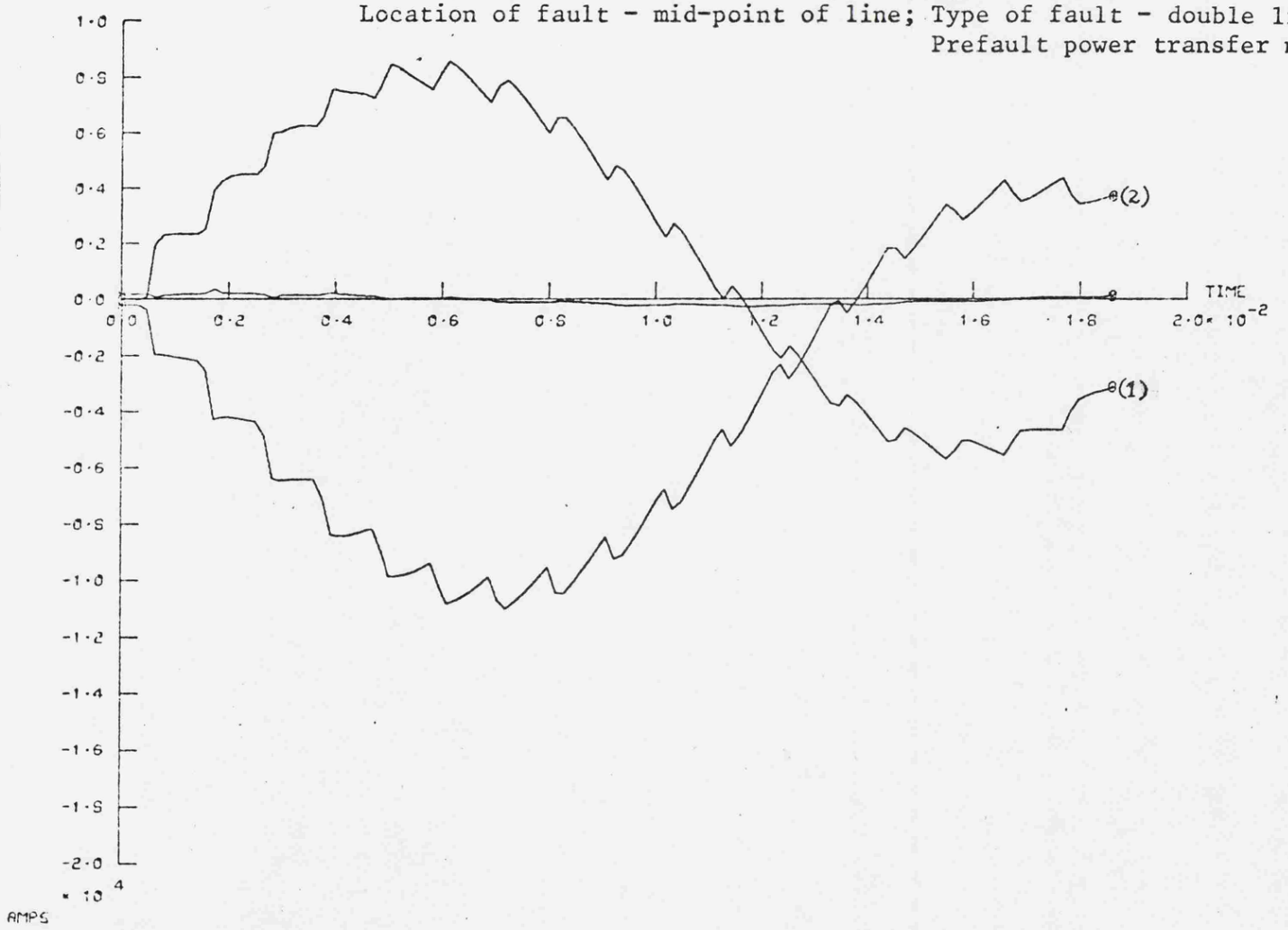

Fig. 7.13b

Transient Fault Current at the Sending End
(400kv, 3-phase double end fed system, 320 km untransposed line
Location of fault - mid-point of line; Type of fault - double line to ground
Prefault power transfer negligible

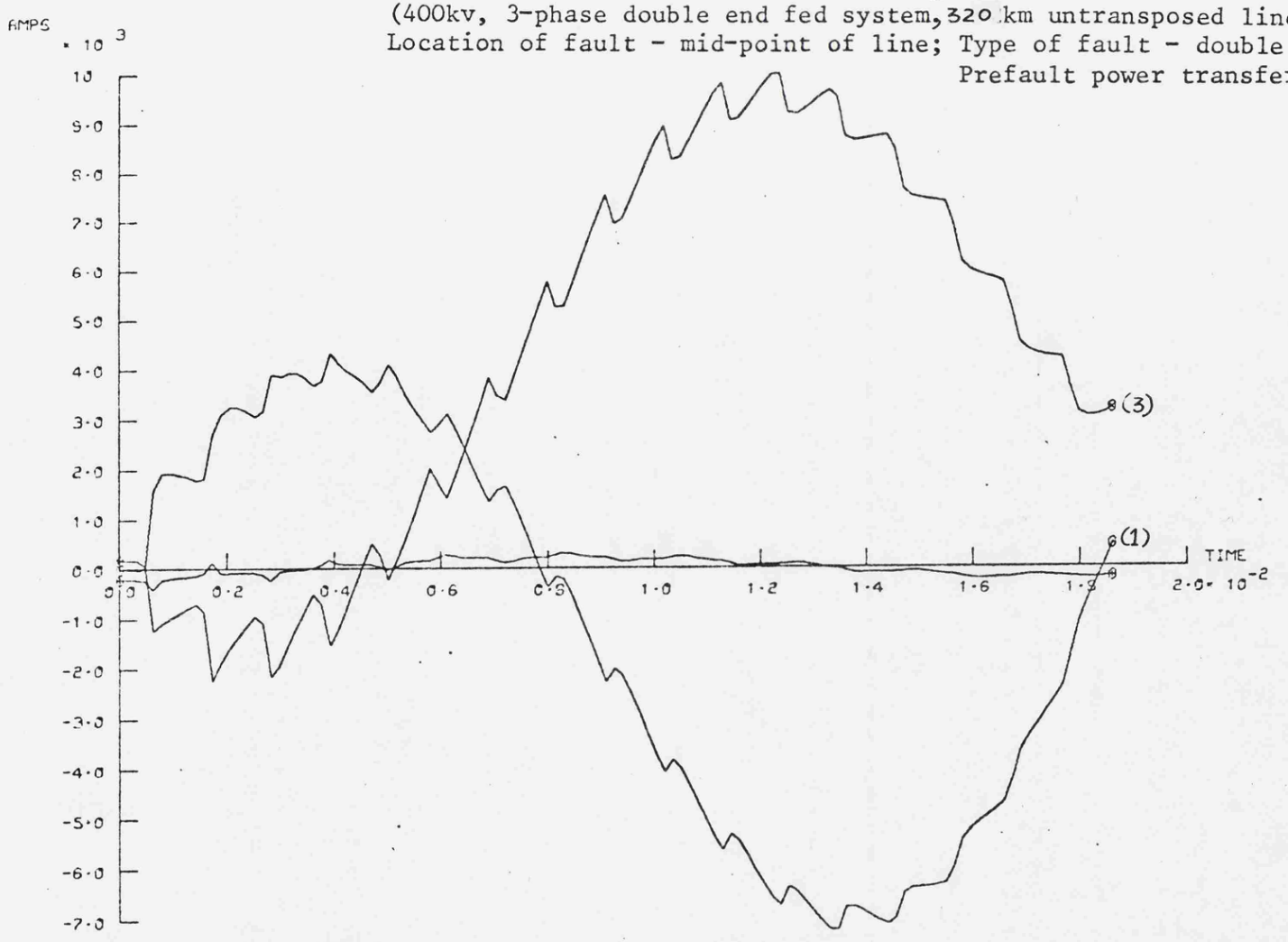

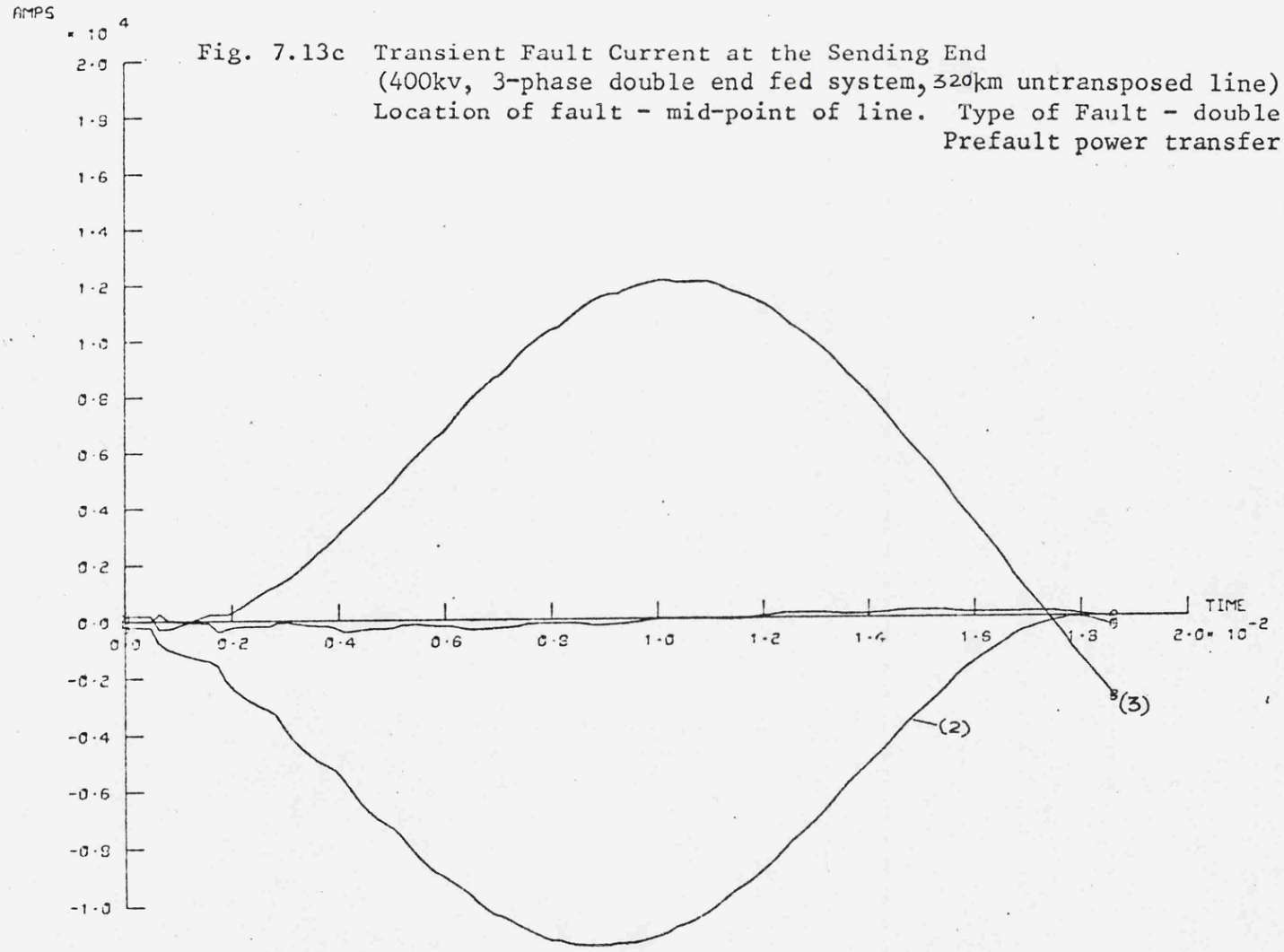

Fig. 7.13c Transient Fault Current at the Sending End
(400kv, 3-phase double end fed system, 320km untransposed line)
Location of fault - mid-point of line. Type of Fault - double line to ground
Prefault power transfer negligible

Fig. 7.14a Transient Fault Current at the Sending End
(400kv, 3-phase, double end fed system, 320km untransposed line)
Location of fault - mid-point of line. Type of Fault - line to line
Prefault power transfer negligible

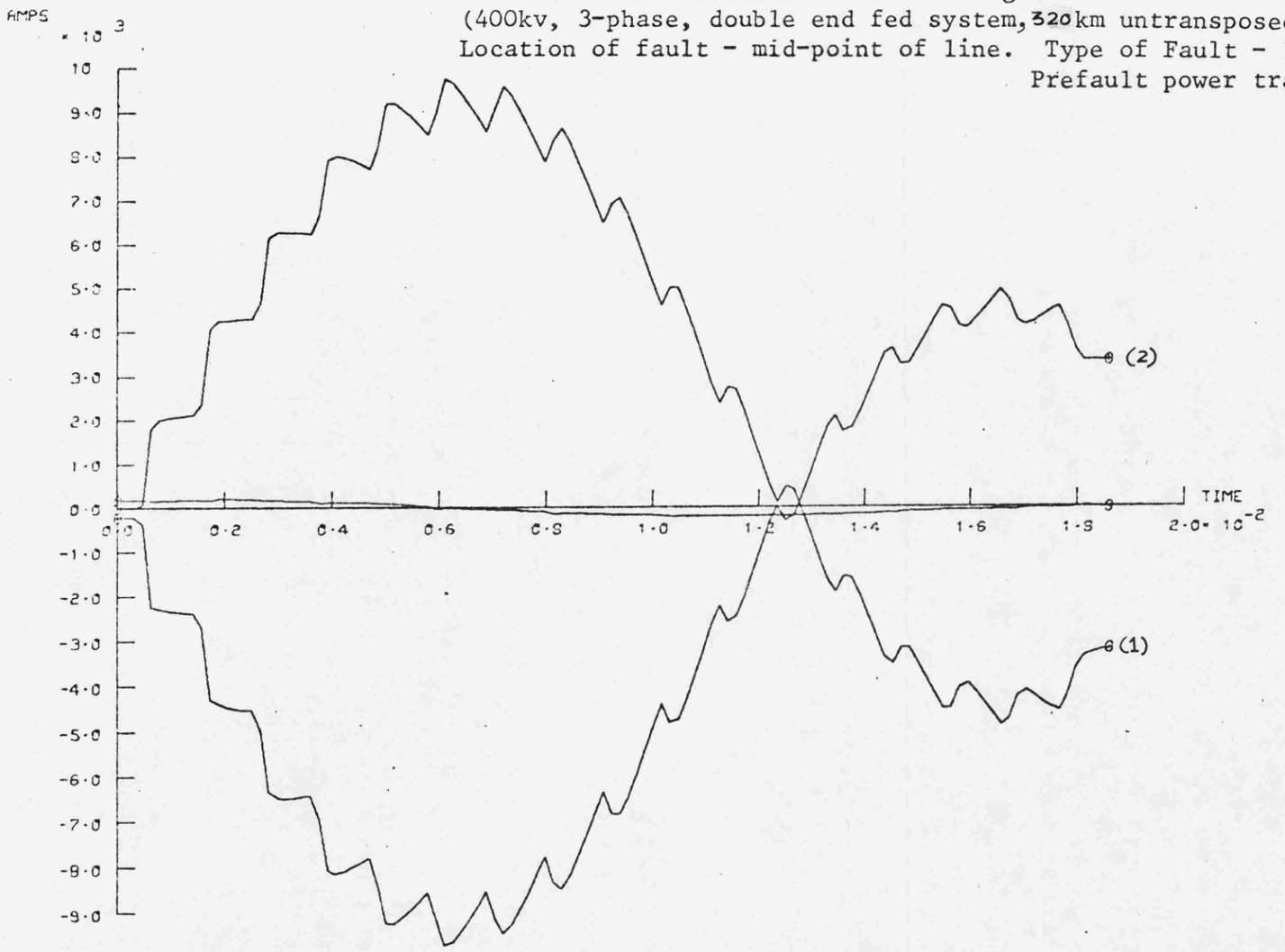

Fig. 7.14b Transient Fault Current at the Sending End
(400kv 3-phase double end fed system, 320km untransposed line)
Location of fault - mid-point of line. Type of fault - line to line
Prefault power transfer negligible

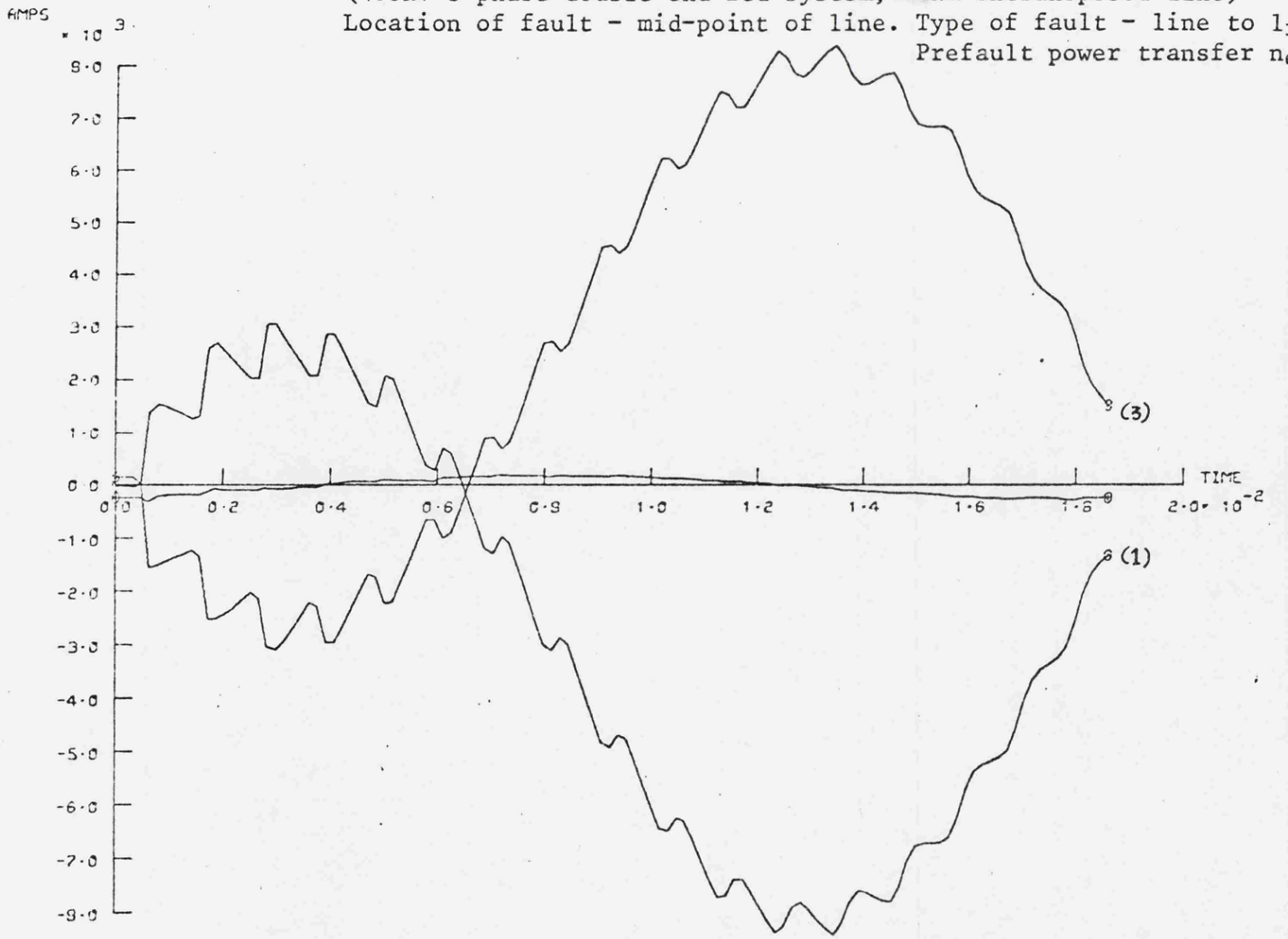

Fig. 7.14c Transient Fault Current at the Sending End
(400kv, 3-phase double end fed system, 320 km untransposed line)
Location of fault - mid-point of line. Type of Fault - line to line
Prefault power transfer negligible

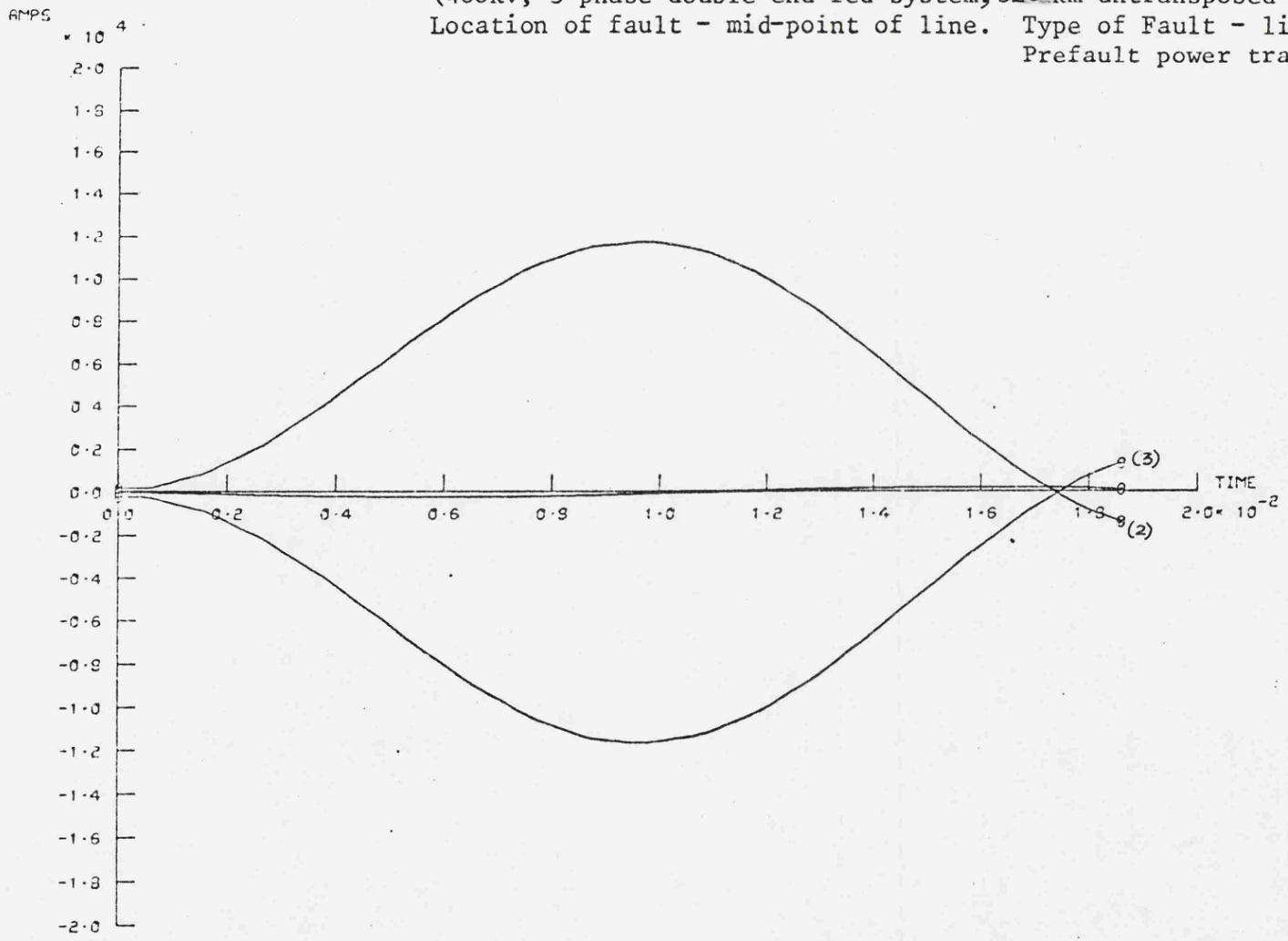

Fig. 7.15 Transient Fault Current at the Sending End
(400kv, 3-phase, double end fed system, 320km untransposed line)
Location of fault - mid-point of line. Type of fault - three-phase
Prefault power transfer negligible

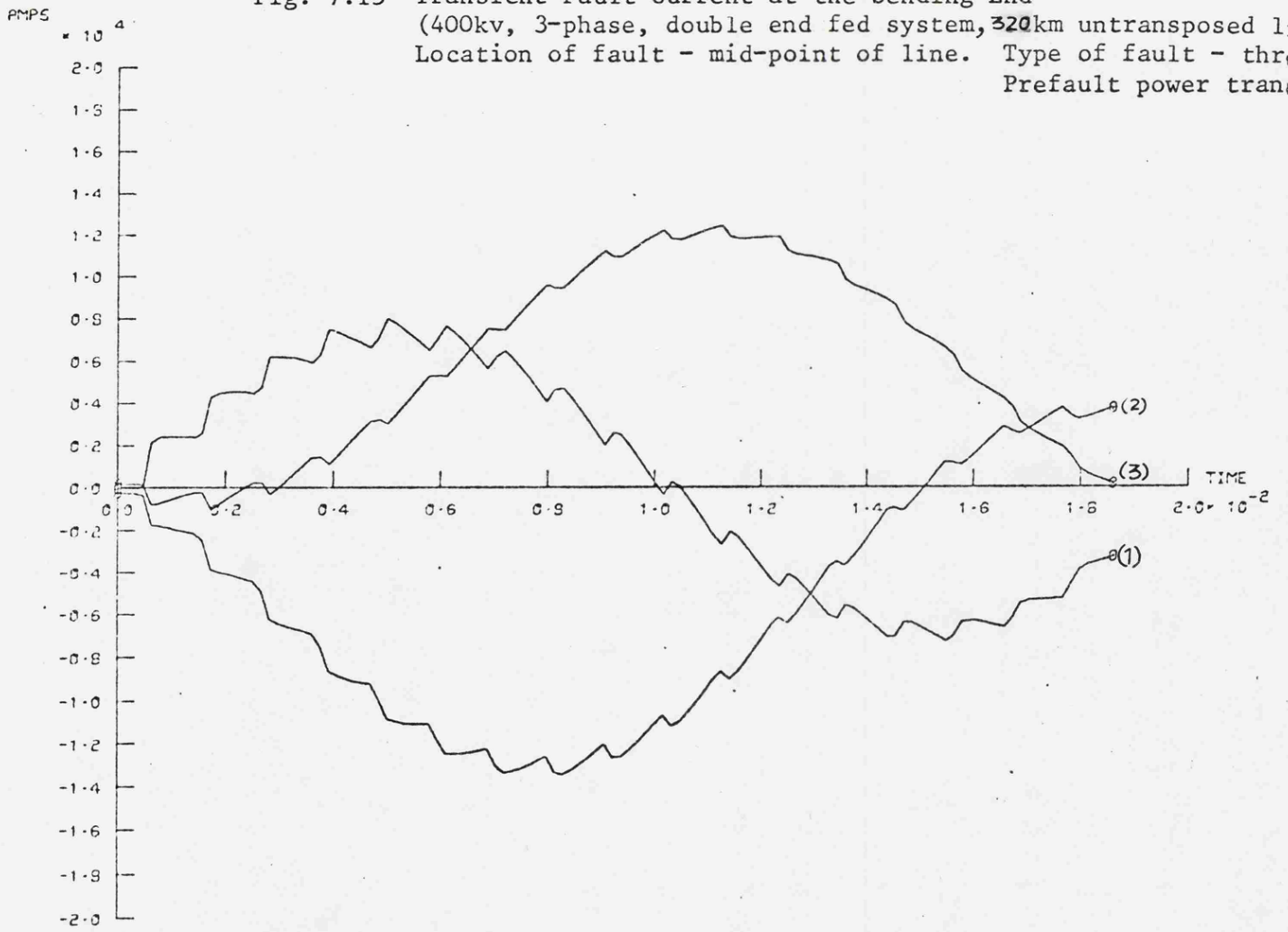

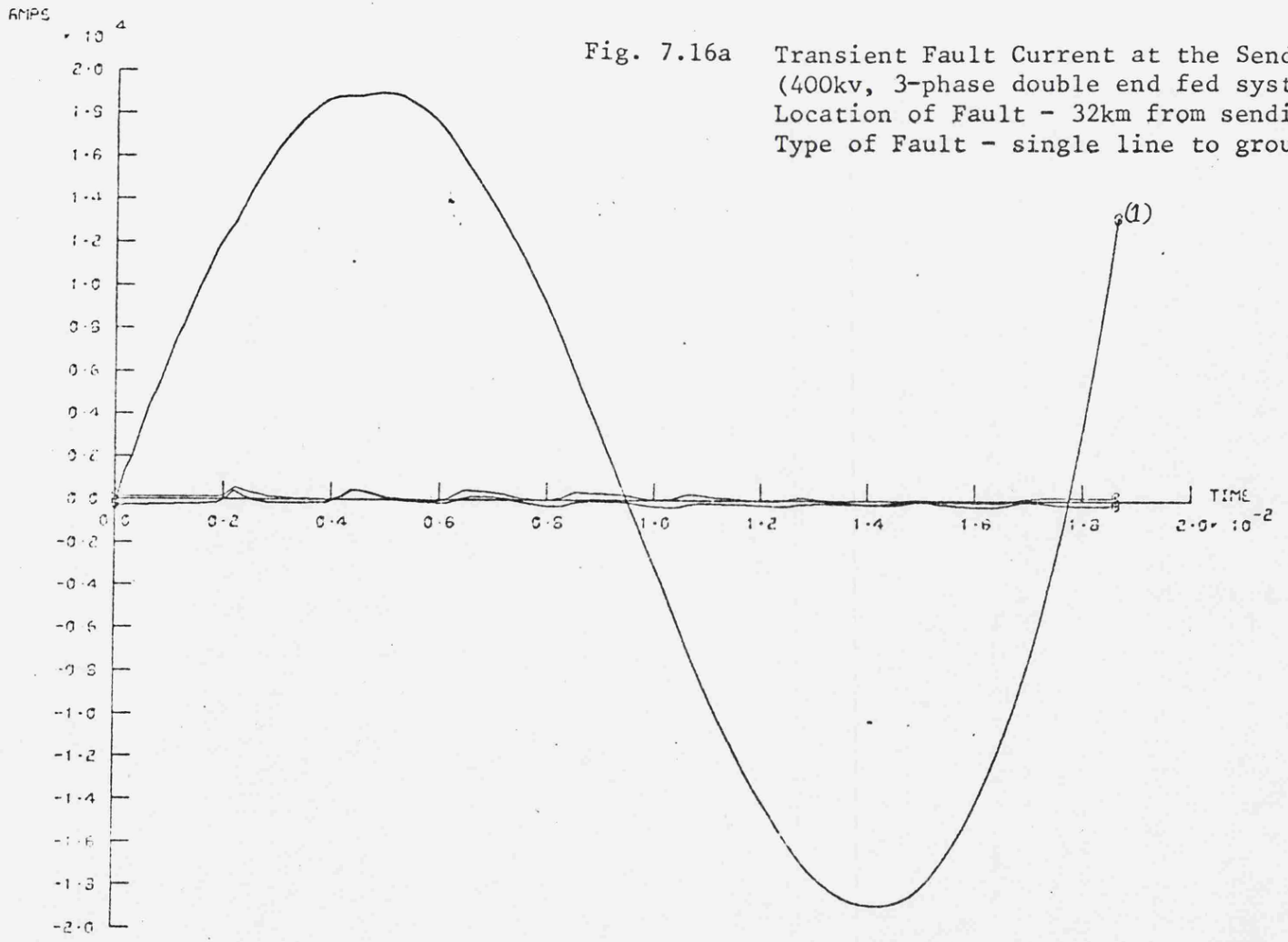

Fig. 7.16a Transient Fault Current at the Sending End
(400kv, 3-phase double end fed system, 320km untransposed line
Location of Fault - 32km from sending end;
Type of Fault - single line to ground

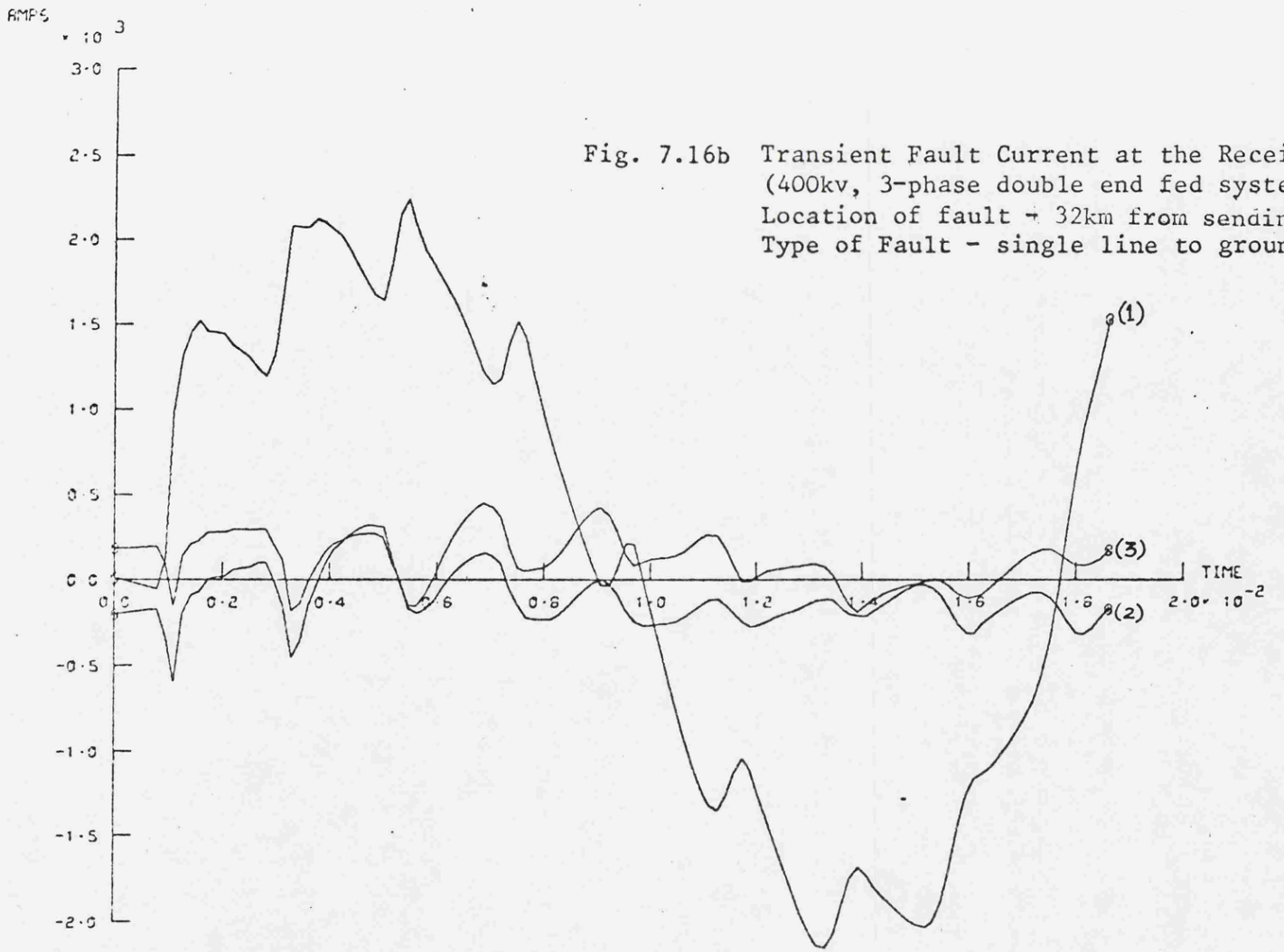

Fig. 7.16b Transient Fault Current at the Receiving End
(400kv, 3-phase double end fed system, 320km untransposed line)
Location of fault - 32km from sending end
Type of Fault - single line to ground

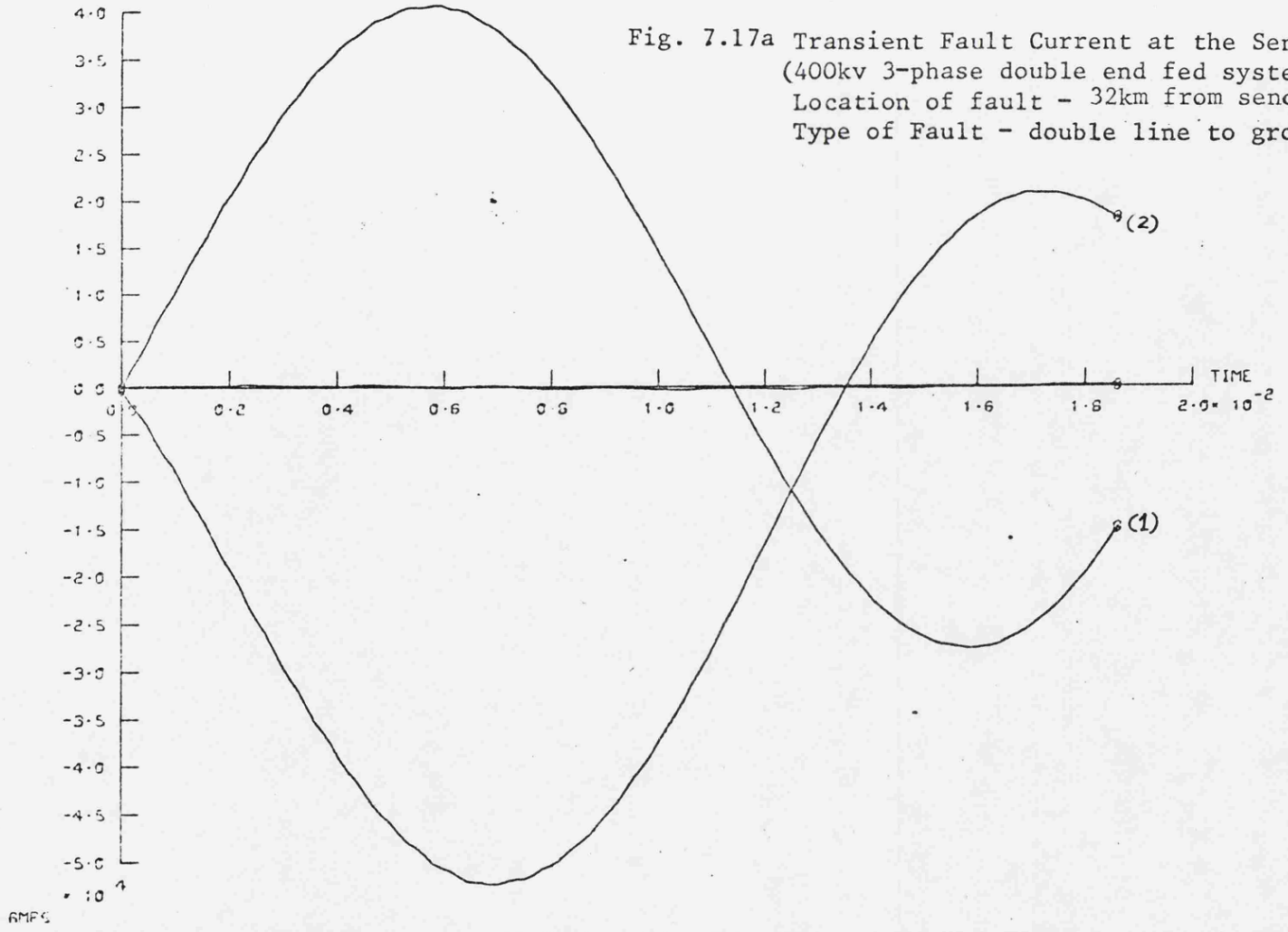

Fig. 7.17a Transient Fault Current at the Sending End
(400kv 3-phase double end fed system, 320km untransposed line)
Location of fault - 32km from sending end
Type of Fault - double line to ground

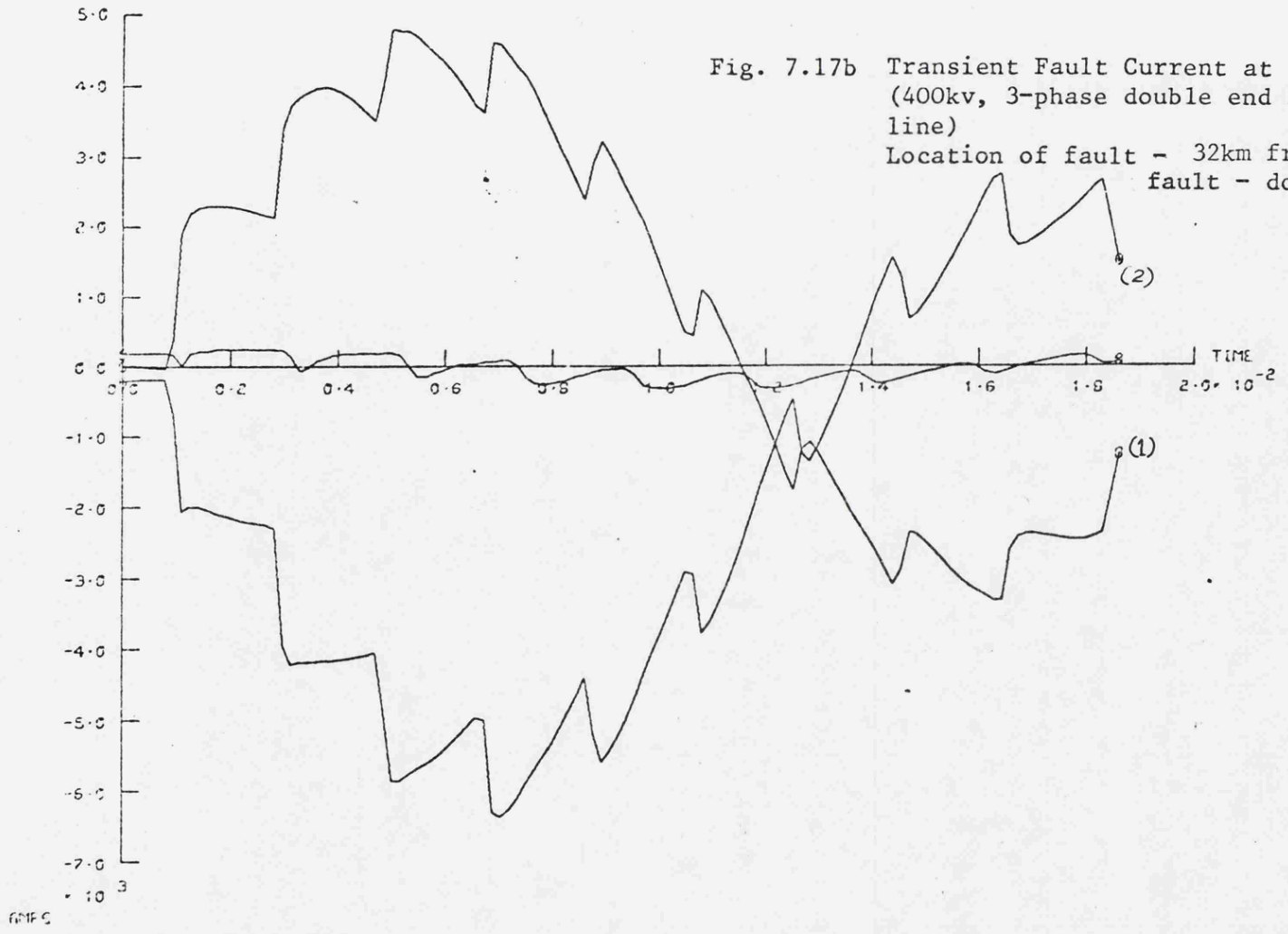

Fig. 7.17b Transient Fault Current at the Receiving End (400kv, 3-phase double end fed system, 320km untransposed line)
Location of fault - 32km from sending end. Type of fault - double line to ground

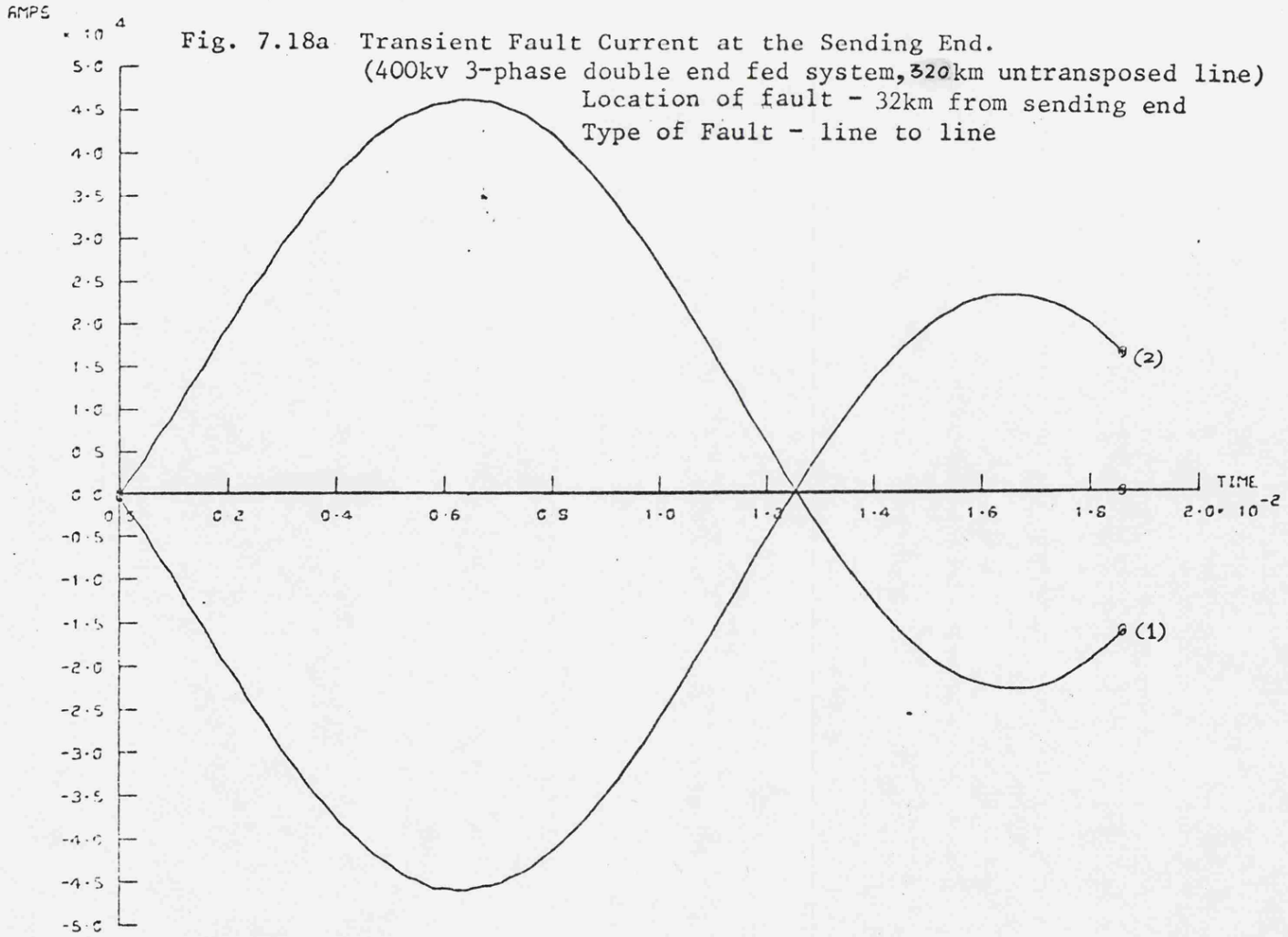

Fig. 7.18a Transient Fault Current at the Sending End.
(400kv 3-phase double end fed system, 320km untransposed line)
Location of fault - 32km from sending end
Type of Fault - line to line

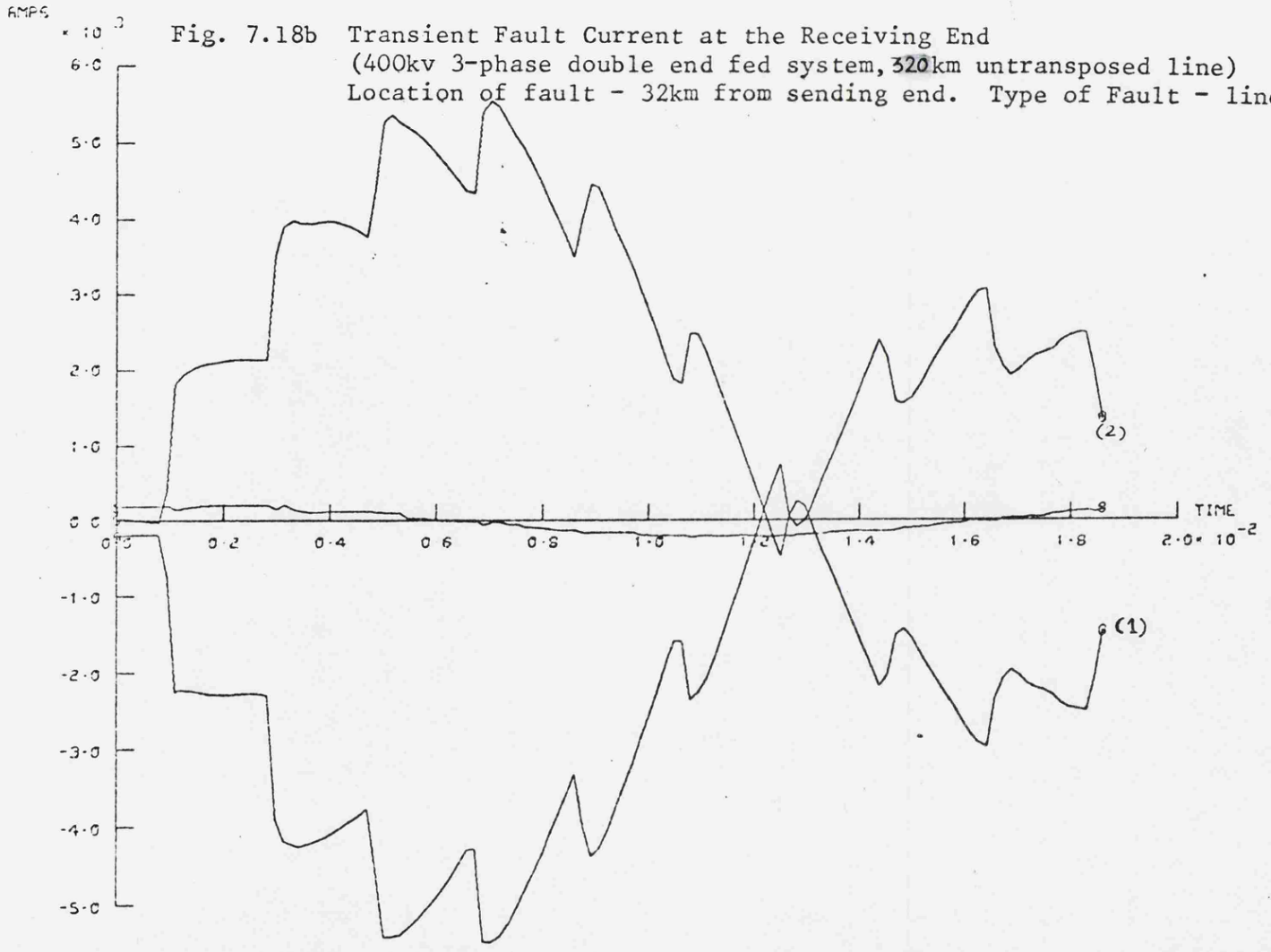

Fig. 7.18b Transient Fault Current at the Receiving End
(400kv 3-phase double end fed system, 320km untransposed line)
Location of fault - 32km from sending end. Type of Fault - line to line

Fig. 7.19a Transient Fault Current at the Sending End
(400kv 3-phase double end fed system, 32km untransposed line)
Location of Fault -320km from sending end
Type of Fault - three-phase

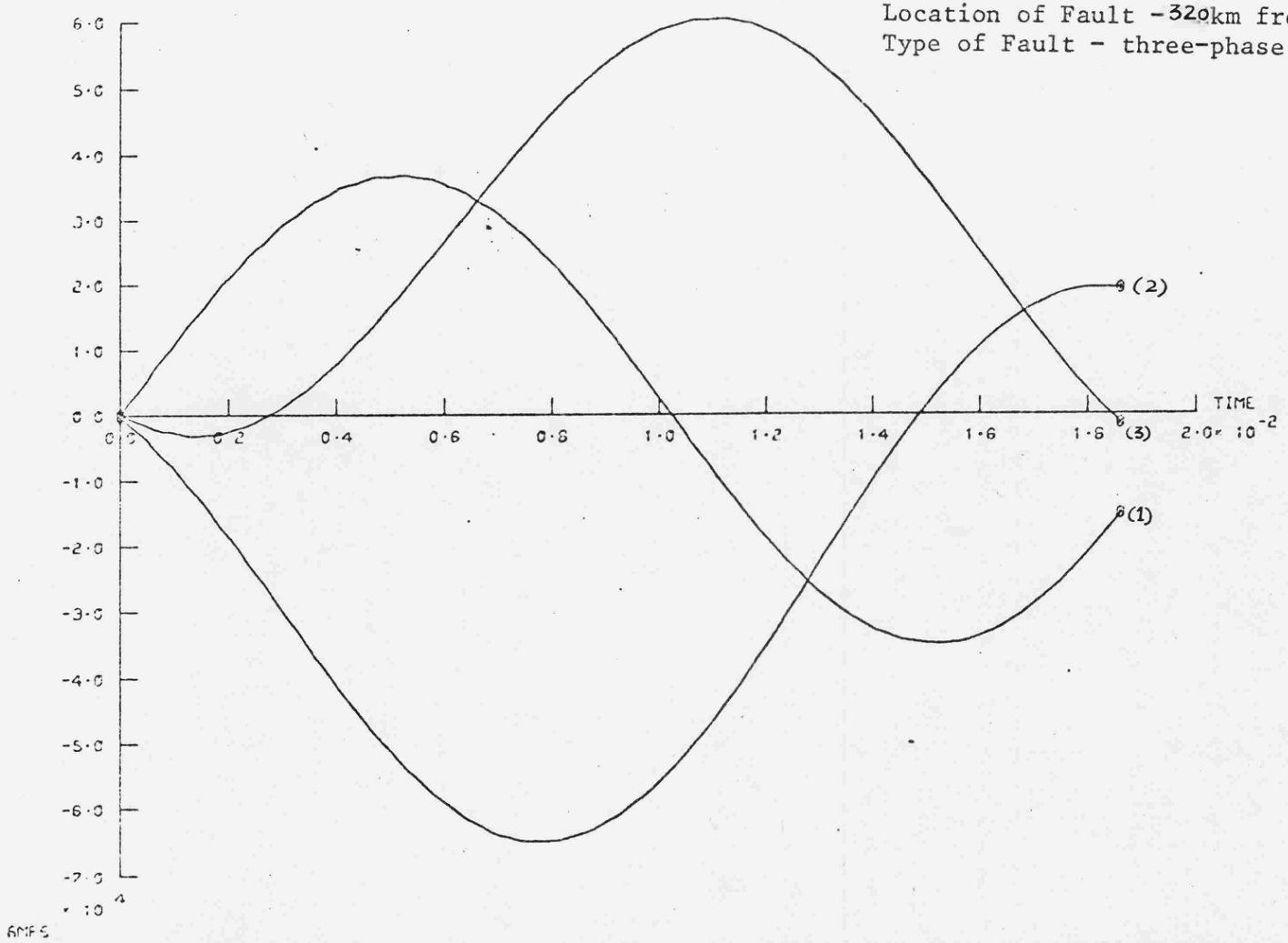

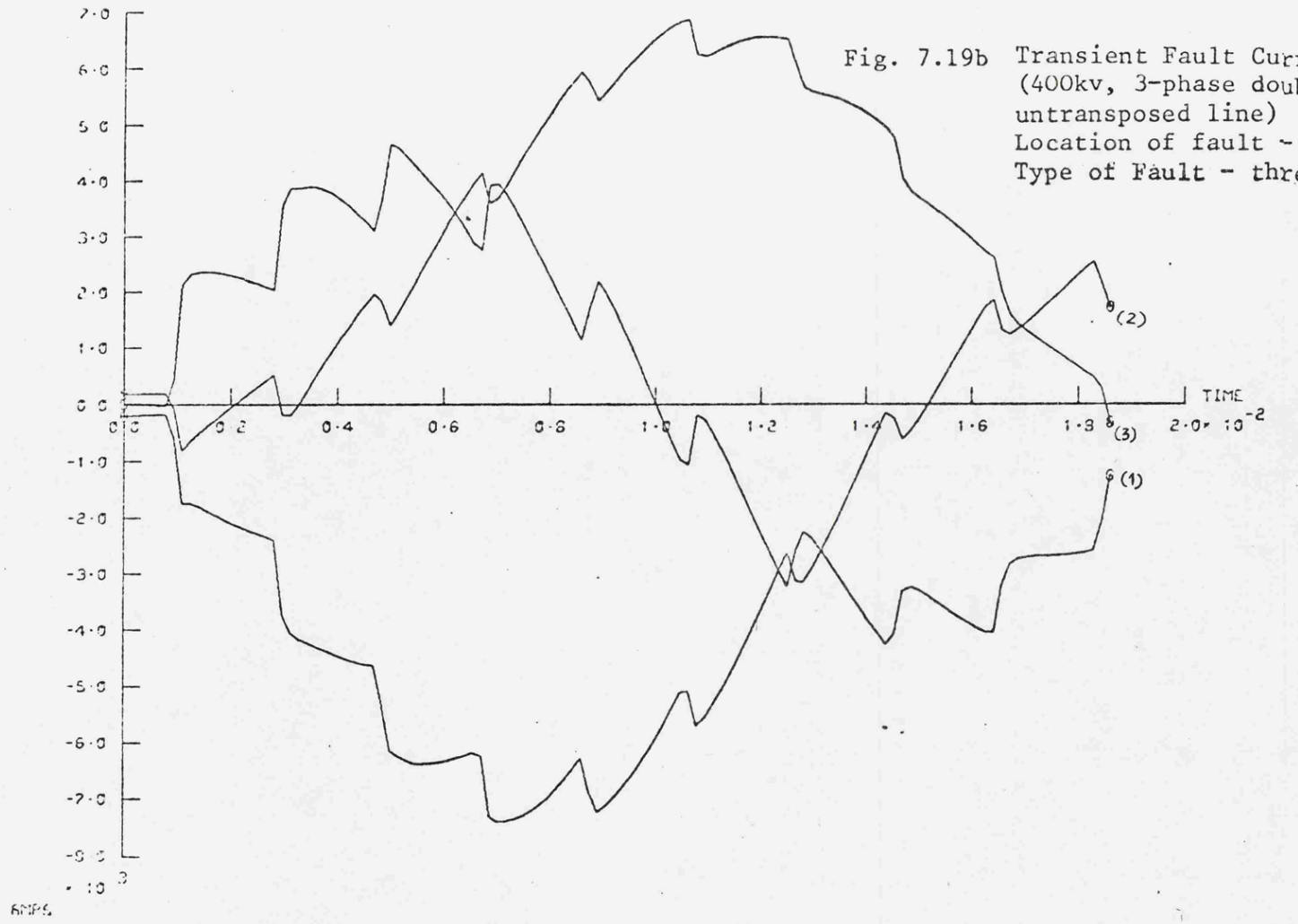

Fig. 7.19b Transient Fault Current at the Receiving End
(400kv, 3-phase double end fed system, 320km untransposed line)
Location of fault - 32km from sending end
Type of Fault - three-phase

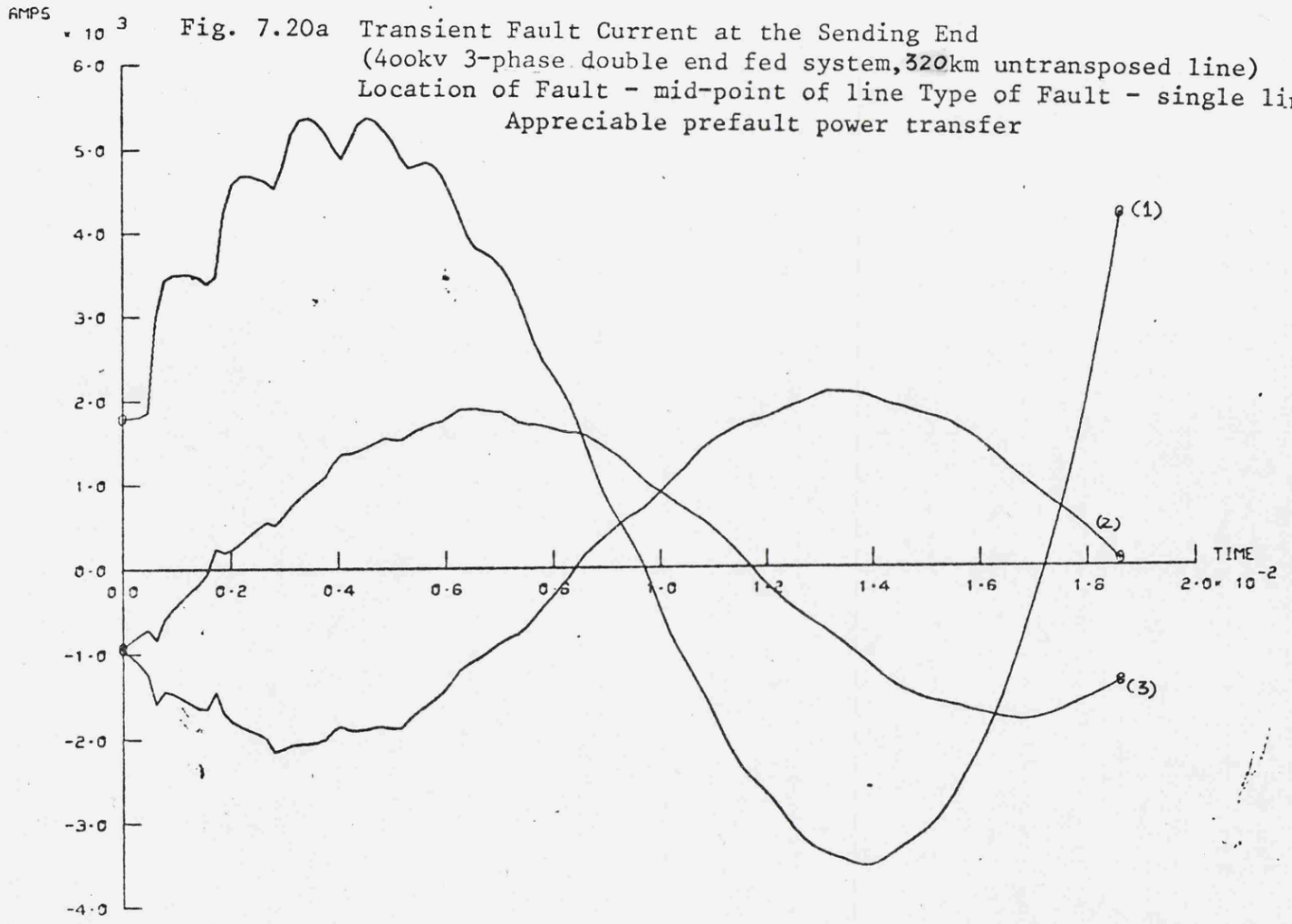

Fig. 7.20a Transient Fault Current at the Sending End
(400kv 3-phase double end fed system, 320km untransposed line)
Location of Fault - mid-point of line Type of Fault - single line to ground
Appreciable prefault power transfer

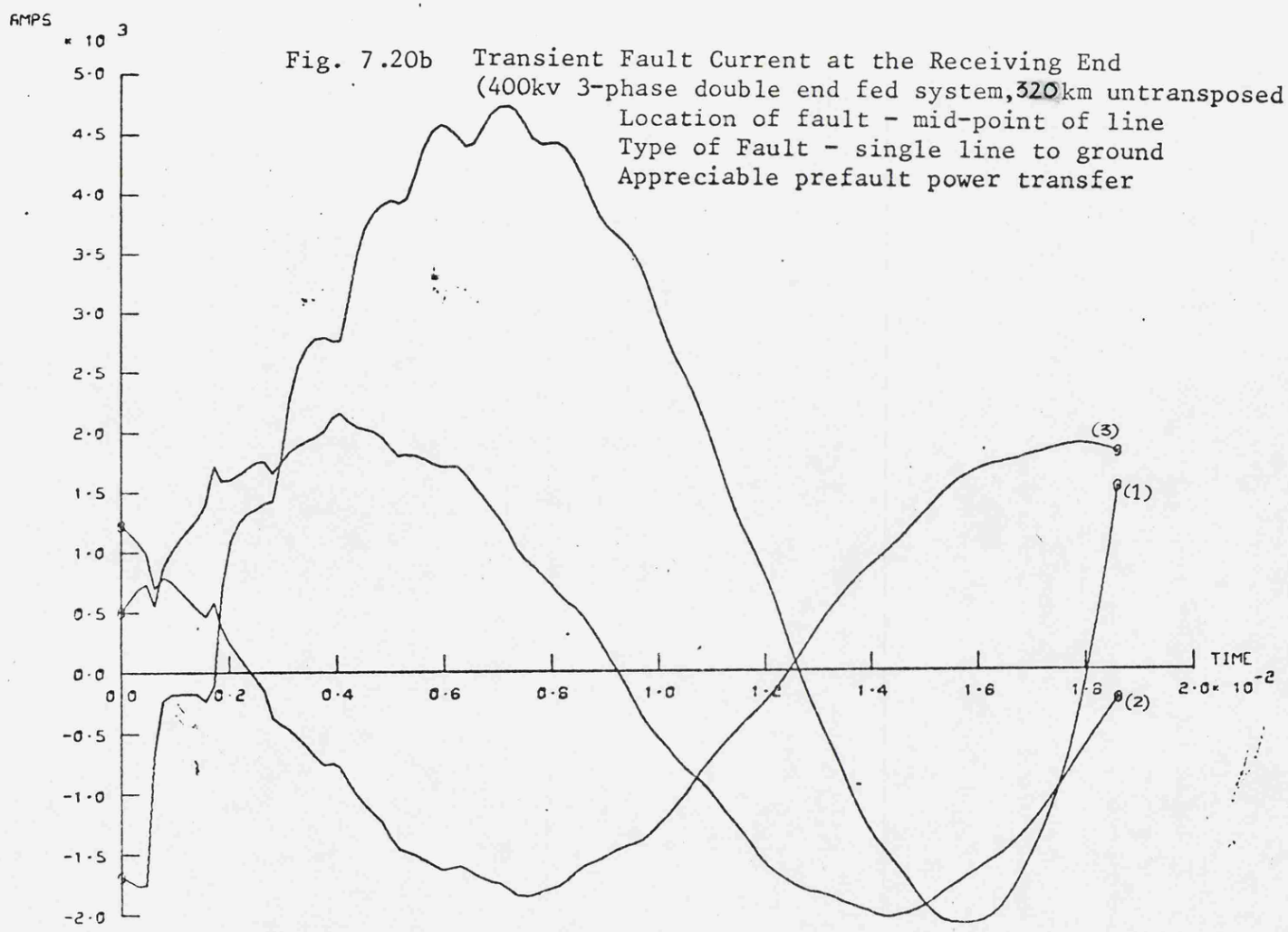

Fig. 7.20b Transient Fault Current at the Receiving End
(400kv 3-phase double end fed system, 320km untransposed line)
Location of fault - mid-point of line
Type of Fault - single line to ground
Appreciable prefault power transfer

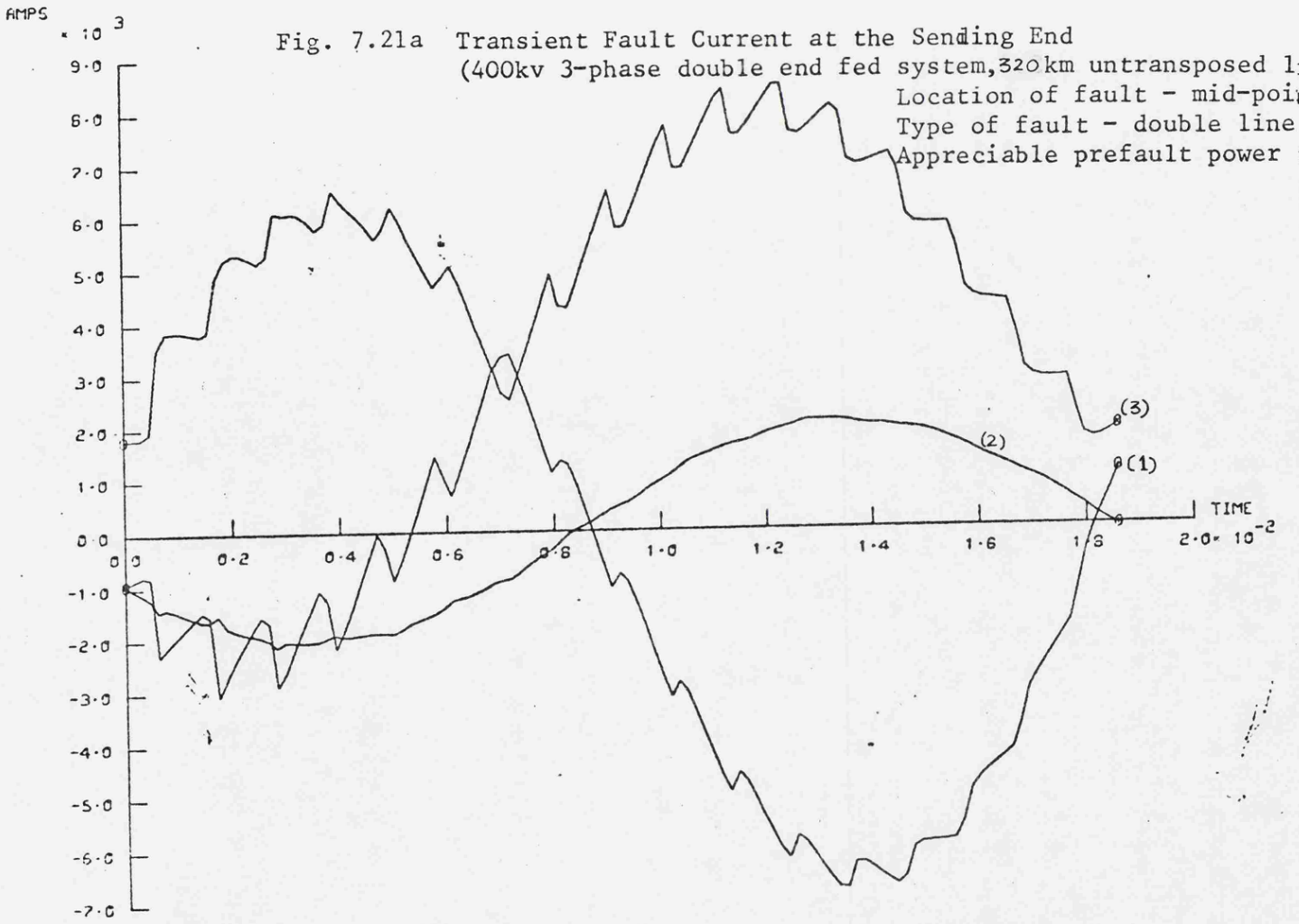

Fig. 7.21a Transient Fault Current at the Sending End
(400kv 3-phase double end fed system, 320km untransposed line)
Location of fault - mid-point of line
Type of fault - double line to ground
Appreciable prefault power transfer

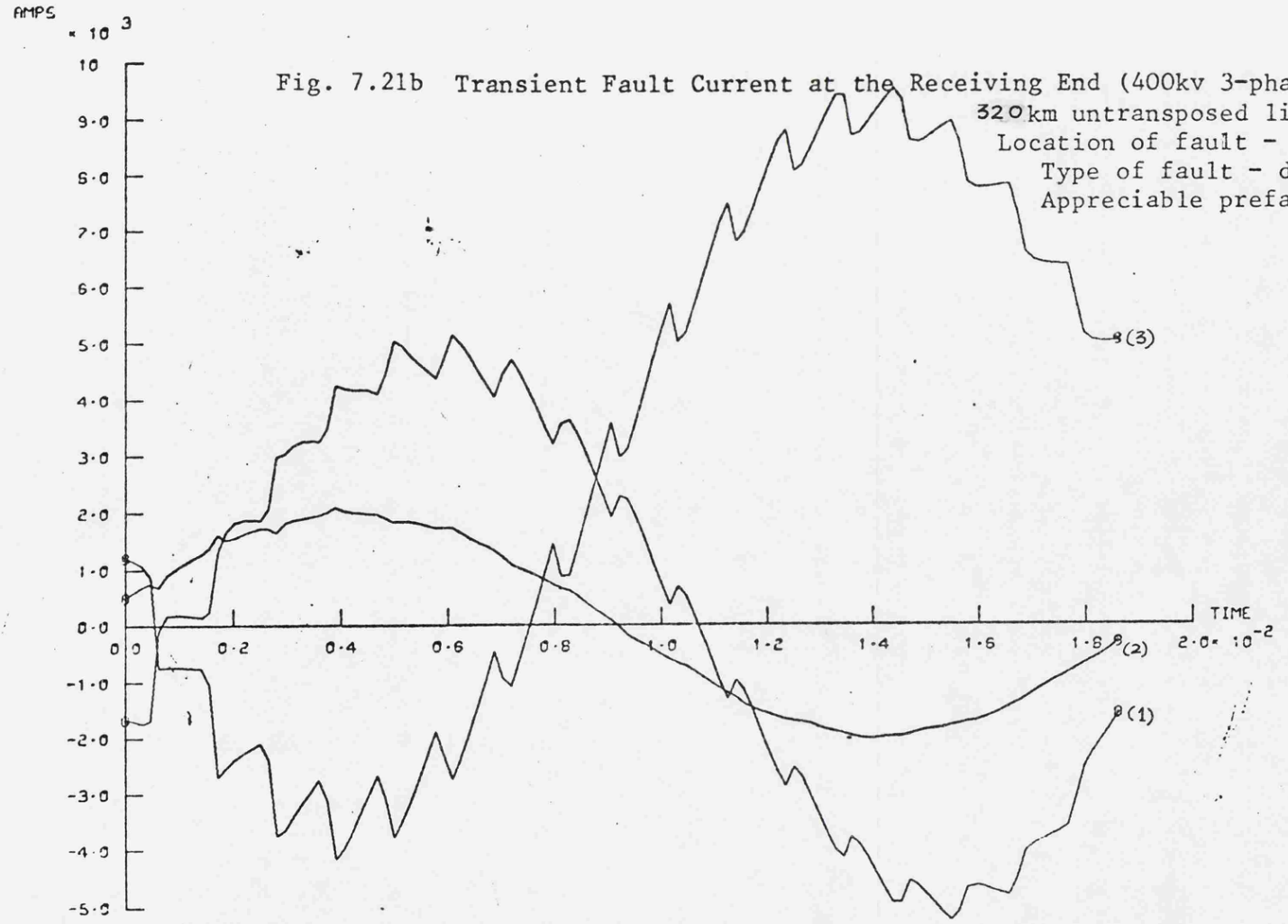

Fig. 7.21b Transient Fault Current at the Receiving End (400kv 3-phase double end fed system
320km untransposed line)
Location of fault - mid-point of line
Type of fault - double line to ground
Appreciable prefault power transfer

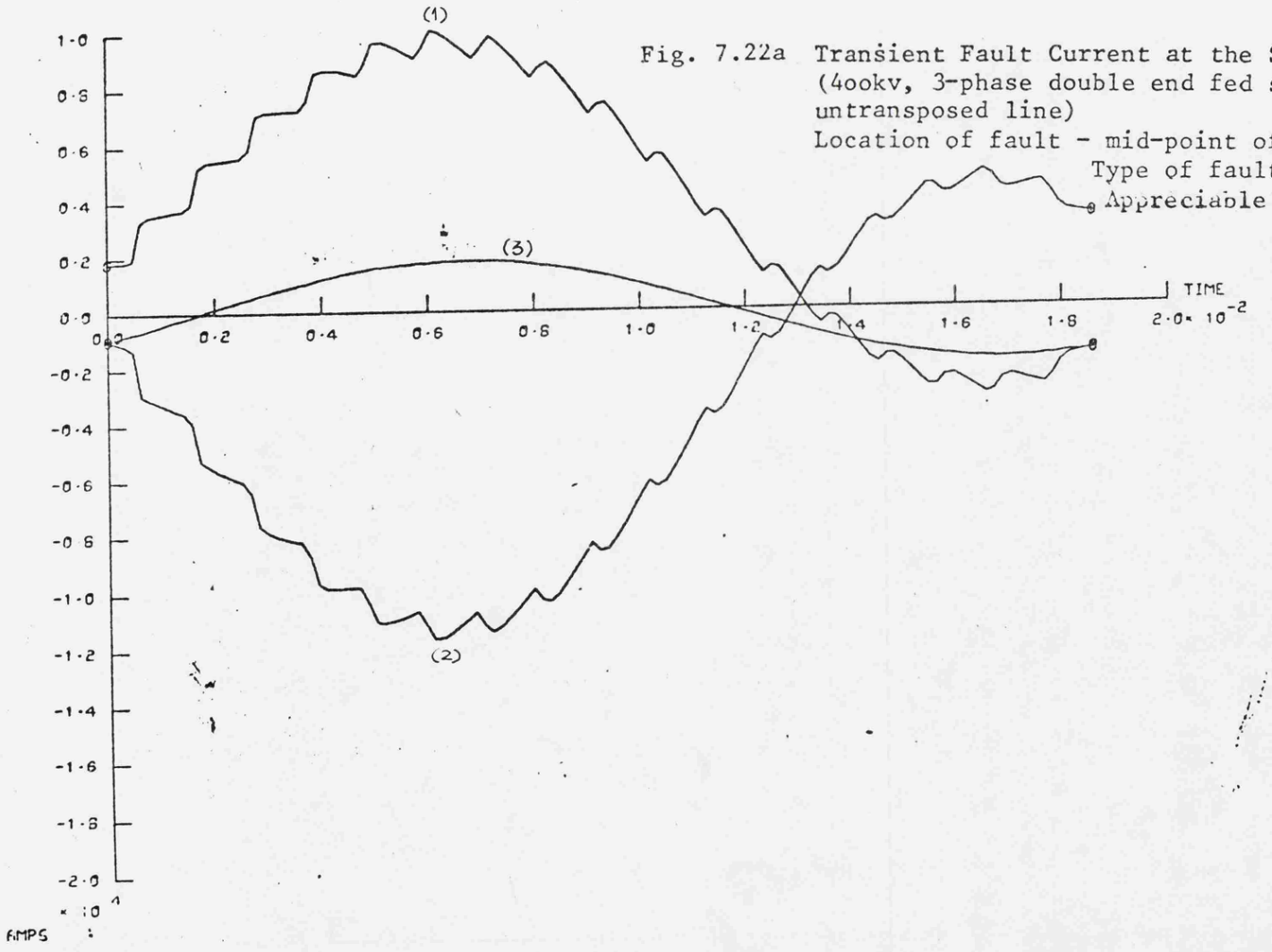

Fig. 7.22a Transient Fault Current at the Sending End
(400kv, 3-phase double end fed system, 320km untransposed line)
Location of fault - mid-point of line
Type of fault - line to line
Appreciable prefault power transfer

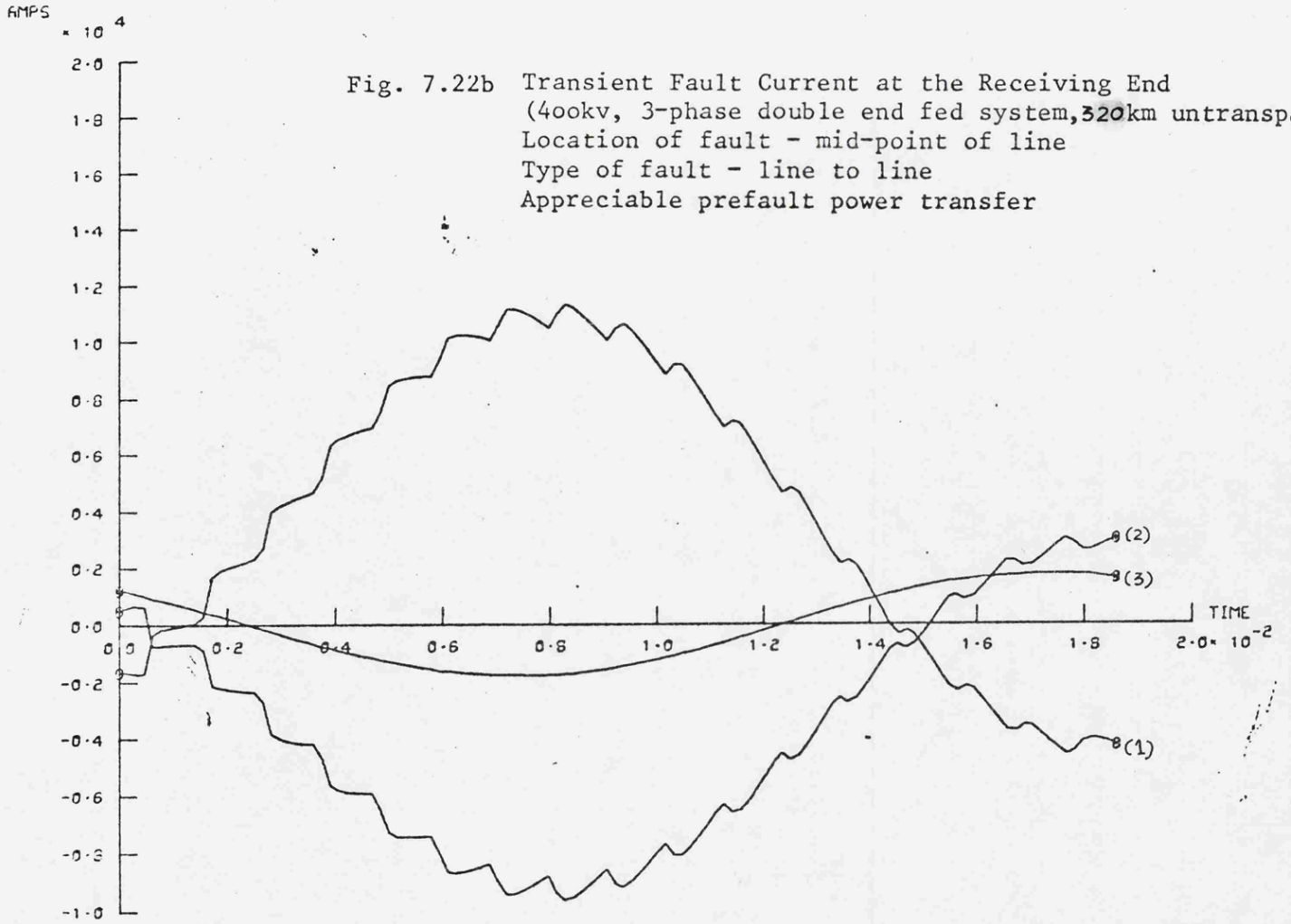

Fig. 7.22b Transient Fault Current at the Receiving End
(400kv, 3-phase double end fed system, 320km untransposed line)
Location of fault - mid-point of line
Type of fault - line to line
Appreciable prefault power transfer

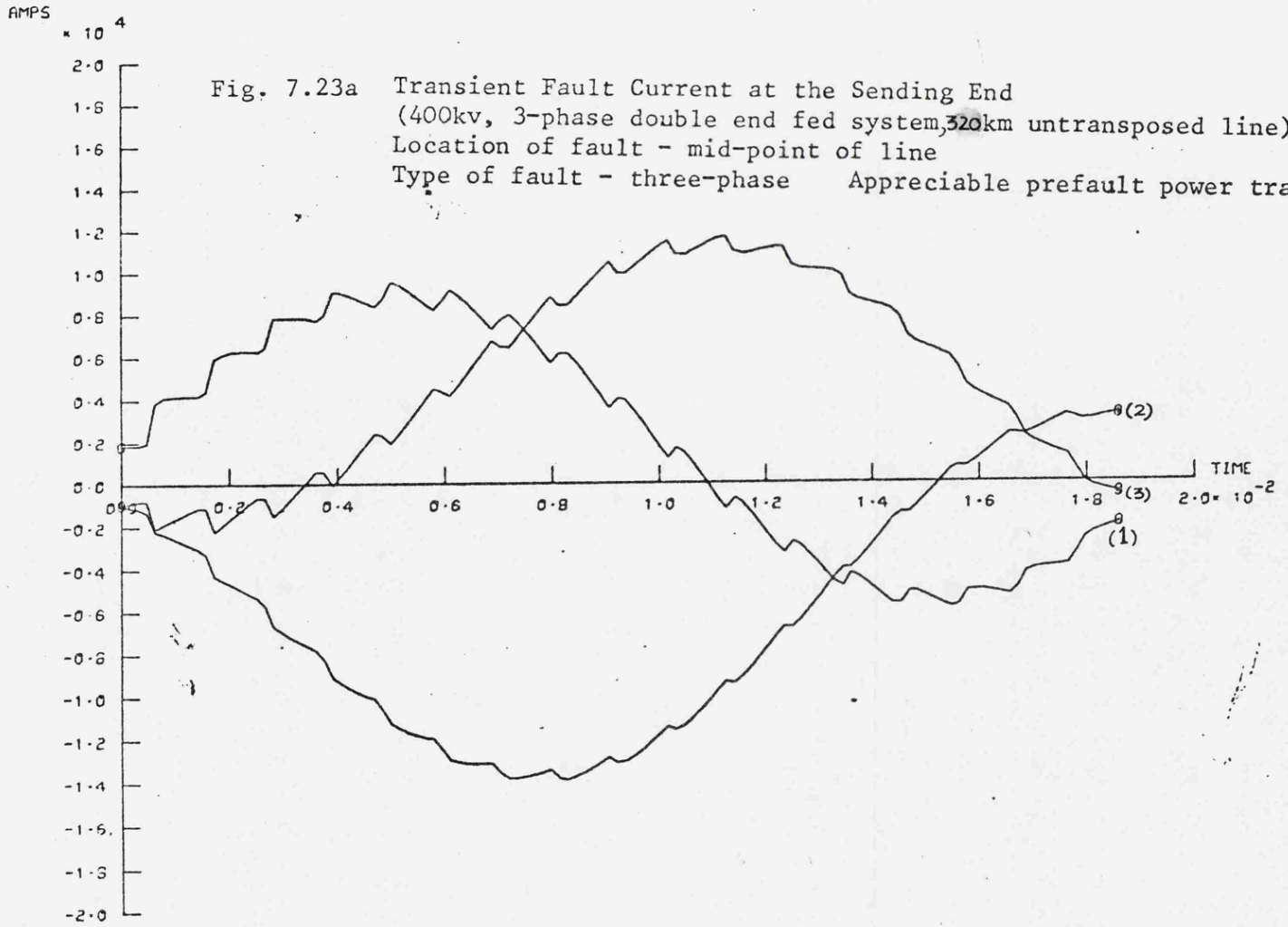

Fig. 7.23a Transient Fault Current at the Sending End
(400kv, 3-phase double end fed system, 320km untransposed line)
Location of fault - mid-point of line
Type of fault - three-phase Appreciable prefault power transfer

Fig. 7.23b Transient Fault Current at the Receiving End (400kv 3-phase double end fed system, 320km untransposed line)

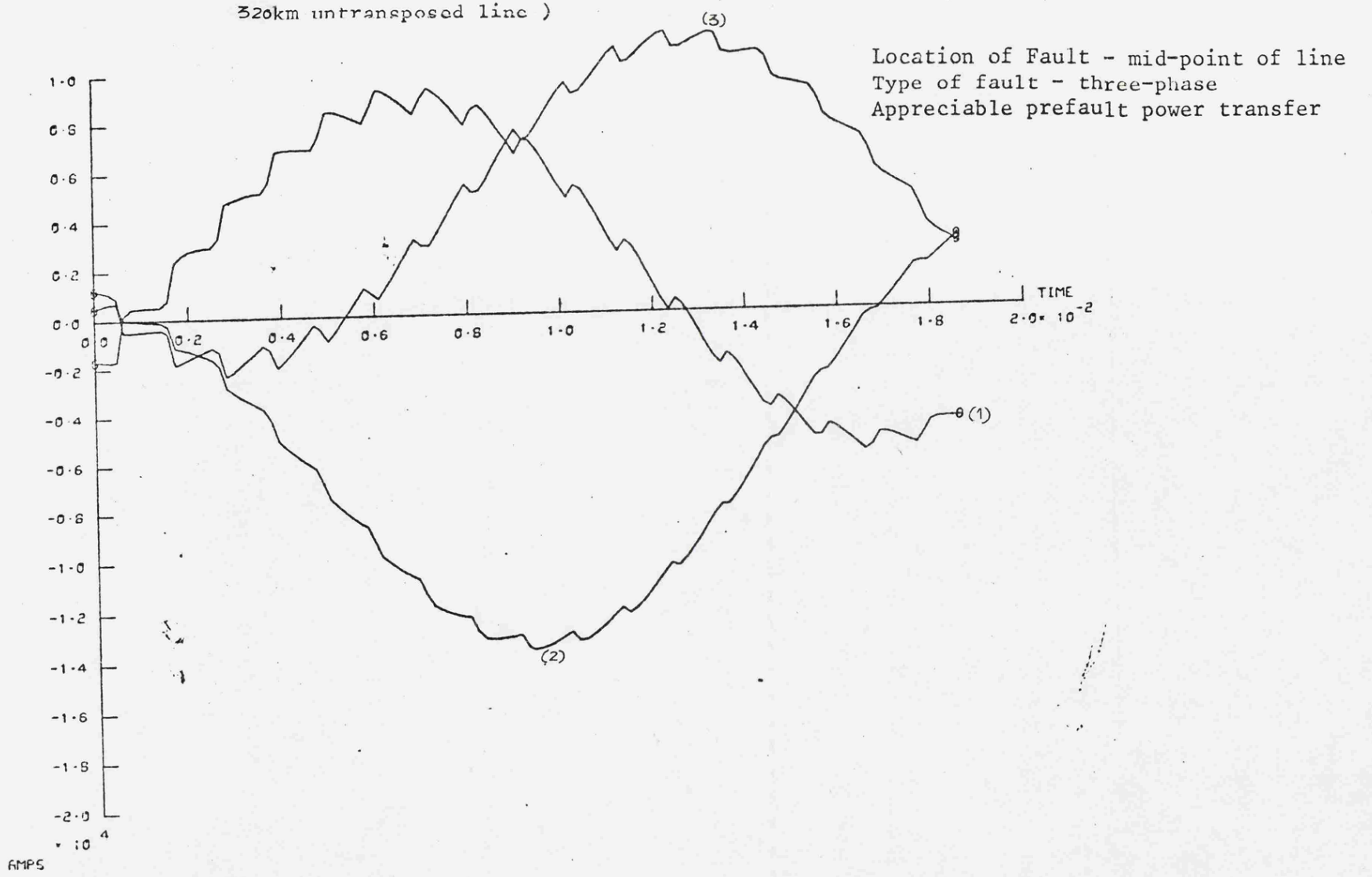

Fig. 7.24a Transient Voltage at the Sending End. (400kv 3-phase lumped parameter source)
Prefault power transfer negligible

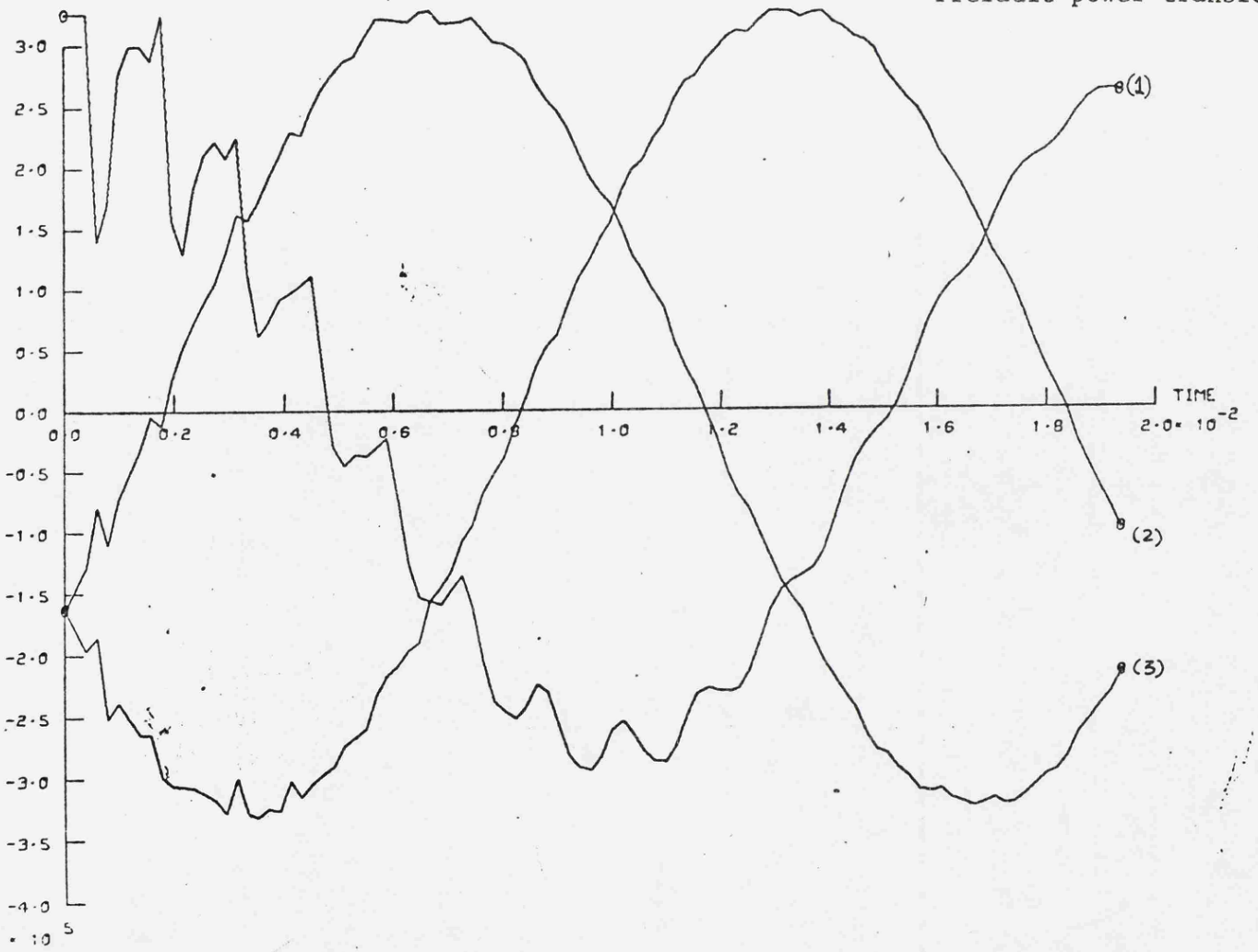

Fig. 7.24b Transient Fault Current at the Sending End

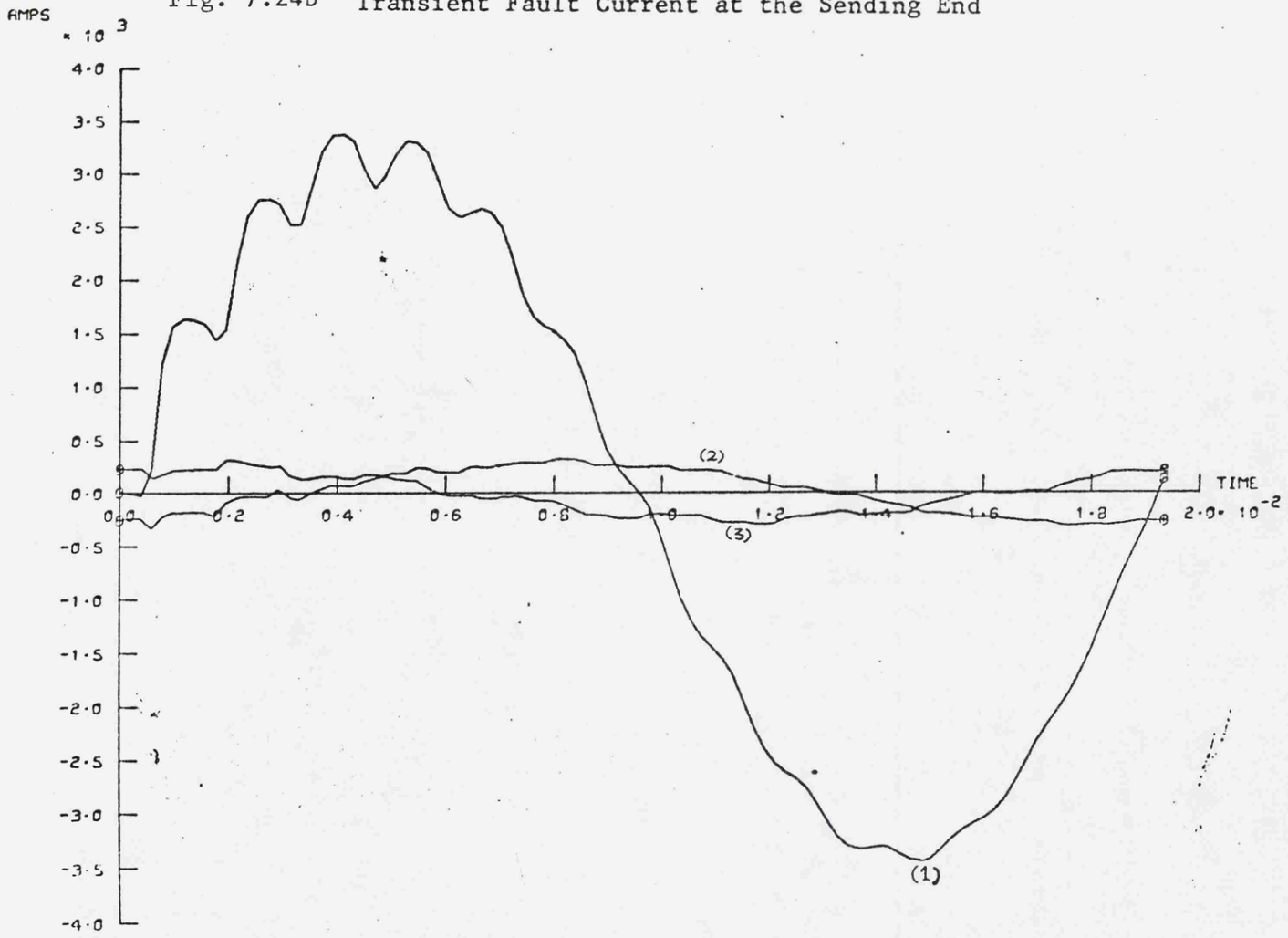

T A B L E 1

PARAMETERS OF TRANSPOSED LINE

Positive Sequence Parameters

r_1 = 0.01875 ohm/Km

ℓ_1 = 0.975 mH/Km

c_1 = 0.0118 μF/Km

Zero Sequence Parameters

r_o = 0.1975 ohm/Km

ℓ_o = 3.6 mH/Km

c_o = 0.00825 μF/Km

Frequency

f = 60 c/s

Series Impedance at 60 c/s (for R=0)

Z_s = j0.697 ohm/Km

Z_m = j0.330 ohm/Km

Shunt Admittance at 60c/s

Y_s = $j\ 0.405 \times 10^{-5}$ mho/Km

Y_m = $-j0.401 \times 10^{-6}$ mho/Km

Surge Impedance at 60 c/s

Z_{cs} = 406.883 ohms

Z_{om} = 119.587 ohms

Surge Admittance at 60 c/s

Y_{os} = 2.83643 mS

Y_{om} = -0.644289 mS

Velocity

V_f = 294664.06 kM/s

V_s = 179460.75 kM/s

TABLE 2 — 160km Transposed Line

	Digital Computer Results (Amps)	Calculated Results (Amps)	T (ms) T_f	T_s
SLG Fault				
I_1	$= 1.58 \times 10^3$ at t = 1.09ms	1.604×10^3	0.544	0.892 ms
I_2	$= 0$	0 (after the arrival of both components)		
I_3	$= 0$	0		
3-LG Fault				
I_1	$= 2.18 \times 10^3$	2.276×10^3		
I_2	$= -1.14 \times 10^3$	-1.138×10^3	0.544 ms	
I_3	$= -1.04 \times 10^3$ t = 0.625 ms	-1.138×10^3		
L_1-L_2 Fault				
I_1	$= 1.66 \times 10^3$ at t = 0.625 ms	1.705×10^3		
I_2	$= -1.66 \times 10^3$	-1.705×10^3	0.544 ms	
I_3	$= 0$	0		
L_1-G & L_2-G				
I_1	$= 2.05 \times 10^3$	2.03×10^3		
I_2	$= -1.57 \times 10^3$ at t = 0.937 ms	-1.38×10^3	0.544 ms	
I_3	$= 0$	0		

The Table shows the comparison of the digital computer results and the results obtained from the approximate calculation. The calculated results are evaluated from the following relation :

$$[I] = -2[Yo][v]$$

where

I = Peak value of the Current at the sending end due to the arrival of the first incident wave of fault surge.

V = Voltage of the hypothetical e.m.f. Source at the instant of fault inception

Yo = Surge-admittance matrix (assumed to be purely conductive)

T_f = Time delay in the arrival of fast component.

T_s = Time delay in the arrival of slow component.

TABLE 3 Untransposed Line

	Digital Computer Results (Amps)	Calculated Results (Amps)	T (ms) T_{f_1}	T_{f_2}	T_s
SLG Fault					
I_1 =	1.719×10^3	1.78×10^3	0.541	0.544	0.707
I_2 =	0	0			
I_3 =	0	0			
L_1-G & L_2-G Fault					
I_1 =	2.359×10^3	2.318×10^3		0.54	
I_2 =	-1.787×10^3	-1.632×10^3		0.54	
I_3 =	0	0			
L_1-L_2 Fault					
I_1 =	2.051×10^3	1.98×10^3		0.54	
I_2 =	$-I_1$	$-I_1$		0.54	
I_3 =	0	0			
3LG Fault					
I_1 =	2.477×10^3	2.48×10^3		0.54	
I_2 =	-1.564×10^3	-1.37×10^3		0.54	
I_3 =	-0.8374×10^3	-0.993×10^3		0.54	

The calculated results for Table 3 are obtained according to the approximate relation defigned in Table 2.

CHAPTER 8

CONCLUSIONS

E.H.V. transmission line demands ultra-high-speed protective schemes. Very realistic and accurate simulation of the post-fault transient behaviour of the transmission line are necessary for the proper design and development of these schemes, and for the proper co-ordination of insulators.

Such simulation has been achieved in this thesis by digital computer studies of very sophisticated mathematical models of transmission systems.

Parameters of the transmission line are highly frequency dependent and influence the transient behaviour of the line. Knowledge of these parameters over a wide range of frequencies are essential for transient studies. Hence, the method of the evaluation of the parameters at any desired frequency are described in detail in Chapter 2.

A very generalised technique for the simulation of faults on transmission lines is described in Chapter 3. The generalised technique is fundamentally based on the property of voltage reduction at the location of fault. The sudden voltage reduction at the location of fault due to fault inception is simulated by switching on a hypothetical emf source with a series impedance. The emf of the hypothetical source is equal and opposite to the prefault voltage and the series impedance is equal to the fault impedance. The hypothetical generator is finally replaced by an equivalent current generator.

The fault transient response is thus defined by the sum total of the combination of all the emf sources in the prefault circuit and the hypothetical emf or current sources simulating the fault.

The system is usually under steady state condition before the fault inception. In this case, fault transients are defined by the super-

position of the prefault steady state condition and the switching transient solution due to the hypothetical source.

Simulation of shunt faults by the equivalent current generators makes the solution very easy and general for all types of shunt faults and is heretofore not available in the literature.

Series(open conductor) fault is simulated by switching on a current generator at the location of fault. The current injected by the current generator being equal and opposite to the prefault current at the location of fault.

The simulation of series fault is described in the Appendix 4. Generally, the system is under steady state condition before the fault inception. Hence, the mathematical models for steady state solution are developed in Chapter 4. The theory of natural modes[1] forms the basis of the mathematical model of multiconductor line and is described in detail in this section.

Mathematical models for fault transients are developed in Chapters 5 and 6. Fault transient models are based on the principle outlined in Chapter 3. The transient solution is evaluated by the technique of modified Fourier transform[49-57]. This technique is used in order to take the frequency dependence of the parameters into account.

In Chapter 5 conventional single-phase representation of ideally transposed three-phase line has been studied. This study is suitable for single phase circuits and for balanced faults on balanced systems. However, the entire picture of the transient behaviour of each phase of the polyphase line, are not always understood from the study of the single-phase circuit. Hence, the study of the practical three-phase line is taken up in Chapter 6. In both of these studies - single-phase

circuit and three-phase circuits - the frequency dependence of the line parameters can be taken into account. Such a rigorous analysis for fault transients is not available in the literature.

In Chapter 7 the digital computer results are presented. The system transient response at the relaying point and the fault induced overvoltage are studied.

Digital computer results presented in this chapter display a very clear picture of the transient behaviour of the transmission system due to the fault initiation.

The following general conclusions may be drawn from the digital computer studies:-

(1) The digital computer results confirm the validity and the generality of the mathematical fault transient models.
This conclusion may be drawn from the following observations:-
   (a) Excellent agreement with Kimbark's field test results for fault induced over voltages due to single line to ground fault in the double-end fed system.
   (b) Excellent agreement of the results of the sophisticated model and the approximate model for short line faults.
   (c) Excellent agreement of the time delay in the arrival of the first incident wave of fault surge, from the location of fault to the relaying point and the time interval between any consecutive reflections.
   (d) Excellent agreement with the surge impedance of the line of the magnitude of the current at the relaying point due to the arrival of the first incident wave of fault surge.

(e) Excellent agreement with Bewley's theory of multivelocity propagation of modal components e.g. In the case of transposed line digital computer results show -

(a) the propogation of two components - fast and slow - in the case of SLG fault.

(b) the propogation of fast components only in the case of line to line fault or three phase fault.

(2) The following information about the fault may be known from the careful observation of the current waveform at the relaying point:-

(a) type of fault

(b) location of fault

(c) the phase angle of the prefault voltage at the location of fault at the instant of fault inception.

The above conclusions are true for shunt faults only at a particular location. However, further investigation is necessary in order to establish that the variation of current due to the initiation of shunt faults is unique and similar variation of current is not caused by any other cause(s).

(3) The influence of untransposition is very insignificant and may be neglected if very high degree of accuracy is not desired. Moreover, the study of this transposed line is justified because of the computational efficiency and the economy in compution time.

(4) Any superspeed relay cannot detect this fault at the instant of fault inception. This is due to the time delay in the arrival of fault initiated surge from the location of fault to the relaying point.

(5) The influence of the frequency dependence of the line parameters is very significant in the case of SLG fault. The hf disturbances are very prominent for comparatively longer duration of time in the case of frequency invariant parameters than in the case of frequency dependent parameters. Thus, the frequency dependence of the parameters is a boon for the slow relays, as the waveform would be less noisy after about one-half cycle or so of the supply frequency. However, the disturbance is very Similar in either case - with frequency dependent or invariant parameters - during a period of 5 ms or less after the fault inception. Hence, the influence of the frequency dependence of the parameters would not be very significant as far as the design of the superspeed relays with operating time 5ms or less are concerned.

(6) The fault induced overvoltages may be evaluated by this analytical technique for transposed line or untransposed line with frequency dependent or invariant parameters. Kimbark's method is applicable for transposed line with frequency invariant parameters only. Moreover, on the basis of this technique the fault induced overvoltages due to off-centre SLG fault, combination of SLG fault and open conductor fault or any other type of fault can be very easily determined. Analysis of such cases may be very complex by Kimbark's method.

(7) By suitable design of line parameters the duration and the peak value of the overvoltage pulse may be reduced.

(8) The computer programme is made very efficient by storing the basic parameters of any line e.g. Yo, γ, Q at the supply frequency and over a wide range of complex frequencies in a data file. The range of complex frequencies is defined by the observation period. The data file takes a very small amount of core-store

and the advantage of storing the basic data is that the same calculations would not have to be repeated over and over again for the evaluation of fault transients under different conditions e.g. for different fypes of faults, different location of faults, different instant of fault inception.

The analytical technique for the evaluation of fault transients is very general and its main features may be summarised as follows:-

(1) The technique is applicable for both transposed and untransposed line with distributed parameters.

(2) The frequency dependence of line parameters can be taken into account.

(3) Transmission line of any configuration may be analysed.

(4) There is no limitation on

  (a) the length of the line

  (b) the location of fault

  (c) the instant of fault inception

(5) Any linear time invariant fault impedance can be taken into account.

(6) Any termination can be taken into account.

(7) Any model of the source can be taken into account provided it is suitably defined in the frequency domain.

(8) The following types of faults can be analysed on the basis of this method

  (a) All types of shunt faults at a particular location.

  (b) All types of series faults (open conductor faults) at a particular location.

  (c) Simultaneous shunt faults or series faults at multiple locations.

  (d) Combination of shunt and series faults at one or multiple locations

Future Work

The work presented in this thesis forms the first stepping-stone for the design and development of superspeed protective schemes. For the achievement of superspeed protective scheme and for simulation of fault transient phenomena in some more practical cases further future work may be carried out along the following lines:-

(1) The primary circuit signals obtained from simulation studies may be used for the development of the digital computer program suitable for high speed protective schemes.

(2) Some of the existing algorithms may be tested and their limitations and suitability established properly on the basis of these realistic signals obtained from simulation studies.

(3) In the present work the single circuit polyphase line has been studied for single- and double-ended systems, but the technique of fault simulation outlined in this thesis is very general and is readily applicable for double-circuit line and for more complex power systems.

(4) If SLG fault is not cleared immediately, then it often escalates to double-line to ground or three-phase faults. The present analysis can be very easily extended for the analysis of sequential faults. In this case, the prefault conditions would be under transient conditions (due to the initiation of SLG fault) instead of being under steady state condition as has been generally considered in the present analysis. The simulation for this case would be very similar to sequential switching.[19]

(5) The present analysis is applicable for any linear time invariant fault resistance or in other words for any constant value of fault resistance.

In actual practice the fault resistance is nonlinear and time dependent. However, fault resistance may be assumed to be constant for short duration faults. This assumption may be justified on the basis of fast fault clearance, and is further confirmed by some recent field test results and approximate arc simulation studies.[5] Further investigation is necessary for properly establishing the characteristics of the arc in the air, so that the fault resistance may be properly defined and simulated.

(6) The representation of source by the simplified models - infinite busbar, and lumped parameter model - is suitable for some practical situations for transient studies.[21] The source influences the system transients to a great degree. In many practical situations, these simplified representations may not be very realistic e.g. the sources with distributed generators and various line infeeds. Better representation is necessary for similar complex arrangements.

(7) In this thesis results of transient variation of voltages and currents on the transmission line at the relaying point have been presented. In practice, these informations are scaled down by transducers and then used for relaying purposes. With the advent of high performance wide-bandwidth transducers these informations would be scaled down without any further distortion and may be used directly for the relays. The present work may be justified on the basis of such future development.

The transducers in common use at present influence the secondary quantities very much and causes further distortion in the relaying signals.

Hence the future work may be directed towards the development of high performance wide-bandwidth transducers. Meanwhile, the present analysis

* Typical value of bandwidth may be defined to be 10-20 kc/s.

may be extended for the evaluation of the response at the secondary terminals of the transducers in common use these days. This would need proper simulation of these transducers in the frequency domain.

(8) Series capacitors and shunt reactors are used in some long ehv lines. The series capacitors reduce the effect of inductive reactance of the line and increase the transmission capability of the line. Shunt reactors offset the line charging current and thereby limit the steady state voltages during light load conditions and limit the voltages during switching operations.

Both of these devices would influence the transient response significantly. Future investigation should be directed towards their proper simulation so that their influences also may be taken into account. However, nonlinearity of these devices pose a very big challenge.

APPENDIX 1

Steady State Solution of the Faulted Three-Phase Transmission Line by the Principle of Superposition

Consider a three-phase transmission circuit fed from infinite busbar source at either end. Let the fault occur at some intermediate point, as shown in Fig.6.1.

The prefault system equations are given by

$$\begin{bmatrix} I_{ss} \\ I_{xs} \end{bmatrix} = \begin{bmatrix} A_1 & B_1 \\ B_1 & A_1 \end{bmatrix} \begin{bmatrix} V_s \\ V_{xp} \end{bmatrix} \qquad (1)$$

$$\begin{bmatrix} -I_{xs} \\ I_{Rs} \end{bmatrix} = \begin{bmatrix} A_2 & B_2 \\ B_2 & A_2 \end{bmatrix} \begin{bmatrix} V_{xp} \\ V_R \end{bmatrix} \qquad (2)$$

where I_{ss}, I_{Rs}. I_{xs} represent the current vectors in the lines in the prefault circuit at the sending end, receiving end and at x in the direction shown in Fig.6.1.

V_s, V_R, V_{xp} represent the voltage vectors of the lines with respect to earth at the sending end, receiving end and at x in the prefault circuit.

From equations (1) and (2), we obtain

$$I_{ss} = A_1 V_s + B_1 V_{xp} \qquad (3)$$

$$I_{Rs} = B_2 V_{xp} + A_2 V_R \tag{4}$$

$$I_{xs} = B_1 V_s + A_1 V_{xp} \tag{5}$$

$$-I_{xs} = A_2 V_{xp} + B_2 V_R \tag{6}$$

Adding equations (5) and (6) we obtain

$$0 = (A_1 + A_2) V_{xp} + B_1 V_s + B_2 V_R$$

or,

$$(A_1 + A_2) V_{xp} = -(B_1 V_s + B_2 V_R) \tag{7}$$

Fig.62 shows the modified circuit in which all the emf sources present in the unfaulted circuit are shorted and leaving their respective source impedances in the circuit. In this circuit the fault impedances are replaced by the equivalent current generators and their shunt admittances.

The system equations for the modified circuit are given by

$$\begin{bmatrix} I_{s_I} \\ I_{s_T} \end{bmatrix} = \begin{bmatrix} A_1 + Y_f & B_1 \\ B_1 & A_1 \end{bmatrix} \begin{bmatrix} V_{xa} \\ 0 \end{bmatrix} \tag{8}$$

$$\begin{bmatrix} I_{s_2} \\ I_{R_T} \end{bmatrix} = \begin{bmatrix} A_2 & B_2 \\ B_2 & A_2 \end{bmatrix} \begin{bmatrix} V_{xa} \\ 0 \end{bmatrix} \tag{9}$$

From equations (8) and (9)

$$I_{s_1} = (A_1 + Y_f)\, V_{xa} \tag{10}$$

$$I_{S_T} = B_1\, V_{xa} \tag{11}$$

$$I_{s_2} = A_2\, V_{xa} \tag{12}$$

$$I_{R_T} = B_2\, V_{xa} \tag{13}$$

Hence fault current at the sending end is given by

$$I_{s_f} = I_{ss} + I_{s_T}$$

$$= A_1\, V_s + B_1\, V_{xp} + B_1\, V_{xa}$$

$$= A_1\, V_s + B_1 (V_{xp} + V_{xa}) \tag{14}$$

$$I_{R_f} = I_{R_s} + I_{R_T}$$

$$= B_2\, V_{xp} + A_2\, V_R + B_2\, V_{xa}$$

$$= A_2\, V_R + B_2\, (V_{xp} + V_{xa}) \tag{15}$$

The current injected by the current generators is given by

$$I_s = I_{s_1} + I_{s_2}$$

Substituting for I_{s_1} and I_{s_2} from equation (10) and (12) we obtain

$$I_s = (A_1 + Y_f)V_{xa} + A_2V_{xa}$$

$$= (A_1 + Y_f + A_2)\, V_{xa} \qquad (16)$$

Also

$$I_s = -Y_f \times V_{xp} \qquad (17)$$

therefore,

$$-Y_fV_{xp} = (A_1 + Y_f + A_2)V_{xa} \qquad (18)$$

Now adding $(A_1+ A_2+ Y_f)V_{xp}$ on each side of equation (18) we obtain

$$(A_1+ A_2)\, V_{xp} = (A_1 + Y_f + A_2)(V_{xa} + V_{xp}) \qquad (19)$$

Substituting for $(A_1+ A_2)V_{xp}$ from equation (7) in equation (11) we obtain

$$-(B_1V_s + B_2V_R) = (A_1+ Y_f+ A_2)(V_{xa}+ V_{xp}) \qquad (20)$$

or,

$$(V_{xa}+ V_{xp}) = -(A_1+ Y_f+ A_2)^{-1}(B_1V_s + B_2V_R)$$

Now substituting for $(V_{xa} + V_{xp})$ in equations (14) and (15)

$$I_{s_f} = A_1V_s + B_1(V_{xp}+ V_{xa})$$

$$= A_1V_s - B_1(A_1+ Y_f+ A_2)^{-1}(B_1V_s + B_2V_R) \qquad (21)$$

$$= \left[A_1 - B_2(A_1 + Y_f + A_2)^{-1}B_1\right] V_s - \left[B_1(A_1 + Y_f + A_2)^{-1}B_s\right] V_s$$

$$I_{R_f} = A_2V_R - B_2(A_1 + Y_f + A_2)^{-1}(B_1V_s + B_2V_R)$$

$$= \left[A_2 - B_2(A_1 + Y_f + A_2)^{-1} B_2\right] V_R - \left[B_2(A_1 + Y_f + A_2)^{-1}B_1\right] V_s \quad (22)$$

Equations (21) and (22) are the same as those obtained by Wedepohl[16] for the currents at the sending end and the receiving end of a faulted three-phase transmission circuit.

Thus it is proved that the principle of superposition is equally applicable for the solution of a faulted transmission circuit and it is also established that the fault impedance may be replaced by a source emf with a series impedance. The series impedance being equal to the fault impedance, and the emf of the source is equal and opposite to the prefault emf across the fault impedances before the occurrence of this fault.

Appendix 2

APPENDIX to CHAPTER FOUR [1]

Evaluation of the Propagation Constants and the Modal Components

It has been shown by Wedepohl[1] by expanding and re-arranging the relation $\gamma^2 = Q^{-1}PQ$ in the following form

$$PQ - Q\gamma^2 = 0 \tag{1}$$

that, if γ^2 is diagonal then

$$[P - \gamma_i^2 \; U] \; [Q]_i = [0] \tag{2}$$

where the matrix P is defined by the product of the matrices Z and Y and is of the order nxn

U = unit matrix of order nxn

γ_i^2 = i^{th} diagonal element of the diagonal matrix γ^2. The matrix γ^2 is of order nxn.

Q_i = i^{th} column of the Q matrix. The matrix Q is of order nxn

and

$[P - \gamma_i^2 \; U] \; (Q)_i$ is the i^{th} column of the resultant matrix $[PQ - Q\gamma^2]$.

The above equation represents a set of homogeneous equations and the vector $(Q)_i$ will have a non-trivial solution, if the following relation is satisfied[1]

$$\det(P - \gamma_i^2 \; U) = 0 \tag{3}$$

or, in general

$$\det (P - \gamma^2 U) = 0 \tag{4}$$

Now, let

$$\det (P - \gamma^2 U) = f(\gamma^2) \tag{5}$$

or,

$$f(\gamma^2) = 0 \tag{6}$$

In general, $f(\gamma^2)$ is a polynomial of degree n and the equation $f(\gamma^2) = 0$ has n roots. This equation is defined to be the characteristic equation of the P matrix and the roots of the characteristic equation are defined to be the eigenvalues and the vector Q corresponding to each root are defined to be the eigenvectors of the matrix P.

The solution of the equation $f(\gamma^2) = 0$ gives the n roots of γ^2 and once the n values of γ^2 are known, the Q matrix may be solved by one column at a time by solving the system of homogeneous simultaneous equations given by the solution

$$\left(P - \gamma_i^2 U\right) Q_i = 0$$

where $i = 1, 2, \ldots\ldots n$

Now for $(Q)_i \neq 0$, the $\det(P - \gamma_i^2 U) = 0$, the vector $(Q)_i$ has an infinite number of solutions, however, each element of the vector $(Q)_i$ or the i^{th} column of the Q matrix are proportional to each other. Hence, any one element may be chosen arbitrarily and the remaining elements are defined in terms of this one, for a particular value of γ_i.

Thus for n = 2, the eigenvalues and the corresponding eigenvectors of the P matrix may be easily evaluated as $f(\gamma^2)$ is a polynomial of second degree. But for n > 2, i.e. if the order of the matrix P is greater than 2 then the direct evaluation of the eigenvalues and the corresponding eigenvector matrix becomes very cumbersome, especially when the elements of the P matrix are complex. However, the eigenvalues and the eigenvectors are easily evaluated by various standard mathematical techniques, e.g. Q-R method, root-squaring method etc. In this thesis, these are evaluated by the root-squaring method[2] by modifying the product of the matrices Z and Y as suggested by Wedepohl[2].

Similarly, the matrices γ^2 and S are defined from the solution

$$\gamma^2 = S^{-1} P_t S \tag{7}$$

and the necessary condition for $[S] \neq [0]$ is given by

$$\det(P_t - \gamma^2 U) = 0 \tag{8}$$

It has been shown in the following section that $\gamma^2 = \gamma^2$ and that the matrices S and Q are related to each other.

Hence, if suffices to evaluate the eigenvalues and the eigenvectors of either matrix P or matrix P_t. Throughout the present work these quantities are evaluated from the matrix P.

The square root of each of the diagonal elements of the eigenvalue matrix γ^2 defines the propagation constant and the corresponding column of the eigenvector matrix Q defines the modal distribution of the components.

Some of the Important Properties of the Wave Equation(1)

In this section some of the important properties of the wave equation described by Wedepohl and others are presented. These properties define the important relations between the component voltages and currents, and are very useful in the mathematical analysis and understanding of the phenomenon of wave propagation on the multiconductor transmission line.

1. Propagation constants of the component voltages and the corresponding component currents are equal to each other.

Consider the relations

$$\det(P - \gamma^2) = 0 \tag{9}$$

and

$$\det(P_t - {}^1\gamma^2) = 0 \tag{10}$$

Now

$$\det(P_t - {}^1\gamma^2) = \det(P_t - {}^1\gamma^2_t) \quad \because \; {}^1\gamma^2 \text{ is a diagonal matrix.}$$

$$= \det(P - {}^1\gamma^2)_t$$

$$= \det(P - {}^1\gamma^2) \tag{11}$$

($\because$ the determinant of a matrix is equal to the determinant of its transpose)

$$\therefore \quad \det(P - {}^1\gamma^2) = 0 = \det(P - \gamma^2) \tag{12}$$

or,

$$\gamma^2 = {}^1\gamma^2 \tag{13}$$

Thus, the eigenvalues of P and P_t are equal and hence the modal propagation constants of the component voltages are equal to the corres-

ponding component currents.

2. From equations 4.25 and 4.26 of Chapter Four it can be observed that for a n-phase line there are n modes of propagation. In the general case (untransposed line), each mode has its own velocity of propagation and attenuation constant. But if the conductors are ideally transposed then there are still n modes of propagation but (n-1) of then are equal and thus, there are only two different propagation constants in the system.[12]

3. If Q and S are solutions to the equations

$$\frac{d^2V}{dx^2} = Q^{-1}PQV \tag{14}$$

and

$$\frac{d^2I}{dx^2} = S^{-1}P_tSI \tag{15}$$

respectively, then Q' and S' are also solutions to the corresponding equations 14 and 15, where Q' and S' are given by the following relations

$$\begin{aligned} Q' &= QD \\ S' &= SD \end{aligned} \tag{16}$$

where D is an arbitrary diagonal matrix.

4. The current and voltage eigenvector matrices are related to each other. Hence the complete solution of the matrix wave equation may be derived in terms of the Q matrix and the S matrix as a derived factor or vice-versa. Some of the important relations between S and Q matrices are given by

$$\text{(a)} \quad S = YQD$$

$$\text{(b)} \quad S = [Q_t]^{-1} D \tag{17}$$

where D is an arbitrary diagonal matrix of order nxn and is sometimes chosen to normalise the columns of Q. Relation (a) is easily proved[11,] as follows:

$$P = ZY$$

Now

$$P = Q \gamma^2 Q^{-1}$$

or,

$$ZY = Q \gamma^2 Q^{-1}$$

and in general

$$ZY = (QD) \gamma^2 (QD)^{-1}$$

or,

$$Z = (QD) \gamma^2 (QD)^{-1} Y^{-1}$$

or,

$$YZ = Y(QD) \gamma^2 (QD)^{-1} Y^{-1} \tag{18}$$

But from equation 4.24 $YZ = S \gamma^2 S^{-1}$ (19)

By comparing equations (18) and (19)

$$S = YQD \tag{20}$$

Similarly the equation (b) can be proved.

5. The component currents are related only to the corresponding current voltages and vice-versa, i.e. there is no mutual interaction between components[1] or in other words, the current of a certain mode can only be produced by the component voltages of the same mode.

Consider the relations

$$\frac{dV}{dx} = -ZI \tag{21}$$

$$\frac{dI}{dx} = -YI \tag{22}$$

then

$$\frac{dV^c}{dx} = -QZSI^c = -D_Z I^c \tag{23}$$

and

$$\frac{dI^c}{dx} = -SYQV^c = -D_Y V^c \tag{24}$$

where

$$D_Z = Q^{-1}ZS \tag{25}$$

and

$$D_Y = S^{-1}YQ \tag{26}$$

Now

$$\frac{d^2V^c}{dx^2} = -D_Z \frac{dI^c}{dx} = D_Z D_Y V^c \tag{27}$$

and

$$\frac{d^2I^c}{dx^2} = -D_Y \frac{dV^c}{dx} = D_Y D_Z I^c \tag{28}$$

From equations 4.21 and 4.23 of Chapter Four

$$\frac{d^2V^c}{dx^2} = \gamma^2 V^c \tag{29}$$

and

$$\frac{d^2I^c}{dx^2} = \gamma^2 I^c \tag{30}$$

$\therefore$ from equations (27) and (28)

$$D_Z D_Y = D_Y D_Z = \gamma^2 \tag{31}$$

$\therefore$ D_Z and D_Y are each a diagonal matrix[1].

Now from equation 4.29 of Chapter Four

$$V^c = e^{-\gamma x} V_{ci} + e^{\gamma x} V_{cr} \tag{32}$$

or,

$$\frac{dV^c}{dx} = -\gamma e^{-\gamma x} V_{ci} + \gamma e^{\gamma x} V_{cr} \tag{33}$$

Now, substituting for $\frac{dV^c}{dx}$ from equation (23) into equation (33) gives

$$D_Z I^c = -\gamma e^{-\gamma x} V_{ci} + \gamma e^{\gamma x} V_{cr} \tag{34}$$

or,

$$\gamma^{-1} D_Z \; I^c = e^{-\gamma x} V_{ci} - e^{\gamma x} V_{cr}$$

or,

$$Z^c I^c = e^{-\gamma x} V_{ci} - e^{\gamma x} V_{cr} \tag{35}$$

where

$$Z^c = \gamma^{-1} D_Z$$

$$= \gamma^{-1} Q^{-1} Z S \tag{36}$$

Z^c is a diagonal matrix since D_Z and γ are each a diagonal matrix. Hence the produce $\gamma^{-1}Q^{-1}ZS$ is a diagonal matrix.

Now, substituting for I^c from equation 4.32 of Chapter Four in equation 35 gives

$$Z^c e^{-\gamma x} I_{ci} + Z^c e^{\gamma x} I_{cr} = e^{-\gamma x} V_{ci} - e^{\gamma x} V_{cr}$$

or,

$$e^{-\gamma x} Z^c I_{ci} + e^{\gamma x} Z^c I_{cr} = e^{-\gamma x} V_{ci} - e^{\gamma x} V_{cr} \tag{37}$$

$$\therefore \quad V_{ci} = Z^c I_{ci} \tag{38}$$

$$V_{cr} = -Z^c I_{cr} \tag{39}$$

Equations (38) and (39) define important relations and are used quite often for the solution of the wave equation.

It is seen from equations (29), (30), and (36) that there is no mutual interaction between components.

Polyphase Surge Impedance

Polyphase surge impedance defines a set of terminal impedances which gives reflection free conditions. In this case the voltages and currents at any point on the multiconductor line are uniquely related by the surge impedance.

Consider the relation

$$\frac{dV}{dx} = -ZI \tag{40}$$

or,

$$I = -Z^{-1}\frac{dV}{dx}$$

$$= -Z^{-1} Q \frac{dV^c}{dx} \qquad (\because V = QV^c)$$

$$= +Z^{-1}Q\gamma \; e^{-\gamma x} V_{ci} - e^{\gamma x} V_{cr} \tag{41}$$

$$(\because V^c = e^{-\gamma x} V_{ci} + e^{\gamma x} V_{cr} \text{ and}$$
$$\frac{dV^c}{dx} = -\gamma\, e^{-\gamma x} V_{ci} - e^{\gamma x} V_{cr})$$

$$= Z^{-1} Q \gamma Q^{-1} \left[Q\, e^{-\gamma x} V_{ci} - Q\, e^{\gamma x} V_{cr}\right]$$

$$= Z^{-1} Q \gamma Q^{-1} \left[Q\, e^{-\gamma x} Q^{-1} V_i - Q\, e^{\gamma x} Q^{-1} V_r\right]$$

$$= Z^{-1}\psi \left[e^{-\psi x} V_i - e^{\psi x} V_r\right] \tag{42}$$

$$= Y_o \left[e^{-\psi x} V_i - e^{\psi x} V_r\right] \tag{43}$$

where

$$\psi = Q \gamma Q^{-1} \tag{44}$$

$$Y_o = Z^{-1}\psi \tag{45}$$

Now for reflection free conditions the voltages and currents at any point is given by

$$V^{c}_{x} = e^{-\gamma x} V_{ci} \qquad (\because [V_{cr}] = [0])$$

or,

$$V_x = Q\, e^{-\gamma x}\, \bar{V}_{ci}$$

$$= Q\, e^{-\gamma x}\, Q^{-1} V_i$$

$$= e^{-\psi x} V_i$$

or,

$$I_x = Y_o V_x \qquad (46)$$

Thus Y_o is defined to be the surge admittance matrix.

The surge impedance matrix is given by

$$Z_o = [Y_o]^{-1}$$

$$= [Z^{-1}\psi]^{-1}$$

$$= \psi^{-1} Z \qquad (47)$$

Some other useful relations defining surge impedance/admittance matrices are as follows:

(a) Z_o and Y_o expressed in terms of Z^c

$$Z_o = \psi^{-1} Z$$

$$= [Q\gamma Q^{-1}]^{-1} Z$$

$$= Q\,\gamma^{-1}\,Q^{-1}\,Z$$

$$= Q(\gamma^{-1}Q^{-1}ZS)S^{-1}$$

$$= Q\,Z^c\,S^{-1} \qquad (48)$$

$$Y_o = Z_o^{-1}$$

$$= [Q\,Z^c S^{-1}]^{-1}$$

$$= S\,Z^{c^{-1}}\,Q^{-1}$$

or,

$$Y_o Q = S\,Z^{c^{-1}} \qquad (49)$$

(b) Y_o expressed in terms of Y

From equation 4.22 of Chapter Four

$$ZY = Q\,\gamma^2\,Q^{-1}$$

or,

$$Z^{-1} = [Q\,\gamma^2\,Q^{-1}Y^{-1}]^{-1}$$

$$= Y\,Q\,\gamma^{-2}\,Q^{-1}$$

or,

$$Y_o = Z^{-1} \psi$$

$$= [YQ\gamma^{-2}Q^{-1}] [Q \gamma Q^{-1}]$$

$$= Y Q \gamma^{-1} Q^{-1} \qquad (50)$$

It has been shown by Wedepohl [1] that Z_o is symmetrical, therefore Z_o and Y_o are bilateral.

Appendix 3

APPENDIX to Chapter Six

Mathematical Analysis of Fault Transients due to Simultaneous Faults

Consider the system shown in Fig. 6.1 fed at either end from infinite busbar source.

Let the shunt faults occur suddenly and simultaneously at distances x and x+d respectively from the receiving end. Assuming the system to be under steady state condition before the occurrence of the fault, the prefault voltages at the locations of fault may be evaluated from the relations defined by equation 6·5. The system conditions at x+d are determined by substituting x+d for x in equation 6.5.

The equivalent current generators simulating the shunt faults at the other locations may be defined as follows:

$$I_{s_{f_1}} = -Y_{F_1} \times V_x \qquad (1)$$

$$I_{s_{f_2}} = -Y_{F_2} \times V_{x+d} \qquad (2)$$

where Y_{F_1} and Y_{F_2} are the shunt admittance matrices defining the faults at x and x+d respectively.

V_x = prefault steady state voltage at x

V_{x+d} = prefault steady state voltage at x+d

The switching transients due to the current generators may be evaluated by solving the circuit shown in Fig. 2.

The Fourier transforms of the system equations for the matrices x, d and y respectively may be defined as follows:

For the section x

$$\begin{bmatrix} \overline{I_{s_{f_{12}}}} \\ \overline{I_{RR_2}} \end{bmatrix} = \begin{bmatrix} A_x & B_x \\ B_x & A_x \end{bmatrix} \begin{bmatrix} \overline{V_{s_{f_1}}} \\ 0 \end{bmatrix} \qquad (3)$$

For the section d

$$\begin{bmatrix} \overline{I_{s_{f_{11}}}} \\ \\ \overline{I_{s_{f_{22}}}} \end{bmatrix} = \begin{bmatrix} A_d & B_d \\ \\ B_d & A_d \end{bmatrix} \begin{bmatrix} \overline{V_{s_{f_1}}} \\ \\ \overline{V_{s_{f_2}}} \end{bmatrix} \tag{4}$$

For the section y

$$\begin{bmatrix} \overline{I_{s_{f_{21}}}} \\ \\ \overline{I_{RR_1}} \end{bmatrix} = \begin{bmatrix} A_y & B_y \\ \\ B_y & A_y \end{bmatrix} \begin{bmatrix} \overline{V_{s_{f_2}}} \\ \\ 0 \end{bmatrix} \tag{5}$$

Equations (3), (4) and (5) yield

$$\overline{I_{s_{f_{12}}}} = A_x \overline{V_{s_{f_1}}} \tag{6}$$

$$\overline{I_{s_{f_{11}}}} = A_d \overline{V_{s_{f_1}}} + B_d \overline{V_{s_{f_2}}} \tag{7}$$

$$\overline{I_{s_{f_{22}}}} = B_d \overline{V_{s_{f_1}}} + A_d \overline{V_{s_{f_2}}} \tag{9}$$

The currents in the shunt admittances at either locations may be defined as follows:

$$\overline{I_{f_1}} = + Y_{F_1} \times \overline{V_{s_{f_1}}} \tag{10}$$

$$\overline{I_{f_2}} = Y_{F_2} \times \overline{V_{s_{f_2}}} \tag{11}$$

Now,

$$\overline{I_{s_{f_1}}} = \overline{I_{s_{f_{11}}}} + \overline{I_{s_{f_{12}}}} + \overline{I_{f_1}} \tag{12}$$

and

$$\overline{I_{s_{f_2}}} = \overline{I_{s_{f_{21}}}} + \overline{I_{s_{f_{22}}}} + \overline{I_{f_2}} \tag{13}$$

Equations (7), (6), (10) and (12) yield

$$\begin{aligned}\overline{I_{s_{f_1}}} &= A_d \overline{V_{s_{f_1}}} + B_d \overline{V_{s_{f_2}}} + A_x \overline{V_{s_{f_1}}} + Y_{F_1} \overline{V_{s_{f_1}}} \\ &= (A_x + A_d + Y_{F_1})\overline{V_{s_{f_1}}} + B_d \overline{V_{s_{f_2}}}\end{aligned} \tag{14}$$

Similarly, from equations (8), (9), (11) and (13), $\overline{I_{s_{f_2}}}$ is given by

$$\begin{aligned}\overline{I_{s_{f_2}}} &= A_y \overline{V_{s_{f_2}}} + B_d \overline{V_{s_{f_1}}} + A_d \overline{V_{s_{f_2}}} + Y_{F_2} \overline{V_{s_{f_2}}} \\ &= B_d \overline{V_{s_{f_1}}} + (A_y + A_d + Y_{F_2})\overline{V_{s_{f_2}}}\end{aligned} \tag{15}$$

Equations (14) and (15) may be expressed in the following form

$$\begin{bmatrix} \overline{I_{s_{f_1}}} \\ \overline{I_{s_{f_2}}} \end{bmatrix} = \begin{bmatrix} A_x+A_d+Y_{F_1} & B_d \\ B_d & A_y+A_d+Y_{F_2} \end{bmatrix} \begin{bmatrix} \overline{V_{s_{f_1}}} \\ \overline{V_{s_{f_2}}} \end{bmatrix} \tag{16}$$

or

$$\begin{bmatrix} \overline{V_{s_{f_1}}} \\ \overline{V_{s_{f_2}}} \end{bmatrix} = \begin{bmatrix} A_x+A_d+Y_{F_1} & B_d \\ B_d & A_y+A_d+Y_{F_2} \end{bmatrix}^{-1} \begin{bmatrix} \overline{I_{s_{f_1}}} \\ \overline{I_{s_{f_2}}} \end{bmatrix} \tag{17}$$

Thus $\overline{V_{s_{f_1}}}$ and $\overline{V_{s_{f_2}}}$ are known in terms of the line constants and the injected currents.

From equations (3) and (5), $\overline{I_{RR_1}}$ and $\overline{I_{RR_2}}$ may be defined as follows:

$$\overline{I_{RR_1}} = B_y \overline{V_{s_{f_2}}} \tag{18}$$

$$\overline{I_{RR_2}} = B_x \overline{V_{s_{f_1}}} \tag{19}$$

Inverse Fourier transforms of $\overline{I_{RR_1}}$ and $\overline{I_{RR_2}}$ gives the switching transients at the sending- and the receiving-end respectively.

Fault transients at the sending- and the receiving-end may now be evaluated by adding the respective steady state and the switching components at either ends. Proceeding similarly the system conditions at any other point may be defined.

On the basis of this approach fault transients due to all types of simultaneous fault - shunt faults, or series faults at multiple locations, combinations of series and shunt faults at the same locations or multiple locations - may be evaluated.

APPENDIX to Chapter Six

Mathematical Analysis of Fault Transients due to Series Faults

Typical series faults constitute open conductors. Due to the opening of the conductors the current in the affected conductors at the location of fault is zero. The series fault may, therefore, be simulated by injecting a current equal and opposite to the prefault current in the affected conductors at the location of fault.

The fault transients at any point on the system due to the series fault may be evaluated according to the principle of superposition by adding the prefault component and the switching transient component due to the injected current, the injected current being equal and opposite to the prefault current at the location of fault.

Consider the system shown in Fig. 6.1 fed at the other end from the infinite busbar source. Let this system be under steady state condition before the occurrence of fault. The prefault steady state condition of the system may be determined according to the relations defined in section 6.2.1.1. Now let a series fault occur at a distance x from the receiving end. The injected currents simulating the series fault may be defined as follows:

(a) Three conductors open:

$$I_{s_{f_y}} = - I_y \qquad (1)$$

$$I_{s_{f_x}} = - I_x \qquad (2)$$

(b) Two conductors open (e.g. conductors 1 and 2 open circuited)

$$\begin{bmatrix} I_{s_{f_{y_1}}} \\ I_{s_{f_{y_2}}} \\ I_{s_{f_{y_3}}} \end{bmatrix} = \begin{bmatrix} -I_{y_1} \\ -I_{y_2} \\ 0 \end{bmatrix} \quad (3) \text{ and } \quad \begin{bmatrix} I_{s_{f_{x_1}}} \\ I_{s_{f_{x_2}}} \\ I_{s_{f_{x_3}}} \end{bmatrix} = \begin{bmatrix} -I_{x_1} \\ -I_{x_2} \\ 0 \end{bmatrix} \quad (4)$$

(c) One conductor open (e.g. for conductor 1 open-circuited)

$$\begin{bmatrix} I_{s_{f_{y_1}}} \\ I_{s_{f_{y_2}}} \\ I_{s_{f_{y_3}}} \end{bmatrix} = \begin{bmatrix} -I_{y_1} \\ 0 \\ 0 \end{bmatrix} \quad (5) \text{ and } \quad \begin{bmatrix} I_{s_{f_{x_1}}} \\ I_{s_{f_{x_2}}} \\ I_{s_{f_{x_3}}} \end{bmatrix} = \begin{bmatrix} -I_{x_1} \\ 0 \\ 0 \end{bmatrix} \quad (6)$$

where

I_y = prefault current entering the section y at the location of fault

I_x = prefault current entering the section x at the location of fault

$I_{s_{f_y}}$ = current injected into the section y at the location of fault

$I_{s_{f_x}}$ = current injected into the section x at the location of fault

The switching transient components due to the injected current may be evaluated by solving the circuit shown in Fig. 1.

The Fourier transform of the system equations for the section y may be defined as follows:

$$\begin{bmatrix} \overline{I_{s_{f_y}}} \\ \overline{I_{RR_1}} \end{bmatrix} = \begin{bmatrix} A_y & B_y \\ B_y & A_y \end{bmatrix} \begin{bmatrix} \overline{V_{s_{f_y}}} \\ 0 \end{bmatrix} \tag{7}$$

From equation (7),

$$\overline{I_{s_{f_y}}} = A_y \overline{V_{s_{f_y}}} \tag{8}$$

or,

$$\overline{V_{s_{f_y}}} = A_y^{-1} \overline{I_{s_{f_y}}} \tag{9}$$

and

$$\overline{I_{RR_1}} = B_y \overline{V_{s_{f_y}}} \tag{10}$$

Similarly, considering the section x, $V_{s_{f_x}}$ is given by

$$\overline{V_{s_{f_x}}} = A_x^{-1} \overline{I_{s_{f_x}}} \tag{11}$$

and $\overline{I_{RR_2}}$ may be evaluated in terms of $\overline{V_{s_{f_x}}}$ as follows:

$$\overline{I_{RR_2}} = B_x \overline{V_{s_{f_x}}} \tag{12}$$

The inverse Fourier transform of $\overline{I_{RR_1}}$ and $\overline{I_{RR_2}}$ defines the switching transient currents as a function of time respectively at the sending- and receiving-end.

The fault transient currents at these points may be obtained according to the relationship defined by equations 6.33 and 6.34.

Appendix to Chapter Six

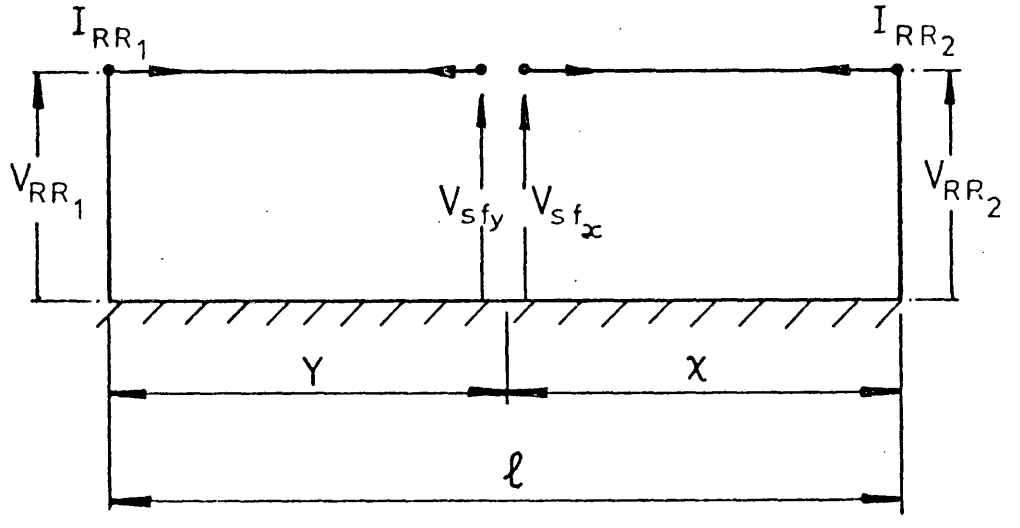

Fig. 1 Simulation of Series Fault

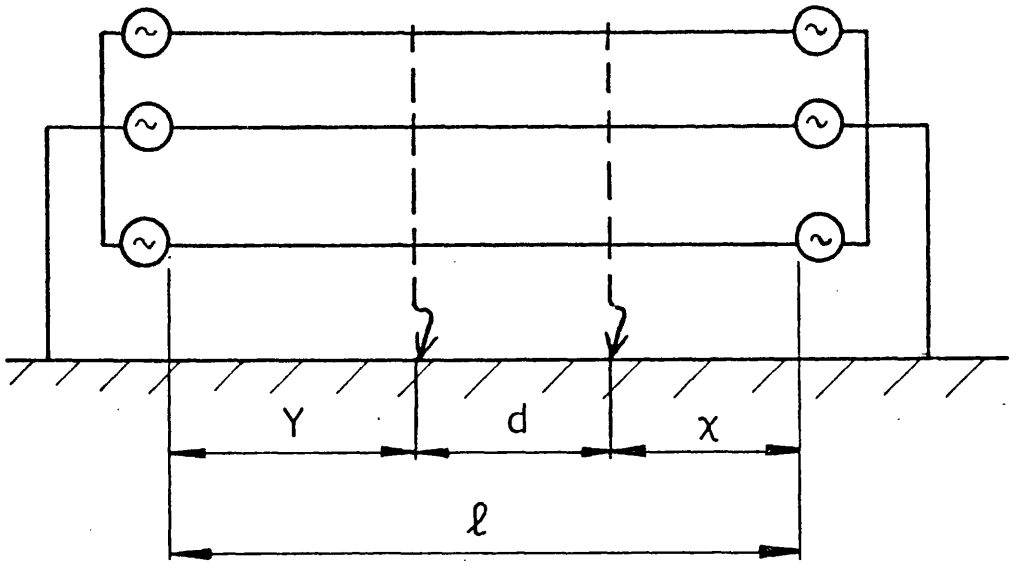

Fig. 2 Simultaneous Fault on Double-End Fed System

APPENDIX 4

Mathematical Analysis of Fault Transients in Short Lines

In this section the mathematical analysis of fault transients due to sudden inception of shunt faults on a simplified three-phase system has been described. In this analysis the distributed shunt admittance of this line is neglected and the line is assumed to be ideally transposed.

The system shown in Fig.6·5ais considered - this system is energised at the sending end and the receiving end is open-circuited before the occurrence of the fault.

Solid fault is applied at the receiving end in each case analysed here and the fault is simulated by using an ideal switch.

The system condition after the fault inception may be defined as follows:

$$[e] = [R][i] + [l]\left[\frac{di}{dt}\right] + [V_f] \qquad (1)$$

where

$$[e] = \begin{bmatrix} e_1 \\ e_2 \\ e_3 \end{bmatrix} \quad ; \quad [i] = \begin{bmatrix} i_1 \\ i_2 \\ i_3 \end{bmatrix} \quad ; \quad \left[\frac{di}{dt}\right] = \begin{bmatrix} \frac{di_1}{dt} \\ \frac{di_2}{dt} \\ \frac{di_3}{dt} \end{bmatrix} ; \quad [V_f] = \begin{bmatrix} V_{f_1} \\ V_{f_2} \\ V_{f_3} \end{bmatrix}$$

$$[R] = \begin{bmatrix} R_s & R_m & R_m \\ R_m & R_s & R_m \\ R_m & R_m & R_s \end{bmatrix} \quad ; \quad [l] = \begin{bmatrix} l_s & l_m & l_m \\ l_m & l_s & l_m \\ l_m & l_m & l_s \end{bmatrix}$$

where the subscripts 1,2 and 3 refer to the phase conductors 1,2 and 3 respectively.

e = instantaneous values of emf

i = instantaneous values of current

R_s = self-resistance of the line per unit length

R_m = mutual resistance of the line per unit length

L_s = self-inductance of the line per unit length

L_m = mutual inductance of the line per unit length

V_f = voltage at the location of fault after the fault inception

l = length of the line

SLG Fault

Let the SLG fault occur on line 1. In this case,

$$i_2 = i_3 = 0 \tag{2}$$

$$v_{f_1} = 0 \tag{3}$$

Substituting for i_2 and i_3 from equation 3 in equation 1 yields

$$e_1 = R_s i_1 + L_s \frac{di_1}{dt} \tag{4}$$

The solution of equation 4 defines i_1 as follows

$$i_1 = I_{m_s} \left\{ \sin(\omega_s t + \phi - \theta) - e^{-\frac{R_s t}{L_s}} \sin(\phi - \theta) \right\} \tag{5}$$

where

$$I_m = \frac{E_m}{Z_e x \ell}$$

$$\theta = \tan^{-1} \frac{\omega_s L_s}{R_s}$$

ϕ = phase angle of the emf source of phase 1 at the instant of fault inception

$$Z_{\ell} = \sqrt{R_s^2 + (\omega_s L_s)^2}$$

Three phase fault

In the case of three-phase fault, the line currents are related as follows

$$i_1 + i_2 + i_3 = 0 \tag{6}$$

and the line voltages at the location of fault are related as follows

$$v_{f_1} = v_{f_2} = v_{f_3}$$

From equations 1 and 6 the following relations may be defined

$$e_1 - v_{f_1} = (R_s - R_m)i_1 + (L_s - L_m)\frac{di_1}{dt} \tag{7}$$

$$e_2 - v_{f_2} = (R_s - R_m)i_2 + (L_s - L_m)\frac{di_2}{dt} \tag{8}$$

$$e_3 - v_{f_3} = (R_s - R_m)i_3 + (L_s - L_m)\frac{di_3}{dt} \tag{9}$$

Adding equations 7, 8 and 9 gives

$$e_1+e_2+e_3 - (v_{f_1} + v_{f_2} + v_{f_3}) = R_s(i_1+i_2+i_3) + (L_s-L_m)\frac{d}{dt}(i_1+i_2+i_3)$$

$$\therefore \quad v_{f_1} = v_{f_2} = v_{f_3} = 0 \qquad \left(\because\ e_1+e_2+e_3 = 0 \text{ and } v_{f_1} \simeq v_{f_2} = v_{f_3} \right) \tag{10}$$

Then the line currents may be evaluated as follows:

$$\dot{i}_k = I_m \left\{ \sin(\omega_s t + \phi_k - \theta) - e^{-\frac{R_e}{L_e} t} \sin(\phi_k - \theta) \right\} \qquad (11)$$

where

$\dot{i}_k$ = current in phase K

$$I_m = \frac{E_m}{Z_e \times 1}$$

$$Z_e = \sqrt{(R_s - R_m)^2 + \omega_s^2 (L_s - L_m)^2}$$

E_{m_k} = peak voltage emf in phase k

ϕ_k = phase angle of e.m.f. of phase k at the instant of fault inception

k = 1, 2 and 3 and refers to phase 1, 2 and 3 respectively.

Line to line fault

Let the conductors 1 and 2 be shorted together. In this case:-

$$\dot{i}_1 = -\dot{i}_2$$
$$\dot{i}_3 = 0 \qquad (12)$$

and

$$v_{f_1} = v_{f_2}$$

Equations 1 and 12 yield

$$e_1 - v_{f_1} = R_s i_1 + R_m i_2 + L_s \frac{di_1}{dt} + L_m \frac{di_2}{dt} \tag{13}$$

$$e_2 - v_{f_2} = R_s i_2 + R_m i_1 + L_s \frac{di_2}{dt} + L_m \frac{di_1}{dt} \tag{14}$$

Subtracting equation 14 from equation 13 gives

$$e_1 - e_2 = (R_s - R_m)(i_1 - i_2) + L_s \frac{d}{dt}(i_1 - i_2) + L_m \frac{d}{dt}(i_1 - i_2)$$

or,

$$e_1 - e_2 = 2(R_s - R_m) i_1 + 2(L_s - L_m) \frac{di_1}{dt} \tag{15}$$

From equation 15 , i_1 may be defined as follows

$$i_1 = I_m \left\{ \sin(\omega t + \phi - \theta) - e^{-\frac{R_e}{L_e} t} \sin(\phi - \theta) \right\} \tag{16}$$

where

$$I_m = \frac{E_m}{Z_e}$$

$$Z_e = 2\sqrt{(R_s - R_m)^2 + \omega_s^2 (L_s - L_m)^2}$$

$$\theta_e = \tan^{-1} \frac{\omega_s (L_s - L_m)}{(R_s - R_m)}$$

ϕ = phase angle of line to line voltage (voltage of line 1 with respect to line 2) at the instant of fault inception

2L-G

Let the lines 1 and 2 be shorted to earth. In this case

$$i_3 = 0$$

and

$$v_{f_1} = v_{f_2} = 0 \tag{17}$$

Equations 1 and 17 yield

$$e_1 = R_s i_1 + R_m i_2 + L_s \frac{di_1}{dt} + L_m \frac{di_2}{dt} \tag{18}$$

$$e_2 = R_m i_1 + R_s i_2 + L_m \frac{di_1}{dt} + L_s \frac{di_2}{dt} \tag{19}$$

Adding and subtracting equations 18 and 19 gives

$$e_a = R_a i_a + L_a \frac{di_a}{dt} \tag{20}$$

$$e_b = R_b i_b + L_b \frac{di_b}{dt} \tag{21}$$

where

$$e_a = e_1 + e_2 \qquad R_a = R_s + R_m \qquad L_a = L_s + L_m$$

$$i_a = i_1 + i_2 \qquad R_b = R_s - R_m \qquad L_b = L_s - L_m$$

$$e_b = e_1 - e_2$$

$$i_b = i_1 - i_2$$

From equations 20 and 21 i_a and i_b may be defined as follows

$$i_a = I_{ma}\left\{\sin(\omega_s t + \phi_a - \theta_a) - e^{-\frac{R_a}{L_a}t}\sin(\phi_a - \theta_a)\right\} \quad (22)$$

$$i_b = I_{mb}\left\{\sin(\omega_s t + \phi_b - \theta_b) - e^{-\frac{R_b}{L_b}t}\sin(\phi_b - \theta_b)\right\} \quad (23)$$

$$I_{ma} = \frac{E_{ma}}{Z_a} \qquad Z_a = \sqrt{R_a^2 + \omega_s^2 L_a^2}$$

$$I_{mb} = \frac{E_{mb}}{Z_b} \qquad Z_b = \sqrt{R_b^2 + \omega_s^2 L_b^2}$$

E_{ma} = peak value of the sum of the voltages of phase 1 and 2 respectively

E_{mb} = peak value of the line to line voltage (voltage of line 1 with respect to 2)

ϕ_a = phase angle of E_{ma} at the instant of fault inception

ϕ_b = phase angle of E_{mb} at the instant of fault inception

In all these cases the same solution may also be achieved by replacing the fault by a hypothetical emf source - the emf being equal and opposite to the prefault voltage at the location of fault.

Appendix 5

Appendix to chapter 7 - II

Description of Digital Computer programme

The important steps of the digital Computer programme for the evaluation of fault transients are as follows:-

(1) Evaluate the steady-state solution of voltages/currents at the desired points and the location of fault.

(2) Define the hypothetical Current generator and the shunt admittance, simulating the fault.

(3) Evaluate the switching transient components at the desired points due to the hypothetical current generator.

(4) Evaluate the fault transients at the desired points - sum of the steady-state solution and the switching transient solution defines the fault transient solution.

The steady-state solution and the switching transient solution of the transmission line are the functions of the basic line data Yo, γ, and Q.

The programme is made very efficient by storing these parameters at the supply frequency and over a wide range of complex frequencies. The range of complex frequencies is defined by the period of observation of the fault transients.

This method needs the evaluation of eigenvalues, eigenvectors and the surge admittance matrix only once at these frequencies for the evaluation of fault transients under varied conditions, e.g.

(a) different types of faults

(b) different locations of fault

(c) different instants of fault inception etc. etc.

Thus by storing the basic data of the line in a data file the Computer programme may be made very efficient and huge amount of computation time may be saved.

REFERENCES

1. Wedepohl, L M
'Application of matrix methods to the solution of travelling wave phenomena in polyphase systems',
Proc. IEE, Vol. 110, 1963, pp. 2200-2212.

2. Galloway, R H; Shorrock, W B; & Wedepohl, L M
'Calculation of electrical parameters for short and long polyphase transmission lines'
Proc. IEE, Vol. 111, No. 12, 1964, pp. 2051-2059.

3. Hedman, D E
'Propagation on overhead transmission lines II - Earth-conduction effects and practical results'
IEEE Trans. on Power & Apparatus, March 1965, pp. 205-211.

4. Hedman, D E
'Propagation on overhead transmission lines I - Theory of modal analysis',
IEEE Trans. on Power & Apparatus, March 1965, pp. 200-204.

5. Balser, S J; Eaton, J R; Krause, P C
'Single pole switching - a comparison of computer results with field test results'
IEEE Trans. on Power & Apparatus, pp. 100-108.

6. Carson, J R
'Wave propagation in overhead wires with ground return'
Bell System Tech. J., pp. 539-554.

7. Kuznetsov, I F
'Electrical parameters of steel-aluminium conductors at industrial and high frequencies'
Izv. Akad. Nauk. SSR Energ i Transp. No. 3, pp. 38-46, May/June 1968.

8. Nakagawa, M; Ametani, A; Iwamoto, K
'Further studies on wave propagation in overhead lines with earth return: impedances of stratified earth'
Proc. IEE, Vol. 120, No. 12, Dec. 1973.

9. Ametani, A
'Stratified earth effects on wave propagation - frequency dependent parameters'
IEEE Trans. on Power & Apparatus, pp. 1233-1239.

10. Guile, A E; Patterson, W
'Electrical power systems Vol.1 '
Oliver & Boyd, Edinburgh, 1969.

11. Chen Mo-Shing; Dillon, W
'Power system modelling'
Proc. IEE, July 1974, pp. 901-915.

12. Greenwood, A
'Electrical transients in power systems',
John Wiley & Sons, 1971.

13. Stevenson, W D
'Elements of power system analysis'
McGraw Hill Book Co. Inc, New York, 1962.

(14) Wasley R.G. - the natural mode theory of high frequency tower resonance effects in multiconductor lines, M.Sc. Thesis, Manchester Univ., 1965.

15. Wedepohl, L M et al
'Wave propagation in multiconductor overhead lines - Calculation of series impedance for multilayer earth'
Proc. IEE, Vol. 113, No. 4, April 1966.

16. Wedepohl, L M et al
'Apparent impedances of very long multiconductor transmission lines'
Proc. IEE, Vol. 117, July 1970.

17. Wedepohl, L M et al
'Multiconductor transmission line'
Proc. IEE, Vol. 110, No. 9, September 1969.

18. Bickford, J P et al
'Calculation of switching transients with particular reference to line energisation'
Proc. IEE, 1967, Vol. 114, No. 4, pp. 465-477.

19. Wedepohl, L M et al
'Transient analysis of multiconductor transmission lines with special reference to nonlinear problems'
Proc. IEE, Vol. 117. No. 5, May 1970, pp. 979-988.

20. Discussion on 'Multiconductor transmission lines, theory of natural modes and Fourier integral applied to transient analysis'
Proc. IEE, Vol. 117, Aug. 1970, pp. 1691-1692.

21. Discussion on 'Calculation of transients on transmission lines with sequential switching and transient analysis of multiconductor transmission lines with special reference to nonlinear problems and frequency-dependent parameters in transmission line analysis',
Proc. IEE, Vol. 118, No. 12, Dec. 1971, pp. 1815-1819.

22. Wedepohl, L M
'Multiple conductor transmission line theory'
Lecture notes - post-experience course, Jan. 1972, Imperial College of Science & Technology, UK.

23. Barthold et al
'Digital travelling wave solutions'
AIEE Trans., PAS, 80, Pt.III, 1961, pp. 812.

24. Slemon, G R et al
'High speed protection of power systems based on improved power system models'
CIGRE Report.

25. Boonyubol, C et al
'A mathematical analysis of transmission line transients related to fault surges'
IEEE Trans. Power Apparatus & Systems, Vol. 89, July/Aug. 1970.

26. Kimbark, E W et al
'Fault surge versus switching surge - a study of transient overvoltages caused by line-to-ground fault'
IEEE Trans. PAS, pp. 1762-1769, Sept. 1968.

27. Uram, R et al
'Mathematical analysis and solution of transmission line transients - Part I - theory',
IEEE Trans. PAS, Vol. 83, pp. 1116-1123, Nov. 1964.

28. Uram, R et al
'Mathematical analysis and solution of transients - Part II - Applications',
IEEE Trans. PAS, Vol. 83, pp. 1123-1137, Nov. 1964.

29. Laughton, M A
'Analysis of unbalanced polyphase networks by the method of phase co-ordinates', Part I.
Proc. IEE, Vol. 115, Aug. 1968.

30. Laughton, M A
'Analysis of unbalanced polyphase networks by the method of phase co-ordinates', Part II
Proc. IEE, Vol. 116, May 1969.

31. Lewis, W P
'Solution of network transients using symmetrical component techniques'
Proc. IEE, Vol. 113, Dec. 1966.

32. Ranjbar, A M; Cory, B J
'An imposed method for the digital protection of high voltage transmission lines',
IEEE Trans. on Power Apparatus & Systems, Vol. PAS-94, Mar/April 1975.

33. Kimbark, E W
'Transient overvoltages caused by monopolar ground fault on bipolar DC line: theory and simulation'
IEEE Trans, Vol. PAS-89, April 1970, pp. 584-593.

34. Colchaser, R G
'Transient overvoltages caused by the initiation and clearance of faults on 1100 kV systems'
IEEE Trans. PAS, Nov./Dec. 1970, pp. 1744-1751.

35. Lago, G V et al
'Transients in electrical circuits'
The Ronald Press Co., New York, 1958.
McCleery, D K - Introduction to Transients', London, Chapman -Hall, 1961.

36. Pipes, L A
'Matrix methods for engineering'
Prentice-Hall Inc., NJ, USA, 1963.

(37) Frazer, R.A., Duncan W.J. and Collar A.R. - Elementary Matrixes

Cambridge University Press, 1938

38. Wagner, C F; Evans, R D
'Symmetrical components'
McGraw Hill Book Co., New York, 1933.

39. Skilling, H H
'Electric transmission lines'
McGraw Hill Book Co. 1951.

40. Skilling, H H
'Transient electric currents'
McGraw Hill Book Co.,

41. Colton, H
'The transmission and distribution of electrical energy',
The English Universities Press Ltd, 1948.

42. Kimbark, E W
'Power system stability Vol. 1'
John Wiley & Sons., New York, 1964.

43. Kimbark, E W
'Power system stability Vol. 2'
John Wiley & Sons., New York, 1962.

44. Bewley, L V
'Travelling waves on transmission systems'
Dover Publications Inc., New York, 1963.

45. Sunde, D E
'Earth conduction effects in transmission systems'
Dover Publications Inc., New York, 1960

46. Warrington, A R C
'Protection relays, their theory and practice' Vol. 1
Chapman and Hall Ltd, 1971.

47. Warrington, A R C
'Protective relays, their theory and practice', Vol. 2
Chapman and Hall Ltd, 1971.

48. Anderson, P M
'Analysis of faulted power systems'
Ames. Iowa, Iowa State University Press, 1973.

49. Day, S et al
'Developments in balancing transient response using Fourier transforms: Gibbs phenomena and Fourier integrals',
IJEE, Vol. 3, No. 4, 1965, P. 501.

50. Day, S
'Developments in obtaining transient response using Fourier transforms: use of modified Fourier transforms'
IJEE, Vol. 4, 1966, p. 31.

51. Ametani, A
'The application of fast Fourier transforms electrical transient phenomena',
IJEE, Vol. 10, pp. 277-287, 1972.

52. Meyer, S et al
'Numerical modelling of frequency dependent transmission line parameters in an electromagnetic transients program'
Trans. IEEE PAS, pp. 1401-1409, 1970.

53. Bhartal, K et al
'Linear circuits and computation'
John Wiley & Sons, New York, 1972.

54. Day, S
'Developments in obtaining transient response by using Fourier transforms: Part IV - survey of the theory'
IJEE, pp. 256-267.

55. Day, S et al
'Developments in obtaining transient responses using Fourier transforms: Part III - global responses'
IJEE , Vol. 6, pp. 259-265, 1968.

56. Hedman et al
'Theoretical evaluation of multiphase propagation'
IEEE Trans. PAS, pp. 2460-2491, 1971.

57. Cooley, W J et al
'An algorithm for the machine calculation of complex Fourier series'
Maths, & Comput., Vol. 19, pp. 297-301, April 1965.

58. The English Electric Co. Ltd, Stafford
'Protective Relays Application Guide.

59. EHV Transmission line reference book - Edison Electric Institute, New York, General Electric Co., Pittsfield, Mass., USA.

60. Electrical transmission and distribution reference book - Westinghouse, Westinghouse Electric Corp., East Pittsburgh, PA, USA, 1950.

61. Peterson, H A
'Transients in power systems'
John Wiley & Sons Inc., New York, 1951.

62. Stagg, G W; El-Abiad, A H
'Computer methods in power system analysis'
McGraw Hill, New York, 1968.

63. McInnes, A D; Morrison, I F
'Real time calculation of resistance and reactance for transmission line protection by digital computer'
Elec. Eng. Trans., March 1971.

64. Battison et al
'British Investigation on the switching of long EHV transmission lines'
CIGRE, Vol. 13-02, 1970.

(65) I.E.E. - International Conference on Developments in power system Protection, March '75.

(66) Rockefeller G.D. - Fault Protection with a Digital Computer, I.E.E.E., Trans. Power Apparatus and Systems, Vol. Pas-88, No. 4, April '69.

(67) Raghavan R et al - Digital Calculation of transient phenomena in ehv systems Part 1, Trans. Power Apparatus and systems, '71.

(68) Laycock et al - Signal processing techniques for power system protection application, I.E.E. Conference publication, March '75.

(69) Kothari G.c. et al - Computer - aided analysis of high-speed protective relays, Proc. I.E.E., Vol. 121, No. 7, 1974.

(70) Mann B.J. and Morrison I.F., Relaying a three-phase transmission line with a digital computer, I.E.E.E., Pas-90, No. 1, 1971.

(71) Wright, A, 1968, Current transformers, Chapman & Hall

(72) Howson D.P. - Mathematics for electrical circuit analysis, Pergamon Press, 1966.

(73) Tucker D.G. - Elementary Electrical network theory, Pergamon Press, 1964.

(74) Fortescue, C.L. Method of Symmetrical Co-ordinates applied to the solution of polyphase networks, Trans. I.E.E.E. , 1918, 37, P. 1027.

(75) Banerjee A.R. - Transient response of faulted transmission line with reference to distance protection, Internal Research Report Univ. of Bath, 1974.

(76) Bramer B and Banerjee A.R. - Fitting of, measured data to a known relationship, Electronics letters, May '73.

Acknowledgements

The author is grateful to Prof. A. J. Eales and Prof. W. Gosling for encouraging him and providing the facilities of the department.

He is also grateful to the Bath University and the British Council for the financial assistances.

He thanks his Supervisor Dr. A. T. Johns.

He is thankful to Mr G. L. Turner, Manager, Dept. of Computer Science, and members of his department, and Dr. B. Bramer, for their suggestions and co-operation.

He is also thankful to Mr A. R. Daniels for encouraging him.

Finally the author expresses his sincere gratitude and thanks to all his well-wishers.